UNIVERSIDADE ESTADUAL DE CAMPINAS

Faculdade de Engenharia Química

VALERIA DA SILVA SANTOS

DEVELOPMENT OF SOLID LIPID NANOPARTICLES AND NANOSTRUCTURED LIPID CARRIERS WITH PHYTOSTEROLS FOR FOOD APPLICATIONS

DESENVOLVIMENTO DE NANOPARTÍCULAS LIPÍDICAS SÓLIDAS E CARREADORES LIPÍDICOS NANOESTRUTURADOS COM FITOESTERÓIS PARA APLICAÇÕES EM ALIMENTOS

CAMPINAS

2018

VALERIA DA SILVA SANTOS

DEVELOPMENT OF SOLID LIPID NANOPARTICLES AND NANOSTRUCTURED LIPID CARRIERS WITH PHYTOSTEROLS FOR FOOD APPLICATIONS

DESENVOLVIMENTO DE NANOPARTÍCULAS LIPÍDICAS SÓLIDAS E CARREADORES LIPIDICOS NANOESTRUTURADOS COM FITOESTERÓIS PARA APLICAÇÕES EM ALIMENTOS

Thesis presented to the Faculty of Chemical Engineering of University of Campinas in partial fulfilment of the requirements for the degree of Doctor.

Tese apresentada à Faculdade de Engenharia Química da Universidade Estadual de Campinas como parte dos requisitos exigidos para a obtenção do título de Doutora em Engenharia Química.

Orientadora: MARIA HELENA ANDRADE SANTANA

Coorientadora: ANA PAULA BADAN RIBEIRO

ESTE EXEMPLAR CORRESPONDE À VERSÃO FINAL DA TESE DEFENDIDA PELA ALUNA VALERIA DA SILVA SANTOS, E ORIENTADA PELA PROFA. DRA. MARIA HELENA ANDRADE SANTANA.

CAMPINAS

2018

Ficha catalográfica
Universidade Estadual de Campinas
Biblioteca da Área de Engenharia e Arquitetura
Luciana Pietrosanto Milla - CRB 8/8129

Informações para Biblioteca Digital

Título em outro idioma: Desenvolvimento de nanopartículas lipídicas sólidas e carreadores lipídicos nanoestruturados com fitoesteróis para aplicações em alimentos
Palavras-chave em inglês:
Nanotechnology
Foods
Oils and fats
Bioactive compounds
Solid lipid nanoparticles
Nanostructured lipid carriers
Área de concentração: Engenharia Química
Titulação: Doutora em Engenharia Química
Banca examinadora:
Maria Helena Andrade Santana [Orientador]
Rita de Kássia de Almeida Garcia
Priscilla Efraim
Samantha Cristina de Pinho
Maria Cristina Chiarinelli Nucci Mascarenhas
Data de defesa: 08-06-2018
Programa de Pós-Graduação: Engenharia Química

Folha de Aprovação da Tese de Doutorado defendida por Valeria da Silva Santos em 08/06/2018, pela Comissão Examinadora constituída pelas Doutoras:

_____

Profa. Dra. Maria Helena Andrade Santana

Orientador

_____

Dra. Rita de Kássia de Almeida Garcia

Membro

_____

Profa. Dra. Priscilla Efraim

Membro

_____

Dra. Samantha Cristina de Pinho

Membro

_____

Dra. Maria Cristina Chiarinelli Nucci Mascarenhas

Membro

Ata da defesa com as respectivas assinaturas dos membros encontra-se no processo de vida acadêmica da aluna.

A minha coorientadora Profa. Dra. Ana Paula Badan Ribeiro por todo apoio, incentivo e oportunidade.

A minha orientadora Profa. Maria Helena Andrade Santana, pela oportunidade e confiança em mim depositada.

Aos membros da Banca avaliadora deste trabalho pelas correções e sugestões.

Gostaria ainda que, todos que de alguma forma contribuíram para a realização deste trabalho e não foram aqui citados, sintam-se agradecidos.

Por fim, e não menos importante, gostaria de agradecer a Deus por me acompanhar e guiar em todos os momentos de minha caminhada.

"Attitudes are more important than abilities,

Motives are more important than methods,

Character is more important than cleverness and the

Heart takes precedence over the head."

Denis Burkitt

RESUMO

Nanopartículas de base lipídica (NL) combinam algumas vantagens, como estabilidade fisica, facilidade de dissolução de compostos bioativos lipofílicos e permeabilidade através da parede do intestino. As NL podem ser compostas apenas de lipídios sólidos, chamadas de Nanopartículas Lipídicas Sólidas (NLS) ou por mistura de lipídios sólidos e líquidos, denominadas como Carreadores Lipídicos Nanoestruturados (CLN). Este trabalho teve como objetivo o desenvolvimento de NLS e CLN para aplicações em alimentos. As NL foram desenvolvidas com matérias-primas alimentícias, comumente empregadas no setor industrial. Para a composição das matrizes lipídicas (ML) foram utilizados óleos de soja e girassol alto oleico (fração líquida) e óleos totalmente hidrogenados a partir dos óleos de soja, canola e crambe, também chamados de *hardfats* (fração sólida). Adicionalmente, foram desenvolvidos CLN com a incorporação de fitoesteróis livres (FL). Os FL são considerados compostos bioativos, capazes de reduzir os níveis de colesterol no organismo, por meio de mecanismo competitivo de absorção, auxiliando na prevenção de doenças cardiovasculares. Os emulsificantes utilizados foram lecitina de soja, monooleato de sorbitano polietoxilado e monoestearato de sorbitano. As nanopartículas foram obtidas em dispersão aquosa através do processo de emulsificação, seguida de homogeneização de alta pressão (HAP) utilizando 3 e 5 ciclos a 800 bar, com posterior cristalização e estabilização da fração lipídica. As NL obtidas foram caracterizadas quanto ao diâmetro médio, polidispersidade e potencial zeta usando espalhamento de luz dinâmico (DLS). As ML e as NL foram submetidas a estudos de comportamento térmico, utilizando calorímetria diferencial de varredura (DSC). Formas polimórficas e fenômenos de polimorfismo foram verificados através de difração de Raio-X (DRX). Microscopia de luz polarizada (MLP) foi empregada para estudar o grau de cristalinidade das ML. As NL apresentaram resultados diferenciados comparados aos materiais em macroescala, principalmente em termos de comportamento térmico. Mostraram-se promissoras para aplicação em produtos alimentícios, e com potencial de utilização em outros segmentos industriais. Cabe ressaltar, que as NL desenvolvidos nesta tese são inéditos, e este estudo encontra-se depositado como privilégio de invenção no INPI (BR 10 2017 006471 9).

Palavras-chaves: Nanotecnologia; Alimentos; Lipídios; Óleos vegetais; *Hardfats*; Fitoesteróis.

ABSTRACT

Lipid nanoparticles (LN) combine some advantages such as chemical stability, easy dissolution of lipophilic bioactive compounds and permeability through the intestine wall. NLs can be composed only of solid lipids, called Solid Lipid Nanoparticles (SLN) or by mixing solid and liquid lipids, called Nanostructured Lipid Carriers (NLC). This work aimed the development of SLN and NLC for food applications. NLs were developed with raw materials commonly used in the food industry sector. For the composition of the lipid matrices (LM), soybean oils and high oleic sunflower (liquid fraction), and fully hydrogenated oils, also called hardfats, were used from the soya, canola, and crambe oils. In addition, CLN was developed with the incorporation of free phytosterols (FP) as a bioactive compound. FPs can reduce blood cholesterol levels, through a competitive mechanism of absorption, aiding in the prevention of cardiovascular diseases. The emulsifiers used were soybean lecithin, ethoxylated sorbitan monooleate, and sorbitan monostearate, individually employed. The nanoparticles were obtained in aqueous dispersion through the emulsification process, followed by high-pressure homogenization (HPH) using 3 and 5 cycles at 800 bar, with subsequent crystallization and stabilization of the lipid fraction. The obtained LN were characterized as the mean hydrodynamic diameter, polydispersity and zeta potential using dynamic light scattering (DLS). The LM and the LN were submitted to studies of the thermal behavior using differential scanning calorimetry (DSC). Polymorphic forms and polymorphism phenomena were verified by X-ray diffraction (XRD). Polarized light microscopy (MLP) was employed to study the degree of crystallinity of lipid matrices. The NL presented different results compared to the materials in macro scale, mainly in terms of thermal behavior. They have shown promise for application in food products, and potential for use in other industrial segments. It should be noted that the systems developed in this thesis are unpublished and present an innovative character, which is deposited as an invention privilege at INPI (BR 10 2017 006471 9).

Keywords: Nanotechnology; Foods; Lipids; Vegetable oils; Hardfats; Phytosterols.

SUMÁRIO

INTRODUÇÃO GERAL

INTRODUÇÃO GERAL

A nanotecnologia é considerada uma ciência recente, que está em constante desenvolvimento e aprimoramento nas mais diversas áreas de pesquisa e aplicação industrial. É uma tecnologia que compreende o desenvolvimento de processos e aplicações de materiais e sistemas em escala nanométrica, através do controle e exploração de fenômenos e propriedades, que se diferenciam do comportamento em micro e macroescala. Deste modo, o constante interesse nesta nova tecnologia motiva a busca por conhecimento em prol da modernização e aperfeiçoamento de processos e produtos.

Na área de alimentos, o interesse da utilização de sistemas em nanoescala reside, principalmente, no carreamento, proteção e liberação controlada de compostos bioativos. Para tal, as nanopartículas lipídicas (NL) combinam algumas vantagens recentemente reportadas na literatura científica como maior facilidade de dissolução de compostos bioativos lipofílicos (ácidos graxos essenciais, tocoferóis, esteróis, carotenóides, etc.), estabilidade química e permeabilidade através da parede do intestino.

As NL podem ser desenvolvidas com matrizes lipídicas (ML) totalmente saturadas denominadas de Nanopartículas Lipídicas Sólidas (NLS) e com misturas de lipídios saturados e insaturados, denominadas como Carreadores Lipídicos Nanoestruturados (CLN). No entanto, as NLS, geralmente apresentam baixa capacidade de incorporação de compostos ativos, devido ao alto grau de organização das moléculas de triacilgliceróis saturados durante a cristalização, formando uma estrutura altamente ordenada e compacta, resultando, consequentemente, em problemas de estabilidade e expulsão dos componentes de inclusão. Tendo em vista esta limitação, os CLN foram desenvolvidos por meio da substituição parcial de lipídios saturados por insaturados. Os lipídios insaturados apresentam comportamento de cristalização diferenciados em relação aos saturados, devido à presença de ligações duplas em suas moléculas. Nos CLN, estes lipídios promovem a formação de estruturas com maior espaçamento intermolecular, caracterizando partículas menos compactas e com maior capacidade de incorporação de compostos bioativos.

Cabe ressaltar, que estas informações, reportadas na literatura científica até o momento, envolvem NL desenvolvidas com materiais de alto grau de pureza, direcionadas para aplicações farmacêuticas e cosméticas. Assim, estes sistemas tornam-se inviáveis para aplicações em alimentos, principalmente devido ao alto custo dos materiais purificados.

Neste contexto, tivemos como objetivo principal deste estudo o desenvolvimento e caracterização de NL a base de óleos e gorduras comestíveis e/ou comercialmente disponíveis no contexto da indústria de alimentos, visando tornar a tecnologia acessível para aplicações em escala industrial, principalmente em termos de custos e aspectos regulatórios e toxicológicos.

Para a concretização desta tese, primeiramente, foi realizada uma revisão bibliográfica sobre NL, abordando desde os conceitos e definições até os materiais lipídicos para a composição da matriz, compostos lipofílicos de inclusão, emulsificantes, métodos de produção e caracterização, aspectos toxicológicos, regulatórios e perspectivas de aplicações da tecnologia na área de alimentos. Este artigo foi submetido para à *Food Research International* (ISSN: 0963-9969) no formato de **Artigo de Revisão**, denominado "*Solid lipid nanoparticles as carriers for lipophilic compounds for applications in foods*" e se encontra em fase de avaliação.

A parte experimental foi divida entre quatro artigos, onde constam o estudo de caracterização das matérias-primas e o desenvolvimento e caracterização de NLS, CLN e CLN com incorporação de compostos bioativos, os fitoesteróis livres (CLN+FL), obtidas através de homogeneização a alta pressão (HAP). Foram utilizados óleos vegetais para composição da fração insaturada e óleos vegetais totalmente hidrogenados para a fração saturada das nanopartículas, ambos materiais comumente empregados na indústria de alimentos. Os óleos vegetais totalmente hidrogenados, também conhecidos como *hardfats,* são obtidos por meio da hidrogenação total de óleos líquidos, que transforma todas as duplas ligações dos ácidos graxos insaturados em saturadas. Os *hardfats* são materiais relativamente novos utilizados como matérias-primas para o desenvolvimento de gorduras interesterificadas *low trans*. Mais recentemente, os *hardfats* têm sido objeto de estudos voltados aos processos de estruturação lipídica, para obtenção de produtos "Zero *Trans"*, e também "*Low Sat"*, sendo uma abordagem totalmente inédita a utilização em NL.

Os fitoesteróis livres (FL), foram selecionados como compostos bioativos para a incorporação nas matrizes lipídicas e nas nanopartículas, pois apresentam estruturas químicas muito semelhantes ao colesterol. Deste modo, a bioatividade dos FL reside na competição em absorção com o colesterol, com consequente redução dos seus níveis no organismo, auxiliando na prevenção de doenças cardiovasculares. Porém, com relação a aspectos tecnológicos, os FL apresentam insolubilidade em água, o que dificulta a aplicação destes compostos em alimentos.

Sendo assim, a solubilização de FL na matriz lipídica dos CLN uma opção para viabilizar a aplicação destes em alimentos.

No contexto experimental da tese, conforme representado esquematicamente na Figura 1, foram realizados estudos preliminares para obtenção das NL realizados com o objetivo de avaliar diferentes condições de processamento e emulsificantes com diferentes balanços-hidrofílicos-lipofílicos (BHL). Assim, foram desenvolvidos CLN e CLN+FL compostos por óleo de soja e *hardfat* de óleo de soja, utilizando 3 e 5 ciclos de HAP a 800 bar e os emulsificantes lecitina de soja desengordurada (BHL=7,0), monoestearato de sorbitano (BHL=4,7) e monooleato de sorbitano etoxilado (BHL=15,0). Os resultados deste estudo compõem o **Artigo 1,** que será submetido para *Food Chemistry* com o título "*Crystallization, polymorphism and stability of nanostructured lipid carriers developed with soybean oil, fully hydrogenated soybean oil and free phytosterols for food applications.*".
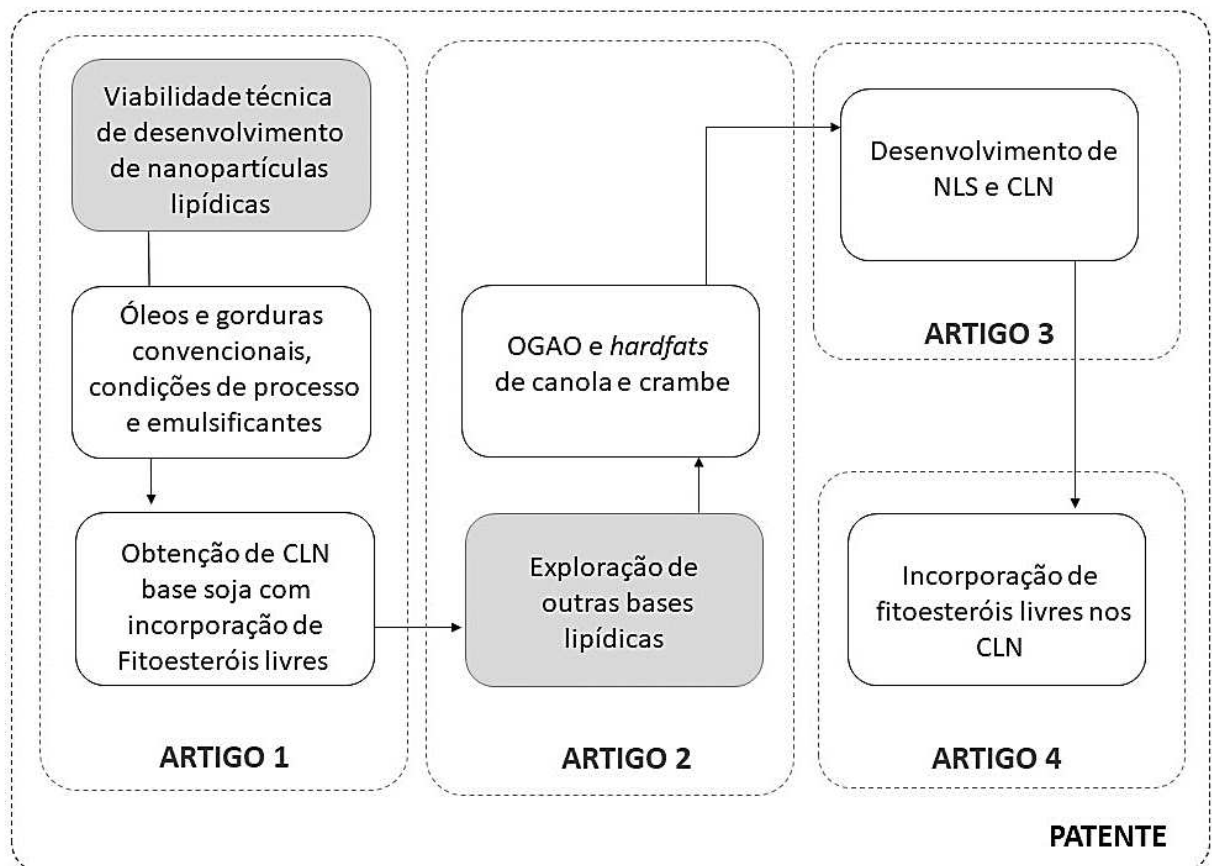
Figura 1. Representação esquemática da parte experimental dos estudos que compreendem os quatro artigos experimentais desta tese.

Para os demais estudos, a composição das ML das nanopartículas foi alterada, visando melhorar os aspectos tecnológicos e nutricionais. Para compor a fração insaturada, foi escolhido o óleo de girassol alto oleico, justificado, principalmente, pela maior estabilidade oxidativa em comparação ao óleo de soja. A fração saturada, composta previamente por *hardfat* do óleo de soja foi substituída pelo *hardfat* de óleo de canola, que também possui o ácido esteárico (C18:0), como principal ácido graxo. Esta substituição foi realizada a fim de reduzir os níveis de ácido palmítico (C16:0) nas formulações. Pois, o ácido palmítico tem sido considerado nutricionalmente inadequado, principalmente em relação a indução de resistência à insulina em casos de diabetes e atividade pró-inflamatória.

Adicionalmente, a fim de estudar a influência do tamanho de cadeia dos ácidos graxos na cristalinidade das ML, foram incluídos no estudo, ácidos graxos de cadeia longa, através do uso de *hardfat* de óleo de crambe. Composto principalmente por ácido behênico (C22:0), que apresenta baixo índice de absorção no organismo (baixa biodisponibilidade). Deste modo, diferentes formulações compostas por óleo de girassol alto oleico e *hardfats* dos óleos de canola e crambe foram desenvolvidas e caracterizadas quanto ao comportamento térmico de cristalização e fusão, hábito polimórfico e cristalinidade, utilizando as técnicas de Calorimetria Diferencial de varredura (DSC), Difração de raios-X (DRX) e Microscopia de Luz Polarizada (MLP). A fim de verificar a influência da composição dos diferentes *hardfats* nos fenômenos de cristalização e polimorfismo das ML desenvolvidas. Os resultados obtidos compoem o **Artigo 2** denominado *"Comportamento térmico e cristalino de matrizes lipídicas com potencial de aplicação em nanopartículas lipídicas"* será submetido à Química Nova.

A partir dos resultados obtidos nos Artigos 1 e 2, foram selecionadas 9 ML e o emulsificante monooleato de sorbitano etoxilado para dar continuidade nos estudos. NLS e CLN foram produzidas por meio de HAP com 3 e 5 ciclos a 800 bar e avaliadas quanto ao diâmetro médio de partículas, índice de polidispersidade e potencial zeta. Adicionalmente, foi aplicado o processo de secagem por liofilização, e foram avaliadas as propriedades térmicas e polimorfismo antes e após a secagem. Estes resultados serão submetidos à *Food Chemistry*, compondo o **Artigo 3** *"Thermal and crystalline properties of lipid nanoparticles developed with conventional vegetable fats and oils for food applications"*.

A última etapa do desenvolvimento das nanopartículas lipídicas consistiu da incorporação de fitoesteróis livres (FL) nas ML e nos CLN. Diferentes sistemas foram

formulados contendo óleo de girassol alto oleico e *hardfats* dos óleos de canola e crambe, com inclusão de 30 e 50% do composto bioativo. Os FL e as ML foram avaliadas quanto ao grau de cristalinidade, polimorfismo e comportamento térmico de fusão. Os CLN foram produzidos através de 3 ciclos de HAP à 800bar, utilizando o emulsificante monooleato de sorbitano etoxilado. Os CLN obtidos foram caracterizados quanto ao diâmetro médio das partículas, índice de polidispersidade, potencial zeta, comportamento térmico e polimorfismo. Os dados obtidos estão reunidos no **Artigo 4**, intitulado *"• Development of nanostructured lipid carriers loaded with free phytosterol for food applications"* que será submetido à *Food Structure*.

Além disso, destaca-se que as nanopartículas desenvolvidas nesta Tese de doutorado são consideradas inéditas, principalmente em termos de composição de ML. Parte deste estudo encontra-se em fase de Pedido de **Patente**, no âmbito de Privilégio de Invenção, com INPI - BR 10 2017 006471 9, registrado como "*Nanopartículas Lipídicas Sólidas (NLS) e Carreadores Lipídicos Nanoestruturados (CLN) para aplicação em alimentos, processo para obtenção de NLS e CLN e uso das NLS e dos CLN*".

Adicionalmente, foi realizado um período de estudos no **"*Centre for Doctoral Training in Complex Particulate Products and Processes*"** da Faculdade de Engenharia Química e de Processos, da Universidade de Leeds, Reino Unido, através do Programa de Doutorado Sanduíche no Exterior (PDSE) da Coordenação de Aperfeiçoamento de Pessoal de Nível Superior (Capes). Este estudo teve a duração de quatro meses, onde foi possível acompanhar experimentos de cristalização de diferentes materiais e o uso do programa *Habit98*. Este programa é utilizado para fornecer informações de energias e interações envolvidas no processo de cristalização de materiais, assim como, para a predição da forma estrutural de cristais. Este programa foi desenvolvido pelo professor Kevin Roberts, que foi o supervisor das atividades no exterior.

OBJETIVO

O objetivo deste trabalho foi o desenvolvimento de nanopartículas lipídicas para a incorporação de fitoesteróis livres, utilizando matérias-primas lipídicas usualmente empregadas na indústria de alimentos.

As metas para alcançar este objetivo foram:

- Estudo do comportamento térmico, hábito cristalino e transição polimórfica das matérias-primas lipídicas e do composto bioativo;

- Desenvolvimento e caracterização de matrizes lipídicas para elaboração das nanopartículas lipídicas;

- Emprego de homogeneização a alta pressão para produção das nanopartículas lipídicas;

- Desenvolvimento de nanopartículas lipídicas com matérias-primas inéditas neste contexto, como óleos de soja e girassol alto oleico, *hardfats* dos óleos de soja, canola e crambe e fitoesteróis livres;

- Avaliação da influência dos emulsificantes e condições de processamento nas características das nanopartículas;

- Obtenção e caracterização das nanopartículas lipídicas sólidas (NLS), carreadores lipídicos nanoestruturados (CLN) e carreadores lipídicos nanoestruturados com fitoesteróis livres (CLN+FL).

ARTIGO DE REVISÃO

"*Solid lipid nanoparticles as carries for lipophilic compounds for applications in foods*" submetido à *Food Research International*.

Solid lipid nanoparticles as carriers for lipophilic compounds for applications in foods

Valeria da Silva Santos[a], Ana Paula Badan Ribeiro[b], Maria Helena Andrade Santana[a]

[a] Department of Biotechnological Processes, School of Chemical Engineering, University of Campinas (UNICAMP), Campinas, SP, Brazil
[b] Department of Food Technology, School of Food Engineering, University of Campinas (UNICAMP), Campinas, SP, Brazil

Graphical abstract
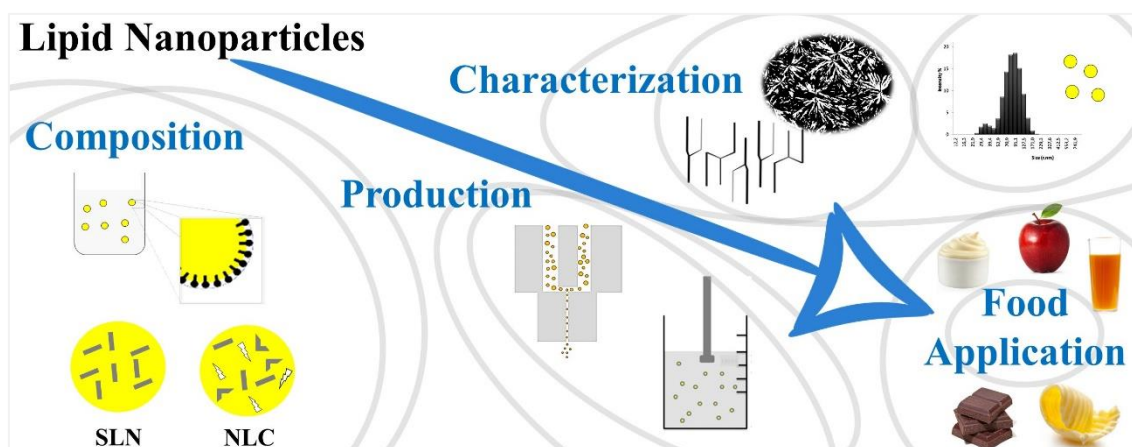
Abstract

Nanotechnology is a new subject of interest in the food industry. Therefore, scientific and technological studies have been intensified in the last 10 years because of the promising results associated with the potential application of functional properties in food products, such as physical and chemical stability, protection and controlled release of bioactive compounds, facilitated solubility of lipophilic compounds and others. Lipids have been used as a raw material for the preparation of nanostructures, mainly due to the solubilization capacity of lipophilic bioactive compounds, and also because of the advantage of potentially using natural ingredients for production on an industrial scale. Thus, in this review we have gathered the information reported in scientific literature on the chemical, physical, crystallization behavior and polymorphisms of lipids used in the preparation of lipid nanoparticles (LN), also

known as solid lipid nanoparticles (SLN) and nanostructured lipid carriers (NLC). Additionally, we reviewed the production methods, properties, characterization, structural components, emulsifying systems and functional lipophilic compounds in SLN and NLC. Important methods for characterizing LN with regards to particle size, polydispersity index, zeta potential, morphology, crystallization behavior and polymorphism are discussed via examples, seeking to support studies that consider stability during the processing and storage. Furthermore, studies on the applications of LN in foods are only found for model systems, justifying the compilation of a series of studies on potential LN applications to encourage future works. In addition, aspects still under discussion are commented, related to the possible risks and regulatory aspects of nanotechnology in food.

Keywords: Nanotechnology; Nanoparticles; Lipids; Crystallization; Bioactive Compounds; Foods.

1. Introduction

Nanotechnology has been a featured science in recent years, and has expanded to several areas of research. The great interest in nanostructured materials is related to different chemical, physical and biological properties that may be present on the nanoscale. This science involves the development, production and application of structures, devices and systems with nanometric dimensions. The basis of knowledge for development of these systems follows the principles of nanodevices found in nature, which have several functionalities, such as the organization of macromolecules including lipoproteins, deoxyribonucleic acid (DNA) and membranes. Nanotechnology materials are in constant development and have been applied in the textile industry, energy production, communication systems, medicine, pharmaceuticals, cosmetics, food industry and others. They include diverse materials and structures, such as nanotubes, nanosensors, nanoparticles, nanofibers and nanosystems carrying bioactive compounds (Cushena, Kerryb, Morrisc, Cruz-Romerob, & Cumminsa, 2012; Tamjidi, Shahedi, Varshosaz, & Nasirpour, 2013; Cerqueira, Pinheiro, Silva, Ramos, Azevedo, Flores-López, Rivera, Bourbon, Ramos, & Vicente, 2014; Beloqui, Solinís, Rodríguez-Gascón, Almeida, & Préat, 2016).

Strategies for the use of nanotechnology in the food industry are differentiated, mainly in terms of preserving integrity and guaranteeing the functionality of bioactive

compounds, as well as biosafety requirements. In this context, it is possible to obtain great benefits from the use of nanotechnology in several areas, for example in food safety for the detection of pathogens, in the development of packaging materials with biodegradable, antimicrobial and barrier properties, as well as edible films for surface coatings, nanosensors, new ingredients, additions, additives, food supplements, foods with functional properties, systems for transporting bioactive compounds and others (Chaudhry & Castle, 2011; Durán & Marcato, 2013; Cerqueira, Pinheiro, Silva, Ramos, Azevedo, Flores-López, Rivera, Bourbon, Ramos, & Vicente, 2014; Wang, Chaudhry, Park, & Juneja, 2015).

The transport of bioactive compounds has been considered an innovative subject in food technology, since it follows the principles of delivery and release of compounds in the body, highly utilized in orally administered drugs. In industrial processing, these carrier systems can also be employed for the protection of compounds of interest against degradation, i.e., preventing undesirable chemical reactions and loss of functional activity as a result of exposure to light and oxygen. Additionally, in foods the use of nanoscale materials with different physicochemical properties could solve some problems found in macro and microstructured systems, such as compatibility with the food matrix resulting from the effects of aggregation and phase separation (Weiss, Takhistov, & McClements, 2006; Aditya & Ko, 2015). It can be seen in scientific literature that studies on the application of nanostructured systems in food are still in the development phase, since knowledge is sought on the behavior of nanostructures to obtain stable and applicable systems. Therefore, this review seeks to gather and present the state of the art on nanostructured lipid systems, associating the subject with consolidated knowledge of lipids on a macroscale, in order to expand the scope on behavior of these systems and discuss their potential application in foods.

2. Lipids and crystallization properties

Lipids are essential nutrients of the human diet, playing a vital role by providing essential fatty acids and energy. Chemically, natural oils and fats consist of multi-component mixtures of triacylglycerols (TAGs), which are esters of glycerol and fatty acids. Each fatty acid can occupy different positions in the glycerol molecule (*sn-1*, *sn-2* or *sn-3*), allowing a great diversity of combinations. However, the distribution of fatty acids in natural TAGs is not random. The taxonomic pattern of oils and fats obeys the 1,3-random-2-random distribution,

with the saturated fatty acids located almost exclusively at the sn-1 and sn-3 positions and the unsaturated fatty acids preferably at the sn-2 position of the TAGs (O'Brien, 2009).

Much of the behavior of lipids depends on the alkyl chain characteristics of the fatty acids present, for example: saturated or unsaturated fatty acids, *cis* or *trans* configuration, chain size, and even or odd carbon numbers. Saturated fatty acids are less reactive and have a higher melting point than the corresponding fatty acid of the same chain size with one or more double bonds. The presence of long and saturated chains increases the melting point of the TAGs due to their linear conformation, resulting in greater interaction of the molecules, and consequently allowing better packing of the fatty acid chains (Scrimgeour, 2005).

The crystallization process refers to the spontaneous ordering of a lipid system, characterized by total or partial movement restriction caused by chemical or physical interactions between triacylglycerol molecules. Differences in the crystalline forms result from different molecular packings. Therefore, a crystal consists of molecules arranged in a fixed pattern known as reticulated. Its high degree of molecular complexity allows that the same set of TAGs be packaged in several different and relatively stable structures (Sato, 2001). Long chain compounds, such as fatty acids and their esters, may exist in differentiated crystalline forms, characterizing polymorphs. The polymorphism can be defined in terms of its ability to manifest different cell unit structures, resulting from various molecular packings (Lawler & Dimick, 2002). In TAGs three specific types of subcellular cells predominate, referring to the polymorphs α, β' and β, according to the current polymorphic nomenclature. The α form is metastable, with hexagonal chain packing. The β' form has intermediate stability and orthorhombic perpendicular packing, while the β form has greater stability and parallel triclinic packing. The melting temperature increases with increasing stability ($\alpha \rightarrow \beta' \rightarrow \beta$) as a result of the density differences of the molecular packing. TAGs initially crystallize into the α and β' forms, although the β form is the most stable. This phenomenon is related to the fact that the β form has higher activation free energy for nucleation. Polymorphic transformation is an irreversible process from the least stable to the most stable form (monotrope phase transformation), depending on the temperature and time involved. At constant temperature, the α and β' forms can transform, as a function of time, into the β form via the liquid-solid or solid-

solid mechanisms (Himavan, Starov, & Stapley, 2006). The transformation rate decreases as the degree of heterogeneity of the TAGs increases (Sato, 2001).

The most important aspect of the physical properties of oils and fats is related to solid-liquid and liquid-solid phase changes, melting and crystallization, respectively. The various thermal phenomena related to oils and fats are verified by monitoring the enthalpy and phase transition changes of the various TAG mixtures. Evaluation of the thermal behavior provides direct measurements of the energy involved in the melting and crystallization processes of lipid systems. Crystallization results in volume contraction associated with an exothermic effect. Melting, contrarily, competes for volume expansion, characterizing an endothermic effect (Tan & Che Man, 2002). The polymorphic characteristics of TAGs complicate the study of the thermal and structural properties of fats. Thermal behavior therefore reflects the general properties of lipid functionality and applicability, and is dependent on TAGs profiles in edible oils and fats (Ribeiro, Basso, Grimaldi, Gioielli, & Gonçalves, 2009).

3. Nanotechnology applied to lipids

Nanoparticles developed from lipids are among the most promising encapsulation technologies in the field of nanotechnology. The initial concept for the development of LN is based on the principles of producing oil-in-water (O/W) emulsions on a nanometric scale, with the substitution of liquid lipids for solid lipids at room temperature. In the last decade, SLN have been developed as an alternative system to emulsions, liposomes and polymeric structures. However, many presented inadequate characteristics related to the unavailability of biocompatible polymers, emulsifiers and the use of organic solvents not approved for food systems (Weiss, Decker, McClements, Kristbergsson, Helgason, & Awad, 2008).

The term "lipids", which is quite general, refers to a wide variety of molecules, including TAGs, partial acylglycerides, fatty acids, steroids, cholesterol and waxes. Compared to conventional encapsulation systems, lipid systems have the advantage of using natural ingredients on an industrial scale, a great differentiation of physicochemical properties, as well as the retention capacity of compounds presenting variable solubility (Kamboj, Bala, & Nair, 2010; Yoon, Park, & Yonn, 2013). In addition, lipids are naturally absorbed by the body, facilitating the transport of bioactive compounds via rapid absorption in the gastrointestinal tract (GIT). Thus, in the pharmaceutical field LN have gained prominence as vehicles for

transporting orally administered drugs, as well as via other methods (Severino, Andreani, Macedo, Fangueiro, Santana, Silva, & Souto, 2012). However, LN for food and drug applications should be produced from lipid materials with high thermal resistance (melting point higher than the body temperature of 37 °C) so that they remain solid during the digestive process in order to protect the bioactive compounds until the time of their absorption in the GIT (Sharma, Diwan, Sardana, & Dhall, 2011).

Solid LN are considered complex systems, presenting spherical shape and dimensions on the nanoscale, although highly variable according to the materials and forms of acquisition. They present high bioavailability due to the use of physiological lipids throughout their composition (Robles, García, Garzón, Hernández, & Vázquez, 2008). They also present advantages including: carriers of bioactive compounds, controlled release and targeting of substances at the site of action, increased stability of the encapsulated compound, ability to include lipophilic substances and absence of toxicity. Besides these factors, they can be produced on a large scale without the use of organic solvents (Gasco, 2007; Lason & Ogonowski, 2011).

Recently there has been a growing interest in studies focused on the development and application of these systems, supported by a large number of scientific publications directed towards production, physicochemical characterization, incorporation capacity of lipophilic compounds and release profile of the incorporated compound (Porter, Willians, & Trevaskis, 2013; Tamjidi, Shahedi, Varshosaz, & Nasirpour, 2013; Choi, K., Aditya, & Ko, 2014; Joseph, Rappolt, Schoenitz, Huzhalska, Augustin, Scholl, & Bunjes, 2015; Zhu, Zhuang, Luan, Sun, & Cao, 2015).

In light of this, the great potential of LN applications is a current focus of research in the food industry, driven by the enormous versatility of these systems since physical properties such as dimensions, structure, load, physical state and preferential crystalline habit can be modulated by means of selecting the specific lipid raw materials, associated with different acquisition parameters (Simovic, Barnes, Tan, & Prestidge, 2012).

4. Solid lipid nanoparticles and nanostructured lipid carriers

Solid LN are currently classified into two categories: solid lipid nanoparticles (SLN) and nanostructured lipid carriers (NLC) (Fig1). The first generation of LN was produced

with only solid lipids (saturated fatty acids) and emulsifiers for the incorporation of bioactive compounds, and denominated SLN. The SLN have a highly ordered crystalline structure and are stabilized by an outer layer consisting of emulsifiers, used alone or in combination (Lason & Ogonowski, 2011). For maintenance of the SLN structure after oral administration, for example, the melting point of the lipid materials used should exceed the body temperature (37 °C), which justifies the use of lipid matrices with high thermal resistance (Sharma, Diwan, Sardana, & Dhall, 2011). In general, it is considered that the lipid phase should totally or partially crystallize at the final application temperature of the SLN. In this sense, SLNs can be produced from a single solid lipid species, such as high melting point TAGs, or by the use of a mixture of lipid classes, where mobility of the incorporated compound is controlled by the physical state of the lipid matrix used and the structure type (Tamjidi, Shahedi, Varshosaz, & Nasirpour, 2013). The structure of SLN allows the incorporation of different types of lipophilic compounds, which are protected against degradative processes by the lipid matrix. In general, the development of SLN requires the knowledge of interactions between the compound of interest and the lipids used as the matrix, the chemical and physical structure of the components, as well as its preferential polymorphic habit. In some cases, SLN produced from high purity lipid matrices can crystallize in a highly ordered manner, which permits less room for incorporation of bioactive compounds, resulting in problems of stability and expulsion of the incorporated component (Lason & Ogonowski, 2011; Weiss, Decker, McClements, Kristbergsson, Helgason, & Awad, 2008).

In order to overcome possible limitations associated with SLN, a second generation of LN, referred to as NLC, appeared with the intent of producing less structured lipid matrices in relation to crystallinity, capable of obtaining better incorporation efficiency and avoiding the release/expulsion of bioactive compounds during storage (Müller, Runge, Ravelli, Mehnert, Thunemann, & Souto, 2006; Garzón, Hernández, Vázquez, Vázquez, & García, 2008; Pardeike, Hommoss, & Müller, 2009; Souto, Severino, Santana, & Pinho, 2011).

The NLC were developed from blends of liquid lipids (unsaturated fatty acids) to solid lipids, which are spatially different, in order to create particles with "imperfect" crystallization characteristics. Therefore, acquiring NLC is accomplished through the combined use of solid and liquid lipid fractions; however, it is important that the blends used have a melting point higher than the body temperature to maintain the structural and stability

characteristics. As a result of imperfections in the crystalline structure of the NLC, the capacity for incorporation of bioactive compounds of the LN can be increased, minimizing expulsion of the compound of interest during the storage period (Yoon, Park, & Yonn, 2013). Müller, Radtke, & Wissing, (2002) stated that the combination of saturated and unsaturated fatty acids promotes less crystalline packing and rigidness of the NLC structure, with greater spacing between the fatty acid chains, facilitating the incorporation of bioactive compounds and minimizing expulsion during polymorphic transitions. Furthermore, according to Tamjidi, Shahedi, Varshosaz, & Nasirpour (2013) the structural organization of NLC is dependent on factors such as the types and concentrations of lipids used in the matrix, the compound incorporated, the interaction between them and the parameters used in production.

TAGs consisting of a single type of fatty acid result in organized structures, with restrictions for accommodation of the incorporated compound, inducing expulsion of the solid lipid matrix compound. Lipid mixtures consisting of heterogeneous TAGs form crystals with a smaller degree of ordering, offering more space to accommodate the molecules of the incorporated compound (Garzón, Vázquez, Vázquez, García, & Hernández, 2009). In this sense, significant differences were verified between monoacid TAGs and complex lipid mixtures, whose polymorphic properties differ significantly (Hou, Xie, Huang, & Zhu, 2003).
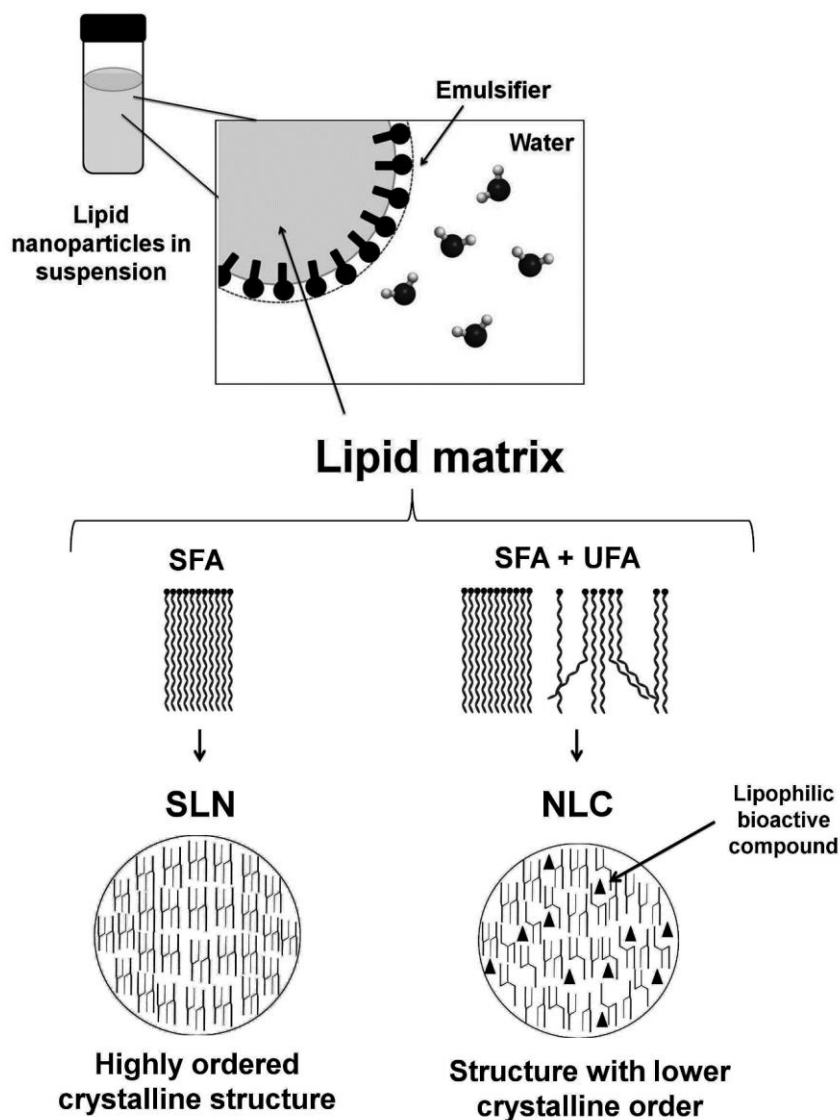
Fig. 1 Schematic representation of the structures of lipid nanoparticles: SLN (solid lipid nanoparticles, composed by SFA - saturated fatty acids) and NLC (Nanostructured Lipid Carriers, composed by SFA-saturated fatty acids and UFA - unsaturated fatty acids).

5. Methods for production of SLN and NLC

The techniques for obtaining SLN and NLC are similar and in literature it is possible to find several production methods, such as homogenization using hot or cold high pressure, solvent emulsification and evaporation, solvent emulsification-diffusion, solvent injection (or solvent displacement, multiple emulsion, ultrasonication, microemulsion, spontaneous

emulsification, phase inversion and others (McClements & Rao, 2011; Tamjidi, Shahedi, Varshosaz, & Nasirpour, 2013). However, most of these methods present disadvantages including the need for high concentrations of emulsifiers and co-emulsifiers, and potentially the presence of organic solvent residues which can cause toxicity problems, complicating their application in the food industry (Wissing, Kayser, & Müller, 2004; Tamjidi, Shahedi, Varshosaz, & Nasirpour, 2013; McClements, 2013).

Homogenization using hot or cold high pressure and ultrasonic homogenization are methods that present greater potential for application in the food industry on an industrial scale, with potential for isolated or integrated application, and are described below.

5.1. High pressure homogenization

High pressure homogenization (HPH) is the technique with greatest potential for the preparation of SLN and NLC, since homogenizers of different capacities are commercially available. In contrast to other production techniques, HPH presents no difficulties of scale transposition and allows for working under aseptic conditions, which characterizes the method as highly versatile and advantageous. The HPH is characterized by the use of a variable pressure from 100 to 2000 bar, in which shear and cavitation forces rupture the larger lipid aggregates to the nanometer scale (Mehnert & Mäder, 2012). In order to obtain LN with a homogeneous size distribution, the entire dispersion must be subjected to the same energy intensity. HPH is characterized by applying the same shear stress to the entire sample, due to the reduced dimensions of the homogenizer outlet orifice, generally less than 30μm (Souto, Severino, Santana, & Pinho, 2011). Two different HPH approaches, denominated hot homogenization and cold homogenization, can be used for the production of SLN and NLC. In both cases, a preparatory step involves mixing the bioactive compound in the lipid matrix, by dissolution or dispersion (Mehnert & Mäder, 2012).

5.1.1. Hot high pressure homogenization

Hot HPH is carried out at temperatures exceeding the melting point of the lipid phase, and may be understood as the homogenization of a pre-emulsion. To obtain this pre-emulsion, the lipid matrix is completely melted, incorporating the active compound by dissolution or by dispersion. To increase the stability of the pre-emulsion, it is possible to incorporate an emulsifier into the liquid lipid phase. This phase is then emulsified in an aqueous

phase containing the emulsifier with the use of mechanical stirring, such as ultra-turrax (Souto, Severino, Santana, & Pinho, 2011). The quality of the pre-emulsion strongly affects the final quality of the LN, and in this step particles with dimensions of a few micrometers should be obtained (Mehnert & Mäder, 2012). Then, the pre-emulsion is subjected to HPH at a temperature dependent on the material, resulting in an O/W type nanoemulsion (Bunjes & Siekmann, 2006; Patel & Martin-Gonzalez, 2012). In general, for this stage two to five HPH cycles are used, with pressure varying between 500 and 1500 bar (Severino, Andreani, Macedo, Fangueiro, Santana, Silva, & Souto, 2012; Liu, Wang, & Xia, 2012). Higher temperatures result in lower particle sizes as a result of the viscosity decrease. In some cases, the increase in the homogenization pressure or the number of cycles can promote an increase in particle size, due to the coalescence phenomenon as a result of the high kinetic energy. The obtained nanoemulsion is then cooled to a temperature at or below room temperature, followed by solidification of the lipids and obtaining the aqueous LN dispersion (Reddy & Shariff, 2013).

It is considered that the physico-chemical characteristics of the LN obtained by hot HPH are affected by a set of parameters, which include solubility of the incorporated component, polymorphism of the lipid matrix, nature and concentration of the lipid and emulsifying phase, process temperature, shear force and number of homogenization cycles performed (Severino, Andreani, Macedo, Fangueiro, Santana, Silva, & Souto, 2012). Cheong & Tan (2010) investigated the effect of pressure, number of cycles and temperature on the properties of the LN obtained with palm oil, verifying that all parameters resulted in a significant effect on the size distribution and morphology of the particles obtained. Several recent studies have been reported to obtain LN using this technique, with favorable results regarding the general physical properties (Attama & Muller-Goymann, 2008; Han, Li, Yin, Liu, & Xu, 2008; Mitri, Shegokar, Gohla, Anselmi, & Müller, 2011; Patel & Martin-Gonzalez, 2012; Liu, Wang, & Xia, 2012; Carvalho, Noronha, Floriani, Lino, Rocha, Bellettini, Ogliari, & Barreto, 2013; Zheng, Zou, Yang, Liu, Xia, Ye, & Mu, 2013).

5.1.2. Cold high pressure homogenization

Cold HPH is suitable for the incorporation of thermolabile or hydrophilic bioactive compounds (Garzón, Hernández, Vázquez, Vázquez, & García, 2008). It was developed in order to overcome problems related to the preservation of bioactive compounds. Among these,

highlighted are decomposition of the active substance subjected to high temperatures and contact with the aqueous phase during the homogenization process, as well as multiple modifications due to the complex crystallization behavior in nanoemulsions (Lason & Ogonowski, 2011; Mehnert & Mäder, 2012).

The first phase of the cold HPH technique is identical to hot HPH and involves the solubilization or dispersion of the bioactive compound in the molten lipid matrix. However, the other phases are quite different. The lipid matrix containing the bioactive compound is rapidly cooled with liquid nitrogen or dry ice, and this high cooling rate favors the homogeneous distribution of the bioactive compound. This mixture is subjected to a fragmentation process and has its size reduced to microparticles (50-100 μm), which are dispersed in a cold solution containing the emulsifier, so as to form a pre-suspension. This is subjected to HPH at room temperature or lower, generally at 500 bar for 5 to 10 cycles, to obtain an aqueous dispersion of LN. However, the greater the number of cycles employed the higher the temperature control has to be, since in each cycle the dispersion increases by 10 to 20 °C. The cold HPH method minimizes exposure of the sample to elevated temperatures, with exception of the first phase, where it is necessary to use a temperature above the melting point of the lipid matrix to disperse the bioactive compound (Lason & Ogonowski, 2011; Mehnert & Mäder, 2012). Another interesting feature is that the use of low temperatures in crystallization of the lipid matrix increases the lipid fragility and favors the acquisition of LN with smaller dimensions (Garzón, Hernández, Vázquez, Vázquez, & García, 2008; Souto, Severino, Santana, & Pinho, 2011). However, the particles obtained by this method are larger in comparison to the hot homogenization process, requiring a greater number of homogenization cycles (Lason & Ogonowski, 2011).

5.2. Ultrasonic Homogenization

Techniques such as ultrasound are used in many industrial applications in the food industry, such as processing, preservation and food safety. This emerging technology has been used as an alternative to conventional food processing operations and has the advantage of ease of adaptation and scale up in several processes (Awad, Moharram, Shaltout, Asker, & Youssef, 2012, Ramisetty, Pandit, & Gogate, 2015).

Ultrasound homogenates using constant or intermittent high intensity ultrasonic waves. The method basically consists of the preparation of a pre-emulsion in an ultra-turrax, followed by homogenization with ultrasound application to obtain a nanoemulsion and subsequent solidification of the lipid fraction. An ultrasound probe is inserted in the pre-emulsion and during the sonication process longitudinal waves are created when a sound wave enters the liquid medium, thus creating alternating regions of compression and expansion which generates levels of intense mechanical turbulence. This favors the formation of gas bubbles which propagate within the liquid and lead to cavitation effects, i.e., formation, growth and collapse of small bubbles in the liquid (Leong, Man, Lai, Long, Misran, & Tan, 2009; McClements & Rao, 2011).

A number of recent studies using ultrasound to produce LN composed of sunflower, canola, soybean, linseed, sesame, and olive oils from nanoemulsions are found in literature (Kentish, Wooster, Ashokkumar, Balachandran, Mawson, & Simons, 2008; Leong, Man, Lai, Long, Misran, & Tan, 2009; Wulff-Perez, Galvez-Ruiz, De Vicente, & Martin-Rodriguez, 2009; Amani, York, Chrystyn, & Clark, 2010). These showed that parameters such as ultrasonic wave intensity, exposure time, type and quantity of emulsifiers and viscosity of the medium should be evaluated to improve LN production processes, in addition to evaluation of lipid oxidation due to the presence of air bubbles in the process.

Leong, Man, Lai, Long, Misran, & Tan (2009) prepared O/W nanoemulsions with 15 % sunflower oil and 5.6% emulsifiers both together and individually (polyoxyethylene sorbitan monooleate - PSM 80, sorbitan monooleate - SM 80 and sodium dodecyl sulfate - SDS). The pre-emulsions were prepared in an ultra-turrax for 1-2 min and then sonicated at the sonication amplitude of 30 μm by immersion of the ultrasound probe in 40 mL of sample for 20 minutes, with temperature control by means of circulated cooling water at 21 - 23 °C. The authors demonstrated that ultrasound is a viable method for producing O/W type nanoemulsions using sunflower oil, with no lipid oxidation and average particle size below 40 nm.

6. Structural components for LN

The essential components for obtaining SLN and NLC are lipids, emulsifiers and water (Aditya & Ko, 2015). The nature and proportion of the lipid phases, emulsifiers, and co-emulsifiers determine the general properties of the LN, such as loading capacity, incorporation

efficiency of bioactive compounds, stability and administration forms (Garzón, Vázquez, Vázquez, García, & Hernández, 2009). Among the materials for the composition of LN, many lipid components and emulsifiers are found within the category GRAS - Generally Recognized as Safe, or with approved regulatory status for the preparation of bioactive compound carrier systems for oral, parenteral or dermal administration (Garzón, Vázquez, Vázquez, García, & Hernández, 2009; Aditya & Ko, 2015).

According to literature, in order to obtain the particulate matrix mixtures, solid lipids are mixed with liquid lipids, preferably in a ratio of 70:30 to 99.9:0.1. The SLN can be obtained in systems composed of 0.1 to 30% (w/w) lipids, with high melting lipid fractions dispersed in aqueous medium and stabilized by emulsifier contents between 0.5 and 5% (w/w); for NLC, the percentage of lipids in the formulation may be greater than 95% (w/w). In both systems, the percentage of the encapsulated compound, relative to the total formulation, is about 5% (w/w). The higher the lipid content in the formulation, the greater the incorporation capacity in the LN obtained, with direct implications on the cost and feasibility for application in foods (Tamjidi, Shahedi, Varshosaz, & Nasirpour, 2013). Different formulations are associated with incorporation efficiencies between 50 and 95% (Jannin, Musakhanian, & Marchaud, 2008). As the concentration of the lipid phase increases the LN size increases, making emulsification in the aqueous phase more difficult. In general, lipid phase percentages greater than 10% result in LN with larger dimensions and more heterogeneous size distribution (Souto, Severino, Santana, & Pinho, 2011).

The lipid matrix represents a fundamental factor in the structure and properties of the LN, since it determines specific molecular configurations related to the functionalities of these structures. The nature of the lipid phase also has a great influence on the biodegradation of nanoparticles. TAGs with long-chain fatty acids present a slower degradation process compared to TAGs with short-chain fatty acids; more unsaturated TAGs are also more susceptible to oxidation than less unsaturated TAGs (Sharma, Diwan, Sardana, & Dhall, 2011). Furthermore, selection of the constituents of the lipid matrix determines the production conditions of the LN, such as the homogenization temperature and cooling rates (Weiss, Decker, McClements, Kristbergsson, Helgason, & Awad, 2008).

Selection of the appropriate lipid matrices for development of SLN and NLC should consider the following aspects: i) the solubility of the bioactive compound in the lipid phase,

the efficiency of incorporation and feasibility of use in the LN obtained; ii) stability of the lipid phase for chemical and enzymatic oxidation processes; iii) use of biodegradable lipid components presenting an acceptable toxicological profile (Tamjidi, Shahedi, Varshosaz, & Nasirpour, 2013).

Factors including crystallization velocity of the lipid phase and microstructural properties affect the general characteristics of the obtained LN, such as geometry and dimensions. The average particle size generally increases with increasing melting point of the lipid matrix, as a result of increasing the viscosity of the dispersed phase (Mehnert & Mäder, 2012).

Specifically, with regards to NLC production, the lipid constituents with high and low melting points must have a very different spatial configuration. This means that the liquid lipid phase should not be incorporated into the solid lipid phase, and that the crystals should not be dissolved by the liquid phase. Additionally, an essential condition to guarantee NLC stability is that the lipid constituents with high and low melting points present complete miscibility at the concentrations of use (Doktorovová, Araújo, Garcia, Rakovský, & Souto, 2010).

The vast majority of the lipid components used to obtain LN consist of synthetic materials, generally of high cost and with varying chemical composition according to different manufacturers, in which small differences in the contents of acylglycerol components may represent difficulties in standardized acquisition and characterization (Garzón, Vázquez, Vázquez, García, & Hernández, 2009; Mehnert & Mäder, 2012). However, the use of TAGs in their purified form is generally economically unfeasible when considering the scale and possibility for application in food systems. Table 1 shows the synthetic lipid components found in literature, used for LN composition and applicable for foods.

The combination of fatty acid characteristics found in common lipid sources in the food industry, such as vegetable oils and fats, is very promising for the development of nanostructured lipid systems with specific release properties. Different mixtures of natural fats represent compatible sources for this purpose, with crystallographic characteristics suitable for SLN and NLC formulation (Garzón, Vázquez, Vázquez, García, & Hernández, 2009). However, to date few studies have been directed at obtaining LN from conventional oils and fats.

Mandawgade & Patravale (2008) developed SLN with the use of different stearin fractions from palm kernel oil. The preparation of SLN from beeswax and animal fat was studied by Attama & Muller-Goymann (2008). The authors verified that the degree of crystallinity of the particles was maintained throughout storage. Joseph & Bunjes (2012) used mixtures of medium chain TAGs (MCT) and soybean oil to obtain LN. Yang, Corona, Schubert, Reeder, & Henson (2014) studied the effect of different synthetic and natural lipid matrices, in concentrations between 2.5 and 20%, on the crystallization properties of NLC. Natural lipid sources composed mainly of TAGs, such as olive oil and palm oil, favored the formation of more homogeneous and stable structures.

Table 1. Commercial materials used in the composition of nanoemulsion and lipid nanoparticles found in the literature

LIPID COMPOSITION [a]	REFERENCE
Solid Lipid	
Stearic acid purified	Sharma, Ganta, Denny, & Garg (2009); Chakraborty, Shukla, Vuddanda, Mishra, & Singh (2010); Eltayeb, Bakhshi, Stride, & Edirisinghe (2013).
TAG purified (trilaurin / trimyristin / tripalmitin / tristearin)	Mühlen, Schwarz, & Mehnert (1998); Bunjes, Steiniger, & Richter (2007); Awad, Helgaso, Kristbergsson, Decker, Weiss, & McClements (2008); Awad, Helgason, Weiss, Decker, & McClements (2009); Severino, Andreani, Macedo, Fangueiro, Santana, Silva, & Souto (2012); Salminen, Helgason, Kristinsson, Kristbergsson, & Weiss (2013); Joseph, Rappolt, Schoenitz, Huzhalska, Augustin, Scholl, & Bunjes (2015).
Mixtures of TAG (65-80%), DAG (10-35%) and MAG (1-5%)	Jores, Haberland, Wartewig, Mäder, & Mehnert (2005).
Glyceryl behenate (5% MAG, 50% DAG and 35% TAG of C22:0)	Mühlen, Schwarz, & Mehnert (1998); Jores, Mehnert, & Mäder (2003); Jores, Mehnert, Drechsler, Bunjes, Johann, & Mäder (2004); Jores, Haberland, Wartewig, Mäder, & Mehnert (2005); Alex, Chacko, Jose, & Souto (2011).

Propylene glycol monostearate (70% mono and distearatoglycol 29% mono and dipalmitatoglycerol and 1% fatty acids (C14:0 and C18:0))	Hentschel, Gramdorf, Müller, & Kurz (2008).
Coconut oil	Ramisetty, Pandit, & Gogate (2015).
Liquid lipid	
49% PUFA, 28% EPA, 12% DHA, 24% MUFA, 27% SFA, 0.25% FFA	Awad, Helgason, Weiss, Decker, & McClements (2009); Lacatusu, Mitrea, Badea, Stan, Oprea, & Meghea (2013); Salminen, Helgason, Kristinsson, Kristbergsson, & Weiss (2013).
Purified medium chain TAG (C8:0 e C10:0).	Jores, Mehnert, & Mäder (2003); Jores, Mehnert, Drechsler, Bunjes, Johann, & Mäder (2004); Jores, Haberland, Wartewig, Mäder, & Mehnert (2005); Severino, Andreani, Macedo, Fangueiro, Santana, Silva, & Souto (2012).
Sunflower oil	Hentschel, Gramdorf, Müller, & Kurz (2008); Leong, Man, Lai, Long, Misran, & Tan (2009).
Flaxseed oil	Kentish, Wooster, Ashokkumar, Balachandran, Mawson, & Simons (2008).
Purified oleic acid	Sharma, Ganta, Denny, & Garg (2009).

[a] TAG - Triacylglycerols; DAG – Diacylglycerols; MAG – Monoacylglycerols; C8:0 - Caprylic acid; C10:0 - Capryc acid; C14:0 - myristic acid; C18:0 - stearic acid; C22:0 - behenic acid; PUFA - polyunsaturated fatty acids; MUFA - monounsaturated fatty acids; SFA - saturated fatty acids; FFA - Free fatty acids; EPA - eicosapentaenoic acid; DHA - docosahexaenoic acid.

6.1. Liquid lipids

Low-melting point lipid components are usually employed in obtaining NLC. The medium-chain triacylglycerols (MCT) and oleic acid are the most common components in the development of this class of NLC (Jannin, Musakhanian, & Marchaud, 2008; Joseph & Bunjes, 2012).

Oleic acid - *cis-9-octadecenoic acid - C18:1 (9)* – is a constituent of most edible oils and fats. It exhibits crystallization at 4 °C and can be obtained by hydrolysis of vegetable

oils. It has a well-documented and established health benefit, as well as less susceptibility to oxidation when compared to linoleic and linolenic acids (Scrimgeour, 2005).

Edible vegetable oils such as canola, soybean and sunflower oil can be used for NLC production. The incorporation of these natural oils alters the crystallinity of the lipid matrix, and in general improves the solubility of the encapsulated components. These raw materials prove to be environmentally appropriate, are low cost, and as additional benefits may contain natural antioxidants that maximize the protection of inclusion compounds. However, the limited use of these oils results from their low oxidative stability (Liu & Wu, 2010; Nguyen, Hwang, Park, & Park, 2012). Therefore, the main liquid components used for the production of LN are oleic and triolein acid in the great majority of available studies (Aditya, Shim, Lee, Lee, Im, & Ko, 2013; Mojahedian, Daneshamouz, Samani, & Zargaran, 2013; Shangguan, Lu, Qi, Han, Tian, Xie, Hu, Yuan, & Wu, 2014), as well as soybean, corn and sunflower oil in LN specifically for application in foods (Liu & Wu, 2010; Hejri, Khosra, Gharanjig, & Hejazi, 2013; Asumadu-Mensah, Smith, & Ribeiro, 2013).

High oleic sunflower oil (HOSO) is considered a premium raw material, which was developed by Russian researchers from chemical mutagenesis and selective crosses of sunflower (*Helianthus annus*), seeking to obtain a stable seed variety for the climate conditions, and therefore with high oleic acid content (O'Brien, 2009). The typical HOSO composition is represented by 3-5% palmitic acid, 2-6% stearic acid, 75-88% oleic acid and less than 1% linolenic acid, which gives the oil ten times greater oxidative stability in relation to soybean oil and the regular sunflower oil itself. The HOSO has a neutral flavor and aroma, and has been used to obtain products of maximum toxicological safety and biodegradability in foods, cosmetics and pharmaceuticals (Gunstone, 2005; McKeon, 2005). These attributes indicate HOSO as a high-quality liquid lipid source to obtain NLC (Tamjidi, Shahedi, Varshosaz, & Nasirpour, 2013; Cerqueira, Pinheiro, Silva, Ramos, Azevedo, Flores-López, Rivera, Bourbon, Ramos, & Vicente, 2014).

6.2. Solid lipids

The solid lipid components employed in the preparation of LN consist mainly of TAGs, fatty acids, monoacylglycerols, diacylglycerols and waxes. The myristic, palmitic and stearic acids, in particular, are compatible with the lipid composition of animal tissues, and as

a consequence have been used as the preferred lipid matrix for the preparation of LN (Eltayeb, Bakhshi, Stride, & Edirisinghe, 2013). Stearic acid consists of an endogenous long-chain fatty acid, and represents a major component in natural oils and fats, with high biocompatibility and low toxicity. It has a melting point of approximately 70 °C and is considered neutral with respect to physiological fluids. From these aspects, both stearic acid and tristearin, or lipid mixtures rich in these components, are highly utilized raw materials for LN composition (Mensink, 2005; Severino, Pinho, Souto, & Santana, 2011; Eltayeb, Bakhshi, Stride, & Edirisinghe, 2013; Wang, Dong, Wei, Zhong, Liu, Yao, Yang, Zheng, Quek, & Chen, 2014). Natural waxes such as carnauba, candelilla and beeswax can also be used directly for the formulation of these structures. These materials are commercially available and are approved as GRAS for direct application in foods, in addition to being characterized by high stability against oxidation processes (Garzón, Vázquez, Vázquez, García, & Hernández, 2009).

6.3. Emulsifiers and co-emulsifiers

Emulsifiers are amphiphilic molecules that exhibit tensoactive properties, due to the presence of a polar (hydrophilic) moiety and an apolar (hydrophobic / lipophilic) moiety in the structure, allowing for actuation at the interface of immiscible substances. They are used in the production of nanoemulsions and LN, because they facilitate dispersion of the lipid matrices in water, reducing the surface tension between the aqueous phase and the oil phase (McClements & Rao, 2011).

The solubility of emulsifiers is characterized by their hydrophilic-lipophilic balance (HLB), an index ranging from 0 to 20, which allows for estimating the hydrophilicity of the emulsifier. The higher the HLB value, greater is its solubility in polar solvents, and the lower the HLB value the greater its affinity with apolar compounds (O'Brien, 2009; Bastida-Rodríguez, 2013).

Most emulsifiers, with the exception of lecithins which are phospholipids, are derived from mono- and diacylglycerols or from alcohols, where the classes most used in foods are: mono- and diacylglycerols, acetylated mono- and diacylglycerols, phosphated mono- and diacylglycerols, propylene glycol esters, sorbitan esters, sucrose esters, polyglycerol esters and lactate esters (O'Brien, 2009).

The emulsifiers can be divided into 3 types:

Ionic Emulsifiers: Most ionic food grade emulsifiers are negatively charged, for example, citric acid esters of monoglycerides (CITREM), diacetyl tartaric esters of fatty acids and glycerol (DATEM) and sodium lauryl sulfate (SLS). Only lauric alginate is positively charged and available for food application. Ionic emulsifiers can be used in the formation of nanoemulsions by low and high energy methods. However, in systems that depend on high concentrations of ionic emulsifiers, utilization may be limited because they may cause allergies (McClementes & Rao, 2011).

Non-ionic Emulsifiers: These are characterized by having hydrophilic groups without charges associated to the fatty acid chains. Examples used for the production of LN can be seen in Table 2. Non-ionic emulsifiers have been widely used for the formation of nanoemulsions by high and low energy methods. They present advantages in food applications because of their low toxicity and irritability (McClementes & Rao, 2011).

Zwitterionic emulsifiers: These have two or more ionizable groups of opposite charge in the molecule. The predominant behavior is dependent on the pH of the medium and may assume positive, negative or neutral charges. The major representatives of this class are phospholipids, substances considered GRAS, which allows for their wide use in foods (Table 2). However, natural phospholipids are inefficient in the formation and stabilization of nanoemulsions when used alone, but may be effective when used in combination with co-emulsifiers (McClementes & Rao, 2011).

In order to improve the efficiency of some emulsifiers, studies reported in literature cite the use of co-emulsifiers, also called co-surfactants (Salminen, Helgason, Kristinsson, Kristbergsson, & Weiss, 2013). Co-emulsifiers are molecules with polar moieties in the structure, such as alcohols and short chain organic acids that alter the physico-chemical characteristics of the emulsifiers. They are generally used to improve the flexibility of the interface of the emulsified systems. They act by promoting the increase in entropy at the oil-water interface, destabilizing the formation of crystalline structures, thus conferring higher viscosity to the systems (McClementes & Rao, 2011).

In studies related to obtaining LN for potential food applications several emulsifiers have been studied, as exemplified in Table 2, where the name, composition and source consulted can be found. These present general characteristics of toxicological safety for use in

foods, obtained from renewable sources and with high stability conferred to lipid nanostructures (Liu, Wang, & Xia, 2012; Dora, Putaux, Pignot-Paintrand, Dubreuil, Soldi, Borsali, & Lemos-Senna, 2012; Patel & Martin-Gonzalez, 2012; Lobato, Paese, Forgearini, Guterres, Jablonski, & Rios, 2013; Qian, Decker, Xiao, & McClements, 2013; Aditya, Shim, Lee, Lee, Im, & Ko, 2013; Carvalho, Noronha, Floriani, Lino, Rocha, Bellettini, Ogliari, & Barreto, 2013; Shangguan, Lu, Qi, Han, Tian, Xie, Hu, Yuan, & Wu, 2014; Choi, Aditya, & Ko, 2014).

Selection of the emulsifiers and their specific concentrations has a great impact on the quality of the LN. High emulsifier concentrations reduce surface tension and facilitate particle partitioning during the production process, promoting an important increase in surface area. The main characteristics affected are particle size and encapsulation efficiency (Awad, Helgaso, Kristbergsson, Decker, Weiss, & McClements, 2008; Souto, Severino, Santana, & Pinho, 2011).

In conventional emulsions, the emulsifier predominantly influences the particle size that can be obtained during homogenization and the stability of the dispersions, providing sufficient repulsive forces to prevent flocculation or coalescence of the systems. However, in LN the emulsifiers present a fundamental additional function, which consists of controlling the crystallization process of the lipid phase. Due to the small dimensions of the nanoemulsions, the number of lipid molecules interacting with the different functional groups of the emulsifiers is large enough for them to act as lipid phase crystallization modulators. Furthermore, the emulsifier may modify the crystallization kinetics and the natural polymorphic habit of the raw lipid materials used, avoiding recrystallization and destabilization problems of LN during storage and application (Weiss, Decker, McClements, Kristbergsson, Helgason, & Awad, 2008).

The different processes for obtaining LN require specific mixtures and concentrations of emulsifiers, incorporated into the lipid or aqueous phase. The optimum concentration of emulsifiers in the formulation is dependent on the lipid matrix used for composition of the nanoparticles. In general, the higher the concentration of emulsifiers, the greater the crystalline structure complexity of the LN. Additionally, different emulsifier compositions require specific homogenization parameters to obtain the highest degree of dispersion, due to the different velocities required to cover the new lipid surfaces formed. Preliminary tests considering the lipid materials used to obtain the LN, emulsifier composition

and concentrations, as well as evaluation of the LN production method, are therefore fundamental for the functionality, quality and applicability characteristics of nanoparticulate lipid systems (Helgason, Awad, Kristbergsson, Decker, McClements, & Weiss, 2009; Mehnert & Mäder, 2012).

There are few studies that address the use of emulsifiers as modifiers of the crystallization process, therefore its effects are still unclear and more studies are needed to elucidate the mechanisms of their actuation. Bunjes, Steiniger, & Richter (2007) reported that fully saturated long chain phospholipids (High Melting Point - HMP lecithins) delayed polymorphic transition from the metastable α form to the more stable β form in SLN composed of tristearin. The authors found that during the cooling process of the nanoemulsion containing SLN, lecithin which has a high melting point due to the presence of fully saturated TAGs chains, crystallized first, forming a solid monolayer around the lipid droplets. This layer served as a template for the crystallization of tristearin which occurred in the metastable α form, with the formation of concentric layers moving from the surface to the center of the SLN. It was observed that during the cold storage period (5-8 °C) the polymorphic transition to the β form occurred more slowly compared to SLN with HMP Lecithin. It is assumed that in this type of system the polymorphic transition is complicated because there is not enough space for molecular rearrangements. In this study, it was also observed that the β-form can be easily induced by increasing the storage temperature. Salminen, Helgason, Kristinsson, Kristbergsson, & Weiss (2013) also evaluated the influence of lecithins on the physical and chemical properties of NLC composed of tristearin with inclusion of omega 3 (ω-3) fatty acids. Oxidation of ω-3 was inhibited by 90% in NLC stabilized with high melting point lecithin compared to the use of low melting point lecithin. This effect was attributed to the induction of interfacial heterogeneous crystallization promoted by the high melting point lecithin, with consequent formation of a solid monolayer around the particles, avoiding expulsion and conferring protection to the encapsulated ω-3. The results showed that the fully saturated lecithin was the key component in control of the crystallization behavior, and thus allowed for the formation of nanoparticles stable to lipid oxidation.

Table 2. Emulsifiers and co-emulsifiers used in the production of Lipid Nanoparticles found in the literature

EMULSIFIERS	REFERENCE
Nonionic Emulsifiers	
Sorbitan monooleate	Bouchemal, Briançon, Perrier, & Fessi (2004); De Morais, Santos, Delicato, Goncalves, & Rocha (2006); Leong, Man, Lai, Long, Misran, & Tan (2009); Ramisetty, Pandit, & Gogate (2015).
Sorbitan monoestearate	De Morais, Santos, Delicato, Goncalves, & Rocha (2006); Robles, García, Garzón, Hernández, & Vázquez (2008).
Sorbitan monolaurate	De Morais, Santos, Delicato, Goncalves, & Rocha (2006); Pey, Maestro, Sole, Gonzalez, Solans, & Gutierrez, (2006).
Polyoxyethylene sorbitan monooleate	Bouchemal, Briançon, Perrier, & Fessi (2004); De Morais, Santos, Delicato, Goncalves, & Rocha (2006); Han, Li, Yin, Liu, & Xu (2008); Hentschel, Gramdorf, Müller, & Kurz (2008); Yuan, Chen, Du, Hu, Zeng, & Zhao (2007); Wooster, Golding, & Sanguansri (2008); Leong, Man, Lai, Long, Misran, & Tan (2009); Amani, York, Chrystyn, & Clark, (2010); Teo, Basri, Zakaria, Salleh, Rahman, & Rahman, (2010); Santos, Pereira, Bender, Colomé, & Guterres (2012); Zhang, Douglas, Guoxun, & Qixin (2013); Lacatusu, Mitrea, Badea, Stan, Oprea, & Meghea (2013); Ramisetty, Pandit, & Gogate (2015); Madureira, Campos, Fonte, Nunes, Reis, Gomes, Sarmento, & Pintado (2015).
Polyoxyethylene sorbitan monostearate	De Morais, Santos, Delicato, Goncalves, & Rocha (2006); Yuan, Chen, Du, Hu, Zeng, & Zhao (2007).
Polyoxyethylene sorbitan monopalmitate	Kentish, Wooster, Ashokkumar, Balachandran, Mawson, & Simons (2008).
Polyoxyethylene sorbitan monolaurate	Bouchemal, Briançon, Perrier, & Fessi (2004); Pey, Maestro, Sole, Gonzalez, Solans, & Gutierrez, (2006); De Morais, Santos, Delicato, Goncalves, & Rocha (2006); Awad, Helgaso, Kristbergsson, Decker, Weiss, & McClements (2008); Yuan, Chen, Du, Hu, Zeng, & Zhao (2007); Wang, Jiang, Wang,

	Huang, Ho, & Huang (2008); Awad, Helgason, Weiss, Decker, & McClements (2009); Mao, Xu, Yang, Yuan, Gao, & Zhao (2009); Yin, Chu, Kobayashi, & Nakajima (2009); Qian & McClements (2011); Badea, Lăcătus, Badea, Ott, & Meghea (2015).

Zwitterionic Emulsifiers[a]

Phospholipids (94% phosphatidylcholine; FAC: 12-17% C16:0, 2-5% C18:0, 11-15% C18:1, 59-70% C18:2 and 3-7% C18:3)	Bunjes, Steiniger, & Richter (2007).
Phospholipids (94% phosphatidylcholine; FAC: 12-16% C16:0, 85-88% C18:0, 2% C18:1 and 1 % C18:2)	Bunjes, Steiniger, & Richter (2007); Joseph, Rappolt, Schoenitz, Huzhalska, Augustin, Scholl, & Bunjes (2015).
Phospholipids (60% hydrogenated phosphatidylcholine; 10% hydrogenated lysophosphatidylcholine; FAC: 85% C18:0, 15% C16:0)	Salminen, Helgason, Kristinsson, Kristbergsson, & Weiss (2013).
Phospholipids (70% phosphatidylcholine; 8.5% phosphatidylethanolamine, 2.2% lysophosphatidylcholine; FAC: 17-20% C16:0, 2-5% C18:0, 8-12% C18:1, 58-65% C18:2, 4-6% C18:3, 0.1-0.2% DL-α tocopeherol)	Salminen, Helgason, Kristinsson, Kristbergsson, & Weiss (2013).

Co-emulsifiers

Sodium Taurodeoxycholate	Chakraborty, Shukla, Vuddanda, Mishra, & Singh (2010); Salminen, Helgason, Kristinsson, Kristbergsson, & Weiss (2013).
Sodium glycollate	Bunjes, Steiniger, & Richter (2007); Han, Li, Yin, Liu, & Xu (2008); Sharma, Ganta, Denny, & Garg (2009); Joseph, Rappolt, Schoenitz, Huzhalska, Augustin, Scholl, & Bunjes (2015).
Sodium Dodecylsulfate	Leong, Man, Lai, Long, Misran, & Tan (2009).

[a] FAC - Fatty acids composition; C16:0 - palmitic acid; C18:0 - stearic acid; C18:1 - oleic acid; C18:2 - linoleic acid; C18:3 - linolenic acid.

7. Properties of SLN and NLC

7.1. Mean diameter and polydispersity index

Mean diameter and particle size distribution, known as the polydispersity index (DPI), are important properties for LN characterization, reported in almost all studies involving the acquisition of these systems. Determination of the mean diameter is fundamental, mainly for scientific and technological reasons as in characterizing and confirming if the desired dimensions were obtained, and especially if they are maintained during storage or subsequent processing (Bunjes, 2005; McClements, 2013; Tamjidi, Shahedi, Varshosaz, & Nasirpour, 2013).

Control of the LN dimensions is essential since this parameter influences the physico-chemical and functional properties, as well as the potential application. Reduction of the mean diameter may promote increased translucency, viscosity, stability and bioavailability of the LN. Generally, this property is related to composition of the lipid matrix and the process used to obtain the LN.

According to McClementes & Rao (2011), lipid systems obtained via emulsification can be considered nanometric materials when they have a mean particle radii ≤ 100 nm. These authors use the mean diameter to characterize emulsions, nanoemulsions and microemulsions, due to several misunderstandings regarding the use of nomenclatures found in literature on these systems and application in LN. They clarified that the emulsion is a thermodynamically unstable system, with tendency for aggregation of particles over time. Characterized by mean radii of the particles in the range of 100 nm - 100 μm, they are cloudy and opaque, because they contain droplets similar in size to the wavelength of light. Systems containing particles with mean radii between 0.1 and 100 nm are considered nanoemulsions, often referred to as mini-emulsions in literature. The relatively low mean diameter, compared to the light wavelength, gives the nanoemulsions a tendency to be transparent or slightly cloudy. A very low mean diameter also indicates that these systems are much more stable to gravitational separation and aggregation of the particles. However, nanoemulsions are still considered thermodynamically unstable

The PDI is another factor related to physical stability of the LN. According to Tamjidi, Shahedi, Varshosaz, & Nasirpour (2013), in order to obtain suspensions with long-

term stability, the PDI values should be in the range of 0.1 - 0.25. Values above 0.5 indicate very broad particle size distribution, characterizing low physical stability.

7.2. *Zeta potential*

Colloidal particles generally exhibit surface charge, as a result of the availability of ionized groups or adsorption of ions from the dispersion medium. These surface charges and the force and extension of the electric field around the particles play a very important role in the mutual repulsion of the LN, and consequently in its electrostatic stability. Because the surface potential of the particles cannot be measured directly, the zeta potential - ZP (electric potential at the hydrodynamic shear surface around the colloidal particles) is generally determined as a characteristic parameter for the LN charge (Robles, García, Garzón, Hernández, & Vázquez, 2008). ZP values of approximately | 30 | mV characterizes colloidal systems with good stability, where ZP values are considered optimal when they are roughly | 60 | mV. The system is susceptible to destabilization between 5 and 30 mV and the occurrence of limited flocculation can be observed; and for ZP values smaller than 5 mV the system presents a great tendency for particle coagulation (Santos, Pereira, Bender, Colomé, & Guterres, 2012; Shah, Eldridge, Palombo, Harding, 2015; Badea, Lăcătus, Badea, Ott, & Meghea, 2015, Madureira, Campos, Fonte, Nunes, Reis, Gomes, Sarmento, & Pintado, 2015).

In the study of LN, determination of the ZP has been mainly used to obtain information about its dispersion behavior. It can also represent an indication of stability of the system, permitting formulation adjustments, and allows for accompanying the interaction behavior with different incorporated compounds. Changes in the ZP can be observed over time, being indicators of system destabilization, with consequent expulsions of the incorporated compounds during the storage period (Bunjes, 2005; Shah, Eldridge, Palombo, Harding, 2015).

Santos, Pereira, Bender, Colomé, & Guterres (2012) found that ZP values varied according to the emulsifying system used. The SLN were developed with an oil phase composed of cupuaçu butter and NLC composed of a mixture of cupuaçu butter and chestnut oil, using the emulsifiers soy lecithin and PSM 80. The ZP values for SLN and NLC in the presence of soy lecithin were - 50.6 ± 2.0 and - 66.4 ± 2.0 mV; when the emulsifiers were used together there was a change in ZP, with values of - 29.0 ± 1.5 and - 16.9 ± 1.0 mV, respectively. According to the authors, this reduction in ZP was expected, since the additional presence of

PSM 80, which is a non-ionic emulsifier and acts by steric stabilization, causes a reduction in the ZP conferred by soy lecithin due to modifications in the shear plane on the surface of the particles.

Madureira, Campos, Fonte, Nunes, Reis, Gomes, Sarmento, & Pintado (2015) also used PSM 80 in their studies, in which they developed SLN with lipid matrix composed of carnauba wax for incorporation of rosmarinic acid. The authors obtained ZP values ranging from - 37.5 to - 40.7 mV, indicating that high electrical repulsion reduces the risk of particle aggregation.

7.3. Crystallinity, polymorphism and stability

Lipid crystallization represents a fundamental issue for the performance of LN. Lipid materials are highly polymorphic, even in the dispersed state. In LN, the crystallization behavior of the matrix can exhibit distinct characteristics in comparison to the continuous system with identical fatty acids and TAGs composition, and polymorphic transitions are usually accelerated in nanostructured complexes (Bunjes, 2005). The degree of crystallinity and polymorphic modifications of lipids comprising LN represent fundamental factors for their development, since these parameters are strongly related to the incorporation capacity of bioactive compounds and release rates. In general, a decline is observed in the carrying capacity of the incorporated bioactive compounds according to the sequence of polymorphic transitions to higher stability crystalline forms (Mehnert & Mäder, 2012; Tamjidi, Shahedi, Varshosaz, & Nasirpour, 2013; Joseph, Rappolt, Schoenitz, Huzhalska, Augustin, Scholl, & Bunjes, 2015).

Stability of the LN should be considered based on two different perspectives related to the behavior of matrix crystallization and particle size distribution (Sharma, Diwan, Sardana, & Dhall, 2011). The relationship between crystalline modification and the incorporated compound exhibits additional influence of interactions between lipids and the emulsifiers used. Additionally, the crystalline structures may be subject to interference from other factors, such as heating and cooling rates, storage temperature and especially the materials used in the formulation, such as liquid and solid lipids, emulsifiers, dispersion medium and bioactive compound, as well as interactions among them (Bunjes & Unruh, 2007).

During storage, rearrangement of the crystalline lattice may occur to the state of greatest stability, and these transitions are generally associated with expulsion of a fraction of

the incorporated active compound. In general, lipid crystals present greater mobility in thermodynamically unstable configurations. Therefore, these configurations show lower crystalline density, and as a result, greater capacity for incorporation of external molecules. The occurrence of polymorphic transformations is usually accompanied by changes in morphology of the LN, namely from spherical forms to the flattened forms, for example platelet forms. The efficacy of nanostructured lipid systems is therefore determined by modifications of the characteristic crystal lattice of a specific set of TAGs (Helgason, Awad, Kristbergsson, Decker, McClements, & Weiss, 2009). In this sense, maintaining the EE and CC parameters resides mainly in the development of strategies to prevent crystalline modifications during the storage of LN. In addition to control of the transitions between the forms α, β' and β, several sub-forms and their interactions with the different emulsifiers should be considered in stability studies of the LN (Souto, Severino, Santana, & Pinho, 2011; Mehnert & Mäder, 2012, Joseph, Rappolt, Schoenitz, Huzhalska, Augustin, Scholl, & Bunjes, 2015). Additionally, in the LN post-crystallization processes the phenomena recognized as agglutination of adjacent surfaces or sintering can be verified, as well as the spontaneous dissolution of specific TAGs, known as Ostwald ripening (Himavan, Starov, & Stapley, 2006; Wu, Zhang, & Watanabe, 2011).

With respect to particle size distribution, the flocculation process, characterized by the association of nanoparticles that maintain their individual integrity, can cause a pronounced increase in the viscosity of the dispersions, which generally results in gelation of the LN (Weiss, Decker, McClements, Kristbergsson, Helgason, & Awad, 2008; Robles, García, Garzón, Hernández, & Vázquez, 2008; Sharma, Diwan, Sardana, & Dhall, 2011).

Considering SLN composed of tripalmitin and polyoxyethylene sorbitan monolaurate (PSM), Awad, Helgaso, Kristbergsson, Decker, Weiss, & McClements (2008) studied the impact of the cooling and heating rates on polymorphic transformations, aggregation and gelatinization of the LN, and verified that increased magnitude of these parameters delayed the α→β transition, i.e., a shorter time for the metastable crystalline structure to rearrange in the most stable form, promoting greater SLN stability. The SLN characterized by the initial α form were spherical and totally covered by the emulsifier; the transformation to the β form, however, modified the SLN morphology as well as the spatial distribution of the emulsifier, resulting in aggregation of the particles by hydrophobic interactions.

Attama & Muller-Goymann (2008) reported the preparation of SLN from beeswax and animal fat. No increase in the degree of crystallinity of the LN was observed during storage; however, the presence of animal fat decreased the crystalline organization. Nik, Langmaid, & Wright (2012) found that the polymorphic habit of SLN was affected by the emulsifier in the composition.

Qian, Decker, Xiao, & McClements (2013) studied the impact of the lipid composition on the physical state and physical-chemical properties of nanostructures containing incorporated β-carotene. An increase in the concentration of unsaturated fatty acids in the structures resulted in greater stability for aggregation and degradation of β-carotene.

Choi, Aditya, & Ko (2014) evaluated the effect of pH and electrolyte concentration of the medium in simulation of the properties of a food matrix, on evolution of the structure, polymorphism and stability of SLN produced with high melting point TAGs and with sorbitan monooleate as an emulsifier. The authors observed that development of the SLN structure was dependent on the polymorphic transition $\beta' \rightarrow \beta$, and that the particle crystallinity decreased with increasing pH and with the electrolyte content in the medium, in the same way as the rate of recrystallization of the LN.

7.4 Morphology and ultrastructure

Morphology of the LN is highly variable. Spherical particles provide greater potential for controlled release and protection of bioactive compounds, with longer diffusion pathways and less contact with aqueous media. Additionally, they require smaller emulsifier quantities for stabilization, due to minimization of the specific surface area. However, anisometric particles may present advantages when the bioactive compounds are incorporated into the emulsifier layer. Emulsifiers that act with stabilizing function demonstrate the ability to form additional colloidal structures, such as vesicles or micelles, through a self-assembly process. These structures contain lipophilic domains that may represent alternative compartments for localization of the bioactive compound. As a consequence, their presence may affect the incorporation and release properties of bioactive compounds (Yoon, Park, & Yonn, 2013). Thus, knowledge on the morphology of the LN is of great importance for the characterization of these systems, since it can directly affect the PI of the particulate systems (Bunjes, 2005).

7.5. Encapsulation efficiency and charge capacity

The encapsulation efficiency (EE) is defined as the ratio between the fraction of the bioactive compound in the LN and the total bioactive compound incorporated in the initial lipid phase (Liu & Wu, 2010; Sharma, Diwan, Sardana, & Dhall, 2011). The EE parameter can be determined after quantification of the free or incorporated fraction of the compound of interest in the LN (Nguyen, Hwang, Park, & Park, 2012). The EE value influences the release properties of the LN and depends on the formulation components and the production method used (Tamjidi, Shahedi, Varshosaz, & Nasirpour, 2013). The EE values reported in literature are generally between 75 and 100% for different lipid materials evaluated, forms of obtaining the LN and bioactive compounds carried (Liu, Wang, & Xia, 2012; Lobato, Paese, Forgearini, Guterres, Jablonski, & Rios, 2013; Aditya, Shim, Lee, Lee, Im, & Ko, 2013; Carvalho, Noronha, Floriani, Lino, Rocha, Bellettini, Ogliari, & Barreto, 2013; Shangguan, Lu, Qi, Han, Tian, Xie, Hu, Yuan, & Wu, 2014).

The charge capacity (CC) of LN can be defined as the ratio of the incorporated bioactive compound in relation to the initial lipid phase. This parameter is predominantly influenced by the preferential polymorphic habit of the lipid system used, by the solubility of the compound incorporated in the lipid matrix in the liquid state, and by the physical structure of the LN (Robles, García, Garzón, Hernández, & Vázquez, 2008; Nguyen, Hwang, Park, & Park, 2012).

8. Characterization of LN

8.1 Laser Diffraction and Photon Correlation Spectroscopy

The analytical methods commonly used to determine the mean diameter and PDI are dynamic light scattering (DLS), also known as photon correlation spectroscopy (PCS), and laser diffraction (LD). DLS/PCS measures the fluctuation of intensity of the scattered light as a result of Brownian motion of the particles. LD is based on the diffraction angle of the focused laser, which is directly related to the mean diameter of the particles in the suspension. The combined use of light beams with different wavelengths allows for measurements ranging from nanometers up to a few millimeters, encompassing a larger spectrum of average particle sizes. It is recommended to use the two techniques for better characterization of the system and to avoid misunderstandings, since these methods do not directly measure the particle size but

rather the light scattering, which is used to calculate the mean diameter (Robles, García, Garzón, Hernández, & Vázquez, 2008; Wu, Zhang, & Watanabe, 2011; Yoon, Park, & Yonn, 2013).

Ghosh, Saranya, Mukherjee, & Chandrasekaran (2013) developed nanoemulsions composed of oil extracted from basil leaf and PSM 80 obtained by ultrasound at the proportions of 1:1, 1:2, 1:3 and 1:4, and by LD obtained a mean diameter and PDI of 41.15nm and 0.09, 31.65 nm and 0.2, 29.6 nm and 0.2, and 29.3 nm and 0.2, respectively. Leong, Man, Lai, Long, Misran, & Tan (2009) produced O/W emulsions by ultrasound for 20 minutes, composed of 15 % sunflower oil and 5.6 % PSM 80, sorbitan monooleate (SM 80) and SDS as a co-emulsifier. They evaluated the average diameter by LD and obtained particles up to 40nm.

8.2. Differential Scanning Calorimetry

Differential scanning calorimetry (DSC) is the thermoanalytical technique most used in the study of lipid materials and allows for evaluating the thermal behavior of lipid matrices used in the composition of LN, providing information on the crystallization and fusion pattern of lipid constituents of the LN (Jannin, Musakhanian, & Marchaud, 2008). It is used in evaluation of the thermal behavior when adding other compounds in the lipid phase, such as emulsifiers and bioactive compounds, and for study of the thermal behavior of suspended LN in the aqueous phase after the production and drying processes, and during storage and its application (Bunjes & Unruh, 2007). Moreover, with this technique it is possible to carry out the complementary investigation of the recrystallization behavior of the lipid materials, using the melting curves obtained in function of the LN storage time. Additionally, the degree of ordering of the lipid structures in the SLN and NLC can be directly associated with the enthalpy values obtained in the different fusion events (Bunjes & Unruh, 2007; Patel & Martin-Gonzalez, 2012). It is recommended to study the specific melting and crystallization events of the raw materials in their isolated form, of the continuous lipid phase and the LN itself, which in general have different thermal behaviors in relation to the original lipid matrix, for example a lower melting point due to the extremely small dimensions (Mehnert & Mäder, 2012).

Awad, Helgaso, Kristbergsson, Decker, Weiss, & McClements (2008) used this technique to evaluate the raw materials and SLN with regards to the crystallization behavior in heating and cooling cycles. The SLNs were made with 10% tripalmitin and 1.5%, obtained by emulsification in hot HPH. The SLNs were maintained in suspension at 37 °C and analyzed by

DSC. According to this method the authors could predict the polymorph formed and observe that the crystallization behavior of the lipid phase is different after the nanoscale emulsification process. The mixture of tripalmitin and PSM crystallized at higher temperatures (39 °C) than SLNs developed with these materials (19 °C). The authors suggested that in SLN, where the lipid phase is distributed as suspended droplets, more energy is necessary to promote nucleation and crystallization of the lipids compared to the bulk mixture. Thus, in the lipid matrix crystallization occurs via the heterogeneous nucleation process, where the presence of catalytic impurities is considered, favoring the quicker initial of crystallization. However, in SLN the lipids are in the form of droplets, distributed on the nanoscale in the emulsion. The authors considered that crystallization is made more difficult because the probability of finding impurities in the droplets is very low, and because this occurs only in individual droplets it is not propagated as occurs in the bulk blend, requiring the use of lower temperatures to promote nucleation and crystallization in LN. Additionally, from the thermal behavior the authors could infer about the polymorphic forms, and observed that for the LN the polymorphic form α was quickly transformed into β, which was not observed in the bulk blend, confirming that the crystallization behavior of the LN is differentiated.

8.3. X-Ray Diffraction

X-ray diffraction is used to determine the identity of crystalline solids based on their atomic structure. Due to the different geometric configurations, the polymorphs diffract X-rays at different angles. X-ray diffraction can be performed in wide-angle X-ray scattering (WAXS) and small-angle X-ray scattering (SAXS). In lipids, WAXS diffractions correspond to the short-spacings of the subcells and allow for verifying the different polymorphs, and SAXS diffractions correspond to the long spacings, and are used to determine the structure of the asymmetric lipid bilayer in unilamellar vesicles (Campos, 2005; Ribeiro, Basso, Grimaldi, Gioielli, & Gonçalves, 2009). In addition, it is possible to obtain such information simultaneously and still use temperature variations over time to monitor polymorphic transitions at certain rates of cooling and heating, with the aid of a DSC coupled to the synchrotron light source via the synchrotron radiation X-ray diffraction (SR-XRD) technique known as DSC/XRDT (Takeuchi, Ueno, & Sato, 2003; Joseph, Rappolt, Schoenitz, Huzhalska, Augustin, Scholl, & Bunjes, 2015).

X-ray diffraction is a fundamental tool for the characterization of crystalline modifications in continuous or particulate lipid systems, and allows for differentiation of amorphous and crystalline LN as well as different polymorphic phases related to the stability study of nanostructured lipid systems (Bunjes & Unruh, 2007; Dion, Ruud, Saskia, & Hans, 2008; Wu, Zhang, & Watanabe, 2011).

8.4. Microscopic Techniques

Analytical resources involving the use of microscopy are important tools for the investigation of morphology, mean size and size distribution of the LN. Polarized light microscopy (PLM), although not sensitive to nanometric dimensions, provides indications regarding the presence of possible microparticles or nanoparticle agglomerates with microdimensions. According to Klang, Matsko, Valenta, & Hofer (2012), scanning electron microscopy (SEM) and transmission electron microscopy (TEM) are essential tools for obtaining information about the basic structural properties of nanoscale systems. SEM, in contrast to methods for determining the particle size distribution, promotes direct identification of the LN morphology, with three-dimensional and surface information (Luykx, Peters, Ruth, & Bouwmeester, 2008). Transmission electron microscopy (TEM) can be used to study the size, shape and internal structure of LN, via two-dimensional images with resolution power close to 0.4 nm, allowing for the identification of colloidal domains that characterize the ultrastructure of the LN (Luykx, Peters, Ruth, & Bouwmeester, 2008; Klang, Matsko, Valenta, & Hofer, 2012). However, these techniques present some limitations related to the direct measurement with electron beams that can damage the LN structure, as well as preparation of the sample for analysis, where it must be dry in the form of powder or film (Domingo & Saurina, 2012; Klang, Matsko, Valenta, & Hofer, 2012). Klang, Matsko, Valenta, & Hofer (2012) highlighted that in order to obtain representative images, both in SEM and in TEM, cryogenic methods (cryo) must be used for sample preparation. Furthermore, the analyses must be performed in equipment with specific conditions for Cryo-SEM and Cryo-TEM. Thus, it is possible to investigate lipid systems under conditions close to preparation and/or application, without the need for heat treatment which may compromise the structure of the LN or even induce undesired polymorphic transitions. Another method used in characterization of these systems is Atomic Force Microscopy (AFM), also recommended for the study of morphology,

size, stability and dynamic processes of LN (Luykx, Peters, Ruth, & Bouwmeester, 2008). Most AFM equipment does not require sample treatment and is compatible with liquid media and atmospheric conditions. Thus, it can provide real information of the lipid systems in three dimensions, with resolution close to 1 nm (Domingo & Saurina, 2012; Tamjidi, Shahedi, Varshosaz, & Nasirpour, 2013).

8.5. *Nuclear Magnetic Resonance*

Study of the coexistence of colloidal structures, such as typical micelles, inverses and liposomes, as well as super-cooled fusions constituted of liquid lipid domains, undesirable in LN, should be considered in the complete characterization of LN. The analytical techniques that meet these requirements include nuclear magnetic resonance (NMR), where active nuclei (1H, 13C, 9F and 31P) of interest are associated with the identification of specific molecules or their segments, as well as the distinction between physical states of lipid components, allowing for differentiation of lipid structures and detection of liquid nanocompartments. The other technique is electronic spin resonance (ESR), a spectroscopic technique that detects species containing unpaired electrons, i.e., paramagnetic species, providing important information regarding the microviscosity and micropolarity of the LN. This tool allows for monitoring the possible expulsion of the bioactive compounds from the LN, as well as measuring the distribution of these compounds between the LN and the non-particulate colloidal structures (Bunjes, 2005; Haskell, 2006; Dion, Ruud, Saskia, & Hans, 2008). It should be noted that both techniques are non-destructive and sensitive to the simultaneous detection of different colloidal species. In recent studies, Yucel, Elias & Coupland (2013) used the ESR technique to evaluate the performance of LN stabilized by sodium caseinate. Berton-Carabin, Coupland, & Elias (2013) investigated the distribution and chemical reactivity of molecules with different degrees of lipophilicity in SLN.

8.6. *Complementary techniques*

Characterization of the chemical stability of bioactive compounds represents an essential step for performance evaluation of the LN, for various applications. In addition, the quantification of these components is fundamental for determination of the EE and CC parameters. The instrumental techniques for these purposes are quite variable according to the incorporated bioactive compound. In general, high performance liquid chromatography

(HPLC), gas chromatography (GC) and ultraviolet/visible spectroscopy (UV/VIS) are very useful for the evaluation of compounds incorporated into LN (Jannin, Musakhanian, & Marchaud, 2008).

9. Functional lipophilic compounds

The incorporation of functional lipophilic components is highly relevant when the carrier systems can be obtained from LN, such as SLN and NLC, due to physicochemical interactions favorable to the acquisition of high stability nanostructured systems with important applications in the areas of food, medicine, cosmetics and pharmaceuticals. Bioactive lipids differ widely in their molecular properties (molecular weight, structure, functional groups, polarity and charge), which results in differences in their physico-chemical and physiological properties, such as solubility, physical state, rheological properties, chemical stability and bioactivity. Therefore, each carrier system for these compounds is characterized by specific properties (McClements, Decker, Park, & Weiss, 2009). In terms of bioactivity, the main functional lipophilic compounds are carotenoids, liposoluble antioxidants (tocopherols and polyphenols), liposoluble vitamins and phytosterols, which have been the focus of recent studies on nanotechnological applications (Mozafari, Flanagan, Matia-Merino, Awati, Omri, Suntres, & Singh, 2006; Huang, Yu, & Ru, 2010; Tamjidi, Shahedi, Varshosaz, & Nasirpour, 2013; Nakajima, Wang, Chaudhry, Park, & Juneja, 2015; Badea, Lăcătus, Badea, Ott, & Meghea, 2015).

9.1. Carotenoids

Carotenoids comprise a diverse group of lipophilic compounds which impart a yellow and red coloration to many foods. They are also bioactive substances, with beneficial effects to health, and some present pro-vitamin A activity (Kamal-Eldin, 2005). Health benefits attributed to carotenoids include immunomodulation and reduced risk of contracting chronic degenerative diseases such as cancer, cardiovascular disease, cataracts and age-related macular degeneration. These physiological activities have been attributed to its antioxidant properties, specifically to the ability to sequester singlet oxygen and interact with free radicals. Endogenous carotenoids in foods are generally stable. However, as additives in food systems these components are relatively unstable as a result of susceptibility to light, oxygen and auto-oxidation processes. They are further characterized by low solubility in water, which affects

their bioavailability. Consequently, the dispersion of carotenoids in processed foods may result in their rapid degradation. An additional challenge for carotenoid incorporation in food results from its high melting point, associated with its crystalline state at body and storage temperatures (Ribeiro & Schubert, 2003; Qian, Decker, Xiao, & McClements, 2012). Thus, the use of nanostructures shows a promising and differentiated alternative for carotenoid carrying and protection in food systems (Mozafari, Flanagan, Matia-Merino, Awati, Omri, Suntres, & Singh, 2006; Weiss, Takhistov, & McClements, 2006).

In this context, several studies have focused on the development and application of nano-structured lipid systems containing carotenoids as bioactive compounds. Tan & Nakajima (2005) studied the preparation of β-carotene nanodispersions for food application, obtained by the emulsification-evaporation process, with stability evaluated at 4 °C. The mean diameter of the particles ranged from 60 to 140 nm, and showed great influence on the degradation of β-carotene, evaluated by HPLC. Helgason, Awad, Kristbergsson, Decker, McClements, & Weiss (2009) evaluated the impact of emulsifier properties on the stability of *β*-carotene incorporated into SLN and NLC structures. Liu & Wu (2010) studied the development of NLC composed of tripalmitin and corn oil, for inclusion of lutein, using response surface methodology. Mitri, Shegokar, Gohla, Anselmi, & Müller (2011) obtained SLN and NLC for incorporation of lutein, with dimensions between 150 and 350 nm, and a formulation containing 9% lipids. The characteristic mean diameter decreased with increase of the proportion of liquid oil in the lipid matrices. The development of LN from bixin, composed of TAGs of capric and capric acids, was reported by Lobato, Paese, Forgearini, Guterres, Jablonski, & Rios (2013) who sought its application in low lipid content foods. The physical stability of the LN was evaluated for 120 days at room temperature, and showed favorable results for incorporation in processed foods with long shelf life. In a study related to the impact of lipid composition on the physicochemical properties of SLN with β-carotene incorporation, Qian, Decker, Xiao, & McClements (2013) verified that higher levels of saturated fatty acids resulted in greater stability for aggregation and degradation of the incorporated component. Nik, Langmaid, & Wright (2012) studied the incorporation of β-carotene into SLN, produced with 10% lipid phase and observed chemical stability during 90 days. Zhang, Douglas, Guoxun, & Qixin (2013), with the objective of preparing NLC for application in functional beverages, used anhydrous milk fat to incorporate carotenoids. Hejri, Khosra, Gharanjig, & Hejazi (2013) optimized the LN formulation for

carrying of β-carotene by using the response surface methodology. The lipid phases were evaluated with concentrations of up to 40% in relation to the total formulation, consisting of palmitic acid and corn oil, which showed a significant effect on the mean diameter of the NLC obtained.

9.2. Tocopherols

Vitamin E is chemically represented by eight different compounds that make up the tocol group, which includes tocopherols and tocotrienols (Wanasundara & Shahidi, 2005). These substances are nonpolar, basically existing in the lipid phase of foods. The action of vitamin E as an antioxidant for the human organism is of extreme importance, where tocopherols are naturally present in cell membranes, acting as a protection factor against endogenous and exogenous oxidation. Literature reports the protection of LDL (Low density lipoprotein) against oxidation by the action of vitamin E, which interferes in the occurrence of cardiovascular diseases. The potential of this vitamin is evaluated for various diseases related to oxidative stress, such as endometriosis, in addition to stimulating cells of the immune system (Mozafari, Flanagan, Matia-Merino, Awati, Omri, Suntres, & Singh, 2006). All tocopherols and tocotrienols are absorbed in the intestine and transported to the liver via chylomicrons. However, α-tocopherol is preferably used. This is due to the presence of specific proteins present in the liver, receptors of tocopherols, with affinity to α-tocopherol and its stereoisomers. For recommendation in diets, only α-tocopherol, including synthetic stereoisomers or natural mixtures containing this compound, are referred to as vitamin E (Kamal-Eldin, 2005).

Because of the antioxidant function of tocopherols and tocotrienols, storage-associated processing may promote significant changes in vitamin E levels in foods. Furthermore, insolubility in water, a characteristic of these compounds, makes it difficult to incorporate them into various food formulations. The use of LN may provide the food industry with significant potential for increasing the solubility, stability and bioavailability of tocopherols, mainly represented by α-tocopherol (Mozafari, Flanagan, Matia-Merino, Awati, Omri, Suntres, & Singh, 2006; Weiss, Takhistov, & McClements, 2006).

Recent studies have reported the incorporation of tocopherols into LN systems. The α-tocopherol can be used as a liquid lipid matrix in the production of NLC nanoparticles (Tamjidi, Shahedi, Varshosaz, & Nasirpour, 2013). It may be present in the concentrated form

(isolated from vegetable oils) or via addition of the oil containing it, such as soybean, sunflower, canola and other oils (Oliveira, Valentim, Goulart, Silva, Bechara, & Trevisan, 2009). In addition to the use of α-tocopherol as liquid lipid constituent of the NLC matrix, it can be used to minimize deterioration of the bioactive lipid compound to be incorporated in the LN, since it is responsible for the inhibition of lipid autoxidation (Oliveira, Valentim, Goulart, Silva, Bechara, & Trevisan, 2009).

Preparation of LN for *β*-tocopherol transport was evaluated by Relkin, Yung, Kalnin, & Ollivon (2008). The joint evaluation by DSC and X-ray diffraction indicated the formation of crystalline globular structures at 20 °C, with adequate protection against degradation. Encapsulation of tocopherols in nanostructured colloidal systems was evaluated by Ziani, Fang, & McClements (2012), who suggested that the extent of tocopherol protection is dependent on the nature of the liquid lipid phase of the formulation. SLN were employed by Abuasal, Lucas, Peyton, Alayoubi, Nazzal, Sylvester, & Kaddoumi (2012) in a model system to verify the increase in γ-tocotrienol bioavailability, for evaluation of possible anticarcinogenic potential. The authors concluded that the dose corresponding to $10 mg.kg^{-1}$ of SLN showed an expressive increase in the oral bioavailability of this compound. Carvalho, Noronha, Floriani, Lino, Rocha, Bellettini, Ogliari, & Barreto (2013) reported the development of SLN composed of glyceryl behenate, using response surface methodology to maximize α-tocopherol inclusion. The optimized condition for the study resulted in SLN with a mean diameter close to 215 nm and ZP value equal to – 41.9 mV, with EE greater than 75.5 %, corresponding to structures containing crystals with the α and β' polymorphs.

9.3. Omega-3 fatty acids

Omega-3 fatty acids (*ω*-3) are considered bioactive compounds that can confer several health benefits, such as anti-inflammatory action directly related to the prevention of cardiovascular diseases. They belong to the groups of polyunsaturated essential fatty acids, such as eicosapentaenoic acid (EPA) and docosahexaenoic acid (DHA) (Rubio-Rodríguez, Jaime, Diego, Sanz, & Carballid, 2010). The *ω*-3 fatty acids are not metabolized by the body, requiring that they are ingested in the diet (Conto, Grosso, & Gonçalves, 2013). Consequently, there is great interest in the food industry to develop functional foods that contain ω-3, since its application in foods is quite limited by the high oxidative instability which gives unpleasant

flavours to the products (Cho, Shim, & Park, 2003). Therefore, effective strategies must be developed to encapsulate and protect ω-3 against oxidation during production, packaging, storage, transport and sale (Awad, Helgason, Weiss, Decker, & McClements, 2009).

Studies reported in literature indicate that the use of ω-3 presents viable crystallization, polymorphism and stability characteristics for LN application. Salminen, Helgason, Kristinsson, Kristbergsson, & Weiss (2013) evaluated the influence of the emulsifying properties of low- and high-melting point soybean lecithin regarding the physical and chemical stability of NLC containing tristearin and fish oil ω-3. The results indicated that the presence of high melting point soybean lecithin delayed the oxidation of ω-3 by 90%, allowing the formation of physically stable and oxidation resistant NLC. Lacatusu, Mitrea, Badea, Stan, Oprea, & Meghea (2013) developed NLC with ω-3 from fish oil for lutein carrying. The NLC showed to efficiently retain lutein (88.5%) and provide antioxidant protection *in vitro* (98.0%), with a better sustained release profile of lutein compared to conventional nanoemulsions. Awad, Helgason, Weiss, Decker, & McClements (2009) evaluated the effect of ω-3 in tripalmitin SLN in suspension. The results demonstrated that ω-3 was successfully incorporated into SLN in suspensions, in addition to increasing the stability against particle aggregation. Crystallization, melting and polymorphism were influenced by the presence of ω-3 30% incorporated in the lipid matrix, with acceleration in the polymorphic transition of lipid crystals from the forms α to β. Holser (2012) evaluated the incorporation of EPA and DHA into SLN composed of different purified TAGs, with favorable results regarding the inhibition of lipid oxidation and stability against degradation in aqueous systems. Salminen, Helgason, Kristinsson, Kristbergsson, & Weiss (2013) developed NLC based on tristearin and fish oil. The authors concluded that modulation of the crystallization behavior of nanostructures is fundamental for the protection of ω-3, and that rapid solidification of the outer lipid layer constituting the LN presents a limiting effect on the diffusion of these fatty acids to the surface, minimizing oxidative processes.

9.4. Phytosterols

Sterols are triterpenic monoalcohols that can be classified according to their origin, such as animal sterols (cholesterol) or vegetable sterols (phytosterols). Phytosterols comprise most of the unsaponifiable fraction of most edible oils and fats, and are present in greatest

quantity as β-sitosterol, campesterol and stigmasterol (Leong, Man, Lai, Long, Misran, & Tan, 2009; Izadi, Nasirpour, & Garousi, 2012).

Phytosterols are considered functional compounds, mainly because of the mechanism of action in reducing the absorption of cholesterol in the intestine. The bioactivity of phytosterols resides in the fact that they have molecular structures very similar to cholesterol, and compete with cholesterol absorption sites in the intestine, reducing its absorption (Nichols & Sanderson, 2003; Leong, Man, Lai, Long, Misran, & Tan, 2009). Several studies have shown that ingestion of 1.5 to 3g of phytosterols per day as an additive or food ingredient decreases cholesterol absorption and reduces LDL-cholesterol levels by approximately 8-15% in the blood (Fernandes & Cabral, 2007; Leong, Man, Lai, Long, Misran, & Tan, 2009).

This functionality has led to great interest in the development of foods enriched with phytosterols. However, its insolubility in water and high melting point (120-140°C) make it difficult to incorporate free phytosterols into foods (Nichols & Sanderson, 2003). An alternative to increase the solubility of phytosterols is the esterification process with fatty acids. Studies have shown that esterified phytosterols exhibit lower absorption when compared to free-form phytosterols (McClements, Decker, & Weiss, 2007). Originally, esterified phytosterols have been added to high fat foods, for example margarines, where solubilization and dispersion are relatively simple. But for incorporation in foods with high water content, it is necessary to develop mechanisms capable of maintaining the phytosterols in suspension, submitting them to the emulsification process or transporting them in LN and/or liposomes.

10. LN for food applications

The application of LN in food must follow some fundamental requirements, such as compatibility with the food to which it will be incorporated, and absence of adverse effects on appearance, aroma, flavor, texture and shelf life. The incorporated bioactive compound must be protected by the LN against degradation during all stages of processing, storage, transport and use. The obtained nanostructures must then be able to control the rate of release of the functional agent at a specific site, and/or in response to a specific environmental stimulus, such as variations in pH, ionic strength and temperature (McClements, Decker, & Weiss, 2007).

Hentschel, Gramdorf, Müller, & Kurz (2008) studied NLC composed of sunflower oil and propylene glycol monostearate (PGMS) for incorporation of β-carotene, to be applied

in functional beverages. The authors obtained LN in the crystalline form α and verified during 30 weeks that the LN remained stable, because no polymorphic transitions occurred. Trujillo & Wright (2010) evaluated the stability and crystallization properties and melting behavior of SLN obtained when using canola stearin, with variable mean diameter in function of the emulsifier concentration and homogenization pressure during 240 days. Nik, Langmaid, & Wright (2012) studied this same lipid matrix for the incorporation of β-carotene into SLN. The authors verified that the polymorphic habit of the LN obtained was affected by the type of emulsifier, obtaining LN with all crystals in the β form and LN with mixtures of crystals in the *β'* and *β* forms. Holser (2012) and Qian, Decker, Xiao, & McClements (2013) produced and evaluated LN obtained with palm oil and cocoa butter for incorporation of EPA/DHA and carotenes, respectively, with excellent results regarding stability and oxidative protection. Asumadu-Mensah, Smith, & Ribeiro (2013) used carnauba wax, candelilla wax and sunflower oil for high melting-point LN composition. Crystal structures were obtained in platelet and needle forms, with melting and crystallization temperatures lower than the corresponding initial mixtures, presenting good crystallinity characteristics for inclusion of lipophilic components. In order to evaluate different lipid matrices for NLC composition. Zheng, Zou, Yang, Liu, Xia, Ye, & Mu (2013) studied LN obtained from mixtures containing hydrogenated sunflower and rapeseed oils, palm oil and its stearin, as well as soybean oil. The mean diameter was significantly affected by the composition of the lipid mixture, for structured systems containing up to 20% of the lipid phase, with good stability properties for the incorporation of conjugated linoleic acid. Shilei, Rui, Guodong, & Qiang (2014) developed NLC with flavonoids (quercetin), using caprylic and capric acid, glyceryl monostearate and glyceryl monolaurate, and applied them in model beverages. They found that NLC showed high efficiency of flavanoid incorporation (93.5 %), remaining stable during 60 days of storage. The NLC were also evaluated after addition in a beverage formulation at pH 3.4, maintained at three different temperatures (4, 25 and 40 °C) for 60 days. An increase in the mean particle diameter was observed only during the first 15 days. Madureira, Campos, Fonte, Nunes, Reis, Gomes, Sarmento, & Pintado (2015) developed SLN using carnauba wax as a lipid matrix for carrying rosmarinic acid, a polyphenol with reported biological activities, including antioxidant, antimutagenic, anti-bacterial and anti-viral capacities. The efficiency of the emulsifier PSM 80 on the system was evaluated, and the authors emphasized the lipid concentrations of 1.0 and

1.5% with 2% (w/w) of the emulsifier as those most effective for stability and rosmarinic acid release during 28 days of storage under refrigeration. Zhu, Zhuang, Luan, Sun, & Cao (2015) prepared an NLC composed of palm stearin and soy lecithin emulsifier to carry Antarctic Krill, an oil rich in EPA, DHA and the carotenoid astaxanthin. The NLC were added to model beverages with pH 3.4. The NLC and NLC-containing beverages were stored for 10 days at different temperatures (4, 25 and 40 °C) and evaluated with regards to mean particle diameter. The results obtained demonstrate that the NLC stored at 4 °C were more stable compared to those stored at room temperature. However, when evaluating the beverages containing the NLCs, it was observed that the mean particle diameter remained more stable in the beverages stored at room temperature.

11. Toxicological and regulatory aspects

Lipids are easily absorbed into the body at the nanoscale, promoting the uptake of active compounds through rapid absorption into the GIT. However, this rapid and efficient absorption of compounds at the nanoscale, due to the increase in surface area, generates some discussion points about undesirable effects in the organism. However, questions of this nature exist not only for LN but for all materials at the nanometric scale, mainly due to the fact that the behavior is differentiated in relation to materials on a macro scale (Sozer & Kokini 2009; Blasco & Picó, 2011; Severino, Andreani, Macedo, Fangueiro, Santana, Silva, & Souto, 2012). Concern with the use of these materials is associated with the fact that there is no information on biological fate, consumption risks and effects on human health and the environment. Therefore, studies on the physico-chemical properties and physiological processes that occur during digestion and absorption of nanosystems are extremely important (Cerqueira, Pinheiro, Silva, Ramos, Azevedo, Flores-López, Rivera, Bourbon, Ramos, & Vicente, 2014).

Some studies in the field of medicine, using standard drugs, were carried out in order to obtain information regarding the behavior of these materials. Garnett & Kallinteri (2006) studied several nanometric material size ranges for potential uses as medicines in order to beneficially exploit these size ranges. They verified that at scales below 100 nm the physico-chemical properties are altered and are accentuated at smaller particle sizes, resulting in increased interaction with the cells. Nanoparticles with a size between 50 and 70 nm can be deposited in lung tissues and trigger inflammatory processes, while at 50 nm they tend to

permeate through cell membranes via passive transport in cells of various tissues. Blood-brain permeability may occur with particles measuring 30 nm and at 10 nm and smaller strong interactions with extra or intracellular macromolecules may also occur. Hoet, Brüske-Hohlfeld, & Salata (2004) found that nanoparticles are generally admitted to the human body via the lungs and intestines, and the penetration of particles through these pathways depends on the size, surface properties and point of contact. However, nanomaterials may present particular characteristics that should be studied on a case-by-case basis.

In foods, behavioral studies of nanosystems in the gastrointestinal tract both *in vitro* and *in vivo* are extremely necessary to elucidate several factors that may represent potential health risks (Cerqueira, Pinheiro, Silva, Ramos, Azevedo, Flores-López, Rivera, Bourbon, Ramos, & Vicente, 2014). For example, studies on the absorption, adsorption, enzymatic degradation and agglomeration processes of SLN and NLC, as well as interactions with lipid transport systems are important (Mehnert & Mäder, 2012), since a number of factors may affect the absorption/adsorption of these systems, including concentration, surface area, surface energy, morphology and others (Rashidi & Khosravi-Darani, 2011).

Currently, the use of nanotechnology in food is not regulated for preparation and application. Efforts have been directed at identifying applications and food safety issues of nanotechnology in the food sector by the World Health Organization (WHO) and the Food and Agriculture Organization of the United Nations (FAO). In the European Union (EU), regulations for nutrition labeling entered into effect in 2014, where ingredients contained in the product in the form of artificial nanomaterials must be clearly indicated in the list of ingredients (Weiss, Takhistov, & McClements, 2006). The Food and Drug Administration (FDA) determined that nanotechnology is an emerging technology that can be used in a wide range of products that are part of regulated items. In 2014, the agency released a guide containing recommendations to evaluate the effects of changes in the manufacturing process with emerging technologies, including nanotechnology, with regards to the safety and regulatory status of foods and food ingredients. This guide does not establish regulatory definitions but is intended to assist industries and sectors in identifying when potential implications should be considered for regulatory, safety, efficacy or public health impact status issues that may arise with the application of nanotechnology to products regulated by the FDA. Therefore, the FDA will request information on its regulated products, including food substances which involve the

application of nanotechnology, where external, internal or surface structure dimensions are on the nanometer scale (about 1 nm to 100 nm), and if a product is designed to exhibit functional, physical, chemical or biological properties due to its size, even if exceeding the limits of the nanoscale, up to one micrometer (1,000 nm). These aspects are intended to provide an initial screening tool, with the understanding that they are subject to changes in the future as new information becomes available (FDA, 2014).

12. Conclusions and perspectives

The use of nanotechnology in the form of SLN and NLC, for improving both the physical and nutritional properties of foods, has shown to be an emerging technology with great potential for exploration and application. The development of these types of nanoparticles with different lipid materials can impart distinct characteristics to various products with properties that can be adapted and used in a wide range of applications due to the numerous materials that can be exploited. In this review, it was possible to find several studies reporting the elaboration and production of LN for application in drugs and foods, using high cost synthetic materials, and in smaller quantity with the use of alternative natural materials. Also observed is the need for adaptation and knowledge of processes seeking the use of materials utilized by food industries, in addition to environmental and health risk assessments, and mainly dissemination of knowledge to the population for insertion of nanotechnology in the market. However, in the food industry, nanotechnology that uses SLN and NLC is little explored and there are not yet any products on the market.

Acknowledgements

References

Abuasal, B. S., Lucas, C., Peyton, B., Alayoubi, A., Nazzal, S., Sylvester, P. W., & Kaddoumi, A. (2012). Enhancement of intestinal permeability utilizing solid lipid nanoparticles increases γ-tocotrienol oral bioavailability. *Lipids, 47*(5): 461–469.

Aditya, N. P., & Ko. S. (2015). Solid lipid nanoparticles (SLNs): delivery vehicles for food bioactives. *RSC Advances, 5*:30902–30911.

Aditya, N. P., Shim, M., Lee, I., Lee, Y., Im, M., & Ko, S. (2013). Curcumin and genistein coloaded nanostructured lipid carriers: in vitro digestion and antiprostate cancer activity. *Journal of Agricultural and Food Chemistry, 61*:1878−1883.

Alex, A. M. R., Chacko, A. J., Jose, S., & Souto, E. B. (2011). Lopinavir loaded solid lipid nanoparticles (SLN) for intestinal lymphatic targeting. *European Journal of Pharmaceutical Sciences, 42*:11–18.

Amani, A., York, P., Chrystyn, H., & Clark, B. (2010). Factors affecting the stability of nanoemulsions - Use of artificial neural networks. *Pharmaceutical Research, 27*(1):37–45.

Asumadu-Mensah, A., Smith, K. W., & Ribeiro, H. S. (2013). Solid lipid dispersions: potential delivery system for functional ingredients in foods. *Journal of Food Science, 78*:1000–1008.

Attama, A. A., & Muller-Goymann, C. C. (2008). Effect of beeswax modification on the lipid matrix and solid lipid nanoparticle crystallinity. *Colloids and Surfaces A: Physicochemical and Engineering Aspects, 315*:189–195.

Awad, T. S., Helgaso, T., Kristbergsson, K., Decker, E. A., Weiss, J., & McClements, D. J. (2008). Effect of cooling and heating rates on polymorphic transformations and gelation of tripalmitin solid lipid nanoparticle (SLN) suspensions. *Food Biophysics, 3*:155–162.

Awad, T. S., Helgason, T., Weiss, J., Decker, E. A., & McClements, D. J. (2009). Effect of omega-3 fatty acids on crystallization, polymorphic transformation and stability of tripalmitin solid lipid nanoparticle suspensions. *Crystal Growth & Design, 9*:3405–3411.

Awad, T. S., Moharram, H. A., Shaltout, O. E., Asker, D., & Youssef, M. M. (2012). Applications of ultrasound in analysis, processing and quality control of food: A review. *Food Research International, 48*:410–427.

Badea, G., Lăcătus, I., Badea, N., Ott, C., & Meghea, A. (2015). Use of various vegetable oils in designing photoprotective nanostructured formulations for UV protection and antioxidant activity. *Industrial Crops and Products, 67*:18–24.

Bastida-Rodríguez, J. (2013). The food additive polyglycerol polyricinoleate (E-476): structure, applications, and production methods. *International Scholarly Research Notices, Chemical Engineering, 2013*:1-21.

Beloqui, A., Solinís, M. Á., Rodríguez-Gascón, A., Almeida, A. J., & Préat, V. (2016). Nanostructured lipid carriers: Promising drug delivery systems for future clinics. *Nanomedicine: Nanotechnology, Biology, and Medicine*, *12*:143–161.

Berton-Carabin, C. C., Coupland, J. N., & Elias, R. J. (2013). Effect of the lipophilicity of model ingredients on their location and reactivity in emulsions and solid lipid nanoparticles. *Colloids and Surfaces A: Physicochemical and Engineering Aspects, 431*:9-17.

Blasco, C., & Picó, Y. (2011). Determining nanomaterials in food. *Trends in Analytical Chemistry, 30*(1):84-99.

Bouchemal, K., Briançon, S., Perrier, E., &Fessi, H. (2004). Nano-emulsion formulation using spontaneous emulsification: Solvent, oil and surfactant optimisation. *International Journal of Pharmaceutics, 280*:241–25.

Bunjes, H., & Siekmann, B. (2006). Manufacture, Characterization, and Applications of Solid Lipid Nanoparticles as Drug Delivery Systems. In S. Benita (Ed.), *Microencapsulation - Methods and Industrial Applications* (pp. 213-268). London CRC Press: Taylor & Francis Group.

Bunjes, H. (2005). Characterization of Solid Lipid Nano and Microparticles. In C. Nastruzzi (Ed.), *Lipospheres in Drug Targets and Delivery: Approaches, Methods, and Applications.* (pp. 43-70) Boca Raton: CRC Press LLC.

Bunjes, H., & Unruh, T. (2007). Characterization of lipid nanoparticles by differential scanning calorimetry, X-ray and neutron scattering. *Advanced Drug Delivery Reviews, 59*:379–402.

Bunjes, H., Steiniger, F., & Richter, W. (2007). Visualizing the Structure of Triglyceride Nanoparticles in Different Crystal Modifications. *Langmuir, 23*(7): 4005–4011.

Campos, R. (2005). Experimental Methodology. In A. J. Marangoni (Ed.), *Fat Crystal Networks* (pp. 267-349). New York: CRC Press: Taylor & Francis Group.

Carvalho, S. M., Noronha, C. M., Floriani, C. L., Lino, R. C., Rocha, G., Bellettini, I. C., Ogliari, P. J., & Barreto, P. L. M. (2013). Optimization of α-tocopherol loaded solid lipid nanoparticles by central composite design. *Industrial Crops and Products*, *49*:278–285.

Cerqueira, M. A., Pinheiro, A. C., Silva, H. D., Ramos, P. E., Azevedo, M. A., Flores-López, M. L., Rivera, M. C., Bourbon, A. I., Ramos, O. L., & Vicente, A. A. (2014). Design of bio-nanosystems for oral delivery of functional compounds. *Food Engineering Reviews, 6*(1):1–19.

Chakraborty, S., Shukla, D., Vuddanda, P. R., Mishra, B., & Singh, S. (2010). Utilization of adsorption technique in the development of oral delivery system of lipid based nanoparticles. *Colloids and Surfaces B: Biointerfaces*, 81(2):563–569.

Chaudhry, Q., & Castle, L. (2011). Food applications of nanotechnologies: An overview of opportunities and challenges for developing countries. *Trends in Food Science & Technology, 22*:595–603.

Cheong, J. N., & Tan, C. P. (2010). Palm-based functional lipid nanodispersions: preparation, characterization and stability evaluation. *European Journal of Lipid Science and Technology, 112*:557–564.

Cho, Y. H., Shim, H. K., & Park, J. (2003). Encapsulation of fish oil by an enzymatic gelation process using TGase cross-linked protein. *Journal of Food Science, 68*:2717–2723.

Choi, K., Aditya, N. P., & Ko, S. (2014). Effect of aqueous pH and electrolyte concentration on structure, stability and flow behavior of non-ionic surfactant based solid lipid nanoparticles. *Food Chemistry, 147*:239–244.

Conto, L. C., Grosso, C. R. F., & Gonçalves, L. A. G. (2013). Chemometry as applied to the production of OMEGA-3 microcapsules by complex coacervation with soy protein isolate and gum Arabic. *LWT-Food Science and Technology, 53*:218–224.

Cushena, M., Kerryb, J., Morrisc, M., Cruz-Romerob, M., & Cumminsa, E. (2012). Nanotechnologies in the food industry e Recent developments, risks and regulation. *Trends in Food Science & Technology, 24*:30-46.

De Morais, J., Santos, O., Delicato, T., Goncalves, R., & Rocha, P. F. (2006). Physicochemical characterization of canola oil/water nano-emulsions obtained by determination of required HLB number and emulsion phase inversion methods. *Journal of Dispersion Science and Technology*, 27(1):109–115.

Dion, M. A. M. L., Ruud, J. B. P., Saskia, M. V. R., & Hans, B. (2008). A Review of Analytical Methods for the Identification and Characterization of Nano Delivery Systems in Food. *Journal of Agricultural and Food Chemistry*, *56*(18):8231–8247.

Doktorovová, S., Araújo, J., Garcia, M. L., Rakovský, E., & Souto, E. B. (2010). Formulating fluticasone propionate in novel PEG-containing nanostructured lipid carriers (PEG-NLC). *Colloids and Surfaces B: Biointerfaces*, *75*(2):538-542.

Domingo, C., & Saurina, J. (2012). Review An overview of the analytical characterization of nanostructured drug delivery systems: Towards green and sustainable pharmaceuticals: A review. *Analytica Chimica Acta*, *744*:8–22.

Dora, C. L., Putaux, J., Pignot-Paintrand, I., Dubreuil, F., Soldi, V., Borsali, R., & Lemos-Senna, E. (2012). Physicochemical and morphological characterizations of glyceryl tristearate/castor oil nanocarriers prepared by the solvent diffusion method. *Journal of the Brazilian Chemical Society*, *23*:1972-1981.

Durán, N., **&** Marcato, P. D. (2013). Nanobiotechnology perspectives. Role of nanotechnology in the food industry: A review. *International Journal of Food Science and Technology, 48*:1127–1134.

Eltayeb, M., Bakhshi, P.K., Stride, E., & Edirisinghe, M. (2013). Preparation of solid lipid nanoparticles containing active compound by electrohydrodynamic spraying. *Food Research International*, *53*:88–95.

Fernandes, P., & Cabral, J. M. S. (2007). Phytosterols: Applications and recovery methods. *Bioresource Technology, 98*:2335–2350.

Food and Drug Administration-FDA (2014) Contains Nonbinding Recommendations: Assessing the Effects of Significant Manufacturing Process Changes, Including Emerging Technologies, on the Safety and Regulatory Status of Food Ingredients and Food Contact Substances, Including Food Ingredients that are Color Additives. Available from: <http://www.fda.gov/RegulatoryInformation/Guidances/ucm257698.htm> Acessed: 2017, April 23.

Garnett, M. C., & Kallinteri, P. (2006). Nanomedicines and nanotoxicology: some physiological principles. *Occupational Medicine, 56*(5):307–311.

Garzón, M. L. S., Hernández, A. L., Vázquez, M. L. R., Vázquez, M. L. R., & García, B. F. (2008). Preparación de nanopartículas sólidas lipídicas (SLN), y de Acarreadores

lipídicos nanoestructurados (NLC). *Revista Mexicana de Ciencias Farmacéuticas, 39*(4):50-66.

Garzón, M. L. S., Vázquez, M. L. R., Vázquez, M. L. R., García, B. F., & Hernández, A. L. (2009) Efecto de los componentes de la formulación em las propriedades de las nanopartículas sólidas. *Revista Mexicana de Ciencias Farmacéuticas, 40*(2):26-40.

Gasco, M. R. G. (2007). Lipid nanoparticles: perspectives and challenges. *Advanced Drug Delivery Reviews*, *59*:377–378.

Ghosh, V., Saranya, S., Mukherjee, A., Chandrasekaran, N. (2013). Cinnamon oil nanoemulsion formulation by untrasonic emulsficantion: investigation of its bactericidal activity. *Journal of Nanoscience and Nanotechnology, 13*(1):114-122.

Han. F., Li, S., Yin, R., Liu, H., & Xu, L. (2008). Effect of surfactants on the formation and characterization of a new type of colloidal drug delivery system: nanostructured lipid carriers. *Colloids and Surfaces A: Physicochemical and Engineering Aspects*, *315*:210–216.

Haskell, R. J. (2006). Physical Characterization of Nanoparticles. In R. B. Gupta, & U. B. Kompella (Eds.), *Nanoparticle Technology for Drug Delivery* (pp. 103-138). Boca Raton: CRC Press.

Hejri, A., Khosra, V. I. A., Gharanjig, K., & Hejazi, M. (2013). Optimisation of the formulation of β-carotene loaded nanostructured lipid carriers prepared by solvent diffusion method. *Food Chemistry,141*:117–123.

Helgason, T., Awad, T. S., Kristbergsson, K., Decker, E. A., McClements, D. J., & Weiss, J. (2009). Impact of surfactant properties on oxidative stability of β-carotene encapsulated within solid lipid nanoparticles. *Journal of Agricultural and Food Chemistry*, *57*:8033–8040.

Hentschel, A., Gramdorf, S., Müller, R. H., & Kurz, T. (2008). β-Carotene-loaded nanostructured lipid carriers. *Journal of Food Science*, *73*(2):1-6.

Himavan, C., Starov, V. M., & Stapley, A. G. F. (2006). Thermodynamic and kinetic aspects of fat crystallization. Advances in Colloid and Interface Science, *122*:3-33.

Hoet, P. H. M., Brüske-Hohlfeld, I., & Salata, O. V. (2004). Nanoparticles - known and unknown health risks. *Journal of Nanobiotechnology*, *2*(12):1-15.

Holser, R. (2012). Encapsulation of polyunsaturated fatty acid esters with solid lipid articles. *Lipid Insights, 5*:1-5.

Hou, D. Z., Xie, C. S., Huang, K. J., & Zhu, C. H. (2003). The production and characteristics of solid lipid nanoparticles (SLNs). *Biomaterials, 24*:1781-1785.

Huang, Q., Yu, H., & Ru, Q. (2010). Bioavailability and delivery of nutraceuticals using nanotechnology. *Journal of Food Science*, *75*:50-57.

Izadi, Z., Nasirpour, A., & Garousi, G. (2012). Optimization of Phytosterols Dispersion in an Oil/ Water Emulsion Using Mixture Design Approach. *Journal of Dispersion Science and Technology*, *33*(12):1715-1722.

Jannin, V., Musakhanian, J., & Marchaud, D. (2008). Approaches for the development of solid and semi-solid lipid-based formulations. *Advanced Drug Delivery Reviews*, *60*:734-746.

Jores, K., Haberland. A., Wartewig, S., Mäder, K., & Mehnert, W. (2005). Solid Lipid Nanoparticles (SLN) and Oil-Loaded SLN Studied by Spectrofluorometry and Raman Spectroscopy. *Pharmaceutical Research, 22*(11):1887-1897.

Jores, K., Mehnert, W., Drechsler, M., Bunjes, H., Johann, C., & Mäder, K. (2004). Investigations on the structure of solid lipid nanoparticles (SLN) and oil-loaded solid lipid nanoparticles by photon correlation spectroscopy, field-flow fractionation and transmission electron microscopy. *Journal of Controlled Release, 95*:217– 227.

Jores, K., Mehnert, W., & Mäder, K. (2003). Physicochemical Investigations on Solid Lipid Nanoparticles and on Oil-Loaded Solid Lipid Nanoparticles: A Nuclear Magnetic Resonance and Electron Spin Resonance Study. *Pharmaceutical Research, 20*(8):1274-1283.

Joseph, S., & Bunjes, H. (2012). Preparation of nanoemulsions and solid lipid nanoparticles by premix membrane emulsfication. *Journal of Pharmaceutical Sciences*, *101*:2479-2489.

Joseph, S., Rappolt, M., Schoenitz, M., Huzhalska, V., Augustin, W., Scholl, S., & Bunjes, H. (2015). Stability of the Metastable α-Polymorph in Solid Triglyceride Drug-Carrier Nanoparticles. *Langmuir*, *31*:6663−6674.

Kamal-Eldin, A. (2005). Minor Components of Fats and Oils. In F. Shahidi (Ed.), *Bailey's Industrial Oil and Fat Products. Edible Oil and Fat Products: Chemistry, Chemical properties, and health effects* (pp. 319−359). Hoboken, New Jersey: John Wiley & Sons.

Kamboj, S., Bala, S., & Nair, A. B. (2010). Solid lipid nanoparticles: an effective lipid bases technology for poorly water soluble drugs. *International Journal of Pharmaceutical Sciences Review and Research*, *5*:78-90.

Kentish, S., Wooster, T. J., Ashokkumar, M., Balachandran, S., Mawson, R., & Simons, L. (2008). The use of ultrasonics for nanoemulsion preparation. *Innovative Food Science and Emerging Technologies*, *9*:170–175.

Klang, V., Matsko, N. B., Valenta, C., & Hofer, F. (2012). Electron microscopy of nanoemulsions: An essential tool for characterization and stability assessment. *Micron, 43*(2–3):85–103.

Lacatusu, I., Mitrea, E., Badea, N., Stan, R., Oprea, O., & Meghea, A. (2013). Lipid nanoparticles based on omega-3 fatty acids as effective carriers for lutein delivery. Preparation and in vitro characterization studies. *Journal of Functional Foods*, *5*:1260–1269

Lason, E., & Ogonowski, J. (2011). Solid lipid nanoparticles – Characteristics, application and obtaining. *Chemik*, *65*(10):964-967.

Lawler, P. J., & Dimick, P. S. (2002). Crystallization and polymorphism of fats. In C. C. Akoh (Ed.), *Food Lipids: Chemistry, Nutrition, and Biotechnology* (pp. 275-300). Boca Raton: CRC Press.

Leong, W. F., Man, Y. B. C., Lai, O. M., Long, K., Misran, M., & Tan, C. P. (2009). Optimization of Processing Parameters for the Preparation of Phytosterol Microemulsions by the Solvent Displacement Method. *Journal of Agricultural and Food Chemistry*, *57*:8426–8433.

Liu, C. H., & Wu, C. T. (2010). Optimization of nanostructured lipid carriers for lutein delivery. *Colloids and Surfaces A: Physicochemical and Engineering Aspects*, *353*(2-3):149–156.

Liu, F., & Tang, C. (2014). Phytosterol Colloidal Particles as Pickering Stabilizers for Emulsions. *Journal of Agricultural and Food Chemistry*, *62*(22): 5133−5141.

Liu, G. Y., Wang, J. M., & Xia, Q. (2012). Application of nanostructured lipid carrier in food for the improved bioavailability. *European Food Research and Technology*, *234*:391–398.

Lobato, K. B. S., Paese, K., Forgearini, J. C., Guterres, S. S., Jablonski, A., & Rios, A. O. (2013). Characterization and stability evaluation of bixin nanocapsules. *Food Chemistry*, *141*:3906–3912.

Luykx, D. M. A. M., Peters, R. J. B., Ruth, S. M. V., & Bouwmeester, H. (2008). A Review of Analytical Methods for the Identification and Characterization of Nano Delivery Systems in Food. *Journal of Agricultural and Food Chemistry*, *56*:8231–8247.

Madureira, A. R., Campos, D. A., Fonte, P., Nunes, S., Reis, F., Gomes, A. M., Sarmento, B., & Pintado, M. M. (2015). Characterization of solid lipid nanoparticles produced with carnauba wax for rosmarinic acid oral delivery. *RSC Advances, 5*:22665-22673.

Mandawgade, S. D., & Patravale, V. B. (2008). Development of SLNs from natural lipids: application to topical delivery of tretinoin. *International Journal of Pharmaceutics*, *363*:132–138.

Mao, L. K., Xu, D. X., Yang, J., Yuan, F., Gao, Y. X., & Zhao, J. (2009). Effects of small and large molecule emulsifiers on the characteristics of beta-carotene nanoemulsions prepared by high pressure homogenization. *Food Technology and Biotechnology*, 47:336–342.

McClements, D. J. (2013). Edible lipid nanoparticles: Digestion, absorption, and potential toxicity. *Progress in Lipid Research, 52*:409–423.

McClements, D. J., & Rao, J. (2011). Food-grade nanoemulsions: formulation, fabrication, properties, performance, biological fate, and potential toxicity. *Critical Reviews in Food Science and Nutrition*, *51*(4):285-330.

McClements, D. J., Decker, E. A., & Weiss, J. (2007). Emulsion-based delivery systems for lipophilic bioactive components. *Journal of Food Science*, *72*:109-124.

McClements, D. J., Decker, E. A., Park, Y., & Weiss, J. (2009). Structural design principles for delivery of bioactive components in nutraceuticals and functional foods. *Critical Reviews in Food Science and Nutrition*, *49*:577–606.

McKeon, T. A. (2005). Transgenic Oils. In F. Shahidi (Ed.) *Bailey's Industrial Oil and Fat Products. Edible Oil and Fat Products: Chemistry, Chemical properties, and health effects* (pp. 155–174) New Jersey: John Wiley & Sons.

Mehnert. W., & Mäder, K. (2012). Solid lipid nanoparticles: production, characterization and applications. *Advanced Drug Delivery Reviews*, *64*:83-101.

Mensink, R. P. (2005). Effects of stearic acid on plasma lipid and lipoproteins in humans. *Lipids, 40*(12):1201-1205.

Mitri, K., Shegokar, R., Gohla, S., Anselmi, C., & Müller, R. H. (2011). Lipid nanocarriers for dermal delivery of lutein: preparation, characterization, stability and performance. *International Journal of Pharmaceutics*, *414*:267– 275.

Mojahedian, M. M., Daneshamouz, S., Samani, S. M., & Zargaran, A. (2013). A novel method to produce solid lipid nanoparticles using n-butanol as an additional co-surfactant according to the o/w microemulsion quenching technique. *Chemistry and Physics of Lipids*, *174*:32– 38.

Mozafari, M. R., Flanagan, J., Matia-Merino, L., Awati, A., Omri, A., Suntres, Z., & Singh, H. (2006). Recent trends in the lipid-based nanoencapsulation of antioxidants and their role in foods. *Journal of the Science of Food and Agriculture*, *86*:2038-2045.

Mühlen, A. Z., Schwarz, C., & Mehnert, W. (1998). Solid lipid nanoparticles (SLN) for controlled drug delivery – Drug release and release mechanism. *European Journal of Pharmaceutics and Biopharmaceutics*, 45(2):149–155.

Müller, R. H., Radtke, M., & Wissing, S. A. (2002). Nanostructured lipid matrices for improved microencapsulation of drugs. *International Journal of Pharmaceutics*, 242(1-2):121-128.

Müller, R. H., Runge, S., Ravelli, V., Mehnert, W., Thunemann, A. F., & Souto, E. B. (2006). Oral bioavailability of cyclosporine: Solid lipid nanoparticles (SLN®) versus drug nanocrystals. *International Journal of Pharmaceutics*, *317*:82–89.

Nakajima, M., Wang, Z., Chaudhry, Q., Park, H. J., & Juneja, L. R. (2015). Nano-Science-Engineering-Technology Applications to Food and Nutrition. *Journal of Nutritional Science and Vitaminology, 61*:S180-2.

Nguyen, H. M., Hwang, I. C., Park, J. W., & Park, H. J. (2012). Enhanced payload and photo-protection for pesticides using nanostructured lipid carriers with corn oil as liquid lipid. *Journal of Microencapsulation*, *29*(6):596-604.

Nichols, D. S., & Sanderson, K. (2003). The nomenclature, structure and properties of food lipids. In Z. E. Sikorski, & A. Kolakowska (Eds.), *Chemical and Functional Properties of Food Lipids* (pp. 29–60). Boca Raton: CRC Press.

Nik, A. M., Langmaid, S., & Wright, A. J. (2012). Nonionic surfactant and interfacial structure impact crystallinity and stability of β-carotene loaded lipid nanodispersions. *Journal of Agricultural and Food Chemistry*, *60*:4126−4135.

O'Brien, R. D. (2009). Fats and oils formulation. In R. D. O'Brien (Ed.), *Fats and oils – Formulating and Processing for Applications* (pp.263-345). Boca Raton: CRC.

Oliveira, A. C., Valentim, I. B., Goulart, M. O. F., Silva, C. A., Bechara, E. J. H., & Trevisan, M. T. S. (2009). Fontes Vegetais Naturais de Antioxidantes. *Química Nova*, *32*(3):689-702.

Pardeike, J., Hommoss, A., & Müller, R. (2009). Lipid nanoparticles (SLN, NLC) in cosmetic and pharmaceutical dermal products. *International Journal of Pharmaceutics*, *366*:170-184.

Patel, M. R., & Martin-Gonzalez, F. S. (2012). Characterization of ergocalciferol loaded solid lipid nanoparticles. *Journal of Food Science*, *71*:8-13.

Pey, C. M., Maestro, A., Sole, I., Gonzalez, C., Solans, C., & Gutierrez, J. M. (2006). Optimization of nano-emulsions prepared by low-energy emulsification methods at constant temperature using a factorial design study. *Colloids and Surfaces a-Physicochemical and Engineering Aspects*, 288(1–3):144–150.

Porter, C. J. H., Willians, H. D., & Trevaskis, N. (2013). Recent advances in lipid-based formulation technology. *Pharmaceutical Research*, *30*:2971–2975.

Qian, C., & McClements, D. (2011). Formation of nanoemulsions stabilized by model food-grade emulsifiers using high pressure homogenization: Factors affecting particle size. *Food Hydrocolloids*, *25*(5):1000-1008.

Qian, C., Decker, E. A., Xiao, H., & McClements, D. J. (2012). Inhibition of β-carotene degradation in oil-in-water nanoemulsions: Influence of oil-soluble and water-soluble antioxidants. *Food Chemistry*, *135*(3):1036-1043.

Qian, C., Decker, E. A., Xiao, H., & McClements, D. J. (2013). Impact of lipid nanoparticle physical state on particle aggregation and β-carotene degradation: potential limitations of solid lipid nanoparticles. *Food Research International*, *52*:342–349.

Ramisetty, K. A., Pandit, A. B., & Gogate, P. R. (2015). Ultrasound assisted preparation of emulsion of coconut oil in water: Understanding the effect of operating

parameters and comparison of reactor designs. *Chemical Engineering and Processing: Process Intensification*, *88*:70–77.

Rashidi, L., & Khosravi-Darani, K. (2011). The Applications of Nanotechnology in Food Industry. *Critical Reviews in Food Science and Nutrition, 51*:723–730.

Reddy, R. N., & Shariff, A. (2013). Solid lipid nanoparticles: an advanced drug delivery system. *International Journal of Pharmaceutical Sciences and Research*, *4*(1):161-171.

Relkin, P., Yung, J. M., Kalnin, D., & Ollivon, M. (2008). Structural behaviour of lipid droplets in protein-stabilized nano-emulsions and stability of α-tocopherol. *Food Biophysics*, *3*:163–168.

Ribeiro, A. P. B., Basso, R. C., & Kieckbusch, T. G. (2013). Effect of the addition of hardfats on the physical properties of cocoa butter. *European Journal of Lipid Science and Technology*, *115*:301-312.

Ribeiro, A. P. B., Basso, R. C., Grimaldi, R., Gioielli, L. A., & Gonçalves, L. A. G. (2009). Instrumental methods for the evaluation of interesterified fats. *Food Analytical Methods, 2*:282-302.

Ribeiro, H. S., & Schubert, H. (2003). Stability of lycopene emulsions in food systems. *Journal of Food Science*, *68*:2730-2734.

Robles, L. V., García, F. B., Garzón, S. M. L., Hernández, L. A., & Vázquez, R. M. L. (2008). Nanopartículas lipídicas sólidas. *Revista Mexicana de Ciências Farmacêuticas*, *39*(1):38-52.

Rubio-Rodríguez, S. B. N., Jaime, I., Diego, S. M., Sanz, M. T., & Carballid, J. R. (2010). Production of omega-3 polyunsaturated fatty acid concentrates: A review. *Innovative Food Science and Emerging Technologies*, *11*:1-12.

Salminen, H., Helgason, T., Kristinsson, B., Kristbergsson, K., & Weiss, J. (2013). Formation of solid shell nanoparticles with liquid ω-3 fatty acid core. *Food Chemistry*, *141*(3):2934–2943.

Santos, G. S., Pereira, G. G., Bender, E. A., Colomé, L. M., & Guterres, S. S. (2012). Desenvolvimento e caracterização de nanopartículas lipídicas destinadas à aplicação tópica de dapsona. *Química Nova*, *35*(7):1388-1394.

Sato, K. (2001). Crystallization behaviour of fats and lipids: a review. *Chemical Engineering Science*, *56*(7):2255-2265.

Scrimgeour, C. (2005). Chemistry of Fatty Acids. In F. Shahidi (Ed.) *Bailey's Industrial Oil and Fat Products. Edible Oil and Fat Products: Chemistry, Chemical properties, and health effects*. (pp. 1-43). New Jersey: John Wiley & Sons.

Severino, P., Andreani, T., Macedo, A. S., Fangueiro, J. F., Santana, M. H. A., Silva, A. M., & Souto, E. B. (2012). Review Article: Current State-of-Art and New Trends on Lipid Nanoparticles (SLN and NLC) for Oral Drug Delivery. *Journal of Drug Delivery,* Doi:10.1155/2012/750891.

Severino, P., Pinho, S. C., Souto, E. B., & Santana, M. H. A. (2011). Crystallinity of Dynasan® 114 and Dynasan® 118 matrices for the production of stable Miglyol® -loaded nanoparticles. *Journal of Thermal Analysis and Calorimetry*, *108*(1):101-108.

Shah, R., Eldridge, D., Palombo, E., & Harding, I. (2015). *Lipid Nanoparticles: Production, Characterization and Stability.* Springer. ISSN 1864-8126.

Shangguan, M., Lu, Y., Qi, J., Han, J., Tian, Z., Xie, Y., Hu, F., Yuan, H., & Wu, W. (2014). Binary lipids-based nanostructured lipid carriers for improved oral bioavailability of silymarin. *Journal of Biomaterials Applications*, *28*:887–896.

Sharma, P., Ganta, S., Denny, W. A., & Garg, S. (2009). Formulation and pharmacokinetics of lipid nanoparticles of a chemically sensitive nitrogen mustard derivative: Chlorambucil. *International Journal of Pharmaceutics*, 367:187–194.

Sharma, V. K., Diwan, A., Sardana, S., & Dhall, V. (2011). Solid lipid nanoparticles system: an overview. *International Journal of Research in Pharmaceutical Sciences*, *2*(3):450-461.

Shilei, N., Rui, S. Guodong, Z., & Qiang, X. (2014). Quercetin loaded Nanostructured Lipid Carrier for food fortification: Preparation, Characterization and in vitro study. *Journal of Food Process Engineering, 38*:93-106.

Simovic, S., Barnes, T. J., Tan, A., & Prestige, C. A. (2012). Assembling nanoparticle coatings to improve the drug delivery performance of lipid based colloids. *Nanoscale, 4*:1220–1230.

Souto, E. B., Severino, P., Santana, M. H. A., & Pinho, S. C. (2011). Nanopartículas de lipídios sólidos: métodos clássicos de produção laboratorial. *Química Nova*, *34*:1762-1769.

Sozer, N., & Kokini, J. L. (2009). Nanotechnology and its applications in the food sector. *Trends in Biotechnology, 27*(2):82-89.

Takeuchi, M., Ueno, S., & Sato, K. (2003). Synchrotron Radiation SAXS/WAXS Study of Polymorph-Dependent Phase Behavior of Binary Mixtures of Saturated Monoacid Triacylglycerols. *Crystal growth & design, 3*(3):369-374.

Tamjidi, F., Shahedi, M., Varshosaz, J., & Nasirpour, A. (2013). Nanostructured lipid carriers (NLC): A potential delivery system for bioactive food molecules. *Innovative Food Science and Emerging Technologies*, *19*:29–43.

Tan, C. P., & Che Man, Y. B. (2002). Differential scanning calorimetric analysis of palm, palm oil based products and coconut oil: effects of scanning rate variation. *Food Chemistry*, *76*:9-102.

Tan, C. P., & Nakajima, M. (2005). β-Carotene nanodispersions: preparation, characterization and stability evaluation. *Food Chemistry*, *92*:661–671.

Teo, B. S. X., Basri, M., Zakaria, M. R. S., Salleh, A. B., Rahman, R. N. Z. R. A., & Rahman, A. M. B. (2010). A potential tocopherol acetate loaded palm oil esters-in-water nanoemulsions for nanocosmeceuticals. *Journal of Nanobiotechnology, 8*(4):1–12.

Trujillo, C. C., & Wright, A. J. (2010). Properties and stability of solid lipid particle dispersions based on canola stearin and poloxamer 188. *Journal of American Oil Chemists' Society*, *87*:715–730.

Wanasundara, P. K. J. P. D., & Shahidi, F. (2005). Antioxidants: Science, Technology, and Applications. In F. Shahidi (Ed.), *Bailey's Industrial Oil and Fat Products. Edible Oil and Fat Products: Chemistry, Chemical properties, and health effects* (pp. 431-489). New Jersey: John Wiley & Sons.

Wang, J. L., Dong, X. Y., Wei, F., Zhong, J., Liu, B., Yao, M. H., Yang, M., Zheng, C., Quek, S. Y., & Chen, H. (2014). Preparation and characterization of novel lipid carriers containing microalgae oil for food applications. *Journal of Food Science*, *79*:169-177.

Wang, X. Y., Jiang, Y., Wang, Y. W., Huang, M. T., Ho, C. T., & Huang, Q. R. (2008). Enhancing anti-inflammation activity of curcumin through O/W nanoemulsions. *Food Chemistry*, *108*(2):419–424.

Weiss, J., Decker, E. A., McClements, D. J., Kristbergsson, K., Helgason, T., & Awad, T. (2008). Solid lipid nanoparticles as delivery systems for bioactive food components. *Food Biophysics*, *3*:146-154.

Weiss, J., Takhistov, P., & McClements, J. (2006). Functional materials in food nanotechnology. *Journal of Food Science*, *71*(9):107-116.

Wissing, S. A., Kayser, O., & Müller, R. H. (2004). Solid lipid nanoparticles for parenteral drug delivery. *Advanced Drug Delivery Reviews*, *56*(9):1257–1272.

Wooster, T., Golding, M., & Sanguansri, P. (2008). Impact of oil type on nanoemulsion formation and Ostwald ripening stability. *Langmuir, 24*(22):12758–12765.

Wu, L., Zhang, J., & Watanabe, W. (2011). Physical and chemical stability of drug nanoparticles. *Advanced Drug Delivery Reviews*, *63*:456-469.

Wulff-Perez, M., Galvez-Ruiz, M. J., De Vicente, J., & Martin-Rodriguez, A. (2010). Delaying lipid digestion through steric surfactant Pluronic F68: A novel in vitro approach. *Food Research International*, *43*(6):1629–1633.

Yang, Y., Corona, A., Schubert, B., Reeder, R., & Henson, M. A. (2014). The effect of oil type on the aggregation stability of nanostructured lipid carriers. *Journal of Colloid and Interface Science*, *418*:261–272.

Yin, L., Chu, B., Kobayashi, I., & Nakajima, M. (2009). Performance of selected emulsifiers and their combinations in the preparation of [beta]-carotene nanodispersions. *Food Hydrocolloids*, 23(6):1617–1622.

Yoon, G., Park, J. W., & Yonn, I. (2013). Solid lipid nanoparticles (SLNs) and nanostructured lipid carriers (NLCs): recent advances in drug delivery. *Journal of Pharmaceutical Investigation*, *43*:353–362.

Yuan, H., Chen, J., Du, Y. Z., Hu, F. Q., Zeng, S., & Zhao, H. L. (2007). Studies on oral absorption of stearic acid sln by a novel fluorometric method. *Colloids and Surfaces B-Biointerfaces*, *58*(2):157–164.

Yucel, U., Elias, R. J., & Coupland, J. N. (2013). Localization and reactivity of a hydrophobic solute in lecithin and caseinate stabilized solid lipid nanoparticles and nanoemulsions. *Journal of Colloid and Interface Science, 394*:20-25.

Zhang, L., Douglas, G. H., Guoxun, C., & Qixin, Z. (2013). Transparent dispersions of milk-fat-based nanostructured lipid carriers for delivery of β-carotene. *Journal of Agricultural and Food Chemistry*, *61*:9435−9443.

Zheng, K., Zou, A., Yang, X., Liu, F., Xia, Q., Ye, R., & Mu, B. (2013). The effect of polymer surfactant emulsifying agent on the formation and stability of α-lipoic acid loaded nanostructured lipid carriers (NLC). *Food Hydrocolloids*, *32*:72-78.

Zhu, J., Zhuang, P., Luan, L., Sun, Q., & Cao, F. (2015). Preparation and characterization of novel nanocarriers containing krill oil for food application. *Journal of Functional Foods, 19*:902– 912.

Ziani, K., Fang, Y., & McClements, D. J. (2012). Encapsulation of functional lipophilic components in surfactant-based colloidal delivery systems: vitamin E, vitamin D, and lemon oil. *Food Chemistry*, *134*:1106–1112.

ARTIGO 1

"Crystallization, polymorphism and stability of nanostructured lipid carriers developed with soybean oil, fully hydrogenated soybean oil and free phytosterols for food application" a ser submetido à *Food Chemistry*.

Crystallization, polymorphism and stability of nanostructured lipid carriers developed with soybean oil, fully hydrogenated soybean oil and free phytosterols for food applications

Valeria da Silva Santos[1], Ana Paula Badan Ribeiro[2], Lisandro Pavie Cardoso[3], Maria Helena Andrade Santana[1]

[1]Department of Biotechnological Processes, School of Chemical Engineering, University of Campinas, 500 Albert Einstein Ave., Campinas, SP 13083-970, Brazil.

[2] Department of Food Technology, School of Food Engineering, University of Campinas, 80 Monteiro Lobato St., Campinas, SP 13083-970, Brazil.

[3] Department of Applied Physics, Institute of Physics Gleb Wataghin, University of Campinas, 777 Sérgio Buarque de Holanda St., 13083-859 Campinas, SP, Brazil.

Abstract

The aim of this work was the development of nanostructured lipid carriers (NLC) with free phytosterols (FP) using conventional fats and oils (soybean oil and fully hydrogenated soybean oil). The thermal and crystalline behavior of the lipid matrices, FP and NLCs were evaluated. NLCs were characterized in size and polydispersity. The FP presented high crystallization (126 °C) and melting (137 °C) temperatures, but this did not avoid its incorporation into NLC. The NLC presented size between 154 to 534 nm and polydispersity ranging from 0.1 to 0.5, the lower limits being obtained with the polyoxyethylenesorbitan monooleate emulsifier (T80). The NLCs were found to require lower temperatures to crystallize and the polymorphic transitions were accelerated. This study indicated that the conventional raw materials were compatible with the development of NLC with FP. In this way, innovative nanoparticles were obtained, mainly in terms of lipid composition, with high potential of food applications.

Keywords: Nanotechnology; Foods; Nanostructured Lipid Carriers; Free phytosterols; High-pressure homogenization.

Abbreviations

DSC	Differential Scanning Calorimetry
FHSO	Fully hydrogenated soybean oil
FP	Free Phytosterols
GTI	Gastrointestinal tract
HLB	Hydrophilic-lipophilic balance
HPH	High-pressure homogenization
INPI	National Institute of Industrial Property
LN	Lipid Nanoparticle
NLC	Nanostructured Lipid Carriers
NLC+FP	Nanostructured lipid carriers with free phytosterols
NLC_{S60}	Nanostructured lipid carriers developed with the sorbitan monostearate emulsifier

NLC$_{SL}$	Nanostructured lipid carriers developed with soybean lecithin emulsifier
NLC$_{T80}$	Nanostructured lipid carriers developed with the polyoxyethylene sorbitan monooleate emulsifier
PDI	Polydispersity index
S60	Sorbitan monostearate
SL	Soybean Lecithin
SO	Soybean Oil
T80	Polyoxyethylenesorbitan monooleate
TAG	Triacylglycerols
XRD	X-ray diffraction
Z-ave	Z-Average size

1. Introduction

Nanotechnology is an extremely current topic, which has been constantly developed in several countries, in the most varied application sectors. This technology involves the development and application of materials and systems at the nanometric scale, through the exploration and control of its phenomena and properties. However, regulatory terms are still inexistent for processing and application of nanosystems in food (CUSHENA, 2012; CERQUEIRA et al.; 2014, TAMJIDI et al., 2013).

In food, lipids have been used as raw material for the development of lipid nanoparticles (LN), mainly for the solubilization capacity of lipophilic bioactive compounds. In addition, LN may improve the chemical stability and permeability of bioactive compounds through the gastrointestinal tract (GIT) and may also facilitate its absorption (AWAD et al., 2009). In this way, LN should preferably be produced by using lipid materials with high thermal resistance (melting point over than the body temperature, 37 ° C), in way that they remain solid during the digestive process, in order to protect the compounds incorporated until their absorption in TGI (SHARMA et al., 2011).

There are currently two types of lipid nanoparticles, solid lipid nanoparticles (NLS), developed with saturated lipids, and nanostructured lipid carriers (NLC), composed of both saturated and unsaturated lipids. The NLCs were developed to overcome possible limitations associated with NLS. The insertion of unsaturated lipids was performed to produce less structured lipid matrices, in relation to crystallinity, obtaining a better incorporation efficiency and avoiding the release/expulsion of bioactive compounds during storage (MÜLLER et al.,

2006; GÁRZON et al., 2008; PARDEIKE et al., 2009; SOUTO et al., 2011; SOUTO et al., 2011).

The lipid matrices of the NLCs are generally produced with high-cost lipids, such as purified triacylglycerols (TAGs) and/or synthetic lipid materials (GARZÓN et al., 2009; MEHNERT, MADER, 2012). These matrices make NLCs economically unfeasible when considering the scale and possibility of application in food systems. Thus, the combination of the characteristics from the lipid sources commonly applied in the food industry, such as vegetable oils and fats, seems to be promising for the development of nanostructured lipid systems. Different mixtures of natural fats represent compatible sources for this purpose, with crystallographic characteristics suitable for NLC formulation (Garzon et al., 2009). However, up to date, few studies have been directed at obtaining LN from conventional oils and fats.

A high potential and low-cost option for application as saturated lipid in LN are the fully hydrogenated vegetable oils, also known as hardfats. These materials have melting points between 40 and 72°C, compatible with the application as the solid material of NLC. Fully hydrogenated vegetable oils are obtained when all the double bonds of the fatty acids are saturated during the total catalytic hydrogenation process of unsaturated oils. Hardfats have been developed as a raw material to replace partially hydrogenated fat, contributing to the development of interesterified low-trans fats by means of the interesterification process. Although they are considered relatively new materials, they are low-cost industrial products. Currently, hardfats have been also the object of studies focused on the modification of fat physical properties, as well as the structuring of liquid oils (RIBEIRO, BASSO, KIECKBUSCH, 2013; HUANG, YU, RU, 2010; TAMJIDI et al., 2013).

In this way, the use of fully hydrogenated vegetable oils combined with polyunsaturated oils such as soybean, canola, and sunflower oil is a promising option for the development of lipid matrices for the incorporation of lipophilic bioactive compounds, such as free phytosterols (FP) in NLC.

The FP is considered a functional compound because it establishes a competitive mechanism during the absorption of cholesterol, reducing cholesterol blood levels, which is closely related to the prevention of cardiovascular diseases (VAIKOUSI et al., 2007). In the scientific literature, it is possible to find several studies demonstrating that regular consumption of FP is also related to the reduction of cancer risk (AWAD, CHINNAM, FINK, BRADFORD,

2007; LEONG et al., 2011a; LEONG et al., 2011b). However, FP has high crystallinity and low solubility in water (NICHOLS, Sanderson, 2003), so few FP products are available for consumption, mainly due to technological application issues.

It's important to take into account that when the raw materials involved in the processing of nanoparticles are oils and fats, the main points of studies are related to the crystallization behavior and lipid polymorphism. These properties are influenced by intrinsic and extrinsic factors, such as chemical composition, production process, thermal recrystallization conditions, among others. Conventional lipids, unlike purified materials, are composed of a variety of TAG groups with different requirements for nucleation energy, molecular diffusion, and the crystal network establishment for each application (SATO 2001; RIBEIRO et al. al. 2009a). The crystallization behavior and the polymorphic transitions of lipid materials at the nanoscale, for the development of LN, is still unclear, but it is directly related to the physical stability of LN.

The main objective of this work was to develop NLC with conventional raw materials from the fats and oils industry, such as soybean oil and fully hydrogenated soybean oil for the incorporation of FP. In addition, the crystallization and polymorphism of the lipid matrices and NLC were evaluated in order to verify the influence of these properties on the physical stability of LN. This NLC development approach, with vegetable oil and hardfats for incorporation of bioactive compounds, is totally unprecedented, giving the authors of this work a patent under the privilege of the invention under registration in the National Institute of Industrial Property - INPI (BR 10 2017 006471 9).

2. Materials and methods

2.1 Materials

Refined soybean oil (SO) was locally purchased, fully hydrogenated soybean oil (FHSO) was supplied by SGS (Piracicaba, SP, Brazil) and free phytosterols (FP) was a courtesy of a local production initiative. The emulsifiers used were deoiled soybean lecithin (SL) composed of 68-73% phosphatidylcholine and a hydrophilic-lipophilic balance (HLB) of 7.0 obtained from Solae[TM] Company (St. Louis, MO, USA), sorbitan monostearate - Span[®]60 (S60)

of HLB 4.7, from Sigma-Aldrich® and ethoxylated sorbitan monooleate - Tween®80 (T80) of HLB 15.0, donated by Croda (Campinas, SP, Brazil).

2.2 Methods

2.2.1. Fatty acid composition

The fatty acid composition of the lipid matrices was performed in triplicate by gas chromatography with capillary column according to the AOCS Ce 1f-96 method (AOCS, 2009). After esterification using Hartman and Lago (1973) method the fatty acid methyl esters were separated on Agilent DB-23 (50% cyanopropyl-methyl polysiloxane) column, dimensions 60 m, internal diameter: 0.25 mm, 0.25 µm film. Chromatographic conditions: oven temperature 110 °C – 5 min, 110 °C – 215 °C (5 °C/ min), 215 °C – 24 min; detector temperature: 280 °C; injector temperature 250 °C; carrier gas: helium; split ratio 1:50; injected volume: 1.0 µL. The qualitative composition was determined by comparing the retention times of the peaks with those of the respective fatty acid standards, while the quantitative composition was performed by peak area normalization, according to the recommendation of the cited method.

2.2.2. Triacylglycerol composition

The determination of the TAG composition was performed in triplicate by dissolving the sample in tetrahydrofuran (THF, 20 mg/mL) and injecting into a gas chromatograph equipped with DB-17HT Agilent Catalog 122-1811 capillary column (50% - phenylmethylpolysiloxane), with 15 meters length, 0.25 mm internal diameter and 0.15 µm film. Analysis conditions: split injection ratio 1:100; column temperature: 250 °C, programmed to 350 °C at 5 °C/min; carrier gas: helium, at a flow rate of 1.0 mL/min; injector temperature: 360 °C; detector temperature: 375 °C; injected volume: 1.0 µL. The identification of the TAG groups was performed by comparing the retention times, according to the procedures of Antoniosi Filho, Mendes, Lanças (1995) and the quantification of the groups was performed by peak area normalization as recommended by the authors.

2.2.3 Free phytosterols profile

To obtain the FP profile, the unsaponifiable matter was first extracted by the Ca 6a-40 method, and then, using the Ch 6-91 method, the sterol profile was determined, and the total sterol content was quantified by means of using internal standard α-cholestanol (1 mg/kg Sigma-Aldrich) (AOCS, 2009), procedures performed in triplicate. In summary: 5 g of FP sample was saponified under reflux with 50 ml of ethanolic 2 N KOH solution during 1h. The unsaponifiable compounds were then extracted with diethyl ether (3 x 80 mL) and the organic phase neutralized by washing with distilled water. The residue (unsaponifiable matter) was fractionated by silica thin layer chromatography (Si-TLC) using plates impregnated with potassium hydroxide. The plate was developed twice with a mixture of diethyl ether: hexane (65:35, v/v). The fraction of the sterols was scraped and extracted with hot chloroform and diethyl ether. The solution was evaporated, derivatized with 500 μL of the 1:3:9 (v / v / v) trimethylchloroxylan: hexamethyldisilazane: pyridine mixture and analyzed by GC. The gas chromatograph (Agilent 6890N, Agilent, Santa Clara, CA) was equipped with a low polar capillary column of fused silica ZB5 (poly (5% diphenyl-95% dimethyl) siloxane, of 30 m length, 0.25 mm i.d., and 0.25 μm film thickness, Zebron) and a flame ionization detector (FID). The oven program was adjusted isothermally at 265 ° C, with a 1:50 split ratio. Helium was used as the carrier gas at a flow rate of 1 mL.min^{-1}. The injector and detector temperatures were 300 °C. Quantitative determination was performed using the internal standard. Data were expressed as the total percentage of phytosterols in the sample, using the ratio of the internal standard peak area, and the total phytosterols peak area, according to the recommendation of the method. Peak identification was performed by calculation of the reaction time and comparison with the standard chromatogram. The FP profile was obtained by the ratio of each phytosterol peak area and the total phytosterols peak area.

2.2.4 Formulation of lipid matrices and lipid nanoparticles

The NLCs were prepared with 10% (m/m) of lipid phase and 90% (m/m) of the aqueous phase. The aqueous phase was composed of distilled water and 2% emulsifier according to Helgason et al. (2009), Qian et al. (2013) and Yang et al. (2014). Regarding the lipid phase, NLC was developed with lipid matrices composed of 50% of liquid lipid (SO) and 50% of solid lipid (FHSO). For NLC with the incorporation of the bioactive compound, the

liquid lipid was partially replaced by 30% FP. The emulsifiers LS, S60 and T80 were used separately in each formulation for evaluation of their individual behavior (Table 1).

Table 1. Lipid fase of nanoparticles formulations (corresponding to 10% of the total suspension) and high-pressure homogenization parameters

ID*	Lipid matrix (%)	Bioactive Compound (%)	Emulsifier	Pressure (bar)	Number of HPH cycles
NLC_{T80}	50 SO + 50 FHSO	-	T80	800	3
NLC_{S60}	50 SO + 50 FHSO	-	S60	800	3
NLC_{SL}	50 SO + 50 FHSO	-	SL	800	3
NLC_{T80}	50 SO + 50 FHSO	-	T80	800	5
NLC_{S60}	50 SO + 50 FHSO	-	S60	800	5
NLC_{SL}	50 SO + 50 FHSO	-	SL	800	5
$NLC + FP_{T80}$	20 SO + 50 FHSO	30 FP	T80	800	3
$NLC + FP_{S60}$	20 SO + 50 FHSO	30 FP	S60	800	3
$NLC + FP_{SL}$	20 SO + 50 FHSO	30 FP	SL	800	3
$NLC + FP_{T80}$	20 SO + 50 FHSO	30 FP	T80	800	5
$NLC + FP_{S60}$	20 SO + 50 FHSO	30 FP	S60	800	5
$NLC + FP_{SL}$	20 SO + 50 FHSO	30 FP	SL	800	5

*NLC - Nanostructured Lipid Carriers; NLC + FP - Lipid Carriers Nanostructured with Free Phytosterols; T80 - Formulation containing 2% of emulsifier Tween®80; S60 - Formulation containing 2% of emulsifier Span®60; LS - Formulation containing 2% of emulsifier soybean lecithin; HPH - high-pressure homogenization.

2.2.5. Preparation of lipid matrices and lipid nanoparticles

The preparation of the lipid matrices consisted of the mixture of the liquid lipids (SO), solids lipids (FHSO), and FP, according to each formulation, in Table 1. Each mixture was stirred, on a magnetic stirrer at 300 rpm for 2 minutes at 90 °C. Thereafter, they were conditioned under specific conditions, described in the sequence, for further characterization.

To obtain the NLC and NLC+FP, the lipid matrices were prepared with the subsequent addition of the aqueous phase containing the emulsifier, at the same temperature (90ºC). The pre-emulsion was obtained in Ultra Turrax IKA T18 Basic (Germany) for 3 minutes at 20,000 rpm. Then, the pre-emulsions were subjected to hot homogenization in high-pressure homogenizer (HPH) (GEA Niro Soavi, model: NS 1001L PANDA 2K, Italy) at 90 °C under two different conditions: 3 and 5 cycles of 800 bar (Table 1), according to Zimmermann, Müller, Mäder, (2000), Bunjes, Steineiger, Richter (2007) and Severino, Santana, Souto (2012). After the HPH process the obtained nanoemulsions were cooled to 5 °C for 24 hours for crystallization of the lipid fraction and obtaining the dispersions containing the NLC and NLC+FP, which were subsequently stored at 25 °C (QIAN et al., 2013 KUMBHAR, POKHARKAR, 2013, YANG et al., 2014). In Table 1 the formulations of the NLC and the

NLC+FP are described according to the emulsifier used: NLC T80 and NLC + FP T80 (2% of Tween®80 emulsifier); NLC_{S60} and $NLC+FP_{S60}$ (2% of Span®60 emulsifier); NLC_{SL} and NLC+ FP_{SL} (2% of SL emulsifier).

2.2.6. Drying processes of lipid nanoparticles

The nanoparticles obtained after HPH in aqueous suspension were submitted to two different drying processes: (a) Heating - the nanoparticles in aqueous dispersion were exposed for 24 h in a drying oven with air circulation at 40 °C (Q317M, Brazil); (b) Lyophilization - the aqueous dispersion containing the nanoparticles was first conditioning in ultrafreezer (-80 °C) for 24 h in order to freezing the aqueous phase, followed by lyophilization in lyophilizer (Liobras L101, Brazil), according to the method described by Zimmermann, Müller , Mäder (2000).

2.2.7. Thermal analysis of lipid matrices and lipid nanoparticles

The thermal analyzes were performed in the lipid matrices and in the NLC in aqueous dispersion using Transmission Differential Calorimetry (DSC) TA Instruments, model Q2000, coupled to the RCS90 refrigeration system (TA Instruments, Waters LLC, New Castle). The data processing system used was Universal V4.7A (TA Instruments, Waters LLC, New Castle), and the analysis conditions are described in the sequence.

Lipid matrices: The official method of AOCS Cj 1-94 (AOCS, 2009) was used, with a maximum the temperature changed from 80 ° C to 150 ° C due to the high melting point of FP. The conditions of analysis were: sample mass: ~ 10 mg; Crystallization events: 150 ° C for 10 min, 150 ° C to -40 ° C (10 °C /min); Melting events: - 40 °C for 30 min, - 40 ° C to 150 °C (5 °C/min.). The following parameters were used to evaluate the results: initial crystallization and melting temperatures (T_{ic} and T_{im}), peak crystallization and melting temperatures (T_{pc} and T_{pm}), enthalpies of crystallization and melting (ΔH_c and ΔH_m) and final temperature of crystallization and melting (T_{fc} and T_{fm}) (CAMPOS, 2005).

Lipid nanoparticles in aqueous suspension: Cooling-heating-cooling cycles (37-5-75-5 °C) adapted from AWAD et al. (2008), were used to study the crystallization behavior and stability. Approximately 10 mg of samples were packed in hermetic aluminum pans at 37 ° C shortly after HPH and were immediately analyzed under inert atmosphere (N2) under the

following conditions: start temperature 37 ºC cooling to 5 °C followed by heating to 75 °C and soon after being cooled again at 5 °C, using a constant rate of 10 ° C/min during all cycles. The following parameters were used to evaluate the results: initial crystallization and melting temperature (T_{ic} and T_{im}), peak crystallization and melting temperatures (T_{pc} and T_{pm}), recrystallization temperature (T_{prc}), enthalpies of crystallization and melting (ΔH_c and ΔH_m), enthalpy of recrystallization (ΔH_{rc}) and completion temperature of crystallization, melting and recrystallization (T_{fc}, T_{fm}, T_{frc}) (CAMPOS, 2005).

2.2.8. Particle size and Polydispersity Index (PDI) of the lipid nanoparticles

The particle size was obtained by means of the hydrodynamic diameter (Z-ave) in nanometers (d.nm) using dynamic light scattering (DLS) with a high-power laser in Zetasizer Nano NS equipment, Malvern, United Kingdom. The NLC and NLC+FP were evaluated in triplicate for the Z-ave and PDI after 24 hours and 15 days of the production process. The samples were diluted with distilled water to reduce the opalescence before the determinations. Data analyzes were performed using the software included in the equipment system.

2.2.9 X-ray diffraction analysis of lipid matrices and lipid nanoparticles

The X-ray diffraction (XRD) of matrices and the dried nanoparticles were determined according to the AOCS method Cj 2-95 (AOCS, 2009). Previously, the lipid matrices were melted at 130 °C, crystallized at 5 °C and stabilized at 25 °C for 24 hours in a temperature-controlled incubator. The measurements were carried out in a Philips diffractometer (PW 1710) using Bragg-Brentano (θ:2θ) geometry with Cu-kα rad radiation (λ= 1.54056 Å, 40 KV voltage and 30 mA current). The measurements were obtained at 25 °C with steps of 0.02° in 2° and acquisition time of 2 seconds, with scans of 1.8 to 40° (2° scale). The identification of the polymorphic forms of triacylglycerols was performed from the Short Spacing (SS) characteristic of the lipid crystals (AOCS, 2009).

2.3. Statistical analysis

Data were statistically analyzed by means of One-Way Analysis of Variance (ANOVA) with the Statistica (V.7) Software (Statsoft Inc., Tulsa, UK). The Tukey test was applied to determine the significant differences between the means, at a level of $p \leq 0.05$.

3. Results and discussion

3.1. Chemical characterization of the lipid phase

In the fatty acid composition of the SO, the predominant content of unsaturated fatty acids was 53.32% of linoleic acid (C18: 2), 23.38% of oleic acid (C18: 1) and 6.66% and linolenic acid (C18: 3). Regarding the saturated fatty acids, palmitic acid (C16: 0) and stearic acid (C18: 0), 10.70% and 4.26%, respectively (Table 2) were predominated. Similar values were reported by Ribeiro et al. (2009 b, c), but it is also possible to find SO with very broad ranges of unsaturated fatty acids, such as 48-59% linoleic acid, 17-30% oleic acid and 4,5-11% linolenic acid (REGITANO-D'ARCE, VIEIRA, 2009).

Table 2. Fatty acid composition of soybean oil (SO) and fully hydrogenated soybean oil (FHSO).

Fatty acids (%)	SO[a]	FHSO [a]
C16:0 - Palmitic acid	10.70±1.12	11.22±0.50
C16:1 - Palmitoleic Acid	0.09±0.02	-
C18:0 - Stearic Acid	4.26±0.26	87.11±0.06
C18:1 - Oleic Acid	23.38±0.96	-
C18:2 - Linoleic Acid	53.32±0.58	-
C18:3 - Linolenic Acid	6.66±0.10	-
C20:0 - Arachidonic acid	0.41±0.03	0.60±0.18
C22:0 - Behenic acid	-	0.75±0.28
Σ Saturated	15.83	100
Σ Unsaturated	83.45	<1

[a] Average of three replicates ± Standard Deviation. Values below of 0.2% were omitted from the table.

During the process of total hydrogenation of oils, the unsaturated fatty acids are transformed into saturated fatty acids (WANG, 2002). Thus, the high content of stearic acid (C18:0) found as a major in FHSO is a consequence of the complete hydrogenation process of soybean oil, which naturally contains high concentrations of unsaturated fatty acids with 18 carbons (O'BRIEN, 2009). The FHSO presented, therefore, 87.11% of stearic acid (C18:0), 11.22% of palmitic acid (C16:0), with small proportions of arachidonic and behenic acids (Table 2). Metabolically, stearic acid is basically used as an energy source, with no influenced the metabolism of hormones, prostaglandins, and leukotrienes. In addition, it has no adverse effect on the risks of cardiovascular diseasesie, it has no atherogenic effect (MARANGONI, ROUSSEAU, 1995; O'BRIEN, 2009). The TAG composition consists of the arrangement of the fatty acids in the glycerol molecule. Table 3 shows the SO and FHSO TAG compositions. The TAG composition, from the technological point of view, is extremely important for the

understanding of the phenomena involved in the crystallization of fats and oils since different TAGs present different crystallization and fusion behavior (BUCHGRABER, ULBERTH, EMONS, & ANKLAN, 2004).

Table 3. Triacylglycerols composition of soybean oil (SO) and fully hydrogenated soybean oil (FHSO).

NC	TAG	SO (%)	FHSO (%)
50	PPS	-	3.19±0.35
	POP	1.58±0.35	-
	PLP	4.63±0.39	-
52	PSS	-	28.84±0.92
	POS	1.03±0.10	-
	POO	6.52±0.54	-
	PLO	13.25±1.13	-
	PLL	19.28±1.86	-
	PLnL	2.39±0.69	-
54	SSS	-	66.21±1.46
	SOO	1.30±0.77	-
	SLO	2.25±0.28	-
	OLO	2.51±0.50	-
	OLL	11.55±0.91	-
	LLL	17.35±1.10	-
	LLnL	18.83±1.21	-
	LLnLn	2.59±0.38	-
56	SSA	-	0.49±0.28
58	SSBe	-	1.28±0.09
Total		**100**	**100**

NC - Number of carbons; P = palmitic acid; S = stearic acid; O = oleic acid; L = acid linoleic; Ln = linolenic acid; A = acid arachidonic; Be = behenic acid
-: not detected.

The SO had 14 TAG species while in the FHSO only 5 were found. The predominant TAGs in the SO were PLO, PLL, OLL, LLL, and LLnL, corresponding to 80.26% of the total content, whereas in FHSO only PSS (28.84%) and SSS (66.21%) were found, as expected. In the literature, similar values are observed for the same TAGs in FHSO, varying between 90 and 95% of the total TAG content (HUMPHREY AND NARINE, 2004; RIBEIRO et al., 2009b).

The FP composition was determined only in the lipophilic bioactive compound since in the other lipidic components this content is irrelevant, less than 1% (GÓMEZ-COCA, PÉREZ-CAMINO, MOREDA, 2015). Table 4 shows the FP profile of the bioactive compound incorporated in LN. FP is 98% pure and the components with the highest concentrations were

β-sitosterol, stigmasterol, and campesterol, with contents of 44.05, 26.77 and 23.53%, respectively.

Table 4. Sterols profile of the bioactive compounds loaded in the lipid nanoparticles

Composition of free phytosterols	(%)[a]
Colesterol	0.60±0.02
Brassicasterol	0.30±0.01
Campesterol	23.56±0.23
Campestanol	0.66±0.11
Stigmasterol	26.77±0.22
Δ-7-Campesterol	0.78±0.04
Δ-5,23- Stigmastadienol	0.48±0.01
β-Sitosterol	44.05±0.15
Sitostanol	1.18±0.08
Δ-5-Avenasterol	0.84±0.04
Δ-5-24-Stigmastadienol	0.14±0.01
Δ-Stigmastenol	0.47±0.02
Δ-7-Avenasterol	0.68±0.01
Total of phytosterols	98.00

[a]Average of three replicates ± Standard Deviation.

3.2. Thermal characterization of lipid matrices

Crystallization curves were obtained by DSC for the lipid bases and their mixtures containing SO, FHSO, emulsifiers (LS, T80, and S60) and the bioactive compound (FP). In Figure 1, the exothermic heat flux is plotted as a function of temperature. The crystallization parameters obtained from the thermal curves are shown in Table 5. The selected parameters include: initial crystallization temperature (T_{ic}), which refers to the beginning of the phase transition; peak crystallization temperature (T_{pc}), where the thermal effect is maximal; (ΔH_c), measured by the area of the curve, and final crystallization temperature (T_{fc}), which indicates the conclusion of the thermal effect (RIBEIRO et al., 2009a).
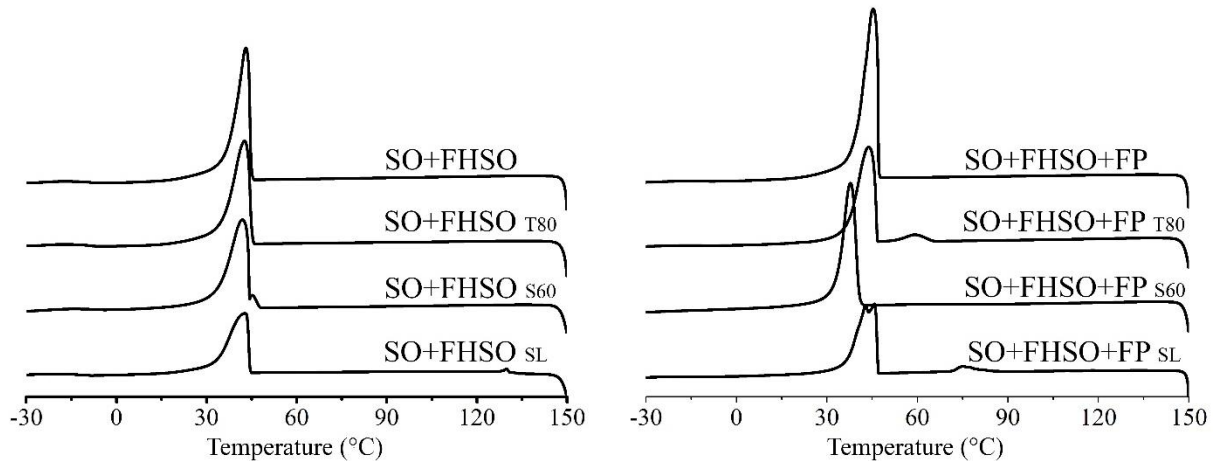
Fig. 1. Crystallization behavior obtained from differential scanning calorimetry (DSC) of the lipid matrices composed by soybean oil (SO) and fully hydrogenated soybean oil (FHSO) and their mixtures containing the three different emulsifiers (soybean lecithin - SL, polyethoxylated sorbitan monooleate - T80 and sorbitan monostearate - S60) and free phytosterols (FP), by cooling from 150 to - 40 °C for samples with FP and by 80 to - 40 °C for others lipid matrices.

Tabela 5. Crystallization behavior of the FHSO, FP and pure lipid matrices and in the presence of emulsifiers and FP, used in the production of NLC. Initial crystallization temperature (T_{ic}), peak crystallization temperature (T_{pc}), enthalpy of crystallization (ΔH_c) and final crystallization temperature (T_{fc})

Samples	T_{ic} (°C)	T_{pc} (°C)		ΔH_c (J/g)		T_{fc} (° C)
		Peak 1	Peak 2	Peak 1	Peak 2	
FHSO	50.41	47.75	nd*	123.40	nd	25.91
FP	126.41	126.37	nd	41.96	nd	119.72
SO+ FHSO	44.83	43.09	nd	72.76	nd	19.70
SO+ FHSO$_{T80}$	45.47	43.03	nd	67.16	nd	19.89
SO+ FHSO$_{S60}$	43.48	41.68	nd	61.46	nd	17.29
SO+ FHSO$_{SL}$	43.69	42.09	nd	41.75	nd	18.36
SO+ FHSO+FP	47.13	45.34	nd	94.93	nd	20.94
SO+ FHSO+FP$_{T80}$	65.06	59.06	43.48	44.42	52.12	49.13
SO+ FHSO+FP$_{S60}$	40.17	38.57	nd	56.28	nd	21.05
SO+ FHSO+FP$_{SL}$	81.25	75.13	45.06	31.29	44.27	70.52

* nd, not detected.

3.2.1. Crystallization behavior of the lipid matrices

The SO was liquid at room temperature and during NLC production, because it is composed mainly of the unsaturated fatty acids, linoleic and oleic, which present low melting points (RIBEIRO et al., 2009b). Therefore, the SO is a suitable raw material for use as liquid lipid in NLC and of great potential for application in these systems, replacing synthetic liquid lipid matrices in terms of cost and regulatory aspects in the food area.

In the crystallization of FHSO, only one peak was observed, reaching maximum crystallization at 47 °C. This behavior was also reported by RIBEIRO and coworkers (2013), it's directly related to the chemical composition since FHSO is composed of approximately 87% of stearic acid. In this way, the FHSO proved to be a compatible lipid material for application in NLC as the solid lipid fraction. Several authors have reported that lipid mixtures rich in stearic acid represent raw materials of great importance for LN composition since they have a melting point higher than body temperature and also because stearic acid is considered metabolic neutral (MENSINK, et al., 2004).

The mixture of these two lipid components, in the proportion of 50% of SO and 50% of FHSO, showed Toc of 43.09 °C. This indicates it as a promising lipid matrix for the development of NLC, with also possibilities for the incorporation of bioactive compounds, providing protection during transport and delivery in the TGI. As Yoon, Park, Yoon (2013) reported, the combined use of solid and liquid lipid fractions in LN is important to maintain structural and stability characteristics, but this mixture should have a melting point higher than the body temperature. In addition, for incorporation of active compounds, the use of both liquid and solid lipid mixture is positive, since it allows the elaboration of a lipid matrix with a low crystallinity degree, offering more spaces to accommodate the bioactive compound (Garzon et al. al., 2009, TAMJIDI et al., 2013). Furthermore, Müller et al. (2002) have also cited that the low crystalline packing and stiffness of the particle structure minimize the undesired expulsion of the bioactive compound during possible polymorphic transitions.

3.2.2. Crystallization behavior of the active compound loaded in the lipid nanoparticles

Knowledge of the crystallization and physical stability of bioactive compounds, such as FP, is extremely important to evaluate its potential for use as functional ingredients in food products. In Figure 2, the crystallization and melting curves of FP can be observed during cooling cycles up to -40 °C and heating up to 150 °C, and Table 5 shows the main parameters involved during the thermal phenomena.

A peak crystallization was observed, with Tpc of approximately 126°C and a melting peak at 137.94 °C, indicating that the predominant fraction of the FP components have similar crystallization and melting properties (Table 5). However, between 50 and 60 °C, some exothermic and endothermic transitions were observed, but at low intensities (Figure 2). Vaikousi et al. (2007) observed similar events with peaks close to 60 °C and also 97 and 105 °C. According to these authors, these thermal events may be related to the loss of hydration water from the crystals remained from the FP obtaining procePss, that undergoes repeated washes with aqueous solutions. Firstly, a part of the hydration water is lost and semi-hydrated crystals are formed (below 60 °C), while the remainder of the hydration water leaves the crystal at approximately 90 °C.
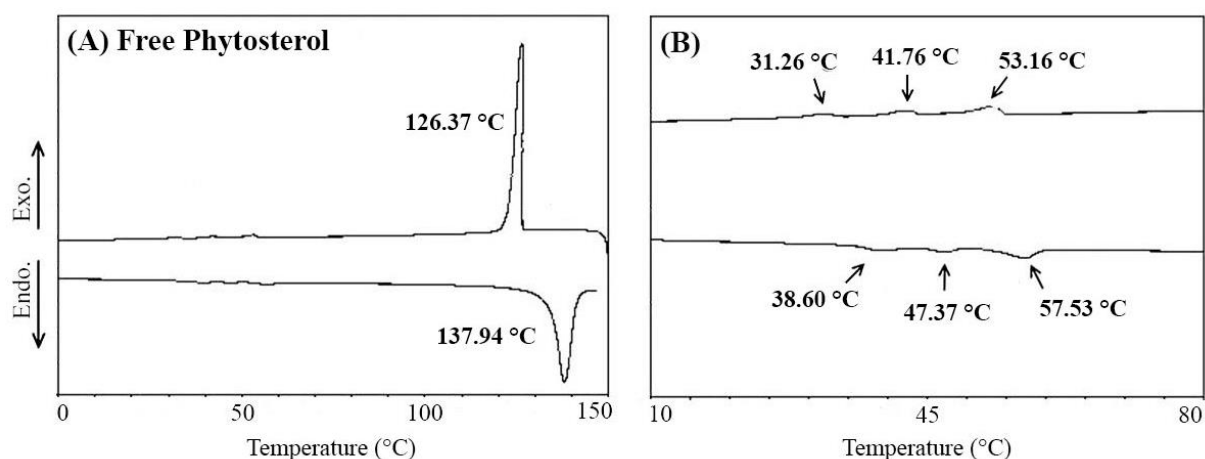
Fig. 2. Crystallization and melting curves of the free phytosterols (A) and zoom of the region with peaks of lower intensities (B), obtained by differential scanning calorimetry (DSC).

As seen, FP has a high melting point, and, in addition, they present a water insolubility, characteristics that result in the great technological challenge for food applications. As reported by Vaikousi et al. (2007) in their studies, the direct delivery of FP in food is considered a technological challenge, since the high crystallinity/insolubility can often become a restrictive factor for the physical stability of several products.

Thus, the incorporation of FP into NLC can be a viable alternative for the enrichment of several food products. In NLC the FP are solubilized in the lipid matrix and assume a different physical behavior, as can be observed in Figure 1 and Table 5, discussed below.

3.2.3. Lipid matrix crystallization behavior in the presence of the active compound

FP were incorporated in the proportion of 30% in the lipid matrix, composed of 50% of FHSO and 20% of SO. Only one crystallization peak was observed, with Toc of 45.34øC. Thus, it is affirmed that FP was incorporated by the Plipid matrix, with the crystallization peak not being observed at approximately 126 °C, confirming its complete co-crystallization in the lipid matrix, as set forth in Table 5. Furthermore, evaluating the impact of the FP in the lipid matrix crystallization, it's possible to observe that the crystallization peak present in the thermogram varies in position, shape, and magnitude. Analyzing the parameters in Table 5, it can be seen that the addition of FP to the lipid matrix resulted in the acceleration of the crystallization start at approximately 2 °C and there was an increase of the enthalpy of crystallization from 72.76 to 94.93 J/g. Thus, it was observed that the inclusion of FP in the lipid matrix, can also contribute to the increase of the thermal resistance of the NLC.

3.2.4. Influence of emulsifiers on the crystallization behavior of lipid matrices

We analyzed the effects of adding 2% of emulsifiers in different lipid matrices used for the production of NLC and NLC+FP. It was noted that the T80 did not interfere in the Tpc of the lipid matrix composed of SO and FHSO. While S60 and LS promoted a reduction of approximately 1 °C in the crystallization events, described in Table 5, which can be considered insignificant for process purposes.

In adition, small influences of the emulsifiers were observed at the T_{oc} of the mixtures containing SO and FHSO (44.83 °C), the presence of T80 delayed the initial crystallization to 45.47 °C, while S60 and LS have anticipated the crystallization event to 43.48

and 43.69 °C respectively (Table 5). More pronounced changes were observed in the crystallization enthalpies when comparing the lipid matrix composed by only the lipid matrices and the same samples in the presence of emulsifiers T80, S60 and LS; noticeable reductions can be noticed in crystallization enthalpies from 72.76 to 67.16, 61.46 and 41.65 J/g respectively. In the exothermic process, the energy released to occur the phase change in the lipid mixture was lower when in the presence of SL than in the presence of other emulsifiers.

In lipid matrices containing FP, were also observed changes in the crystallization behavior with the addition of emulsifiers. In the lipid matrices containing T80 and SL, two crystallization peaks were observed, with different intensities, the second being more intense than the first (Figure 1). This effect may be related to the possible induction of FP crystallization, caused by the presence of emulsifiers. The acceleration of crystallization was observed through the T_{pc} for peak 1 of each sample, from 45.34 °C to 59.06 and 75.13 °C, for T80 and SL respectively. However, the higher phase transitions were observed in the second peaks, which presented higher values for the crystallization enthalpy (Table 5). A different behavior was verified in the presence of S60, in which the crystallization curve showed only one peak (Figure 1); the values obtained for T_{oc} and T_{pc} indicate that this emulsifier has delayed the crystallization of the lipid matrix in the presence of FP and the enthalpy of crystallization was not affected (Table 5).

Differentiated behaviors were observed during the crystallization of the lipid matrices evaluated in this study when in the presence of emulsifiers. The results are in agreement with those related in the literature, which indicates that the presence of certain emulsifiers interferes with the crystallization behavior of lipid materials, slowing or speeding up this process (MASUCHI et al, 2014; Oliveira et al, 2015; Domingues et al., 2016). In addition, it is important to note that all the lipid matrices evaluated have presented thermal characteristics that make feasible its use for the development of NLC and NLC+FP.

3.3. Processing of lipid nanoparticles

The pre-emulsification method followed by HPH, used for the production of NLC and NLC+FP, proved to be efficient for the systems developed in this study. It was possible to obtain NLC with desirable colloidal characteristics using 3 and 5 cycles of homogenization at 800bar, according to results presented and discussed in the following topic.

It is important to highlight that, the emulsifiers used in the nanoparticle formulations combined with the production method, have a great influence on the obtention, viability, and stabilization of the aqueous dispersions. It was observed that the LS emulsifier was not compatible with the FP containing formulation since during the pre-emulsion stage the system showed high viscosity limiting processing in HPH. The other systems remained liquid and were submitted to HPH, with no viscosity increase during processing.

3.4. Particle size and Polydispersity Index (PDI) of the lipid nanoparticles

Z-ave and particle size distribution (PDI), are important properties for LN characterization. The determination of Z-ave is fundamental, mainly, for scientific and technological reasons, such as, to characterize and confirm if that the desired dimensions were obtained after the processing, and especially if they are maintained during storage (McClements, 2013, TAMJIDI et al., 2013). Table 6 shows the Z-ave and PDI of NLC and NLC+FP obtained through 3 and 5 cycles of HPH, evaluated after 24 hours and 15 days of production, developed with T80, S60 and SL.

In Figure 3 and 4, it is possible to observe the particle size distribution expressed according to intensity ($I\alpha d^6$) and number ($N\alpha d$), for the systems developed with 3 and 5 cycles of HPH. The results were expressed in terms of scattered light intensity, I distribution, the proportional diameter to the sixth power ($I\alpha d^6$), and in terms of the number of particles, N distribution, proportional to the predominant diameter in the sample ($N\alpha d$).

The NLC T80 and NLC+FP$_{T80}$ obtained at 3 and 5 cycles, analyzed after 24 hours of production, had a Z-ave of approximately 164 nm, with no significant difference (at a 5%) between them. It was noted that the increase in the number of cycles (from 3 to 5 cycles) of homogenization did not interfere in the Z-ave. However, it was effective in reducing the PDI without the inclusion of the bioactive compound, ranging from 0.176 ± 0.009 to 0.165 ± 0.007, as can be observed in Table 6. Similar behavior was observed for the NLC$_{SL}$ evaluated during 24 hours of processing, in which no significant differences were observed for both parameters in 3 and 5 cycles.

Table 6. Particle size in hydrodynamic diameter (d.nm) and polydispersity index of NLC and NLC+FP evaluated after 24 hours and 15 days of production using 3 and 5 cycles of high pressure homogenization

Samples*	Z-ave (d.nm)**	PDI**
3 Cycles de HPH – 24 h		
NLC $_{T80}$	167.34±0.13^j	0.176±0.009^{de}
NLC $_{S60}$	283.30±5.31^{cd}	0.424±0.056^{abcd}
NLC $_{LS}$	250.20±3.21^{efg}	0.346±0.006^{abcde}
NLC+FP$_{T80}$	164.97±1.98^j	0.235±0.006^{cde}
NLC+FP$_{S60}$	437.60±22.54^b	0.485±0.086^{ab}
NLC+FP$_{SL}$	-	-
3 Cycles de HPH - 15 days		
NLC $_{T80}$	161.15±0.44^j	0.170±0.002^e
NLC $_{S60}$	215.47±7.41^{hi}	0.212±0.012^{de}
NLC $_{LS}$	271.80±2.32^{cde}	0.373±0.005^{abcde}
NLC+FP$_{T80}$	160.98±1.95^j	0.254±0.019^{bcde}
NLC+FP$_{S60}$	297.60±7.84^c	0.481±0.071^{abc}
NLC+FP$_{SL}$	-	-
5 Cycles de HPH – 24 h		
NLC$_{T80}$	160.79±0.74^j	0.165±0.007^e
NLC$_{S60}$	259.80±1.63^{def}	0.304±0.020^{bcde}
NLC$_{SL}$	228.47±0.38^{ghi}	0.330±0.005^{bcde}
NLC+FP$_{T80}$	163.69±2.80^j	0.269±0.021^{bcde}
NLC+FP$_{S60}$	681.70±15.11^a	0.590±0.244^a
NLC+FP$_{SL}$	-	-
5 Cycles de HPH - 15 days		
NLC$_{T80}$	155.38±1.00^j	0.144±0.011^e
NLC$_{S60}$	211.00±1.88^i	0.170±0.004^e
NLC$_{SL}$	241.00±2.24^{fgh}	0.342±0.110^{bcde}
NLC+FP$_{T80}$	154.82±1.20^j	0.246±0.012^{bcde}
NLC+FP$_{S60}$	288.30±5.14^c	0.307±0.090^{bcde}
NLC+FP$_{LS}$	-	-

* NLC: nanostructured lipid carriers - containing 2% T80 emulsifier: Tween®80; S60: Span®60 and LS: Soy lecithin; ** Values represent the average of three replicates ± standard deviation. Different letters in the same column indicate significant differences by the Tukey test at the 5% probability level (p≤0.05).
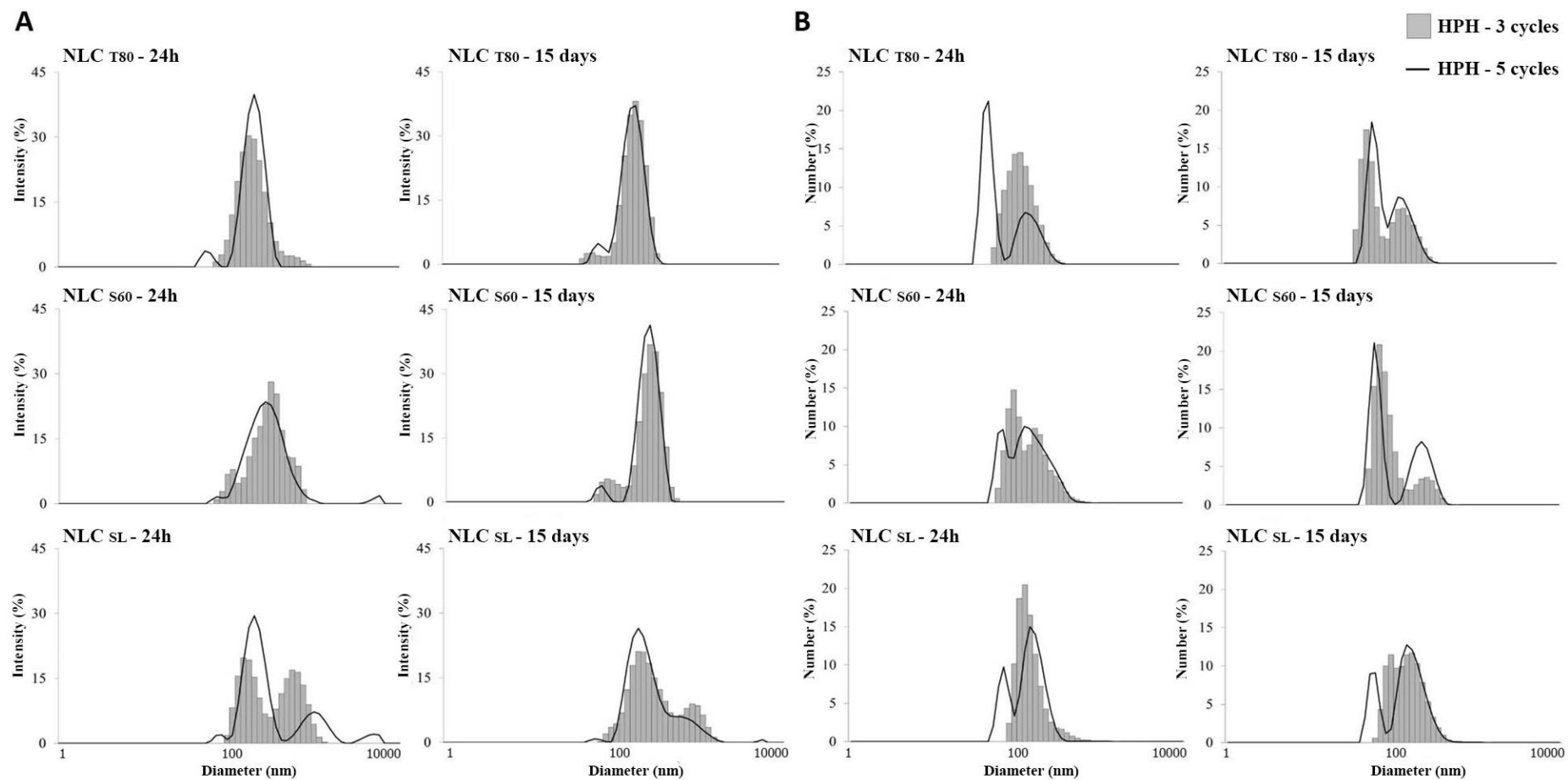
Fig. 3. Hydrodynamic particle size distribution (d.nm) of the NLC with different emulsifiers: T80; S60 and SL, submitted to 3 and 5 cycles of high-pressure homogenization (HPH), analyzed after 24 h and 15 days of production, expressed as (A) intensity ($I\alpha d^6$) and (B) number ($N\alpha d$).
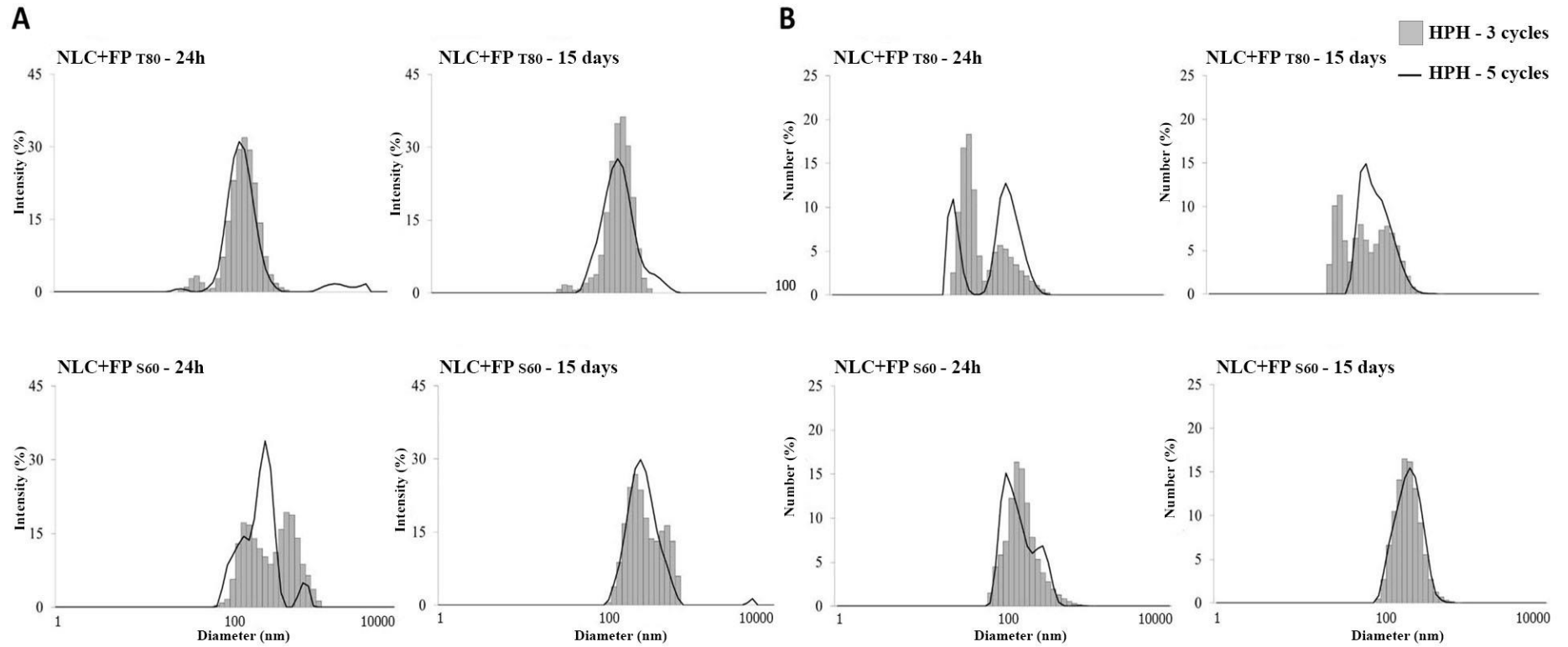
Fig. 4. Hydrodynamic particle size distribution (d.nm) of the NLC+FP developed with different emulsifiers: T80; S60 and SL, submitted to 3 and 5 cycles of high-pressure homogenization (HPH), analyzed after 24 h and 15 days of production, expressed as (A) intensity (Iαd^6) and (B) number (Nαd).

The NLC$_{S60}$ submitted to 3 and 5 cycles of HPH, evaluated after 24 hours of processing, was not different (p≥0.05), presenting approximately 321 and 254 nm Z-ave and PDI of 0.4 and 0.3, respectively. The use of S60 in NLC+FP produced from 3 and 5 cycles of HPH caused a significant increase (p≥0.05) of Z-ave, which varied between 392 and 534 nm, respectively, as well as the PDI that assumed values above 0.4 (Table 6). Therefore, it has been observed that the use of a greater number of HPH cycles for FP-containing system was not suitable. According to Tamjidi et al. (2013), the PDI is related to the physical stability of LN; PDI values should be in the range of 0.1 to 0.25 to provide dispersions with long-term stability, and values above 0.5 indicate very broad particle size distribution, characterizing low physical stability.

Engel and Schubert (2005) evaluated three different systems with tristearin, triolein, and Miglyol®840 (decanoic acid) containing 2.0% SL as crystallization inhibitor and 2.5% FP, dispersed in the aqueous phase containing 1.0% Tween®20 in HAP at 1000 bar. The Z-ave obtained for each system was 131 nm, 100 nm, and 102 nm, respectively. The authors reported that FP had little influence on Z-ave while they are dispersed in the oil phase, however, when they come in contact with the aqueous phase, the crystallization of FP occurs and the Z-ave of the particles increases significantly, destabilizing the system (Table 6).

In addition, in order to verify the physical stability of the lipid particles over time, particle size and PDI evaluations were performed after 15 days of storage at 25 ° C. The systems developed with the T80 emulsifier, both in the presence and absence of FP, remained stable without significant difference (p≥0.05) for Z-ave and PDI after 15 days. In the systems developed with S60 and LS, there were more pronounced differences (p≥0.05) can be noticed in Z-ave and PDI. In general, reductions in Z-ave of the particles were observed, with consequent reduction of PDI. It should be noted that this behavior was positive for the nanoparticles developed with S60, as can be observed in Figure 4, mainly in relation to the number distribution of particles (Nαd), presenting a more uniform behavior. The most relevant results were obtained for the NLC+FP$_{S60}$ developed with 5 cycles of HAP, showing a reduction of Z-ave from 681.70 to 288.30 nm and PDI from 0.590 to 0.307, after 15 days. Even so, by the value of PDI above 0.25, this system is still susceptible to destabilization.

This behavior, related to reductions in Z-ave of the particles, has been already reported by other research groups. According to Salminen (2013) and coworkers, these Z-ave reductions commonly occur in nanostructured lipid systems developed with fully saturated TAGs, being closely related to polymorphic transitions. The authors have mentioned that the polymorphic transition tends to reach equilibrium and the transition to the more stable polymorphic form ends up occurring. In addition, the authors state that if the system is exposed to temperature changes during storage the polymorphic transition is can be easily induced.

The distributions presented in Figure 3 show that for NLC_{T80} and NLC_{S60} the size differences between cycles occurred within 24 hours, with similar distributions in 15 days, as observed in I distributions. In both cases, there was a predominance of the population with diameters between 80-100nm, according to N distribution. For the NLC_{SL}, the behavior of the I distribution was similar, but for both cycles the populations of 80-100 and 100-200nm predominated, indicating a higher polydispersity. The incorporation of the FP caused changes in the distributions in both cycles (Figure 4). In this case, the greatest difference was the predominance of a single population with diameters between 100 and 200nm, according to N distributions. Therefore, as observed from the results obtained, polymorphic transitions possibly occurred during the 15 days of storage for all developed systems. It should be noted that the emulsifier T80 provided the best results in the stabilization of developed nanoparticles.

3.5 Thermal behavior of lipid nanoparticles

In Figure 5A, can be found the thermograms of the lipid matrices used for the production of the NLC and NLC+FP with the emulsifier T80 obtained by crystallization (75 to 5 °C) and melting (5 to 75 °C). In addition, in order to evaluate the thermal behavior of lipids at the nanoscale, the aqueous dispersions containing the NLC and NLC+FP were also evaluated in DSC, through cycles of crystallization, melting and recrystallization (37-5-75-5 °C), the thermograms are shown in Figure 5B.
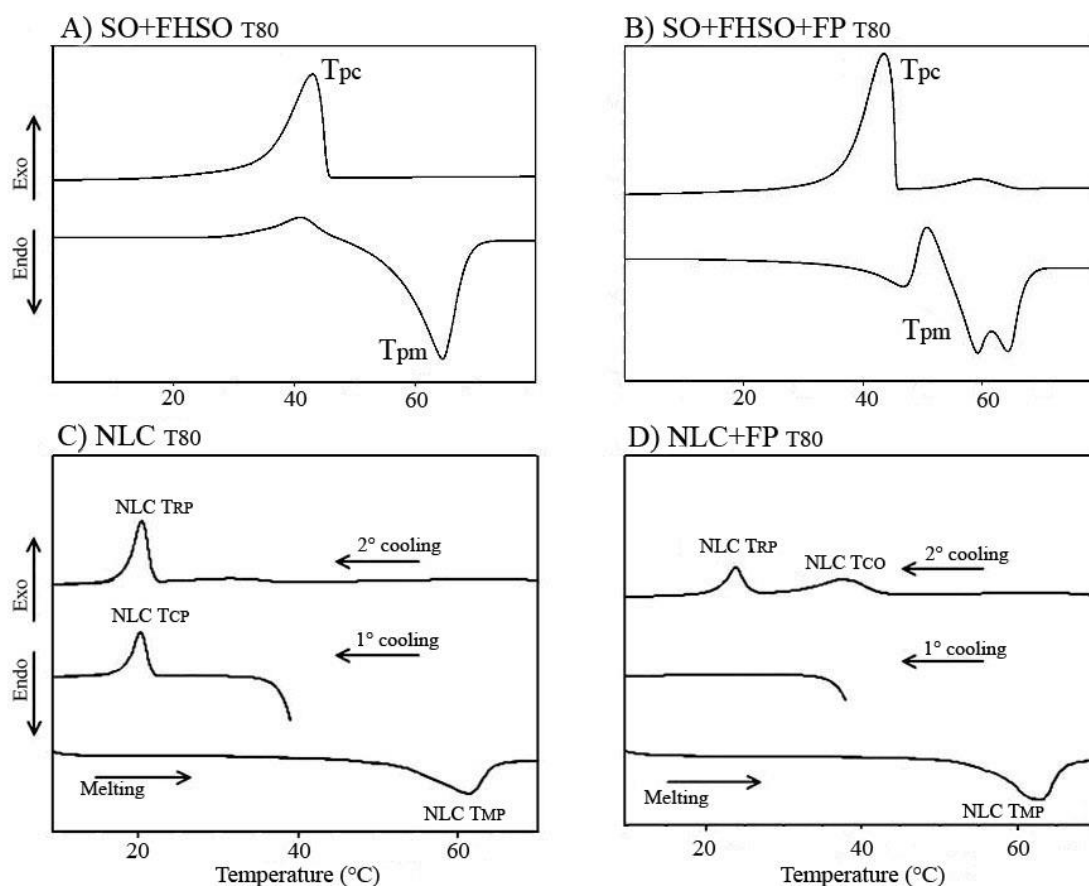
Fig. 5. DSC thermograms of: A) Lipid matrix and B) Lipid matrix with free phytosterols using temperature cycles of 75-5-75 °C; C) NLC$_{T80}$ and D) NLC+FP$_{T80}$ using temperature cycles of 37-5-75-5 °C. All cycles with a crystallization and melting rates of 10 °C/min. Where: Tpc = Maximum crystallization temperature of the lipid matrices; Tpm = Maximum melting temperature of the lipid matrices; CLN T$_{PC}$ = Maximum crystallization temperature; CLN T$_{PM}$ = Maximum melting temperature; CLN T$_{PR}$ = Maximum recrystallization temperature; CLN T$_{CO}$ = Maximum lipid coalescence temperature.

During the first NLC cooling cycle, an exothermic peak was observed at 20.09 °C (NLC T$_{pc}$), approximately 23 °C lower than the Tpc of the lipid matrix used for the production of the lipid nanoparticles (T$_{pc}$ = 43.03 °C) (Figure 5A). Similar results were obtained by Awad et al. (2008) in a study with SLN in aqueous suspension, composed of tripalmitin and Tween®20 as the emulsifier, using the same crystallization rate (10 °C/min). The authors have observed that the lipid matrix has crystallized at a higher temperature (T$_{pc}$ = 39 °C) than the corresponding NLS (T$_{pc}$ = 19 °C). Walstra (2003) explains that the conventional crystallization of macroscale materials generally occurs through the heterogeneous nucleation process, from the presence of catalytic impurities, such as monoacylglycerols in lipids. It is considered that the presence of these impurities favors the initial of crystallization. However, in emulsified

systems, such as SLN and NLC, crystallization becomes more difficult since the lipid material is finely divided into tiny droplets. Thus, the crystallization occurs into each droplet and the probability of being modulated by impurities is reduced. Thus, crystallization is not propagated as in a continuous lipid matrix, being necessary to use lower temperatures to initiate lipid crystallization in LN.

In the NLC+FP no crystallization peak was observed during the first cooling cycle (Figure 5D). It has been noted that the crystallization behavior of this system is different, probably because of the presence of FP. As can be seen in Figure 5A, in the lipid matrix containing FP two crystallization peaks were observed, one of lower intensity at 59.06 °C and the other at 43.48 °C. This early crystallization of the components that crystallized at higher temperature, is represented by the FP and possibly trisaturated TAG of the lipid matrix. These components have may act as crystallization inducers inside the droplets, favoring the crystallization and concluding the NLC phase transition (liquid-solid) at temperatures above 37 °C. During the NLC heating cycle, only one endothermic peak was observed at 61.39 ° C, as well as the corresponding lipid matrix. In the NLC+FP, also only one melting peak was observed, at approximately 63 °C. However, two endothermic peaks were observed in the lipid matrix, one at approximately 48 °C, followed by another crystallization peak at 60-70 °C. It was observed that this last peak had two maximum points, at 60 and 65 °C approximately, they probably are associated with the polymorphic transition in the lipid matrix from β'-form to the more stable β-form. Generally, endothermic peaks can be used to suggest about the polymorphic forms of TAGs, but these can be only confirmed by the XRD analysis discussed in the next topic.

In the second cooling cycle, performed after the melting, the peaks observed in the NLC+FP maintained a similar behavior to the lipid matrix. In addition, it was also found that the phase transition occurred at lower temperatures during this recrystallization compared to the crystallization of the lipid matrix. For NLC a different bePhavior was noticed during the second cooling cycle. Two recrystallization peaks were observed, one of lower intensity at approximately 38 ° C, which may be related to the destabilization of some LN after the melting process. This phenomenon was also observed in the research developed by Awad et al. (2008). The authors reported that when the NLS composed of tripalmitin was cooled for the second time, two exothermic peaks were observed at approximately 19 and 39 °C. The peak at 19 °C

was attributed to crystallization of NLC, while the peak at 39 ° C was attributed to a system destabilization. Thus, the first peak (39 ºC) was attributed to the crystallization of tripalmitin, which may be contained in large (coalesced) droplets.

Even though, it should be noted that the higher intensity recrystallization peak (NLC Tpr) observed in the NLC was very close to the peak observed in the first cycle (NLC Tpc = 20.23 °C and NLC T_{pc} = 20.09 °C, respectively), indicating a high stability of the NLC system. This NLC stability was confirmed in the evaluation of Z-ave and PDI after 15 days from processing, as already discussed.

3.6. X-ray diffraction analyses of lipid matrices and lipid nanoparticles

The X-ray diffraction (XRD) technique is widely used to determine the crystalline polymorphic forms of TAGs. These materials have the ability to exist under various crystalline forms. The most common types of TAG packaging are hexagonal, orthorhombic and triclinic, which are designated as the crystalline forms, α, β' and β, respectively. The lipids are considered monotropic, which is a transition process in different polymorphic forms until reaching the most stable ($\alpha \rightarrow \beta' \rightarrow \beta$) (SATO, 2001).

In Table 7 can be found the SS and the polymorphic forms of the lipid matrices, NLC, and NLC+FP, after drying processes of lyophilization and in the oven and. In Figure 5 the diffractograms obtained by XRD are presented. It should be noted that the soybean oil is liquid at the analysis temperature, making it impossible to characterize by XRD. In addition, the XRD analyzes were performed for the LN obtained with 5 cycles of HPH, since they were the ones that presented the best results of Z-ave and PDI, as previously discussed.

In the results of the characterization of the raw materials through XRD, it was possible to observe FHSO a high-intensity peak for FHSO, with SS at 4.15 Å, which is characteristic of the α form (Figure 6A). For the FP, evaluating from the point of view of theta-2theta system (θ:2θ) a series of peaks was identified: 5.20, 12.18, 12.80, 15.08, 15.80, 16.92, 17.86, 18.64, 19.70, 20.88, 21.82, 22.96, 24.06 and 25.28 Å. Among these, the peaks of higher intensities were highlighted in Figure 5E and were similar to those found by Vaikousi et al. (2007). It should be noted that some diffraction peaks are very similar to those used for the identification of the TAG polymorphs. The atoms of the TAG molecules have regular distances between them, already established and well documented in the scientific literature, allowing the

identification of polymorphic forms α in 0.41 nm, β' in 0.42 and 0.38 nm and β with high peak intensity at 0.46 nm and lower intensity at 0.38 and 0.37 nm (SATO, 2001). For this reason, depending on the percentage of FP incorporated in lipid matrices and NLC, the FP can interfere in the identification of the polymorphic forms of the TAG.

Table 7. Triacylglycerols polymorphic forms, short spacings and peak intensities in the diffractogram from lipid matrices and NLC obtained through 5 cycles of HPH, heated (oven dried) and lyophilized

Lipid matrix	*Short spacing* (nm)					TAG Polymorphic form
	0.46	0.41	0.42	0.38	0.36	
FHSO	-	0.406 s	-	-	-	α
SO+ FHSO	0.443 M	-	0.412 M	0.370 M	-	$\beta' + \beta$
SO+ FHSO+FP	0.449 M	-	0.414 S	0.371 M	0.362 VW	$\beta' + \beta$
SO+ FHSO$_{T80}$	0.445 M	-	0.412 M	0.373 M	0.361 VW	$\beta' + \beta$
SO+ FHSO$_{S60}$	0.442 M	-	0.411 M	0.372 M	-	$\beta' + \beta$
SO+ FHSO$_{SL}$	0.447 F	-	0.412 M	0.375 M	0.362 W	$\beta' + \beta$
SO+ FHSO+FP$_{T80}$	0.450 M	-	0.414 S	0.377 M	0.365 VW	$\beta' + \beta$
SO+ FHSO+FP$_{S60}$	0.449 VW	-	-	0.380 M	0.366 W	β
SO+ FHSO+FP$_{SL}$	0.451 S	-	0.413 VW	0.379 M	-	$\beta' + \beta$
NLC $_{heated}$						
NLC$_{T80}$	0.456 VW	-	-	0.382 M	0.366 M	β
NLC$_{S60}$	0.452 S	-	-	0.382 M	0.365 M	β
NLC$_{SL}$	0.456 VW	-	-	0.382 M	0.366 M	β
NLC+FP$_{T80}$	0.454 VS	-	-	0.382 VS	0.365 VS	β
NLC+FP$_{S60}$	0.453 VS	-	-	0.383 M	0.367 M	β
NLC $_{lyophilized}$						
NLC$_{T80}$	0.457 M	-	-	0.384 M	0.368 M	β
NLC$_{S60}$	0.460 VS	-	-	0.388 M	0.371 M	β
NLC$_{SL}$	0.460 M	-	-	0.387 M	0.370 M	β
NLC+FP$_{T80}$	0.459 M	-	-	0.386 M	0.369 M	β
NLC+FP$_{S60}$	0.460 VS	-	-	0.389 W	0.371 W	β

Peak intensity: V - very, W - weak, M - medium, S - strong.
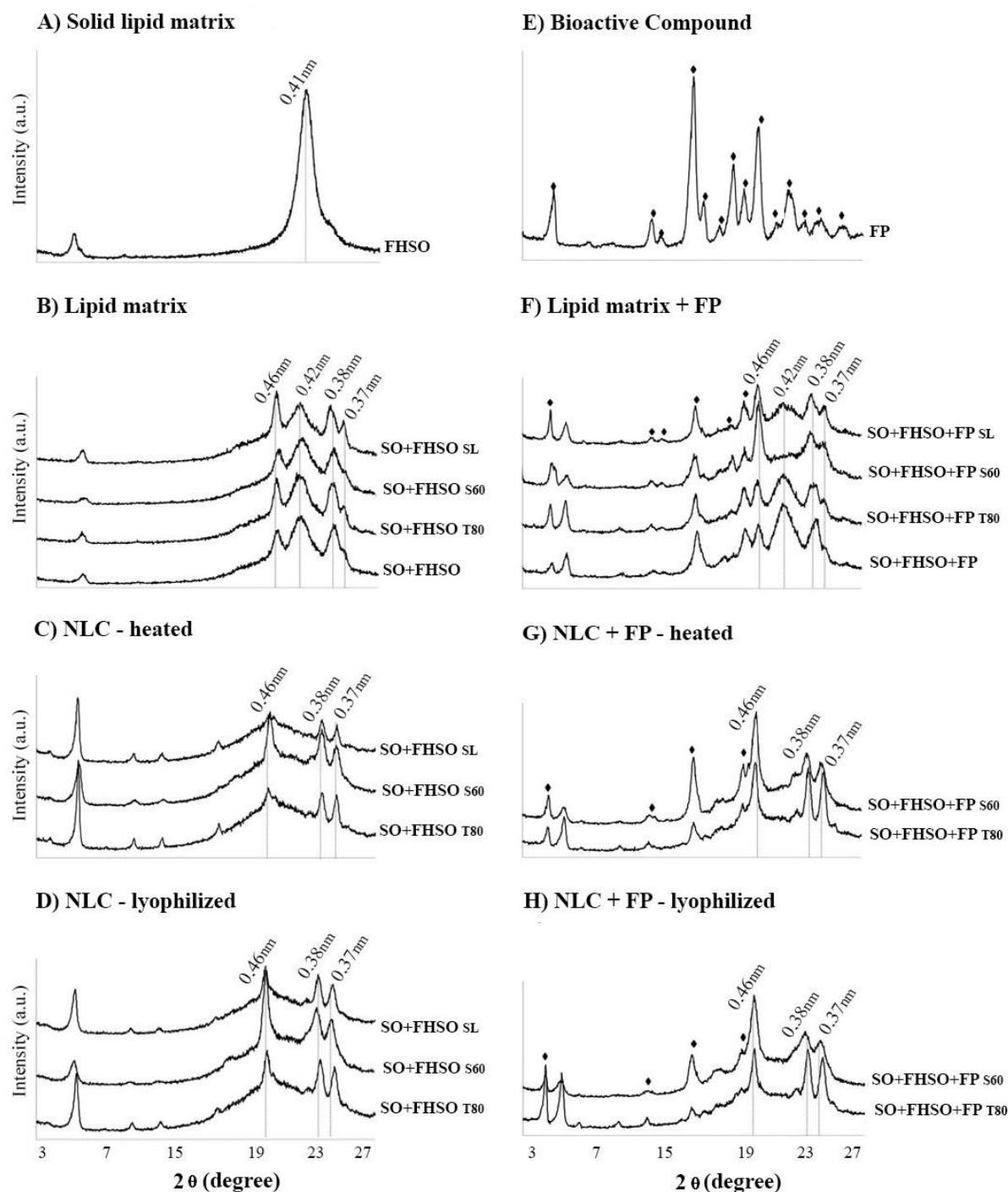
Fig. 6. X-ray diffraction patterns obtained at 25 °C: A) Fully hydrogenated soybean oil - FHSO; B) Lipid matrices developed with different emulsifiers (SL, T80 and S60) used in the NLC production; C) NLC heated (oven dried); D) NLC lyophilized; E) Free phytosterols - FP; F) Lipid matrix with free phytosterols and different emulsifiers (SL, T80 and S60) used in the NLC+FP; G) NLC+FP heated (oven dried), and H) NLC+FP lyophilized.

Evaluating the diffraction patterns of the lipid matrices, shown in Figure 5B and 5F, it was possible to observe diffraction peaks at SS 4.2 and 3.8 Å characteristics of the β'-

form and also in 4.6 Å, SS that characterizes the presence of crystals in the β-form. In this way, it was observed that in these lipid matrices there is a mixture of crystals in both β' and β forms, indicating that these materials are in polymorphic transition ($\alpha \rightarrow \beta' \rightarrow \beta$). Zeitoun et al. (1993) and Ribeiro et al. (2009d) also characterize mixtures of SO with FHSO, in the same proportion used in our studies (50:50 mm) and observe the simultaneous presence of β' and β crystals. With the exception of the lipid matrix developed with FP and S60 (Figure 6F), where only the characteristic SS of the most stable polymorphic form, β, were observed. Probably, the polymorphic transitions were facilitated by the presence of the S60 emulsifier.

In the diffractograms corresponding to the NLC and NLC+FP obtained after the oven drying (Figures 6C and G) and lyophilization (Figures 5D and H), it was possible to observe only SS characteristics of crystals in the β-form. Thus, it can be affirmed that the polymorphic transitions were facilitated in LN as compared to the corresponding LM. It is noteworthy that both lipid matrices, and LN, were subjected to the same crystallization conditions (5 °C/ 24h followed by stabilization at 25 °C) and XRD analysis. Thus, it is suggested that the stabilization in the β-form may be related to the additional processes of LN drying. Salminen and coworkers (2013) described that polymorphic transitions in LN are facilitated when temperature increases in the system. However, the results obtained here showed that after both drying treatments of LN, using heating (oven) and low temperatures (lyophilization), crystals were observed in the most stable form (β). Moreover, for the NLC+FP, similar diffractograms were obtained for both lyophilized and oven dried LN (Figures 5G and H). Being the SS at 4.6 nm, characterized as very strong intensity for the NLC+FP with S60 and of medium intensity, for the NLC+FP containing T80, as described in Table 7. The drying process, heating or lyophilization, did not interfere in the NLC+FP polymorphism. However, the different emulsifiers were found to interfere in the NLC+FP crystallinity, the systems developed with the T80 emulsifier were less crystalline when compared to those containing S60 (Figures 5H and 5G).

On the other hand, polymorphic transitions of β' to β were hampered in the oven drying process of the NLC (Figures 6C and 5D). It was mainly observed in the systems developed with SL and T80, which presented very weak intensities of SS peaks at 4.6 Å, referring to the β polymorph (Table 7). Probably, a partial melting of some TAGs, of an intermediate melting point, may have occurred during the heating drying, hindering the mobility

of the crystalline structure to the most stable form (β). This was not observed in the nanoparticles developed with FP, because they presented higher thermal resistance due to the high melting point of FP.

Finally, the obtaining of nanostructured systems in the β-form, which is the most stable form, guarantees that during the application of these systems in food, no more polymorphic transitions will occur, which could be associated to the destabilization of the product during storage.

4. Conclusions

Soybean oil and fully hydrogenated soybean oil were found to be compatible materials for the development of NLC and NLC+FP. The HPH process was effective to obtain the NLC and NLC+FP, mainly by maintaining the high temperature of the systems during processing, avoiding the crystallization of the solid lipids and FP. The number of HPH cycles did not interfere with the particle size and polydispersity of the LN, but it did contribute to the reduction of the PDI of the NLC+FP. The T80 emulsifier was more effective in the stabilization of the systems, providing the smallest values of size and polydispersity for LN.

The LN in aqueous dispersion, compared to the lipid matrices, required lower temperatures for crystallization. The systems developed with FP presented higher thermal resistance. The polymorphic transitions were accelerated after the drying processes of the LN, with crystals predominating in the β-form, while in the lipid matrices mixtures of crystals in the β' and β forms were found. The drying method did not interfere in the polymorphism of carriers with phytosterols, but for those without phytosterols, the polymorphic transitions were hampered in the oven drying process. In addition, in both NLC and NLC+FP systems, the systems with T80 were less crystalline. Obtaining LN through HPH is easily scalable for industrial processes and NLs have high thermal resistance, which is compatible with the incorporation into different areas and food processes. Thus, it can be concluded that the systems developed in this study are innovative systems, mainly in terms of compositions of lipid matrices and present high potential for food application. We suggest the use of NLC+FP in aqueous based foods, where FP dispersion is hampered by their high melting point and limited solubility. In addition, it's possible to apply the oven dried or lyophilized NLC, as crystallization seeds in lipid-based foods, for the induction of β-form.

References

AMERICAN OIL CHEMISTS' SOCIETY. Official methods and recommended practices of the American Oil Chemists' Society, AOCS Press, Urbana. IL (USA), 2009.

ANTONIOSI FILHO, N.; MENDES, O. L.; LANÇAS; F. M. Computer prediction of triacylglycerol composition of vegetable oils by HRGC. *Chromatographia*, v.40, p.557–562, 1995.

AWAD, A. B.; CHINNAM, M.; FINK, C. S.; BRADFORD, P. G. D-Sitosterol activates Fas signaling in human breast cancer cells. *Phytomedicine*, v.14, n.11, p.747–754, 2007.

AWAD, T. S.; HELGASON, T.; WEISS, J.; DECKER, E. A.; MCcLEMENTS, D. J. Effect of omega-3 fatty acids on crystallization, polymorphic transformation and stability of tripalmitin solid lipid nanoparticle suspensions. *Crystal Growth & Design*, v.9, p.3405–3411, 2009.

AWAD, T. S.; HELGASON, T.; KRISTBERGSSON, K.; DECKER, E. A.; WEISS, J.; McCLEMENTS, D. J. Effect of cooling and heating rates on polymorphic transformations and gelation of tripalmitin solid lipid nanoparticle (SLN) suspensions. *Food Biophysics*, v.3, p.155–162, 2008.

BUCHGRABER, M.; ULBERTH, F.; EMONS, H.; ANKLAN, E. Triacylglycerol profiling by using chromatographic techniques. *European Journal of Lipid Science and Technology*, v.106, n.9, p. 581-651, 2004.

BUNJES, H. Characterization of Solid Lipid Nano and Microparticles. In.: C. Nastruzzi (Ed.), *Lipospheres in Drug Targets and Delivery: Approaches, Methods, and Applications*. (pp. 43-70). Boca Raton: CRC Press LLC, 2005.

BUNJES, H.; STEINIGER, F.; RICHTER, F. W. *Visualizing the Structure of Triglyceride Nanoparticles in Different Crystal Modifications*. Langmuir, v.23, p.4005-401, 2007.

CAMPOS, R. Experimental Methodology. In.: A. J. Marangoni (Ed.), *Fat Crystal Network*s (pp.267-349). New York: CRC Press: Taylor & Francis Group., 2005.

CERQUEIRA, M. A.; PINHEIRO, A. C.; SILVA, H. D.; RAMOS, P. E.; AZEVEDO, M. A.; FLORES-LÓPEZ, M. L.; RIVERA, M. C.; BOURBON, A. I.; RAMOS, O. L.; VICENTE, A. A. Design of bio-nanosystems for oral delivery of functional compounds. *Food Engineering Reviews*, v.6, n.1, p.1–19, 2014.

CUSHENA, M.; KERRYB, J.; MORRISC, M.; CRUZ-ROMEROB, M.; CUMMINSA, E. Nanotechnologies in the food industry e Recent developments, risks and regulation. *Trends in Food Science & Technology*, v.24, p.30-46, 2012.

DOMINGUES, M. A. F.; SILVA, T. L. T.; RIBEIRO, A. P. B.; CHIU, M. C.; GONÇALVES, L. A. GUARALDO. Sucrose behenate as a crystallization enhancer for soft fats. *Food Chemistry*, v.192, p.72–978, 2016.

ELTAYEB, M.; BAKHSHI, P.K.; STRIDE, E.; EDIRISINGHE, M. Preparation of solid lipid nanoparticles containing active compound by electrohydrodynamic spraying. Food *Research International*, v.53, p.88–95, 2013.

ENGELT, R.; SCHUBERT, H. Formulation of phytosterols in emulsions for increased dose response in functional foods. *Innovative Food Science and Emerging Technologies*, v.6, p.233– 237, 2005.

GARZÓN, M. L. S.; HERNÁNDEZ, A. L.; VÁZQUEZ, M. L. R.; VÁZQUEZ, M. L. R.; GARCÍA, B. F. Preparación de nanopartículas sólidas lipídicas (SLN), y de Acarreadores lipídicos nanoestructurados (NLC). *Revista Mexicana de Ciencias Farmacéuticas,* v.39, n.4, p.50-66, 2008.

GARZÓN, M. L. S.; VÁZQUEZ, M. L. R.; VÁZQUEZ, M. L. R.; GARCÍA, B. F.; HERNÁNDEZ, A. L. Efecto de los componentes de la formulación em las propriedades de las nanopartículas sólidas. *Revista Mexicana de Ciências Farmacéuticas,* v.40, n.2, p.26-40, 2009.

GÓMEZ-COCA, R. B.; PÉREZ-CAMINO, M. C.; MOREDA, W. Analysis of Neutral Lipids: Unsaponifiable. In.: *Handbook of Food Analysis*, 3rd ed.; Nollet, L.; Toldrá F. Eds.; CRC Press: Boca Raton, (pp.459-491), 2015.

HARTMAN, L.; LAGO, R. Rapid preparation of fatty acid methyl esters from lipids. *Laboratory Practice*, v.22, p.475–476, 1973.

HELGASON, T.; AWAD, T. S.; KRISTBERGSSON, K.; DECKER, E. A.; McCLEMENTS, D. J.; WEISS, J. Impact of surfactant properties on oxidative stability of β-carotene encapsulated within solid lipid nanoparticles. *Journal of Agricultural and Food Chemistry*, v.57, p.8033–8040, 2009.

HUANG, Q.; YU, H.; RU, Q. Bioavailability and delivery of nutraceuticals using nanotechnology. *Journal of Food Science*, v.75, p.50-57, 2010.

HUMPHREY, K. L.; NARINE, S. S.; A comparison of lipid shortening functionality as a function of molecular ensemble and shear: microstructure, polymorphism, solid fat content and texture. *Food Research International,* v.37, n.1, p.28-38, 2004.

KUMBHAR, D. D.; POKHARKAR, V. B. Engineering of a nanostructured lipid carrier for the poorly water-soluble drug, bicalutamide: Physicochemical investigations. *Colloids and Surfaces A: Physicochemical and Engineering Aspects*, v. 416, p.32– 42, 2013.

LASON, E.; OGONOWSKI, J. Solid lipid nanoparticles – Characteristics, application and obtaining. *Chemik*, v.65, n.10, p.964-967, 2011.

LEONG, W. F.; LAI, O. M.; LONG, K.; CHE MAN, Y. B.; MISRAN, M.; TAN, C. P. Preparation and characterisation of water-soluble phytosterol nanodispersions. *Food Chemistry*, v.129, p.77–83, 2011a.

LEONG.; MAN, W. F. Y. B. C.; LAI, O. M.; LONG, K.; NAKAJIMA, M.; TAN, C. P. Effect of sucrose fatty acid esters on the particle characteristics and flowproperties of phytosterol nanodispersions. *Journal of Food Engineering*, v.104, p.63–69, 2011b.

MARANGONI, A. G., ROUSSEAU, D. Engineering triacylglicerols: the role of interesterification. *Trends in Food Science and Technology*, v.6, p.329-336, 1995.

MASUCHI, M. H.; GRIMALDI, R.; KIECKBUSCH, T. G . Effects of Sorbitan Monostearate and Monooleate on the Crystallization and Consistency Behaviors of Cocoa Butter. *Journal of the American Oil Chemists' Society* (Online), v. 91, p. 1111-1120, 2014.

McCLEMENTS D. J. Edible lipid nanoparticles: Digestion, absorption, and potential toxicity. *Progress in Lipid Research*, v. 52, p.409–423, 2013.

McCLEMENTS, D. J.; RAO, J. Food-grade nanoemulsions: formulation, fabrication, properties, performance, biological fate, and potential toxicity. *Critical Reviews in Food Science and Nutrition*, v.51, n.4, p.285-330, 2011.

MEHNERT. W.; MÄDER, K. Solid lipid nanoparticles: production, characterization and applications. *Advanced Drug Delivery Reviews*, v.*64*, p.83-101, 2012.

MENSINK, R. P. Effects of stearic acid on plasma lipid and lipoproteins in humans. *Lipids*, v.40, n.12, 1201-1205, 2005.

MÜLLER, R. H.; RADTKE, M.; WISSING, S. A. Nanostructured lipid matrices for improved microencapsulation of drugs. *International Journal of Pharmaceutics*, v.242, n.1-2, p.121-128, 2002.

MÜLLER, R. H.; RUNGE, S.; RAVELLI, V.; MEHNERT, W.; THUNEMANN, A. F.; SOUTO, E. B. Oral bioavailability of cyclosporine: Solid lipid nanoparticles (SLN[®]) versus drug nanocrystals. *International Journal of Pharmaceutics*, v.*317, p.*82–89, 2006.

NICHOLS, D. S; SANDERSON, K. The nomenclature, structure and properties of food lipids. In.: Sikorski, Z. E; Kolakowska, A.; editors. *Chemical and Functional Properties of Food Lipids*. Boca Raton: CRC Press. (pp.29–60), 2003.

O'BRIEN, R. D. *Fats and Oils: Formulating and Processing for Applications*, CRC Press, New York (USA) 2009.

OLIVEIRA, G. M.; STAHL, M. A.; RIBEIRO, A. P. B.; GRIMALDI, R.; CARDOSO, L. P.; KIECKBUSCH, T. G. Development of zero trans/low sat fat systems structured with sorbitan monostearate and fully hydrogenated canola oil. *European Journal of Lipid Science Technology*, v.117, p.1762-1771, 2015.

PARDEIKE, J.; HOMMOSS, A.; MÜLLER, R. Lipid nanoparticles (SLN, NLC) in cosmetic and pharmaceutical dermal products. *International Journal of Pharmaceutics*, v.366, p.170-184, 2009.

QIAN, C.; DECKER, E. A.; XIAO, H.; McCLEMENTS, D. J. Impact of lipid nanoparticle physical state on particle aggregation and β-carotene degradation: potential limitations of solid lipid nanoparticles. *Food Research International*, v.52, p.342–349, 2013.

REGITANO-D'ARCE, M. A. B.; VIEIRA, T. M. F. S. *Fuentes de Aceites y Grasas*. In.: BLOCK, J. M.; BARRERA-ARELLANO, D. (Org.). Temas Selectos en Aceites y Grasas - Volumen 1/ Procesamiento. 1 ed. São Paulo: Blucher, 2009, v.1, p.1-29.

RIBEIRO, A. P. B.; BASSO, R. C.; GRIMALDI, R.; GIOIELLI, L. A.; GONÇALVES, L. A. G. Instrumental methods for the evaluation of interesterified fats. *Food Analytical Methods*, v.2, p.282-302, 2009a.

RIBEIRO, A. P. B; MASUCHI, M. H.; GRIMALDI, R.; GONÇALVES, L. A. G. Interesterificação química de óleo de soja e óleo de soja totalmente hidrogenado: influência do tempo de reação. *Química Nova*, v.32, n.4, p.939-945, 2009b.

RIBEIRO, A. P. B.; GRIMALDI, R.; GIOIELLI, L. A.; GONÇALVES, L. A. G. Zero trans fats from soybean oil and fully hydrogenated soybean oil: Physico-chemical properties and food applications. *Food Research International*, v.42, p.401–410, 2009c.

RIBEIRO, A. P. B.; GRIMALDI, R.; GIOIELLI, L. A.; SANTOS, A. O.; CARDOSO, L. P.; GONÇALVES, L. A. G. Thermal Behavior, Microstructure, Polymorphism, and Crystallization Properties of Zero Trans Fats from Soybean Oil and Fully Hydrogenated Soybean Oil. *Food Biophysics*, v.4, p.106–118, 2009d.

RIBEIRO, A. P. B.; BASSO, R. C.; KIECKBUSCH, T.G. Effect of the addition of hardfats on the physical properties of cocoa butter. *European Journal of Lipid Science and Technology*, v.115, p.301–312, 2013.

SALMINEN, H.; HELGASON, T.; KRISTINSSON, B.; KRISTBERGSSON, K.; WEISS, J. Formation of solid shell nanoparticles with liquid ω-3 fatty acid core. *Food Chemistry*, v.141, n.3, p.2934–2943, 2013.

SATO, K. Crystallization behaviour of fats and lipids: a review. *Chemical Engineering Science*, v.56, n.7, p.2255-2265, 2001.

SEVERINO, P.; PINHO, S. C.; SOUTO, E. B.; SANTANA, M. H. A. Crystallinity of Dynasan® 114 and Dynasan® 118 matrices for the production of stable Miglyol® -loaded nanoparticles. *Journal of Thermal Analysis and Calorimetry*, v.108, n.1p.101-108, 2011.

SEVERINO, P.; SANTANA, M. H. A.; SOUTO, E. B. Optimizing SLN and NLC by 2^2 full factorial design: effect of homogenization technique. *Materials Science and Engineering*, v.2, n.6, p.1375-1379, 2012.

SHARMA, V. K.; DIWAN, A.; SARDANA, S.; DHALL, V. Solid lipid nanoparticles system: an overview. *International Journal of Research in Pharmaceutical Sciences*, v.2, n.3. p.450-461, 2011.

SOUTO, E. B.; SEVERINO, P.; SANTANA, M. H. A. PINHO, S. C. Nanopartículas de lipídios sólidos: métodos clássicos de produção laboratorial. *Química Nova*, v.34, p.1762-1769, 2011.

TAMJIDI, F.; SHAHEDI, M.; VARSHOSAZ, J.; NASIRPOUR, A. Nanostructured lipid carriers (NLC): A potential delivery system for bioactive food molecules. *Innovative Food Science and Emerging Technologies*, v.19, p.29–43, 2013.

VAIKOUSI, H.; LAZARIDOU, A.; BILIADERIS, C. G.; ZAWISTOWSKI, J. Phase Transitions, Solubility, and Crystallization Kinetics of Phytosterols and Phytosterol-Oil Blends. *Journal of Agricultural and Food Chemistry*, v.55, p.1790-1798, 2007.

WALSTRA, P. *Physical Chemistry of Foods*, Marcel Decker, New York, NY., 2003.

WANG, J. L.; DONG, X. Y.; WEI, F.; ZHONG, J.; LIU, B.; YAO, M. H.; YANG, M.; ZHENG, C.; QUEK, S. Y.; CHEN, H. Preparation and characterization of novel lipid carriers containing microalgae oil for food applications. *Journal of Food Science*, v.79, p.169-177, 2014.

WANG, T. Soybean oil. In: GUNSTONE, F. D. *Vegetable Oils in Food Technology Composition, Properties and Uses*. Boca Raton, Florida, U.S.A: CRC Press LLC, (pp. 18-52), 2002.

YANG, Y.; CORONA, A.; SCHUBERT, B.; REEDER, R.; HENSON, M. A. The effect of oil type on the aggregation stability of nanostructured lipid carriers. *Journal of Colloid and Interface Science*, v. 418, p.261–272, 2014.

YOON, G.; PARK, J.W.; YONN, I. Solid lipid nanoparticles (SLNs) and nanostructured lipid carriers (NLCs): recent advances in drug delivery. *Journal of Pharmaceutical Investigation*, v. 43, p.353–362, 2013.

ZEITOUN, M. A. M.; NEFF, W. E. MOUNTS, T. L. Physical properties of interesterified fat blends. *Journal of the American Oil Chemists' Society*, v.70, n.5, p.467-471, 1993.

ZIMMERMANN, E.; MÜLLER, R.H; MÄDER, K. Influence of different parameters on reconstitution of lyophilized SLN. *International Journal of Pharmaceutics*, v.196, p. 211–213, 2000.

ARTIGO 2

"Comportamento térmico e cristalino de matrizes lipídicas com potencial de aplicação em nanopartículas lipídicas" a ser submetido à Química Nova.

COMPORTAMENTO TÉRMICO E CRISTALINO DE MATRIZES LIPÍDICAS COM POTENCIAL DE APLICAÇÃO EM NANOPARTÍCULAS LIPÍDICAS

Valeria da Silva Santos[1], Maria Helena Andrade Santana[1], Bruno de Brito Braz[1], Alan Ávila da Silva[2], Lisandro Pavie Cardoso[3], Ana Paula Badan Ribeiro[2]

[1]Departamento de Engenharia de Materiais e Bioprocessos, Faculdade de Engenharia Química, Universidade Estadual de Campinas (UNICAMP), SP, Brasil.

[2]Departamento de Tecnologia de Alimentos, Faculdade de Engenharia de Alimentos, Universidade Estadual de Campinas (UNICAMP), SP, Brasil.

[3]Instituto de Física *Gleb Wataghin*, Departamento de Física Aplicada, Universidade Estadual de Campinas (UNICAMP), SP, Brasil.

ABSTRACT

THIS WORK AIMED TO EVALUATE THE THERMAL AND CRYSTALLINE BEHAVIOR OF LM OF FOOD GRADE WITH THE POSSIBILITY OF APPLICATION IN SOLID LIPID NANOPARTICLES (SLN) AND NANOSTRUCTURED LIPID CARRIERS (NLC). High oleic sunflower oil (HOSO) and the hardfats of canola (CA) and crambe (CR) oils were used. After characterized (fatty acid and triacylglycerols compositions) the LM were obtained by mixing and melting, with crystallization at 5 °C/24h and stabilization at 25 °C/24h. LMs were evaluated for solid fat content (SFC), the thermal behavior of crystallization and melting, polymorphism and microstructure. All LMs had a melting point over the body temperature and the incorporation of HOSO delayed the crystallization start. A eutectic effect was observed promoting the reduction of melt temperature mainly in the blends of CA and CR (50:50). In the LM of hardfats crystals found in the α-form, after the incorporation of HOSO, crystals were in β' and β forms. The lower crystal diameter was obtained for the LMs that presented crystals in the β-form. The results showed that the LM composed by HOSO, CA and CR are compatible with the application in SLN and NLC and of an innovative character.

Keywords: *Hardfats*, Canola, Crambe, High Oleic Sunflower Oil, Nanotechnology, Foods.

Abbreviations

CLN	Carreadores lipídicos nanoestruturados
CA	*Hardfat* do óleo de canola
CR	*Hardfat* do óleo de crambe
CAG	Composição em ácidos graxos
DRX	Difração de raios-X
DSC	Calorimetria Diferencial de Varredura
INPI	Instituto Nacional da Propriedade Industrial
ML	Matrizes lipídicas
MLP	Microscopia de luz polarizada

NL   Nanopartículas lipídicas
NLS   Nanopartículas lipídicas sólidas
OGAO   Óleo de girassol alto oleico
SFC   Conteúdo de gordura sólida
TAG   Triacilgliceróis
TGI   Trato gastrointestinal

INTRODUÇÃO

A nanotecnologia é uma ciência emergente, com grande potencial de aplicação em alimentos. Nos últimos 15 anos, diversos estudos de sistemas em escala nanométrica vêm sendo publicados na área de alimentos, abordando componentes estruturais, métodos de produção e caracterização, propriedades químicas e físicas, carreamento, proteção e liberação de compostos bioativos, direcionados ao desenvolvimento de novos produtos alimentícios [1-4].

Neste contexto, os sistemas lipídicos estão em destaque devido as propriedades físicas e químicas diferenciadas dos óleos e gorduras, muito promissoras para o desenvolvimento de nanopartículas lipídicas. As nanopartículas lipídicas (NL) combinam algumas vantagens, como, maior facilidade de dissolução de compostos bioativos lipofílicos (ácidos graxos essenciais, tocoferóis, esteróis, carotenóides, entre outros), estabilidade química, permeabilidade e solubilidade através da parede do intestino [5].

As NL podem ser desenvolvidas com matrizes lipídicas (ML) totalmente saturadas denominadas de nanopartículas lipídicas sólidas (NLS) e com misturas de lipídios saturados e insaturados, conhecidas como carreadores lipídicos nanoestruturados (CLN) [1,6,7].

Este trabalho tem como proposta central estudar a viabilidade de aplicação óleos e gorduras comestíveis e/ou comercialmente disponíveis no contexto da indústria de alimentos em substituição às ML sintéticas, compostas por triacilgliceróis (TAGs) puros e suas misturas, geralmente utilizadas em fármacos e cosméticos, que se mostram pouco viáveis para aplicações alimentícias, principalmente em termos de custo e aspectos regulatórios [3].

Neste ponto de vista, uma fonte lipídica muito promissora para compor a fração líquida dos CLN é o óleo de girassol alto oleico (OGAO), pois geralmente é utilizado em aplicações alimentícias que requerem elevada estabilidade oxidativa. O OGAO é considerado uma matéria-prima *premium*, que foi desenvolvida por pesquisadores russos a partir da mutagênese química e cruzamentos seletivos do girassol (*Helianthus annus*), visando a

obtenção de uma variedade de semente estável às condições climáticas e com alto teor de ácido oleico [8]. A composição típica do OGAO é representada por 3-5% de ácido palmítico, 2-6% de ácido esteárico, 75 a 88% de ácido oleico e menos de 1% de ácido linolênico, que confere a este óleo estabilidade oxidativa dez vezes superior em relação aos óleos de soja, canola e ao próprio óleo de girassol de composição regular. O OGAO possui sabor e aroma neutros, característica associada ao seu alto potencial de aplicação em alimentos, cosméticos e fármacos, e tem sido direcionado à obtenção de produtos de máxima segurança toxicológica e biodegradabilidade [9,10].

Uma opção de alto potencial e totalmente inédita neste contexto, para o uso como lipídio sólido na obtenção de NL consiste na utilização de óleos vegetais totalmente hidrogenados, também conhecidos como *hardfats*. Estes materiais lipídicos são obtidos quando todas as duplas ligações dos ácidos graxos são saturadas no processo de hidrogenação catalítica de óleos líquidos. Os *hardfats* são considerados materiais relativamente novos, foram desenvolvidos como matéria-prima para substituição da gordura parcialmente hidrogenada, contribuindo para o desenvolvimento de gorduras *low trans* por meio do processo de interesterificação. Atualmente, os *hardfats* têm sido objeto de estudos voltados aos processos de modificação lipídica e na estruturação de óleos líquidos. *Hardfats* específicos, provenientes de uma determinada fonte oleosa, apresentam perfil triacilglicerólico único e diferenciado, embora sejam compostos, em sua totalidade, por TAG trissaturados. Sua composição em ácidos graxos e em TAG é um dos fatores mais importantes na determinação do efeito modulador dos processos de cristalização em fases lipídicas contínuas [11].

O hardfat do óleo de crambe (CR) é obtido da hidrogenação total do óleo de crambe, rico em ácido erúcico (C22:1), que quando hidrogenado transforma-se em ácido behenico (C22:0). Portanto, o *hardfat* de carmbe é composto basicamente de ácido behênico (~60%), e ácido esteárico (30% de C18:0). Devido ao grande tamanho de cadeia, o ácido behênico possui baixo índice de absorção no organismo (baixa biodisponibilidade), fato pelo qual mostra-se favorável em termos de metabolismo, uma vez que, apesar de ser saturado não é totalmente absorvido. Enquanto que o ácido esteárico é considerado metabolicamente neutro, sendo basicamente utilizado como fonte energética, não influenciando, portanto, no metabolismo de hormônios, prostaglandinas e leucotrienos [12]. Outro *hardfat* disponível na indústria de alimentos é o *hardfat* obtido pela hidrogenação do óleo de canola. O óleo de canola é rico em

ácido oleico (C18:1), portanto o *hardfat* do óleo de canola (CA) é composto de cerca de 90% de ácido esteárico. Além de serem ricos em compostos considerados neutros no ponto de vista metabólico, os *hardfats* do óleo de crambe e canola apresentam conteúdo de ácido palmítico (C16:0) reduzido. Alguns estudos associam o ácido palmítico com efeitos metabólicos negativos, principalmente quanto a indução de resistência à insulina em casos de diabetes e atividade pró-inflamatória [12,13]. Desta maneira, estes *hardfats* são considerados de alto potencial como fração sólida de NLS e CLN para aplicação em alimentos.

Cabe destacar que esta abordagem de utilização de *hardfats* como matérias-primas para desenvolvimento de NL ainda não foi verificada na literatura científica. Nosso grupo de pesquisa, recentemente adquiriu o Privilégio de Invenção (INPI - BR 10 2017 006471 9) para o desenvolvimento de NLS e CLN com estas matérias-primas. Até o presente momento, foram desenvolvidos CLN com óleo de soja e *hardfat* do óleo de soja para carreamento de fitoesteróis livres, onde foram otimizadas condições de processamento e sistemas emulsificantes, mostrando resultados promissores [14]. Desta maneira, é fundamentalmente importante o conhecimento das características químicas e físicas de outras matérias-primas, como CA, CR e OGAO possibilitando a ampliação e disseminação desta tecnologia para obtenção de sistemas nanoestruturados compatíveis com aplicações em alimentos. Estas investigações podem fornecer informações valiosas sobre a viabilidade de utilização da nanotecnologia na indústria de alimentos, uma vez que, estas matérias-primas apresentam maior biocompatibilidade e disponibilidade em relação aos lipídios sintéticos.

Por todo exposto, o objetivo deste trabalho foi avaliar o comportamento térmico e cristalino de matrizes lipídicas desenvolvidas com óleo de girassol alto oleico e *hardfats* dos óleos de canola e crambe para utilização em sistemas lipídicos nanoestruturados para aplicação em alimentos.

PARTE EXPERIMENTAL

Material e métodos

Materiais

Para a realização dos experimentos foram utilizados os seguintes produtos:

- Óleo de girassol alto oleico (OGAO) fornecido pela Cargill Agrícola S. A. (Mairinque – SP, Brasil);

- *Hardfats* dos óleos de canola (CA) e crambe (CR), ambos obtidos a partir do processo de hidrogenação catalítica total dos óleos de canola e crambe, respectivamente, fornecidos pela SGS Agricultura e Indústria Ltda© (Ponta Grossa - PR, Brasil).

Métodos

Formulação e preparo das bases lipídicas

Os CA e CR foram utilizados para desenvolver 5 ML totalmente saturadas e 21 ML contendo a mistura de ácidos graxos saturados e insaturadas, compostas pelos óleos totalmente hidrogenados (CA e/ou CR) e com substituição parcial por OGAO, nas proporções de 20, 40 e 60%. Estas ML foram produzidas por mistura simples dos seus componentes, seguida da fusão à temperatura de 90°C sob agitação magnética (300 rpm) durante 2 minutos. Logo após as amostras foram acondicionadas conforme cada procedimento de análise para as caracterizações químicas e físicas, descritos na sequência.

Composição em ácidos graxos (CAG)

A composição em ácidos graxos das matérias-primas foi realizada em triplicata através de cromatografia gasosa com coluna capilar de acordo com o método AOCS Ce 1f-96 [15]. Após esterificação utilizando método de Hartman and Lago [16] os ésteres metílicos de ácidos graxos foram separados em coluna DB – 23 Agilent (50% cianopropil-metilpolisiloxano), dimensões 60 m, diâmetro interno: 0,25 mm, 0,25 μm filme. Condições cromatográficas: temperatura do forno de 110°C – 5 min., 110°C – 215°C (5°C/ min.), 215°C – 24 min.; temperatura do detector: 280°C; temperatura do injetor 250°C; gás de arraste: hélio; razão split 1:50; volume injetado: 1,0 μL. A composição qualitativa foi determinada por comparação dos

tempos de retenção dos picos com os dos respectivos padrões de ácidos graxos, enquanto que a composição quantitativa foi realizada por normalização de área, de acordo com a recomendação do método citado.

Composição em Triacilgliceróis (TAG)

A determinação da composição em TAG das matérias-primas foi realizada em triplicata, mediante a dissolução da amostra em tetrahidrofurano (THF, 20 mg/mL) e injeção em cromatógrafo gasoso equipado com coluna capilar DB-17HT *Agilent Catalog* 122-1811 (50%-fenilmetilpolisiloxano), com 15 metros de comprimento, 0,25 mm de diâmetro interno e 0,15 μm de filme. Condições de análise: injeção split, razão de 1:100; temperatura da coluna: 250ºC, programada até 350ºC à razão de 5ºC/min.; gás de arraste: hélio, em vazão de 1,0 mL/min.; temperatura do injetor: 360ºC; temperatura do detector: 375ºC; volume injetado: 1,0 μL. A identificação dos grupos de TAG foi realizada através da comparação dos tempos de retenção, segundo os procedimentos de Antoniosi, Mendes and Lanças [17], e a quantificação dos grupos foi realizada por normalização de área segundo recomendado pelos autores.

Conteúdo de gordura sólida (SFC)

O conteúdo de gordura sólida das matrizes lipídicas foi determinado utilizando Espectrômetro de Ressonância Magnética Nuclear (RMN) *Bruker pc120 Minispec*, com auxílio de banhos secos de alta precisão, *Tcon* 2000 (*Duratech*, EUA). O procedimento foi realizado de acordo com o método AOCS Cd 16b- 93: método direto, com leitura das amostras em série, a temperaturas de 10, 15, 20, 25; 30, 35, 40, 45, 50, 55, 60, 65 e 70°C [15]. Para o CR foi necessário modificar a temperagem padrão, conforme prescrito pelo Método Cd 16b-93 para amostras não estabilizadas [15]. Portanto, o CR foi mantido a 0°C durante 2h e as leituras foram realizadas após 1h em cada temperatura, a fim de garantir a estabilização da cristalização, conforme descrito por Ribeiro, Grimaldi, Gioielli and Gonçalves [18].

Comportamento Térmico

Foram realizadas 2 análises térmicas distintas nas ML, utilizando calorímetro diferencial de varredura (DSC), TA Q2000 acoplado ao RCS90 *Refrigerated Cooling System* (*TA Instruments, Waters LLC*, *New Castle*). O sistema de processamento de dados utilizado foi o *Universal* V4.7A (TA *Instruments, Waters LLC, New Castle*). As determinações foram:

Comportamento térmico na cristalização: foi realizado conforme o método AOCS Cj 1-94 [15], com modificação da temperatura máxima de 80°C para 100°C. As condições de análise foram: massa da amostra: ~10 mg; Eventos de cristalização: 100ºC por 10 min, 100ºC a -40ºC (10ºC/min). Foram utilizados os seguintes parâmetros para avaliação dos resultados: temperatura inicial de cristalização (T_{OnC}), temperatura máxima do pico de cristalização (T_{pc}), entalpia de cristalização (ΔH_c) e temperatura de conclusão de cristalização (T_{fc}) [19].

Comportamento Térmico na fusão: As amostras foram acondicionadas em cápsulas herméticas de alumínio, como massa de ~10 mg e submetidas a um tratamento prévio a 90°C durante 2 minutos para apagar o histórico cristalino. Logo após, foram armazenadas em câmara incubadora com controle de temperatura, a 5°C durante 24h seguidas de mais 24h a 25°C. Após este tratamento prévio as amostras foram avaliadas em DSC com atmosfera inerte (N_2) utilizando as seguintes condições: manutenção de condição isotérmica: 25°C por 10 minutos; eventos de fusão avaliados entre 25 e 100°C sob a taxa de 10°C/min. [20]. Foram utilizados os seguintes parâmetros para avaliação dos resultados: temperatura inicial de fusão (T_{if}), temperatura máxima do pico de fusão (T_{pf}), entalpia de fusão (ΔH_f) e temperatura de conclusão da fusão (T_{ff}) [19].

Hábito Polimórfico

As formas polimórficas das ML foram determinadas por difração de raios-X (DRX), segundo o método AOCS Cj 2-95 [15]. Previamente, as ML foram fundidas a 90°C para apagar a memória cristalina e foram cristalizadas a 5°C, seguida de estabilização a 25 °C durante 24 horas em incubadora com temperatura controlada. As determinações de DRX foram realizadas em difratômetro *Philips* (PW 1710), utilizando a geometria *Bragg-Bretano* (θ:2θ) com radiação de Cu-kα (λ = 1.54056Å, tensão de 40KV e corrente de 30mA). As medidas foram obtidas a 25°C com passos de 0,02° em 2θ e tempo de aquisição de 2s, com varreduras de 15 a 30° (escala 2θ). A identificação das formas polimórficas foi realizada a partir dos *shorts spacings* (distâncias entre os grupos acila paralelos dos TAG) característicos dos cristais lipídicos [15].

Microestrutura

A determinação da microestrutura (morfologia e cristalinidade) das amostras foi realizada por microscopia sob luz polarizada (MLP). As amostras foram fundidas à temperatura de 90°C em estufa. Com o auxílio de um tubo capilar, uma gota de amostra foi colocada sobre uma lâmina de vidro pré-aquecida à temperatura de 90ºC, que foi coberta com uma lamínula. As lâminas foram acondicionadas a 5°C/24h seguidas de 24h à temperatura de análise (25°C). A morfologia dos cristais foi avaliada com o uso de microscópio biológico com ótica de correção infinita *UIS*, marca *Olympus*, modelo BX51, acoplado a câmera colorida de vídeo digital, marca *Media Cybernetic*, modelo *Evolution MicroPublisher* 5.0Mpixel. As imagens foram obtidas com luz polarizada e com ampliação de 200 vezes, e capturadas utilizando o *software Image-Pro Plus* versão 7.01, marca *Media Cybernetic*. Para cada lâmina foram focalizados três campos visuais que foram utilizados para as medidas dos cristais e apenas um foi escolhido para compor a figura presente neste trabalho representando os cristais observados. Os parâmetros de avaliação selecionados para a análise quantitativa das imagens foram o diâmetro médio dos cristais e a porcentagem de área cristalizada [19].

RESULTADOS E DISCUSSÃO

Composição em ácidos graxos

Os ácidos graxos predominantes na composição do OGAO foram os ácidos graxos insaturados, oleico (C18:1, ~78%) e linoleico (C18:2, ~11%) e em menores quantidades os ácidos graxos saturados, palmítico (C16:0, ~4,31%), esteárico (C18:0, ~3,16%) e behênico (C22:0, ~0,88%), conforme pode ser observado na Tabela 1. O elevado valor de C18:1, confere ao OGAO, alta estabilidade oxidativa em comparação com outros óleos vegetais comumente utilizados na indústria alimentícia, como por exemplo, soja e canola [21]. O OGAO, devido a elevada estabilidade oxidativa, pode ser considerado como fonte de ácidos graxos insaturados ideal para o desenvolvimento de ML estáveis quimicamente, para obtenção de nanopartículas lipídicas.

Tabela 1. Composição em ácidos graxos do óleo de girassol alto oléico (OGAO) e dos *hardfats* dos óleos de canola (CA) e crambe (CR)

Ácidos Graxos (%)	OGAO[a]	CA[a]	CR[a]
C16:0 - Ácido Palmítico	4,31 ± 0,71	5,24 ± 0,04	3,20 ± 0,10
C18:0 - Ácido Esteárico	3,16 ± 0,42	93,82 ± 0,15	31,70 ± 0,34
C18:1- Ácido Oleico	78,60 ± 2,94	-	-
C18:2 - Ácido Linoleico	11,41 ± 1,06	-	-
C20:0 - Ácido Araquidônico	-	0,94 ± 0,01	6,70 ± 0,06
C22:0 - Ácido Behênico	0,88 ± 0,03	-	56,30 ± 0,44
C24:0 – Ácido Lignocérico	-	-	2,10 ± 0,03
Σ saturados	9,32	100,00	100,00
Σ insaturados	90,68	-	-

[a]Média de três repetições ± Desvio Padrão. Médias inferiores a 0,5% foram omitidas da tabela.

Os CA e CR apresentaram 100% de ácidos graxos saturados provenientes do processo de hidrogenação catalítica total dos óleos de canola e crambe, respectivamente. O ácido graxo predominante no CA foi o ácido graxo esteárico (C18:0, ~93%), apresentando também, em menores proporções, os ácidos graxos palmítico (C16:0, ~5%) e araquidônico (C20:0, <1%). Enquanto que, no CR os ácidos graxos majoritários foram o ácido graxo behênico (C22:0, ~56%) e ácido graxo esteárico (C18:0, ~31%), seguidos dos ácidos graxos araquidônico (C20:0, ~6%), palmítico (C16:0, ~3%) e lignocérico (C24:0, ~2%) (Tabela 1), estando estes valores de acordo com a literatura consultada [11,22,23].

Como visto na composição em ácidos graxos do CA e CR (Tabela 1), através do processo de hidrogenação total, todas as ligações insaturadas presentes nos óleos vegetais foram convertidas em saturadas, conferindo propriedades diferenciadas aos materiais obtidos [11]. Por este motivo, estas matérias-primas (*hardftats*) se apresentam totalmente sólidas a temperatura ambiente, podendo ser empregadas como fração saturada de ML para desenvolvimento de sistemas lipídicos nanopartículados.

Além disto, destaca-se, do ponto de vista metabólico os efeitos nutricionais dos principais ácidos graxos de cada *hardfat* utilizado neste estudo. O ácido esteárico, apresenta efeito neutro sobre o perfil de lipoproteínas plasmáticas [23]. E o ácido graxo behênico é considerado um lipídio de baixo valor calórico. Uma vez que, apresenta em sua estrutura molecular cadeia carbônica longa, composta por 22 carbonos e totalmente saturada, com consequente baixa biodisponibilidade no organismo. Deste modo, o ácido graxo behênico atua promovendo o aumento de excreção e redução da absorção de TAG no intestino.

Adicionalmente, este efeito benéfico do ácido graxo behênico vem sendo relacionado à prevenção de obesidade e doenças cardiovasculares [23,24].

Composição em triacilgliceróis (TAG)

TAG são constituídos por três ácidos graxos combinados a três carbonos de uma molécula de glicerol por meio de ligações ésteres [25]. Na composição em TAG do OGAO foi possível verificar a predominância de trioleína (OOO), representando aproximadamente 65% do total, seguidos de OLO (~15%), POO (~10%) e OLL/PLO (~3%). O CA apresentou 4 TAG distintos em sua composição, sendo majoritários o SSS (~80%) e PSS (~13%). No CR foram encontrados 9 diferentes TAG, entres estes os predominantes foram SBeBe (~38%), SSBe (~17%), SABe (~17%), conforme descrito na Tabela 2. Os valores obtidos estão muito próximos aos resultados encontrados por outros autores em seus estudos utilizando as mesmas matérias-primas [11,26,27].

Os principais TAG do OGAO são triinsaturados com cadeias carbônicas compostas por 54 carbonos e os TAG constituintes do CA e CR são trissaturados compostos por 56 a 69 carbonos, todos considerados TAG de cadeias longas (Tabela 2). No caso dos CA e CR, estas características dos TAG trissaturados, conferem alta resistência térmica relacionada ao elevado ponto de fusão dos ácidos graxos constituintes das moléculas. De acordo com O'Brien [8], o ponto de fusão aumenta com o aumento da cadeia carbônica dos ácidos graxos e diminui com a presença de insaturações, sendo de 16°C para o ácido graxo oleico, 69,6°C para o ácido graxo esteárico e de 79,9°C para o ácido graxo behênico, os quais são os principais constituintes do OGAO, CA e CR, respectivamente, como visto anteriormente na Tabela 1. Cabe destacar que estes valores de ponto de fusão são referentes a compostos purificados. Neste trabalho, utilizamos óleos e gorduras vegetais que apresentam misturas destes componentes em suas composições, logo, espera-se comportamentos térmicos diferenciados dos materiais isolados, que serão discutidos na sequência deste estudo.

Tabela 2. Composição em triacilgliceróis (TAG) do óleo de girassol alto oléico (OGAO) e dos *hardfats* dos óleos de canola (CA) e crambe (CR)

NC	TAG	OGAO	CA[a]	CR[a]
52	PSS	-	13,05±1,06	0,52±0,03
	POS	0,84±0,40	-	-
	POO	10,04±0,40	-	-
	PLO	2,93±0,44	-	-
50	PPS	-	3,65±0,23	-
54	SSS	-	80,33±1,40	1,12±0,05
	SOO	2,03±1,23	-	-
	OOO	65,95±1,74	-	-
	OLO	15,34±0,59	-	-
	OLL	2,87±0,23	-	-
56	SSA	-	2,98±0,12	-
	PSBe	-	-	2,14±0,37
58	SSBe	-	-	17,65±0,06
60	SABe	-	-	16,92±0,61
62	SBeBe	-	-	38,64±1,04
64	ABeBe	-	-	6,00±0,81
66	BeBeBe	-	-	8,93±0,65
69	BeBeLg	-	-	8,08±0,90

[a]Média de três repetições ± Desvio Padrão; NC – Número de carbonos; P = ácido palmítico; S = ácido esteárico; O = ácido oleico; L = ácido linoleico; A = ácido araquidônico; B = ácido behênico; Lg = ácido lignocérico -: não detectado.

Conteúdo de gordura sólida (SFC)

Os resultados obtidos através das curvas do conteúdo de gordura sólida permitem a observação do comportamento global de materiais lipídicos para a formulação e desenvolvimento de novos produtos. Valores de SFC abaixo de 25°C caracterizam a dureza da gordura, entre 20 e 25 °C podem indicar a resistência térmica do produto à temperatura ambiente, em 37°C estão relacionados ao comportamento da gordura na temperatura corporal e valores acima de 40°C podem fornecer informações sobre o perfil de derretimento das gorduras [8].

Para o desenvolvimento de nanopartículas lipídicas deseja-se que as ML apresentem resistência térmica à temperatura corporal. Assim, as nanoestruturas são preservadas durante todo o processo digestório, favorecendo o carreamento dos compostos bioativos até o trato gastrointestinal, onde os lipídios são emulsionados pelos sais biliares, absorvidos e metabolizados [7]. Além disto, do ponto de vista tecnológico de aplicação, a resistência térmica das nanopartículas lipídicas também é desejável, podendo ser inseridas em alimentos processados termicamente, mantendo as propriedades estruturais e funcionais.
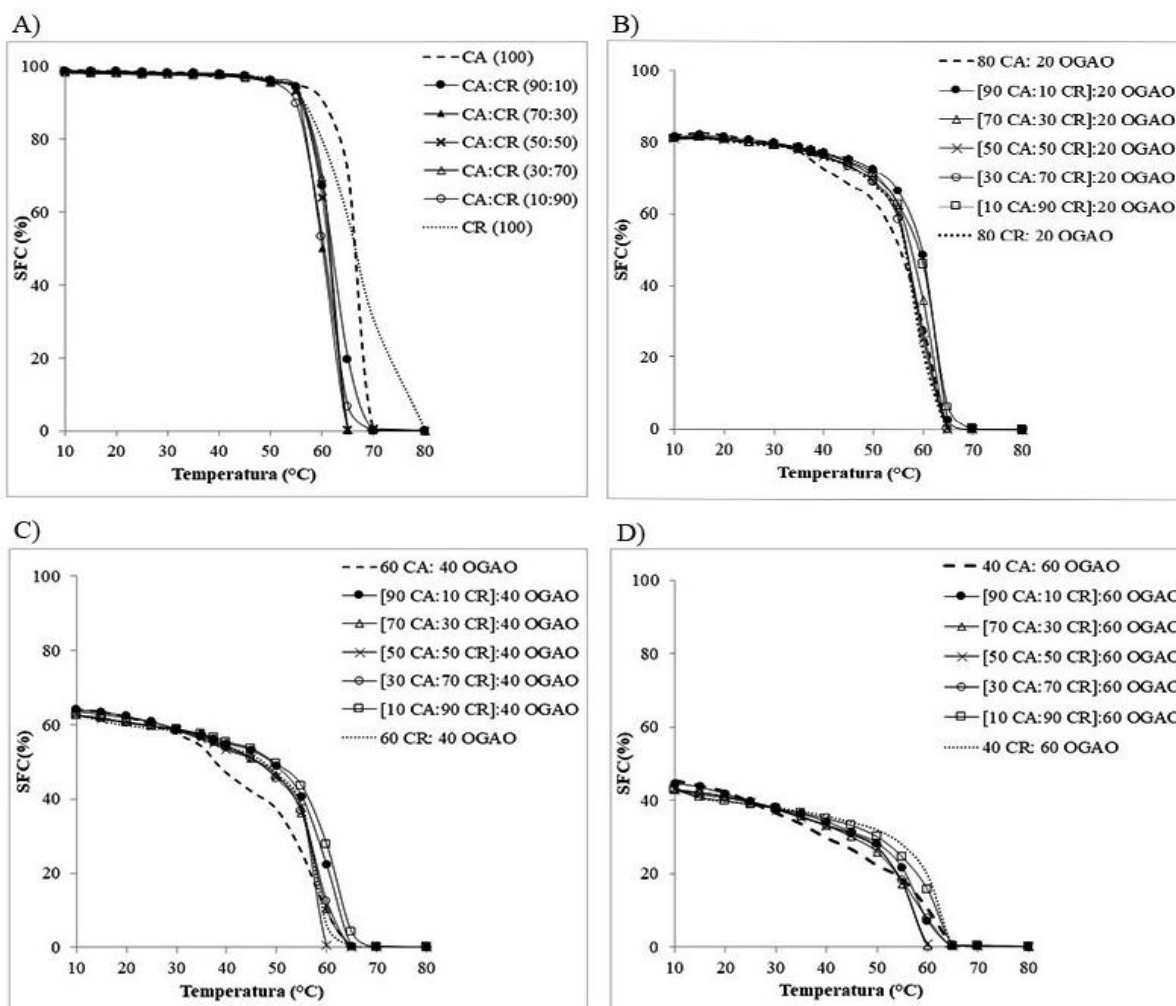
Figura 1. *Curvas do conteúdo de gordura sólida em função (SFC) da temperatura: **A**) hardfats dos óleos de canola (CA) e crambe (CR) e matrizes lipídicas com misturas de CA e CR; **B**) Matrizes lipídicas de CA e CR com incorporação de óleo de girassol alto oleico (OGAO) na proporção de 20%; **C**) Matrizes lipídicas de CA e CR com incorporação de óleo de girassol alto oleico (OGAO) na proporção de 40%; **D**) Matrizes lipídicas de CA e CR com incorporação de óleo de girassol alto oleico (OGAO) na proporção de 60%.*

As ML desenvolvidas neste estudo, conforme exposto na Figura 1, apresentaram elevado conteúdo de gordura sólida até atingir a temperatura de 60°C. As ML desenvolvidas apenas com os lipídios totalmente saturados (Fig. 1A), apresentaram conteúdo de gordura sólida acima de 90%, decaindo apenas na faixa de 60 a 80°C. Este comportamento está relacionado ao elevado ponto de fusão dos TAG trissaturados constituintes dos CA e CR, como visto anteriormente na Tabela 2.

A presença de OGAO, nas matrizes lipídicas reduziu o SFC proporcionalmente a sua incorporação de 20, 40 e 60%, devido a inclusão de ácidos graxos insaturados de baixo

ponto de fusão. Mas, mesmo assim estas ML apresentaram alta resistência térmica, compatível com o desenvolvimento de CLN, apresentando-se sólidas a temperatura corpórea (37°C).

Deste modo, verificamos que o uso dos CA e CR é viável para o desenvolvimento de ML com alto ponto de fusão, pois esta característica física é extremamente importante para o desenvolvimento dos sistemas nanoestruturados, tanto de NLS quanto CLN. Além disso, o emprego de ácidos graxos saturados e insaturados, provenientes de óleos e gorduras vegetais de grau alimentício, conferiu características diferenciadas quanto ao perfil de derretimento das ML desenvolvidas, mostrando-se resistentes à altas temperaturas. Assim, estas ML apresentam potencial de utilização na formulação de NLS e CLN, em substituição de ML purificadas para aplicação em produtos alimentícios, além disso com grande potencialidade de utilização em alimentos processados termicamente.

Comportamento térmico na cristalização

O processo de cristalização lipídica é iniciado pela nucleação cristalina seguida do crescimento dos cristais, até a formação de uma rede cristalina autossustentada [28]. Os parâmetros avaliados para discutir o comportamento de cristalização do CA e CR e suas misturas com OGAO obtidos através de DSC foram: Temperatura inicial de cristalização inicial (T_{ic}) que se refere ao início da transição de fase líquido-sólido; temperatura máxima do pico de cristalização (T_{pc}) ponto onde ocorre o efeito térmico máximo; entalpia de cristalização (ΔH_c) energia necessária para que ocorra a mudança de fase, mensurada através da área da curva; e temperatura final de cristalização (T_{fc}) que indica a conclusão dos efeitos térmicos [29], estes resultados encontram-se descritos na Tabela 3.

Notou-se que o incremento de 20, 40 e 50% de OGAO nas ML retardou o início da cristalização do CA de 50,90°C para 48,72; 46,53 e 43,07°C e do CR de 57,32°C para 55,04; 52,68 e 49,81°C, respectivamente. Além disso, como pode ser observado na Tabela 3, também ocorreram reduções nas T_{pc}, devido a inclusão dos TAG triinsaturados predominantes no OGAO, conforme discutido anteriormente na Tabela 2. A incorporação de TAG triinsaturados influenciou diretamente as características de cristalização dos sistemas, pois, provavelmente, promoveu o espaçamento entre as moléculas de TAG saturadas, pela presença das insaturações, reduzindo o ponto de fusão e a cristalinidade. Ainda, como consequência, promovendo a formação de redes cristalinas menos compactas [30], que será discutido na sequência. De acordo

com Tamjidi, Shahedi, Varshosaz and Nasirpour [1], para o desenvolvimento de CLN estas características menos compactas das ML são desejáveis, principalmente, pelo favorecimento da incorporação de compostos bioativos, e também, por evitar a expulsão indesejável dos compostos de inclusão durante o armazenamento.

As diferenças observadas nos valores de entalpia de cristalização dos CA e CR e o efeito de aceleração da cristalização promovido pela presença de CR nas ML, como pode ser observado na Figura 2, através das curvas de cristalização, estão diretamente relacionados aos TAG trissaturados presentes na composição de cada *hardfat*. Como visto anteriormente na Tabela 2, o CR apresentou uma mistura de diferentes TAG, com predominância de TAG compostos pelo ácido graxo behênico (C22:0), como o SBeBe (~39%), SSBe (~18%), SABe (~17%) e em menores quantidades ABeBe, BeBeBe e BeBeLg, que apresentam maior ponto de fusão que os TAG compostos pelo ácido graxo esteárico (C18:0, ~80% de SSS), predominante no CA. Deste modo, favorecendo a cristalização e aumentando o efeito térmico de transição de fase nas ML desenvolvidas com CR.

Tabela 3. Comportamento térmico de cristalização das ML desenvolvidas com os *hardfats* dos óleos de canola (CA) e crambe (CR) e suas misturas com incorporação de 20, 40 e 60% de óleo de girassol alto oleico (OGAO) a taxa de 10°C/min. Temperatura inicial de cristalização (T_{ic}), temperatura máxima do pico de cristalização (T_{pc}), entalpia de cristalização (ΔH_c) e temperatura final de cristalização (T_{fc})

Matrizes lipídicas	T_{ic} (°C)	T_{pc} (°C)	T_{fc} (°C)	ΔH_c (J/g)
CA e CR				
CA (100)	50,90±0,09	49,39±0,14	16,84±3,00	135,97±0,74
CA:CR (90:10)	50,41±0,05	49,30±0,03	18,07±1,43	129,90±1,35
CA:CR (70:30)	51,44±0,08	50,53±0,38	17,98±0,99	133,60±1,71
CA:CR (50:50)	53,08±0,03	51,23±1,07	19,65±0,36	135,23±3,93
CA:CR (30:70)	54,63±0,03	53,61±0,15	14,46±1,29	136,97±0,65
CA:CR (10:90)	56,40±0,00	55,42±0,03	17,18±0,59	132,45±0,25
CR (100)	57,32±0,02	56,44±0,07	21,27±1,75	141,60±1,71
Incorporação de 20% de OGAO				
80 CA: 20 OGAO	48,72±0,03	46,91±0,03	9,98±0,80	103,20±0,38
[90 CA:10 CR]:20 OGAO	48,59±0,02	47,68±0,09	10,75±0,44	109,13±0,25
[70 CA:30 CR]:20 OGAO	49,48±0,08	48,71±0,10	12,04±1,48	108,73±1,86
[50 CA:50 CR]:20 OGAO	51,06±0,03	50,19±0,15	11,56±0,88	107,17±0,29
[30 CA:70 CR]:20 OGAO	52,73±0,07	51,97±0,01	10,94±1,49	106,43±4,83
[10 CA:90 CR]:20 OGAO	54,30±0,06	53,43±0,09	12,56±1,10	115,63±1,68
80 CR: 20 OGAO	55,04±0,00	54,25±0,02	13,98±0,58	103,90±0,12
Incorporação de 40% de OGAO				
60 CA: 40 OGAO	46,53±0,00	45,13±0,03	6,46±1,67	84,41±1,15
[90 CA:10 CR]:40 OGAO	46,07±0,01	45,22±0,12	7,70±1,12	88,92±0,98
[70 CA:30 CR]:40 OGAO	47,07±0,01	46,46±0,14	7,65±1,19	87,31±0,65
[50 CA:50 CR]:40 OGAO	48,73±0,04	48,40±0,17	7,61±2,37	89,88±1,74
[30 CA:70 CR]:40 OGAO	50,29±0,05	49,84±0,02	6,89±0,13	91,66±1,79
[10 CA:90 CR]:40 OGAO	51,91±0,01	51,25±0,04	9,95±0,60	89,10±0,29
60 CR: 40 OGAO	52,68±0,04	52,00±0,15	11,70±1,02	84,11±0,19
Incorporação de 60% de OGAO				
40 CA: 60 OGAO	43,07±0,21	41,62±0,23	4,08±0,57	63,46±0,97
[90 CA:10 CR]:60 OGAO	42,67±0,08	41,88±0,15	4,74±0,85	59,54±0,89
[70 CA:30 CR]:60 OGAO	44,01±0,07	43,95±0,05	5,65±1,23	64,75±0,54
[50 CA:50 CR]:60 OGAO	45,88±0,03	45,82±0,02	4,65±0,84	67,28±0,98
[30 CA:70 CR]:60 OGAO	47,68±0,00	47,57±0,01	6,32±1,18	70,12±0,64
[10 CA:90 CR]:60 OGAO	49,09±0,09	48,94±0,10	7,93±0,39	64,24±0,05
40 CR: 60 OGAO	49,81±0,03	49,29±0,05	8,89±0,33	59,82±0,35
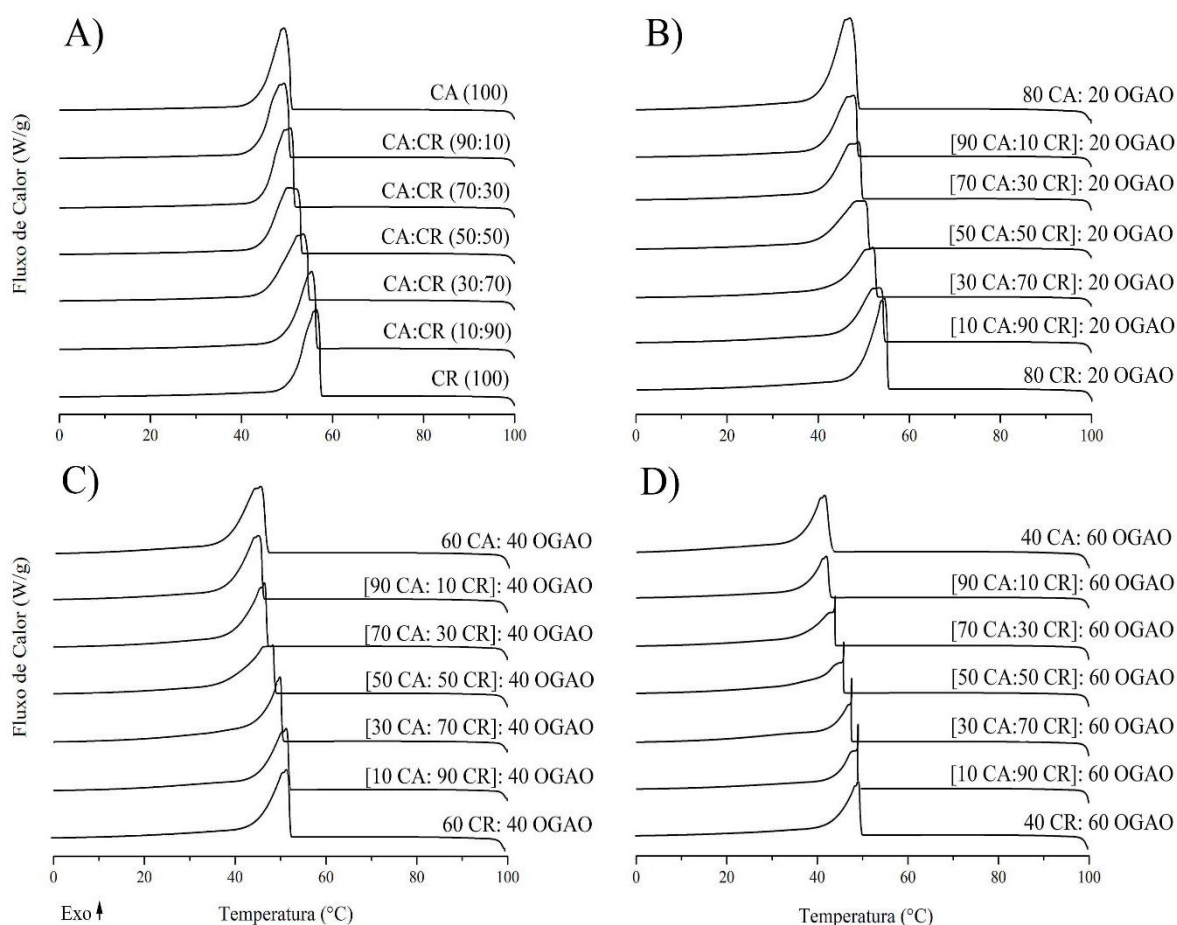
Figura 2. *Curvas de cristalização à taxa de 10°C/min.: **A**) hardfats dos óleos de canola (CA) e crambe (CR) e matrizes lipídicas com misturas de CA e CR; **B**) Matrizes lipídicas de CA e CR com incorporação de óleo de girassol alto oleico (OGAO) na proporção de 20%; **C**) Matrizes lipídicas de CA e CR com incorporação de óleo de girassol alto oleico (OGAO) na proporção de 40%; **D**) Matrizes lipídicas de CA e CR com incorporação de óleo de girassol alto oleico (OGAO) na proporção de 60%.*

Comportamento térmico na fusão

O conhecimento das propriedades de fusão das ML é extremamente importante para o desenvolvimento de NL com alta resistência térmica com possibilidade de aplicação em produtos alimentícios processados termicamente. Assim, estas características são imprescindíveis para o direcionamento de aplicação. Somado a isto, as estruturas cristalinas das NL precisam ser mantidas para que possam proteger e carrear os compostos bioativos ao longo de todo o sistema digestório, até absorção no intestino [31]. Na Tabela 4 é possível observar os resultados obtidos para o comportamento térmico de fusão do CA e CR e das ML desenvolvidas com suas misturas e incorporação de 20, 40 e 60% de OGAO, avaliados a taxa de 10°C/min.

após tratamento térmico de cristalização a 5°C/24h, seguidos de estabilização cristalina a 25°C/24h. Os parâmetros selecionados para avaliação foram: Temperatura inicial de fusão (T_{If}), temperatura máxima do pico de fusão (Tp_f), entalpia de fusão (ΔH_f) e temperatura final de fusão (T_{ff}).

O CR apresentou um único pico de fusão à 62,04°C, indicando que a mistura dos TAG presentes em sua composição, apresentaram comportamento térmico de fusão semelhantes. Enquanto que, no CA foi possível observar dois picos de fusão, um a 55,24°C e o outro em 69,20°C (Figura 3). Provavelmente, o primeiro pico que apresentou maior valor de ΔH_f (-88,96 J/g) está relacionado a fusão da triestearina (SSS) que representa aproximadamente 80% da composição do CA e o segundo pico com ΔH_f (-30,82 J/g) refere-se a fusão dos demais TAG, presentes em quantidades reduzidas (SSA, PSS e PPS). Estes resultados estão abaixo dos valores informados por O'Brien [8] para TAG purificados, sendo de aproximadamente, 73°C o ponto de fusão da SSS e dos demais TAG constituintes do CA, o ponto de fusão varia entre 62 a 65°C. Segundo Sato [28] esta diferença nos valores entre os materiais puros e os encontrados em óleos e gorduras vegetais convencionais, ocorre porque os óleos e gorduras vegetais são compostos por misturas de TAG, com consequente redução do ponto de fusão.

Tabela 4. Comportamento térmico de fusão dos óleos totalmente hidrogenados de canola (CA) e crambe (CR) e das matrizes lipídicas desenvolvidas com suas misturas e incorporação de 20, 40 e 60% de óleo de girassol alto oleico (OGAO) a taxa de 10 °C/min. Temperatura inicial de fusão (T_{If}), temperatura máxima do pico de fusão (T_{pf}), entalpia de fusão (ΔH_f) e temperatura final de fusão (T_{ff})

Matrizes lipídicas	Pico	T_{IF} (°C)	T_{pf} (°C)	T_{ff} (°C)	ΔH_f (J/g)
CA (100)	1	52,55±0,05	55,24±0,02	62,00±0,50	-88,96±1,62
	2	65,81±0,09	69,20±0,09	78,03±0,29	-30,82±1,45
CA:CR (90:10)	1	52,54±0,04	55,66±0,09	75,01±0,72	-111,23±2,78
CA:CR (70:30)	1	52,88±0,14	56,59±0,54	75,33±1,83	-114,25±0,65
CA:CR (50:50)	1	53,41±0,02	58,46±0,23	73,79±1,73	-112,10±2,80
CA:CR (30:70)	1	55,42±0,09	60,19±0,18	76,34±0,61	-112,25±3,25
CA:CR (10:90)	1	58,00±0,24	62,03±0,18	78,75±3,53	-115,15±10,45
CR (100)	1	58,66±0,04	62,04±0,17	73,89±2,12	-113,20±1,10
Incorporação de 20% de OGAO					
80 CA: 20 OGAO	1	62,16±0,00	70,22±0,13	82,27±0,36	-120,10±5,20
[90 CA: 10 CR]: 20 OGAO	1	57,86±0,11	66,20±0,07	79,97±2,16	-117,80±1,10
[70 CA: 30 CR]: 20 OGAO	1	56,79±0,06	63,65±0,01	80,26±0,35	-115,10±0,00
[50 CA: 50 CR]: 20 OGAO	1	54,92±0,03	62,57±0,25	76,38±1,44	-113,00±1,40
[30 CA: 70 CR]: 20 OGAO	1	54,56±0,05	63,22±0,01	80,37±0,82	-107,75±3,85
[10 CA: 90 CR]: 20 OGAO	1	55,46±0,02	65,09±0,09	80,80±1,55	-113,90±3,70
80 CR: 20 OGAO	1	56,20±0,05	65,38±0,02	81,62±0,29	-102,33±3,77
Incorporação de 40% de OGAO					
60 CA: 40 OGAO	1	60,02±0,10	68,66±0,02	83,53±1,98	-88,63±0,91
[90 CA: 10 CR]: 40 OGAO	1	56,09±0,06	64,42±0,07	79,07±0,32	-91,15±2,51
[70 CA: 30 CR]: 40 OGAO	1	54,56±0,66	61,93±0,46	78,38±1,37	-86,20±3,54
[50 CA: 50 CR]: 40 OGAO	1	54,18±0,04	61,70±0,23	78,46±1,36	-85,80±3,48
[30 CA: 70 CR]: 40 OGAO	1	53,05±0,05	62,46±0,01	78,85±1,4	-83,53±0,25
[10 CA: 90 CR]: 40 OGAO	1	53,66±0,03	64,44±0,03	78,86±0,33	-84,04±1,14
60 CR: 40 OGAO	1	55,32±0,05	65,45±0,03	82,45±1,04	-83,15±1,67
Incorporação de 60% de OGAO					
40 CA: 60 OGAO	1	57,62±0,07	66,27±0,10	81,01±0,32	-55,82±0,78
[90 CA: 10 CR]: 60 OGAO	1	45,53±2,68	61,61±0,42	76,49±0,39	-57,09±3,85
[70 CA: 30 CR]: 60 OGAO	1	52,68±0,42	59,96±0,44	76,70±1,33	-54,89±2,43
[50 CA: 50 CR]: 60 OGAO	1	51,59±0,04	58,94±0,03	74,04±1,05	-56,21±0,90
[30 CA: 70 CR]: 60 OGAO	1	50,60±0,25	60,10±0,02	76,92±0,32	-53,42±3,26
[10 CA: 90 CR]: 60 OGAO	1	52,85±0,37	62,74±0,03	76,56±0,46	-52,15±0,15
40 CR: 60 OGAO	1	55,27±0,09	64,17±0,18	80,51±0,54	-52,97±0,44

Na Figura 3 estão expostas as curvas de fusão das ML, onde é possível visualizar as diferenças entre os comportamentos térmicos de fusão das amostras. Na Figura 3A correspondente as ML desenvolvidas apenas com as misturas dos *hardfats*, é visualmente perceptível que ocorreu o aumento da temperatura de fusão com o incremento do CR nas

misturas, comportamento esperado, pois o ponto de fusão do CR foi mais elevado do que o do CA. As temperaturas dos picos de fusão dessas ML variaram entre 52 e 58°C, aproximadamente. Mostrando-se viáveis para utilização em NLS, que são compostas apenas por lipídios saturados. Adicionalmente, como discutido anteriormente, a temperatura de fusão acima da temperatura corpórea (±37°C) possibilita o emprego destas ML para proteção e carreamento de compostos bioativos, ao longo do trata gastrointestinal até absorção no intestino, pois provavelmente a integridade estrutural não será comprometida.

Na Figura 3 estão expostas graficamente as curvas do comportamento térmico de fusão das ML desenvolvidas com a mistura de CA, CR e com incorporação de 20, 40 e 60% de OGAO. As T_{pf} para estas ML variaram entre, aproximadamente, 62 e 70°C, 61 e 69°C e 59 e 66°C, e para a ΔH_f os valores ficaram na faixa de -102 e -120 J/g, -83 a -91J/g e -52 a -56 J/g, respectivamente. Notou-se que o incremento de OGAO nas ML reduziu, de maneira geral a T_{pf} dos sistemas, devido a presença dos TAG triinsaturados, que apresentam ponto de fusão inferior em comparação aos TAG saturados dos *hardfats*. A ΔH_f também foi influência pela presença dos TAG triinsaturados, deste modo, reduzindo a cristalinidade da ML e possivelmente facilitando a transição de fases, que será discutida no decorrer do estudo. Porém, foi possível verificar que ocorreu um efeito eutético entre os componentes das ML e este efeito foi mais pronunciado nas ML contendo 50% de CA e 50% de CR, em todos os níveis de incorporação de OGAO (Figura 3B, C e D). O efeito eutético está diretamente relacionado a incompatibilidades entre os constituintes dos sistemas, podendo estar associado a diferenças entre os volumes moleculares, formas e/ou polimorfos preferenciais, com consequente redução da temperatura de fusão em comparação com os componentes isolados [32].

Avaliando a composição em TAG dos constituintes das ML, pode-se verificar que a OOO é o principal TAG do OGAO (~66%), apresentando em sua composição 54 carbonos e peso molecular de 885,45 g/mol. Valores muito semelhantes ao principal TAG do CA (~80% de SSS) que apresenta forma molecular composta por 54 carbonos e peso molecular de 891,50 g/mol, decorrentes das diferenças das insaturações das moléculas dos ácidos graxos oleico (C18:1) e esteárico (C18:0). Enquanto que, o CR é composto, aproximadamente, por 56% de do ácido graxo behênico e 31% de ácido graxo esteárico, distribuídos em diferentes TAG trissaturados (SSBe, SABe, SBeBe, ABeBe, BeBeBe e BeBeLg), compostos ainda pelos ácidos graxos araquidônico e lignocérico em menores quantidades, mas que apresentam maior

tamanho de cadeia carbônica que o ácido graxo behênico. Portanto, mesmo a BeBeBe não sendo majoritária, utilizamos suas informações a título de comparação com a SSS, ou seja, a BeBeBe apresenta formula molecular composta por 66 carbonos e peso molecular de 1059,83 g/mol. Deste modo, sugerimos que neste estudo o efeito eutético ocorreu devido as diferenças entre os tamanhos das cadeias carbônicas das moléculas dos componentes sólidos do sistema, os *hardfats*. E ainda, pela presença de TAG triinsaturados que possuem organização espacial diferente dos TAG trissaturados, devido a presença de insaturações.

Contudo, este comportamento pode ser positivo para o desenvolvimento de CLN, uma vez que, está incompatibilidade entre os componentes, favoreceu a redução da cristalinidade das ML. Assim, possivelmente, este efeito pode aumentar a capacidade de carga dos CLN e estabilidade ao longo do armazenamento, em relação a sistemas lipídicos mais cristalinos, como as ML desenvolvidas apenas com o CA ou CR.
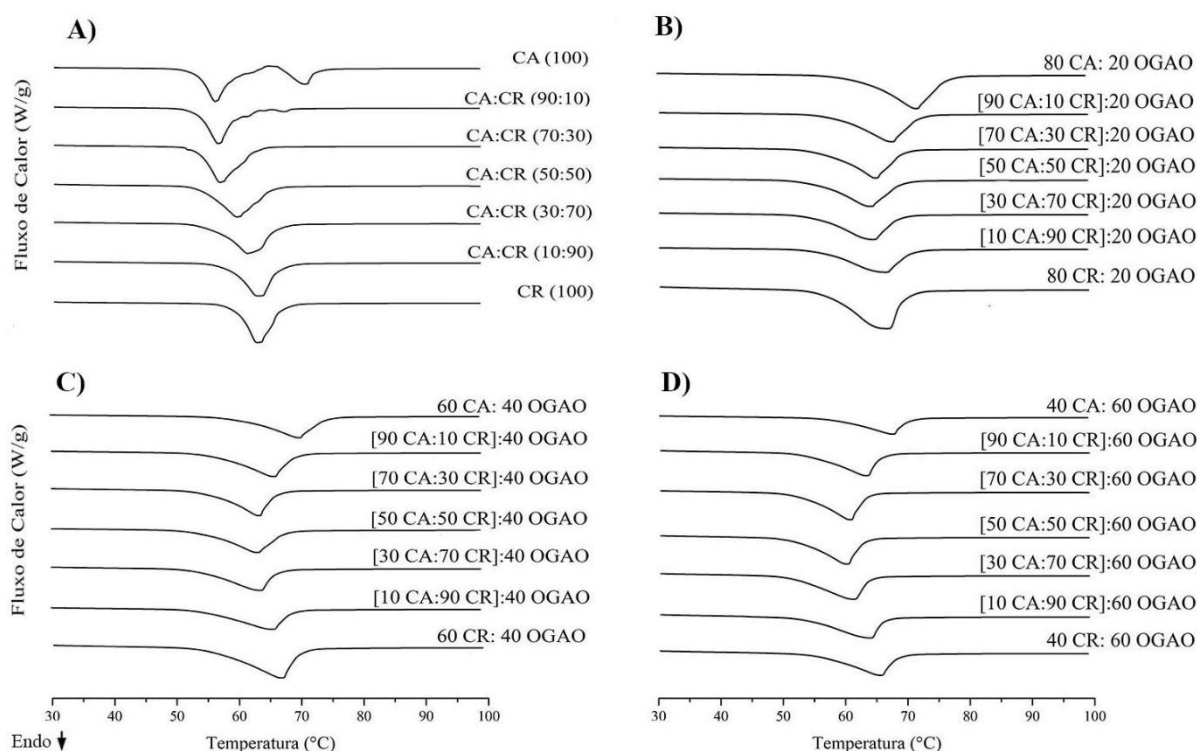
Figura 3. *Curvas de fusão a taxa de 10°C/min.:* ***A****) óleos totalmente hidrogenados de canola (CA) e crambe (CR) e matrizes lipídicas com misturas de CA e CR;* ***B****) Matrizes lipídicas de CA e CR com incorporação de óleo de girassol alto oleico (OGAO) na proporção de 20%;* ***C****) Matrizes lipídicas de CA e CR com incorporação de óleo de girassol alto oleico (OGAO) na proporção de 40%;* ***D****) Matrizes lipídicas de CA e CR com incorporação de óleo de girassol alto oleico (OGAO) na proporção de 60%, respectivamente.*

Hábito Polimórfico

A identificação das formas polimórficas é realizada com base no *short spacings* dos cristais lipídicos, obtidos através de DRX de alto ângulo. Os tipos mais comuns de empacotamento de TAG são hexagonal, ortorrômbico e triclínico, os quais são designados como as formas cristalinas, *α*, *β'* e *β*, respectivamente [28,33]. A transformação polimórfica das gorduras é monotrópica, ou seja, sempre ocorrendo na direção da forma mais estável (α→β'→β), podendo passar ou não através da forma (β') [34].

Na Tabela 6 estão descritos os *short spacings,* intensidades dos picos e as formas polimórficas obtidos após tratamento térmico de cristalização a 5°C/24h seguidos de 25°C/24h para estabilização cristalina dos CA e CR e das ML desenvolvidas com as suas misturas e incorporação de 20, 40 e 60% de OGAO. Adicionalmente, na Figura 2 constam os respectivos difratogramas.

Verificou-se que as matérias-primas (CA e CR) e suas misturas apresentaram apenas uma linha de difração em 4,15 Å, que é referente a cristais na forma *α* (Figura 4A). Os cristais α são considerados instáveis, indicando que estes sistemas ainda passarão por transições polimórficas durante o armazenamento [28].

Observou-se que a incorporação de OGAO em todos os sistemas (Figura 4B, C e D) promoveu a transição polimórfica de *α* para as formas *β'* e *β,* sendo possível verificar picos de difração em 4,2 e 3,8 Å, que correspondem a presença de cristais na forma intermediária *β'* e em 4,6 Å referente a forma *β*. Além disso, o incremento de OGAO favoreceu a redução da cristalinidade dos sistemas desenvolvidos, sendo possível verificar através da redução da intensidade dos picos. Cabe destacar que as ML com incorporação de 20% de OGAO, contendo 80% de CA e composta pela mistura de CA (90%) e CR (10%) apresentaram maior intensidade de difração em 4,6 Å, podendo indicar a predominância de cristais na forma mais estável (*β*). Segundo Oliveira, Stahl, Ribeiro, Grimaldi, Cardoso and Kieckbusch [22] estes sistemas tendem a atingir o equilíbrio termodinâmico na forma *β*, pois o habito polimórfico do CA é a forma mais estável. Enquanto que, nos demais sistemas compostos por 20% de OGAO a intensidade em 4,2 Å foi aumentando com o incremento de CR nas formulações (*β'>>β*). Estes resultados, estão de acordo com os obtidos por Ribeiro, Basso and Kieckbusch [11], que após estudo de estabilização polimórfica do CR, verificaram que o habito polimórfico deste *hardfat* é a mistura de cristais nas formas *β'* e *β*. Comportamento semelhante foi verificado para a incorporação de

40 e 60% de OGAO, onde a maior parte dos sistemas desenvolvidos apresentam misturas de cristais nas formas β' e β. Com exceção das ML compostas por 60% de CA (Figura 4C); 40% de CA; e com a mistura de CA e CR (90:10) (Figura 4D), onde foi possível verificar apenas cristais na forma β.

Sato [28] afirma que as formas polimórficas apresentam características distintas de grande importância tecnológica para o direcionamento de aplicação de ML. Uma vez que, cada forma polimórfica apresenta propriedades físicas particulares, podendo influenciar, tanto nos aspectos físicos de um produto, como consistência, estabilidade e espalhabilidade, quanto nas características sensoriais. De acordo com Sato [28] os cristais α são instáveis e de vida curta, os cristais na forma β' são metaestáveis, com tamanho relativamente pequeno e geralmente incorporam grande quantidade de óleo líquido na rede cristalina, contribuindo para a formação de gorduras mais macias, com boa aeração e propriedades de cremosidade. Ao contrário da forma polimórfica β, que é densamente empacotada e mais estável, o que implica em maior consistência e baixo potencial de aeração. Além disso, inicialmente, os cristais β são pequenos, mas tendem a crescer em grandes aglomerados em forma de agulhas, promovendo uma sensação de arenosidade quando consumidos. Cabe destacar que todas as características descritas por Sato [28] são consideradas para sistemas lipídicos com cristalização em escala macroscópica, podendo apresentar comportamento diferenciado quando nanoestruturados.

Tabela 5. Formas polimórficas, *short spacings* e intensidades dos picos nos difratogramas referentes aos óleos totalmente hidrogenados de canola (CA) e crambe (CR) e das matrizes lipídicas desenvolvidas com as suas misturas e incorporação de 20, 40 e 60% de óleo de girassol alto oleico (OGAO)

Matrizes lipídicas	*Short spacings* (Å)					Forma polimórfica
	4,6*	4,1	4,2	3,8	3,7	
CA (100)	-	$4,15_{mF}$	-	-	-	α
CA:CR (90:10)	-	$4,16_{mF}$	-	-	-	α
CA:CR (70:30)	-	$4,14_{mF}$	-	-	-	α
CA:CR (50:50)	-	$4,16_{mF}$	-	-	-	α
CA:CR (30:70)	-	$4,13_{mF}$	-	-	-	α
CA:CR (10:90)	-	$4,16_{mF}$	-	-	-	α
CR (100)	-	$4,16_{mF}$	-	-	-	α
Incorporação de 20% de OGAO						
80 CA: 20 OGAO	$4,58_{mF}$	-	$4,23_{mf}$	$3,88_{M}$	$3,74_{M}$	$\beta'+\beta$
[90 CA:10 CR]:20 OGAO	$4,59_{mF}$	-	$4,24_{mf}$	$3,88_{M}$	$3,75_{M}$	$\beta'+\beta$
[70 CA:30 CR]:20 OGAO	$4,67_{M}$	-	$4,24_{M}$	$3,85_{M}$	-	$\beta'+\beta$
[50 CA:50 CR]:20 OGAO	$4,54_{M}$	-	$4,21_{M}$	$3,81_{M}$	-	$\beta'+\beta$
[30 CA:70 CR]:20 OGAO	$4,69_{M}$	-	$4,21_{F}$	$3,88_{M}$	-	$\beta'+\beta$
[10 CA:90 CR]:20 OGAO	$4,65_{M}$	-	$4,23_{mF}$	$3,85_{M}$	-	$\beta'+\beta$
80 CR: 20 OGAO	$4,57_{mf}$	-	$4,20_{mF}$	$3,81_{M}$	-	$\beta'+\beta$
Incorporação de 40% de OGAO						
60 CA: 40 OGAO	$4,55_{mF}$	-	-	$3,84_{M}$	$3,69_{M}$	β
[90 CA:10 CR]:40 OGAO	$4,59_{mF}$	-	$4,21_{mf}$	$3,87_{M}$	$3,71_{M}$	$\beta'+\beta$
[70 CA:30 CR]:40 OGAO	$4,65_{M}$	-	$4,24_{mF}$	$3,88_{M}$	-	$\beta'+\beta$
[50 CA:50 CR]:40 OGAO	$4,58_{mF}$	-	$4,21_{M}$	$3,84_{M}$	-	$\beta'+\beta$
[30 CA:70 CR]:40 OGAO	$4,63_{mF}$	-	$4,22_{mF}$	$3,90_{mf}$	$3,82_{mf}$	$\beta'+\beta$
[10 CA:90 CR]:40 OGAO	$4,60_{f}$	-	$4,22_{mF}$	$3,83_{M}$	-	$\beta'+\beta$
60 CR: 40 OGAO	$4,58_{mf}$	-	$4,20_{mF}$	$3,82_{M}$	-	$\beta'+\beta$
Incorporação de 60% de OGAO						
40 CA: 60 OGAO	$4,58_{mF}$	-	-	$3,77_{M}$	$3,62_{M}$	β
[90 CA:10 CR]:60 OGAO	$4,53_{mF}$	-	-	$3,85_{M}$	$3,69_{M}$	β
[70 CA:30 CR]:60 OGAO	$4,57_{mF}$	-	$4,23_{mf}$	$3,85_{M}$	$3,70_{M}$	$\beta'+\beta$
[50 CA:50 CR]:60 OGAO	$4,68_{mF}$	-	$4,24_{mf}$	$3,86_{M}$	$3,72_{M}$	$\beta'+\beta$
[30 CA:70 CR]:60 OGAO	$4,60_{M}$	-	$4,22_{M}$	$3,84_{f}$	-	$\beta'+\beta$
[10 CA:90 CR]:60 OGAO	$4,64_{mf}$	-	$4,22_{mF}$	$3,81_{M}$	-	$\beta'+\beta$
40 CR: 60 OGAO	$4,60_{mf}$	-	$4,21_{mF}$	$3,82_{M}$	-	$\beta'+\beta$

* Intensidade dos picos: m – muito; f – fraco; M – médio; F- forte.
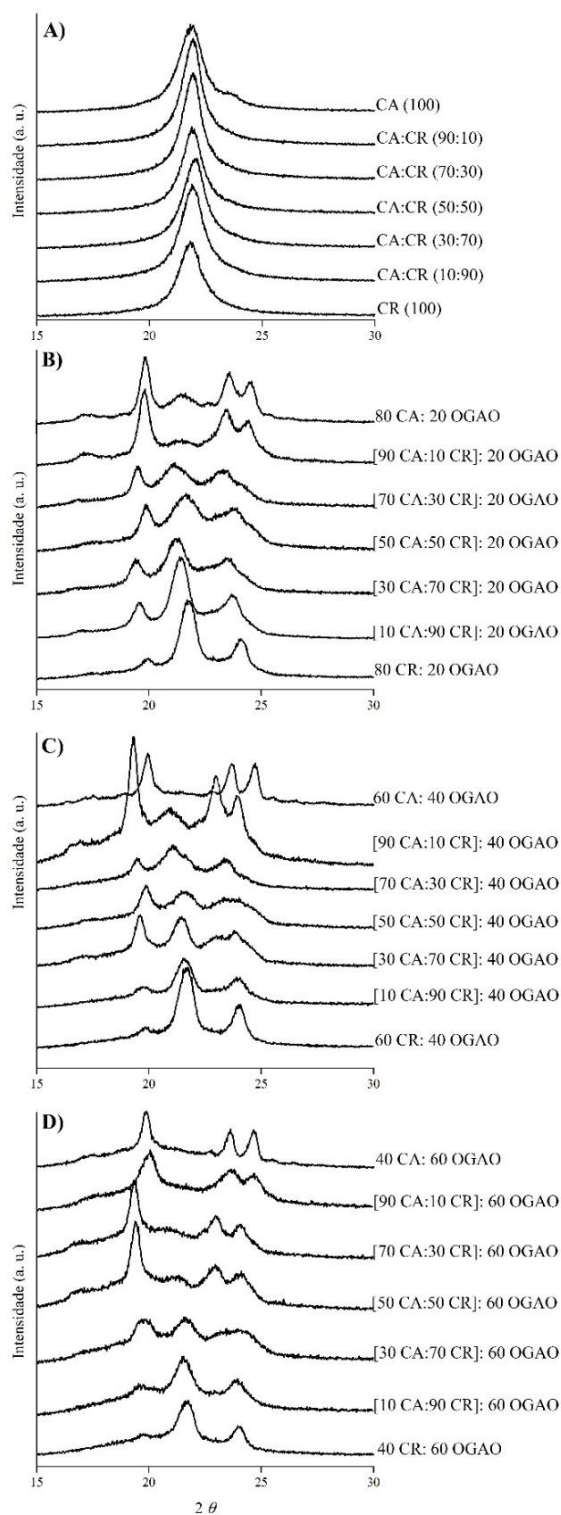
Figura 4. *Padrões de difração de: **A**) óleos totalmente hidrogenados de canola (CA) e crambe (CR) e das matrizes lipídicas desenvolvidas com suas misturas; **B**) Matrizes lipídicas de CA e CR com incorporação de óleo de girassol alto oleico (OGAO) na proporção de 20%; **C**) Matrizes lipídicas de CA e CR com incorporação de óleo de girassol alto oleico (OGAO) na proporção de 40%; **D**) Matrizes lipídicas de CA e CR com incorporação de óleo de girassol alto oleico (OGAO) na proporção de 60%.*

Assim, sugere-se neste estudo que as ML desenvolvidas apenas com lipídios sólidos (CA e CR) apresentaram-se muito promissoras para o desenvolvimento de NLS, mesmo que os cristais na forma α sejam considerados instáveis. Estudos recentes afirmam que nanopartículas que se mantem na forma α apresentam-se esféricas, com menor susceptibilidade a agregação quando estão em suspensão aquosa. Porém, pela elevada cristalinidade, conferida pela composição totalmente saturada, estes sistemas apresentam pouca capacidade de incorporação de compostos bioativos [5,6]. Deste modo, os sistemas que apresentaram misturas de cristais na forma β' e β, com predominância de cristais na β' mostraram-se mais promissores para o carreamento de compostos bioativos. Principalmente do ponto de vista de incorporação de lipídio líquido na rede cristalina, o que pode favorecer a inclusão de compostos bioativos. Além disso, as ML que apresentaram cristais na forma β podem ser empregadas no desenvolvimento de CLN para aplicação como sementes de cristalização em gorduras, visando o desenvolvimento de produtos com redução de saturados. Possivelmente, a redução de escala macro para manométrica pode reduzir os efeitos sensoriais indesejáveis nos produtos.

Microestrutura

A estrutura de uma rede de cristalina formada por gorduras é caracterizada principalmente pela morfologia (tamanho e forma) dos cristais. A morfologia pode ser diretamente observada usando MLP, porque os cristais lipídicos são birrefringentes. Deste modo, sob o MLP, os cristais de gordura aparecem brilhantes, enquanto que o óleo líquido é referente a parte escura da imagem, podendo-se assim, obter também informações referente a cristalinidade do sistema [33]. O nível microestrutural de uma rede cristalina de gordura pode ser definido como estruturas com dimensões variando entre 0,5 e 200 mm [35,36]. As diferenças na formação destas redes cristalinas influenciam diretamente nas propriedades físicas dos produtos onde são adicionadas as ML em macroescala. Assim, a MLP vem sendo muito utilizada para elucidar diferenças na textura de misturas de gorduras e para detectar tipos cristalinos ou alterações morfológicas durante o crescimento de cristais [36].

Na Figura 5 estão expostas as MLP obtidas a partir das ML desenvolvidas neste estudo, onde é possível verificar as redes cristalinas formadas e o formato dos cristais. Valores do diâmetro médio dos cristais e as porcentagens de áreas cristalizadas são apresentados na Tabela 6. O CA e de CR apresentaram cristais com DM de 1,79 e 3,19μm, com

aproximadamente 14 e 27% de área cristalizada, respectivamente. As misturas destes *hardfats*, apresentaram DM dos cristais variando entre 2,00 a 3,28μm e a presença do CR aumentou a porcentagem de área cristalizada (variando entre 23 e 28%). Como pode ser observado na Figura 5, a partir da incorporação de 30% de CR os cristais mudaram de tamanho e formato, adquirindo características mais próximas aos cristais do CR. Notou-se também que as redes cristalinas se tornaram mais densas com o aumento do CR nos sistemas. Segundo, Tang and Marangoni [37] a cristalização de TAG trissaturados ocorre através de eventos de nucleação, onde pequenos cristais crescem e interagem entre si através de forças não covalentes, de modo a formar uma rede cristalina contínua. Após a conclusão da cristalização, os TAG trissaturados agregam-se para formar os cristais de gordura, que entram em contato e formam aglomerados denominados de *clusters*. Estes *clusters* formam agregados maiores, em flocos, a partir de ligações fracas, e dão origem a uma rede macroscópica cristalina altamente organizada. Geralmente, apresentam cristais na forma α, e a alta densidade e organização da rede cristalina dificulta a mobilidade dos cristais para formas cristalinas mais estáveis. Como visto no tópico anterior, através da DRX, o CA e CR e as ML compostas por suas misturas apresentaram cristais na forma α, provavelmente a transição polimórfica destes sistemas foi dificultada pela formação de estruturas altamente compactas e organizadas pela presença de TAG totalmente saturados.

A incorporação de OGAO, de maneira geral favoreceu a redução do DM dos cristais e da cristalinidade de algumas ML, sendo visível a redução da cristalinidade pelos maiores espaçamentos entre os cristais na Figura 5. Além disso, notou-se que para a maioria das ML os cristais apresentaram um núcleo com ramificações alongadas. Esta característica, segundo Rousseau and Marangoni [38], ocorre geralmente para TAG que cristalizam inicialmente em cristais do tipo esferulitos e que crescem radialmente a partir dos mesmos núcleos centrais, decorrentes da agregação de lamelas cristalinas, e podem desenvolver ramificações durante o armazenamento.

Cabe ressaltar que os menores DM dos cristais foram de 1,85 e 1,26 μm paras as ML compostas por CA com incorporação de 40 e 60% de OGAO, respectivamente, e para a ML desenvolvida com a mistura de CA e CR, na proporção de 90:10 (m/m) e incorporação de 60% de OGAO, apresentando DM dos cristais de 1,86μm.
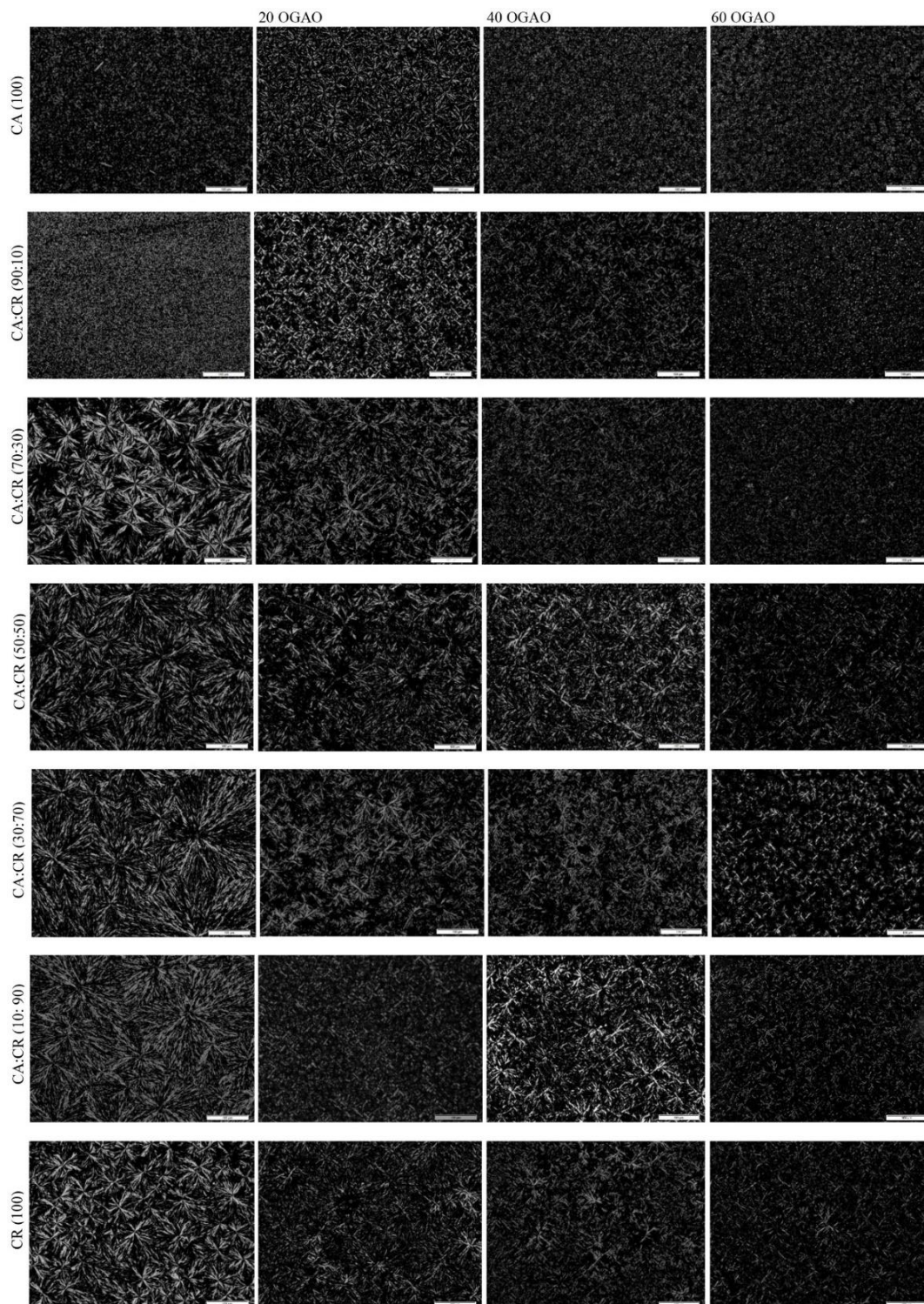
Figura 5. *Imagens das matrizes lipídicas desenvolvidas com óleos totalmente hidrogenados de canola (CA) e crambe (CR) e das matrizes lipídicas desenvolvidas com incorporação de óleo de girassol alto oleico (OGAO) na proporção de 20, 40 e 60%, obtidas através de cristalização estática a 25°C com aumento de 200X, após tratamento térmico de cristalização a 5°C/24h seguido de estabilização cristalina à 25°C/24h. A barra indica 100 micrometros.*

Estes menores diâmetros, podem estar relacionados a presença de TAG triinsaturados provenientes do OGAO, que aumentou o espaçamento entre os cristais, reduzindo a cristalinidade e favorecendo a transição polimórfica para a forma mais estável *β*.

Além disso, apresentando redes cristalinas mais homogêneas. Destaca-se que a ML que apresentou a menor cristalinidade (10%) e o menor DM de cristais (0,91 µm) foi a ML composta por CA e CR, na proporção de 10:90m/m, com 60% de OGAO. Está ML apresentou segundo a DRX uma mistura de cristais nas formas *β'* e *β*, assim como os demais sistemas desenvolvidos.

Tabela 6. Diâmetro médio dos cristais e porcentagem de área cristalizada das matrizes lipídicas desenvolvidas com os óleos totalmente hidrogenados de canola (CA) e crambe (CR) e das matrizes lipídicas (ML) desenvolvidas com as suas misturas e incorporação de 20, 40 e 60% de óleo de girassol alto oleico (OGAO)

Matrizes Lipídicas	Diâmetro médio dos cristais (µm)	Área Cristalizada (%)
CA (100)	1,79±1,82	13,69±0,54
CA:CR (90:10)	2,00±1,52	24,40±3,71
CA:CR (70:30)	3,28±4,64	27,63±2,48
CA:CR (50:50)	2,88±3,68	23,62±0,42
CA:CR (30:70)	2,91±3,74	27,58±0,43
CA:CR (10:90)	2,78±3,20	23,26±0,79
CR (100)	3,19±4,24	26,77±3,06
Incorporação de 20% de OGAO		
80 CA: 20 OGAO	2,70±2,94	26,75±0,37
[90 CA:10 CR]:20 OGAO	5,19±7,41	20,00±1,69
[70 CA:30 CR]:20 OGAO	2,20±2,62	14,30±0,54
[50 CA:50 CR]:20 OGAO	2,74±3,03	17,41±0,92
[30 CA:70 CR]:20 OGAO	3,89±6,51	15,51±1,36
[10 CA:90 CR]:20 OGAO	6,95±7,74	20,94±1,24
80 CR: 20 OGAO	2,34±2,47	17,81±0,54
Incorporação de 40% de OGAO		
60 CA: 40 OGAO	1,85±1,60	16,25±0,69
[90 CA:10 CR]:40 OGAO	2,60±4,65	14,01±0,26
[70 CA:30 CR]:40 OGAO	3,23±4,67	14,66±0,61
[50 CA:50 CR]:40 OGAO	2,85±3,25	25,03±0,65
[30 CA:70 CR]:40 OGAO	4,05±5,66	13,68±1,42
[10 CA:90 CR]:40 OGAO	6,73±8,46	20,33±2,60
60 CR: 40 OGAO	2,06±2,14	12,46±1,32
Incorporação de 60% de OGAO		
40 CA: 60 OGAO	1,26±1,23	12,88±1,10
[90 CA:10 CR]:60 OGAO	1,86±3,27	15,83±0,60
[70 CA:30 CR]:60 OGAO	3,07±4,15	13,49±0,90
[50 CA:50 CR]:60 OGAO	2,05±2,21	12,49±0,91
[30 CA:70 CR]:60 OGAO	6,27±7,37	11,91±1,19
[10 CA:90 CR]:60 OGAO	0,91±1,21	10,90±0,45
40 CR: 60 OGAO	2,19±2,17	13,19±0,58

CONCLUSÃO

Neste estudo foi comprovado que o OGAO, CA e CR, que são óleos e gorduras vegetais presentes no cenário industrial apresentaram comportamento térmico e cristalino com grande potencial para desenvolvimento de nanopartículas lipídicas. A utilização destas matérias-primas lipídicas conferiu as ML desenvolvidas características diferenciadas em termos de cristalização e fusão. Destaca-se o efeito eutético, que pode ser benéfico para o desenvolvimento de NLS e CLN com nanoestruturas cristalinas menos compactas, o que pode favorecer a incorporação de compostos bioativos. Além disso, a incorporação de compostos bioativos também pode ser potencializada pela presença de óleos vegetais, como o OGAO, que também colaborou para a redução da cristalinidade das ML. A exploração das *hardfats* e óleos de outras fontes vegetais, pode contribuir para expandir a nanotecnologia na área de alimentos, possibilitando o desenvolvimento de ML com propriedades diferenciadas. Assim, pode-se concluir que o uso de óleos e gorduras vegetais tem potencial de aplicação em sistemas cristalinos nanoestruturados, principalmente pelas misturas de TAG presentes em suas composições, o que confere características de cristalização e fusão diferenciadas de matérias-primas purificadas.

AGRADECIMENTOS

REFERÊNCIAS

(1)   Tamjidi, F.; Shahedi, M.; Varshosaz, J.; Nasirpour, A. Nanostructured lipid carriers (NLC): A potential delivery system for bioactive food molecules. *Innovative Food Science & Emerging Technologies* **2013**, *19*, 29-43.

(2)   McClements, D. J. Nanoscale Nutrient Delivery Systems for Food Applications: Improving Bioactive Dispersibility, Stability, and Bioavailability. *J Food Sci* **2015**, *80*, N1602-1611.

(3)   Rashidi, L.; Khosravi-Darani, K. The Applications of Nanotechnology in Food Industry. *Critical Reviews in Food Science and Nutrition* **2011**, *51*, 723-730.

(4)   Jafari, S.: *Nanoencapsulation of Food Bioactive Ingredients.*, 2017; Vol. 1.

(5)   Weiss, J.; Decker, E. A.; McClements, D. J.; Kristbergsson, K.; Helgason, T.; Awad, T. Solid Lipid Nanoparticles as Delivery Systems for Bioactive Food Components. *Food Biophysics* **2008**, *3*, 146-154.

(6)   Lasón, E.; Jan, O. Solid lipid nanoparticles – Characteristics, application and obtaining. *Chemik* **2011**, *65*, 964-967.

(7)   Sharma, V. K.; Diwan, A.; Sardana, S.; Dhall, V. Solid lipid nanoparticles system: an overview. *International Journal of Research in Pharmaceutical Sciences* **2011**, *2*, 450-461.

(8)   O'Brien: *Fats and oils formulation*: Boca Raton, 2009.

(9)   Gunstone, F. D.: Vegetable Oils. In *Bailey's Industrial Oil and Fat Products. Edible Oil and Fat Products: Chemistry, Chemical properties, and health effects*; Shahidi, F., Ed.; Hoboken, John Wiley & Sons: New Jersey, 2005; Vol. 2.

(10)   McKeon, T. A.: Transgenic Oils. In *Bailey's Industrial Oil and Fat Products. Edible Oil and Fat Products: Chemistry, Chemical properties, and health effects*; Shahidi, F., Ed.; John Wiley & Sons: Hoboken, New Jersey, 2005; Vol. 2.

(11)   Ribeiro, A. P. B.; Basso, R. C.; Kieckbusch, T. G. Effect of the addition of hardfats on the physical properties of cocoa butter. *European Journal of Lipid Science and Technology* **2013**, *115*, 301-312.

(12)   Costales, R.; Fernandez, A.: Hidrogenación e interesterificación. In *Temas Selectos en Aceites y Grasas - Volumen 1/ Procesamiento.* ; Block, J. M. B.-A., D., Ed.; Blucher: São Paulo, 2009; Vol. 1; pp 1-29.

(13)   Lovejoy, J. C.; Smith, S. R.; Champagne, C. M.; Most, M. M.; Lefevre, M.; Delany, J. P.; Denkins, Y. M.; Rood, J. C.; Veldhuis, J.; Bray, G. A. Effects of Diets Enriched in Saturated (Palmitic), Monounsaturated (Oleic), or trans (Elaidic) Fatty Acids on Insulin Sensitivity and Substrate Oxidation in Healthy Adults. *Diabetes care* **2002**, *25*, 1283-1288.

(14)   Santos, V. S.; Ribeiro, A. P. B.; Cardoso, L. P.; Santana, M. H. A. Crystallization, polymorphism and stability of nanostructured lipid carriers developed with

soybean oil, fully hydrogenated soybean oil and free phytosterols for food application. *Food Chemistry* **2018**, *a ser submetido.*

(15)   AOCS: *Official methods and recommended practices of the American Oil Chemists' Society*; AOCS Press: Urbana (USA), 2009.

(16)   Hartman, L.; Lago, R. Rapid preparation of fatty acid methyl esters from lipids. *Laboratory Practice* **1973**, *22*, 475-476.

(17)   Antoniosi, F. N. R.; Mendes, O. L.; Lanças, F. M. Computer prediction of triacylglycerol composition of vegetable oils by HRGC. *Chromatographia* **1995**, *40*, 557-562.

(18)   Ribeiro, A. P. B.; Grimaldi, R.; Gioielli, L. A.; Gonçalves, L. A. G. Zero trans fats from soybean oil and fully hydrogenated soybean oil: Physico-chemical properties and food applications. *Food Research International* **2009**, *42*, 401-410.

(19)   Campos, R.: Experimental methodology. In *Fat Crystal Networks*; Marangoni, A., Ed.; Marcel Dekker: New York, 2005; Vol. 1; pp 267-349.

(20)   Wang, J. L.; Dong, X. Y.; Wei, F.; Zhong, J.; Liu, B.; Yao, M. H.; Yang, M.; Zheng, C.; Quek, S. Y.; Chen, H. Preparation and characterization of novel lipid carriers containing microalgae oil for food applications. *J Food Sci* **2014**, *79*, E169-177.

(21)   Alberio, C.; Izquierdo, N. G.; Galella, T.; Zuil, S.; Reid, R.; Zambelli, A.; Aguirrezábal, L. A. N. A new sunflower high oleic mutation confers stable oil grain fatty acid composition across environments. *European Journal of Agronomy* **2016**, *73*, 25-33.

(22)   Oliveira, G. M. d.; Stahl, M. A.; Ribeiro, A. P. B.; Grimaldi, R.; Cardoso, L. P.; Kieckbusch, T. G. Development of zero trans/low sat fat systems structured with sorbitan monostearate and fully hydrogenated canola oil. *European Journal of Lipid Science and Technology* **2015**, *117*, 1762-1771.

(23)   Kojima, M.; Tachibana, N.; Yamahira, T.; Seino, S.; Izumisawa, A.; Sagi, A.; Arishima, T.; Kohno, M.; Takamatsu, K.; Hirotsuka, M.; Ikeda, I. Structured triacylglycerol containing behenic and oleic acids suppresses triacylglycerol absorption and prevents obesity in rats. *lipids health disease journal* **2010**, *9*, 77.

(24)   Moreira, D. K. T.; Ract, J. N. R.; Ribeiro, A. P. B.; Macedo, G. A. Production and characterization of structured lipids with antiobesity potential and as a source of essential fatty acids. *Food Research International* **2017**, *99*, 713-719.

(25)   Curi, R.; Pompeia, C.; Miyasaka, C. K.; Procopio, J.: *ENTENDENDO A GORDURA: OS ÁCIDOS GRAXOS*; 1 ed.; EDITORA MANOLE LTDA: Brasil, 2002; Vol. 1.

(26)   Guedes, A. M. M.; Ming, C. C.; Ribeiro, A. P. B.; da Silva, R. C.; Gioielli, L. A.; Gonçalves, L. A. G. Physicochemical Properties of Interesterified Blends of Fully Hydrogenated Crambe abyssinica Oil and Soybean Oil. *Journal of the American Oil Chemists' Society* **2014**, *91*, 111-123.

(27)   Ribeiro, M. D. M. M.; Ming, C. C.; Lopes, T. I. B.; Grimaldi, R.; Marsaioli, A. J.; Gonçalves, L. A. G. Synthesis of structured lipids containing behenic acid from fully hydrogenated Crambe abyssinica oil by enzymatic interesterification. *Journal of Food Science and Technology* **2017**, *54*, 1146–1157.

(28)   Sato, K.: *Crystallization behaviour of fats and lipids: a review*: Oxford, 2001; Vol. 56. pp. 2255-2265.

(29)   Ribeiro, A. P. B.; Masuchi, M. H.; Grimaldi, R.; Gonçalves, L. A. G. Interesterificação química de óleo de soja e óleo de soja totalmente hidrogenado: influência do tempo de reação. *Química Nova* **2009**, *32*, 939-945.

(30)   Yoon, G.; Park, J. W.; Yoon, I.-S. Solid lipid nanoparticles (SLNs) and nanostructured lipid carriers (NLCs): recent advances in drug delivery. *Journal of Pharmaceutical Investigation* **2013**, *43*, 353-362.

(31)   Severino, P.; Andreani, T.; Macedo, A. S.; Fangueiro, J. F.; Santana, M. H.; Silva, A. M.; Souto, E. B. Current State-of-Art and New Trends on Lipid Nanoparticles (SLN and NLC) for Oral Drug Delivery. *J Drug Deliv* **2012**, *2012*, 750891.

(32)   Himawan, C.; Starov, V. M.; Stapley, A. G. Thermodynamic and kinetic aspects of fat crystallization. *Adv Colloid Interface Sci* **2006**, *122*, 3-33.

(33)   Ramel, P. R.; Co, E. D.; Acevedo, N. C.; Marangoni, A. G. Structure and functionality of nanostructured triacylglycerol crystal networks. *Prog Lipid Res* **2016**, *64*, 231-242.

(34)   Timms, R. E.: *Crystallization of fats*; Blackie Academic: London, 1995.

(35)   Marangoni, A. G.; Acevedo, N.; Makely, F., Co, E. Structure and functionality of edible fats. *Soft Matter* **2012**, *8*, 1275-1300.

(36)   Ribeiro, A. P. B.; Basso, R. C.; Gonçalves, L. A. G.; Gioielli, L. A.; Oliveira dos Santos, A.; Cardoso, L. P.; Kieckbusch, T. G. Physico-chemical properties of Brazilian cocoa

butter and industrial blends. Part II - Microstructure, polymorphic behavior and crystallization characteristics. *Grasas y Aceites* **2012**, *63*, 89-99.

(37)   Tang, D.; Marangoni, A.: *Quantitative study on the microstructure of interface techniques*; CRC Press: Boca Raton, 2006; Vol. Science. pp. 257-265.

(38)   Rousseau, A. G.; Marangoni, A.: *Food lipids: chemistry, nutrition, and biotechnology.*; CRC Press: New York, 2002.

ARTIGO 3

"Thermal and crystalline properties of lipid nanoparticles developed with conventional vegetable fats and oils for food applications" a ser submetido a *Food Chemistry.*

Thermal and crystalline properties of lipid nanoparticles produced with conventional vegetable fats and oils for food applications

Valeria da Silva Santos[1], Bruno Brito Braz[1], Alan Ávila da Silva[2], Lisandro Pavie Cardoso[3], Maria Helena Andrade Santana[1], Ana Paula Badan Ribeiro[2]

[1]*Department of Biotechnological Processes, School of Chemical Engineering, University of Campinas, 500 Albert Einstein Ave., Campinas, SP 13083-970, Brazil.*
[2] *Department of Food Technology, School of Food Engineering, University of Campinas, 80 Monteiro Lobato St., Campinas, SP 13083-970, Brazil.*
[3] *Department of Applied Physics, Institute of Physics Gleb Wataghin, University of Campinas, 777 Sérgio Buarque de Holanda St., 13083-859 Campinas, SP, Brazil.*

Abstract

In this work, solid lipid nanoparticles (SLN) and nanostructured lipid carriers (NLC) with conventional vegetable oils and fats (high oleic sunflower oil and fully hydrogenated canola and crambe oils) were developed. NLS and CLN were characterized for size, polydispersity (PDI) and zeta potential (ZP) during 60 days. The thermal and crystalline properties were evaluated. The NLS presented gelation characteristics, associated with lipid polymorphic transitions to the β-form. The CLN remained liquid during the evaluations, presenting size from 156.33 to 208.10nm, PDI from 0.099 to 0199, and PZ from -13,23 to -25,10mV. They exhibited high thermal resistance, melting between 64 and 72°C and polymorphic habit in the β' and β forms. Besides that, an eutectic effect was observed indicating lipid materials incompatibility. However, this effect was beneficial, with consequent reduction of crystallinity and size. The NLS and CLN obtained with conventional oils and fats presented thermal and crystalline characteristics compatible with different food applications and high potential for bioactive compounds incorporation.

Keywords: Nanotechnology; Foods; Lipids, SLN; NLC; High-Pressure Homogenization.

Abbreviations

CA	Fully hydrogenated canola oil
CR	Fully hydrogenated Crambe oil
DLS	Dynamic light scattering
DSC	Differential Scanning Calorimetry
FAC	Fatty acids composition
GTI	Gastrointestinal tract
HLB	Hydrophilic-lipophilic balance
HOSO	High oleic sunflower oil
HPH	High-pressure homogenizer
INPI	National Institute of Industrial Property
LM	Lipid matrix

LN   Lipid Nanoparticles
NLC   Nanostructured Lipid Carriers
PDI   Polydispersity index
T80   Polyoxyethylene sorbitan monooleate
TAG   Triacylglycerols
XRD   X-ray diffraction
Z-ave   Average diameter
ZP   Zeta Potential

1. Introduction

Lipids are essential nutrients of the human diet by providing essential fatty acids and energy. Chemically, natural fats and oils are a multi-component triacylglycerol (TAG) blends, which are esters of glycerol and fatty acids. Conventional vegetable fats and oils are composed of a mixture of about 20 fatty acids in different proportions. Each fatty acid can occupy different positions in the glycerol molecule (sn-1, sn-2 or sn-3), allowing a big diversity of TAG combinations with different thermal and crystalline behaviors (Marangoni, Acevedo, Maleky, Co, Peyronel, Mazzanti, et al., 2012).

The crystalline lipid behavior on macroscale depends directly on the fatty acid chain characteristics, such as the presence of saturated or unsaturated fatty acids, cis or trans configuration, and chain size. Saturated fatty acids have a higher melting point than the corresponding unsaturated fatty acid with one or more double bonds. The presence of long and saturated chains of fatty acids increases the melting point of TAGs, due to their linear conformation, resulting in a higher interaction of the molecules and, consequently, a highly ordered crystalline packaging (Scrimgeour, 2005).

The crystallization process refers to the spontaneous ordering of the lipid system characterized by total or partial movement restriction caused by physical interactions between TAG molecules in different temperatures. Differences in crystalline forms result from different molecular packaging. A crystal, therefore, consists of molecules arranged in a fixed pattern, known as reticulate. Its high degree of molecular complexity allows the same set of TAGs to be packaged and crystallized in different structures, and also be able to transit in different polymorphic forms, characterizing the polymorphism (Sato, 2001).

The polymorphism can be defined in terms of the ability to manifest different cell unit structures resulting from various molecular packaging. In TAGs three specific types of sub-cells predominate, referring to the polymorphs α, β 'and β, according to the current polymorphic nomenclature for lipids. The polymorphic transformation in TAGs is monotropic, that is, it is an irreversible process from the least stable to the most stable ($\alpha \rightarrow \beta' \rightarrow \beta$), depending on the temperature and time involved in the crystallization and stabilization of the crystals (Martini, Awad, & Marangoni, 2006).

It is possible to determine the general properties of lipid functionality and applicability, which are therefore dependent on the TAG profiles of the fats and oils used. In the scientific literature, it is possible to find several studies on the crystallization behavior and polymorphism, for both purified TAGs and of edible fats and oils in micro and macro-scale (Basso, Ribeiro, Masuchi, Gioielli, Gonçalves, Santos, et al., 2010; Sato, 2001).

Currently, there is a great interest in studying the lipid properties at the nanoscale, due to the great discoveries of differentiated behaviors of nanostructured materials, such as nanotubes, nanosensors, nanoparticles, nanofibers, drug delivery nanosystems, among others. These systems can be applied in a wide range of industrial areas, for instance, in the textile, energy production, communication, medicine, pharmaceuticals and cosmetics (Cerqueira, Pinheiro, Silva, Ramos, Azevedo, Flores-López, et al., 2014; Tamjidi, Shahedi, Varshosaz, & Nasirpour, 2013).

Regarding nanoscale lipids for food application, solid lipid nanoparticles (SLN) and nanostructured lipid carriers (NLC) are the most promising nanostructured systems in terms of viability for industrial application. SLN are developed only with saturated lipids and NLC with the mixture of saturated and unsaturated lipids. This difference of chemical composition provides to these systems, different thermal and crystalline properties (Muller, Runge, Ravelli, Mehnert, Thunemann, & Souto, 2011). The main technological characteristic of SLN and NLC is the physical stability of nanostructures. They are developed with lipid materials that have a melting point above body temperature (37 °C), maintaining structural integrity throughout the digestive system, where they will be absorbed and can be used to protect, transport and deliver bioactive compounds in food products. In addition, the high thermal resistance of the SLN and NLC may be an interesting feature from the point of view of applicability in thermally processed products. This technology has already been used in the pharmaceutical and

biomedical areas, through the oral administration of SLN and NLC, presenting positive results for the sustained delivery and release of drugs in the organism (Severino, Andreani, Macedo, Fangueiro, Santana, Silva, et al., 2012).

Recently, we have unprecedented proposed the SLN and NLC production using raw materials, commonly used in food products, generally recognized as safe (GRAS), such as natural and modified fats and oils, which gave to our research group the Invention Privilege (INPI-BR 10 2017 006471 9). NLC developed with soybean oil and soybean oil hardfat, were used as carriers of free phytosterols, where processing conditions and emulsifying systems were optimized (V. S. Santos, Ribeiro, Cardoso, & Santana, 2018). This work made possible the dissemination of the application of lipid nanoparticles in food in terms of volume and costs since it eliminated the need for purified materials for the production of SLN and NLC.

The aim of this work was to develop SLN and NLC using a new range of vegetable oils and fats available in the industrial scenario. As well as, to study the thermal and crystalline behavior of these lipids in nanostructured systems, still little explored in food science and technology.

2. Materials and methods

2.1. Materials

The solid lipid raw materials used for the development of the SLN and NLC were the fully hydrogenated canola (CA) and crambe (CR) oils provided by SGS Agricultura e Indústria Ltda[©] (Ponta Grossa - PR, Brazil), obtained from total catalytic hydrogenation process of the canola and crambe oils, respectively. High oleic sunflower oil (HOSO), supplied by Cargill Agrícola S.A (Mairinque - SP, Brazil), was used as liquid lipid in the NLC composition. The HOSO and both, CA and CR, were characterized according to the fatty acid (FAC) and triacylglycerols (TAG) compositions in a previous study(V. S. Santos, Santana, Braz, Silva, Cardoso, & Ribeiro, 2018). The HOSO have 90.68% of unsaturated fatty acids (78,60% of oleic acid, O, C18:1, and 11,41% of linoleic acid, L, C18:2). The CA and CR presented 100% of saturated fatty acids. CA has 93.82% of stearic acid (S, C18:0), 5.24% of palmitic acid (P, C16:0) and 0.94 % arachidonic acid (A, C20:0). While CR has 56.30% behenic acid (Be, C22:0), 31.70% stearic acid (S, C18:0), 6.70 % of arachidonic acid (A, C20:0), 3.20% of palmitic acid (P, C16:0) and 2.10% of lignoceric acid (Lg, C24:0). The TAGs present in the HOSO were: OOO

65%, followed by OLO (~15%), OOP (~10%) and OLL/PLO (~3%). The CA presented 4 different TAGs in its composition, with the majority being SSS (~80%) and PSS (~13%). In the CR, 9 different TAGs were found, among which the predominant ones were SBeBe (~38%), SSBe (~17%), SABe (~17%) and in smaller proportions ABeBe (~6%), BeBeBe (~9%), BeBeLg (~8%), PSBe (~2%) and PSS (~0.5%). The polyoxyethylene sorbitan monooleate P1754 (Tween®80, T80), with hydrophilic-lipophilic balance (HLB) of 14.0, was purchased from Sigma-Aldrich (St. Louis, Missouri, USA).

2.2. Methods

2.2.1. Formulation of lipid nanoparticles

Two distinct nanoparticle systems were developed, the SLN developed only with saturated lipids and the NLC composed by the mixture of saturated and unsaturated lipids. The general formulation of these nanoparticles was composed of 10% (m/m) of lipid phase and 90% (m/m) of the aqueous phase. The aqueous phase was composed of distilled water and 2% emulsifier, according to recommendations of (Qian & McClements, 2011; Yang, Corona, Schubert, Reeder, & Henson, 2014). The emulsifier used was the T80.

The lipid fraction was selected from an earlier study conducted by our research group. In this work, we have shown that different lipid matrices (LM) have been developed and evaluated for thermal and crystalline behavior and are compatible with the SLN and NLC application (V. S. Santos, Santana, Braz, Silva, Cardoso, & Ribeiro, 2018). Thus, 3 LM composed of only saturated lipids (CA and/or CR) for the development of SLN and 9 LM containing the mixture of saturated (CA and/or CR) and unsaturated lipids (20, 40 and 60% of HOSO) for application in NLC. In Figure 1, the SLN and NLC formulations developed in this study are illustratively set forth.
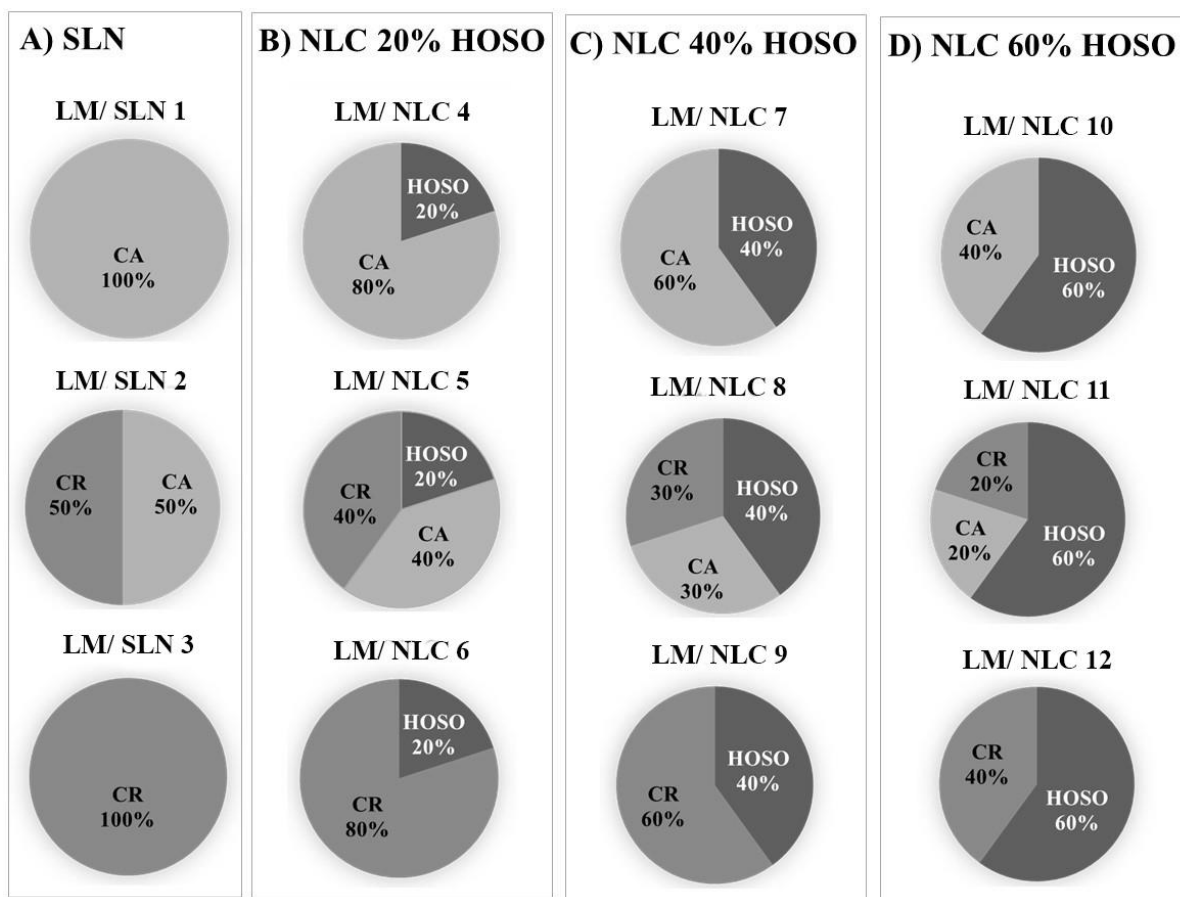
Fig. 1. Schematic representation of Solid Lipid Nanoparticle (SLN) and Nanostructured Lipid Carriers (NLC) formulation with their respective lipid matrices: A) LM/SLN composed only of solid lipids (CA and CR); B) LM/ NLC compounds with mixtures of solid and liquid lipids (20% of the HOSO and CA and/or CR); C) LM/NLC compounds with mixtures of solid and liquid lipids (40% of the HOSO and CA and/or CR); D) LM/NLC compounds with mixtures of solid and liquid lipids (60% of the HOSO and CA and/or CR).

2.2.2. Production process of lipid nanoparticles

Obtaining the lipid nanoparticles involved basically four steps: i) LM fusion, ii) emulsification, iii) nanoemulsification, and iii) crystallization and lipid stabilization. The LM were melted and homogenized on magnetic stirrer at 300 rpm for 2 minutes. Subsequently, the aqueous phase containing the emulsifier was added at 90øC and the pre-emulsion was obtained in Ultra Turrax IKA T18 Basic (Germany) at 20,000rpm for 3 minutes homogenization. Then, the pre-emulsion was subjected to different homogenization cycles (3 and 5 cycles) at 800bar in a high-pressure homogenizer (HPH) (GEA Niro Soavi, model: NS 1001L PANDA 2K, Italy), according to Zimmermann, Müller, and Mäder (2000) and Severino, Santana, and Souto (2012). After the HPH process, the obtained nanoemulsions were stored at 5 °C for 24 hours for the

crystallization of the lipid fraction and obtaining the dispersions containing the SLN and NLC followed by 24 h of crystalline stabilization at 25 °C (Qian & McClements, 2011; Yang, Corona, Schubert, Reeder, & Henson, 2014).
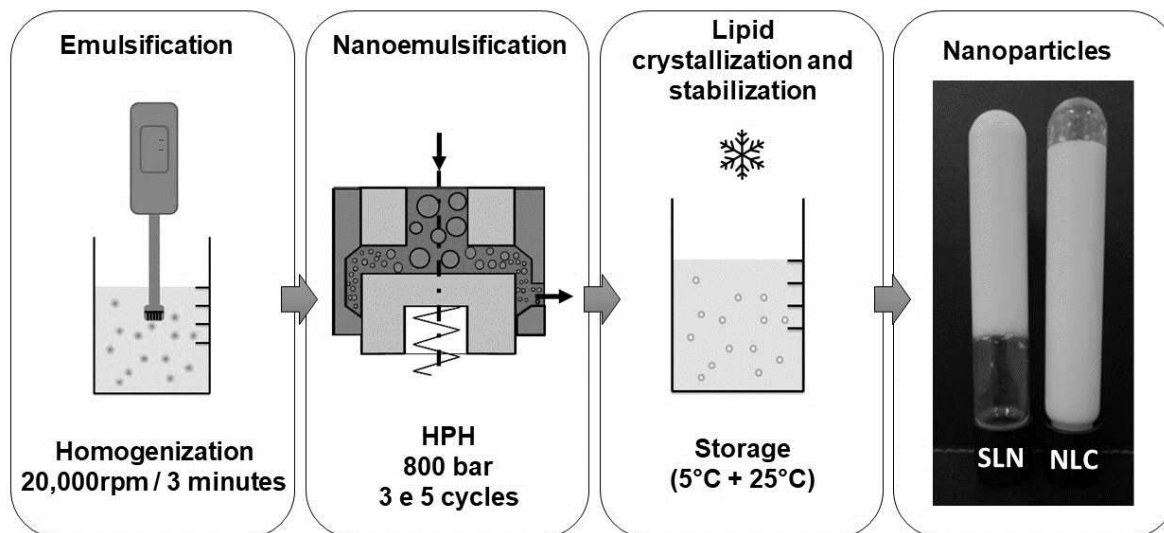
Fig. 2. Illustrative image of the solid lipid nanoparticles (SLN) and Nanostructured Lipid Carriers (NLC) production by high-pressure homogenization (HPH).

2.2.3. Additional drying process of lipid nanoparticles

The nanoparticles in aqueous suspension, shortly after step 4 of crystallization and crystalline stabilization, were subjected to lyophilization. The drying process involved the conditioning of the aqueous dispersion containing the nanoparticles in ultrafreezer (-80 °C) for 24 hours, for freezing the aqueous phase, followed by lyophilization in lyophilizer (Liobras L101, Brazil), according to the method described by Zimmermann, Müller, and Mäder (2000).

3.4. Size, Polydispersity Index and Zeta Potential

The LNs in aqueous dispersion produced by 3 and 5 cycles of HPH were evaluated for particle size by means of the hydrodynamic diameter (Z-ave) in nanometers (d.nm) using dynamic light scattering (DLS) with a high-power laser in Zetasizer Nano NS equipment, Malvern, United Kingdom. Besides that, the LNs were evaluated for the polydispersity index (PDI) and zeta potential (ZP) after 24 hours, 15, 30 and 60 days of the production process. The samples were diluted in distilled water to reduce the opalescence before measurements. Data analysis was performed using the software included in the equipment system.

2.2.4. Melting thermal behavior

The evaluation of the thermal behavior in the melting of the SLN and the lyophilized NLC was performed by means of the Differential Scanning Calorimetry (DSC) TA Instruments, model Q2000, coupled to the RCS90 Refrigerated Cooling System (TA Instruments, Waters LLC, New Castle). The samples (~10 mg) were packed in hermetic aluminum capsules and evaluated in DSC with an inert atmosphere (N_2) using the following conditions: isothermal condition at 25 °C for 10 minutes; the melting events were evaluated from 25 to 100 °C at a rate of 10 °C/min. The data processing system used was Universal V4.7A (TA Instruments, Waters LLC, New Castle) and the following parameters were used for evaluation of the results: initial melt temperature (T_{im}), maximum melt peak temperature (T_{max}), final melting temperature (T_{off}) and melt enthalpy (ΔH_m) (Campos, 2005). Only the particles obtained through 3 cycles of HPH were analyzed, the reasons for the exclusion of particles obtained with 5 cycles of HPH will be further discussed based on particle sizes in the topic of results and discussion.

2.2.5. X-ray diffraction

The polymorphic forms of SLN and lyophilized NLC, obtained through 3 cycles of HPH, were determined by X-ray diffraction (XRD), according to the AOCS method Cj 2-95 (AOCS, 2009). The analyzes were carried out using a Philips diffractometer (PW 1710) using Bragg-Brentano (θ:2θ) geometry radiation with Cu-αK (λ= 1.54056Å, 40 KV voltage and 30 mA current). The measurements were obtained at 25 °C, with steps of 0.02° in 2° and acquisition time of 2 seconds, with scans of 15 to 40° (2θ scale). The identification of the polymorphic forms was performed from the short spacings characteristic of the lipid crystals (AOCS, 2009).

2.2.6. Statistical analysis

Z-ave, PDI, and ZP data were statistically analyzed by means of *One-Way* Analysis of Variance (ANOVA) with *Statistica* (V.12) *Software* (*Statsoft Inc., Tulsa, UK*). The *Tukey* test was applied to determine the significant differences between the means, at a level of p≤0.05.

3. Results and discussion

3.1. Processing and obtaining nanoparticles

The choice of the emulsifying system and the lipid raw materials associated with the production process are extremely important for obtaining stable and potential applications for nanostructured systems. The T80 emulsifier was selected from preliminary studies conducted by our research group, where different NLC formulations were developed with soybean oil (53.32% linoleic, C18:2 and 23.38% oleic, C18:1) and soybean oil hardfat (87.11% stearic, C18:0 and 11.22% palmitic, C16:0). By using T80, NLC were obtained with lower Z-ave and PDI (167nm and 0.176 with 3 cycles of HPH and 160nm and 0.165 with 5 cycles of HPH, respectively), compared to other emulsifiers with lower HLB, such as lecithin of (HLB = 7.0) and sorbitan monostearate - Span®60 (HLB = 4.7), remaining stable for 15 days of evaluation (V. S. Santos, Ribeiro, Cardoso, & Santana, 2018). These results demonstrated that the particle size and distribution profile are dependent on the type of emulsifying system employed, as well as on the conditions of the homogenization process.

As for the method used, we can say that it was possible to obtain the nanoparticles proposed in this study using HPH with 3 cycles and 5 cycles of HPH at 800 bar. Regarding the efficiency of the method, related to the particle size characteristics, dispersion and stability of the systems, the results will be discussed in the following topic according to Z-ave, PDI and ZP parameters as a function of the number of cycles of HPH and stability to over 60 days of storage.

Through visual evaluation, as shown in Figure 1, it can be affirmed that through systems with saturated lipids (SLN) and saturated and unsaturated lipid systems (NLC) systems, they have shown different visual physical characteristics. The NLC were completely fluid (liquid) after the HPH process, followed by static crystallization at 5 °C/24h and crystalline stabilization at 25 °C/24h. This behavior was not verified for the nanoparticles developed only with saturated lipids, the SLN. It was verified that the SLNs systems were totally solid, it was possible to invert the storage flask without changing the characteristics. This solid behavior of SLN has been reported in the literature as a gelation process, which can be caused by the effect of emulsifying systems, processing conditions, and lipid polymorphism.

Westesen and Siekmann (1997) also observed this effect on phospholipid stabilized tripalmitin (PPP) SLN. According to the authors, this behavior was attributed to possible

coalescence and aggregation of crystals in the form of platelets, which were not completely coated by the emulsifier (Awad, Helgason, Weiss, Decker, & McClements, 2009), also verified the gelation mechanism in LN composed of PPP. For this reason, they performed studies evaluating different storage temperatures and associated the SLN gelation to the polymorphic transition of LM. Thus, the authors suggested that the surface area of the nanoparticles increased during the change from a spherical to the platelet form, reducing the efficiency of the emulsifying system in terms of nanoparticle coating and surface tension maintenance. Thus, favouring the attraction between the nanoparticles, causing the coalescence, with consequent formation of a three-dimensional lipid network with water imprisonment, giving the system a gel appearance. Other research has shown that lipid nanoparticles are spherical soon after the process of production, related to the crystallization of TAGs in α polymorphic formα. However, during storage, these spherical particles become elongated, platelet-shaped, due to the polymorphic transition to the more stable form of the lipid crystals, β-form (Awad, Helgason, Weiss, Decker, & McClements, 2009; Bunjes & Unruh, 2007; Salminen, Helgason, Kristinsson, Kristbergsson, & Weiss, 2013).

From this information, we can affirm that the gelation of nanostructured systems, reported for SLN developed with purified TAGs, such as PPP, also occurs with SLN produced with conventional LM. Since the three different SLNs developed in this study (Figure 1), from a mixture of TAGs in their characteristic compositions of natural vegetable oils and fats, showed the similar gelling effect to the SLN produced with purified TAGs.

3.2. Mean diameter, Polydispersity index, and Zeta potential

The determination of the mean hydrodynamic diameter Z-ave through the DLS technique is based on the Stokes-Einstein equation, which considers the hydrodynamic motion of spherical particles in a fluid at a given viscosity, depending on the temperature of the system (Bunjes, Steiniger, & Richter, 2007; Tamjidi, Shahedi, Varshosaz, & Nasirpour, 2013). Thus, as seen in the previous topic, in the SLN, which presented the gelling effect, it was not possible to perform the determination of Z-ave, PDI and ZP, since these results would not represent the behaviour of nanoparticles systems, for comparison purposes with NLC, showing erroneous values of Z-ave, related to crystalline aggregates and not nanoparticles.

The determinations of Z-ave, PDI and ZP were performed to characterize and monitor the physical stability of the NLC after the crystallization step and stabilization of the lipid fraction. In other words, after maintaining for 24h at 5 ° C, followed by 24h at 25 ° C, and after 15, 30 and 60 days of processing. The results are shown in Table 1 and the distribution of the particles (d.nm) expressed in intensity ($I\alpha d^6$) and number ($N\alpha d$) are shown in Figures 3 and 4, for the NLCs obtained through 3 and 5 cycles of HPH. After 24 hours of processing, the NLCs obtained with 3 cycles of HPH presented particles populations range from 150 to 190nm, whereas with 5 cycles particles populations between 160-210nm. The lowest values of Z-ave found for 3 and 5 cycles of HPH referred to NLC 11 and the highest values to NLC 6 (Table 1). In addition, as can be seen in Figures 3 and 4, the NLCs showed a very similar population particles as a function of intensity after 24 hours of processing for both 3 and 5 cycles of HPH, presenting low polydispersity. Only a few systems were bimodal in number distribution ($N\alpha d$), but all the results very close to the Z-ave, showing neither very small nor very large particles, which could cause instability to these systems.

This behavior is directly related to the PDI values, a parameter also obtained through DLS, which provides information about the physical stability of systems. PDI values range from 0 to 1, PDI close to 1 indicates a large variation in particle size, while values close to 0 indicate a monodisperse population of particles. In addition, according to Tamjidi, Shahedi, Varshosaz, and Nasirpour (2013), for nanoparticle systems such as NLC, to obtain suspensions with long-term stability, PDI values should be in the range of 0.10 to 0.25. Thus, ECP results for NLC obtained through 3 cycles of HPH ranged from 0.105 to 0.181 and from 0.099 to 0.199 to 5C of HPH, conferring high stability for systems developed with 3 and 5 cycles of HPH.

Table 1. Mean hydrodynamic diameter, polydispersity index and zeta potential of nanostructured lipid carriers (CLN) obtained by 3 and 5 cycles of high-pressure homogenization (HPH) at 800bar, evaluated after 24h, 15, 30 and 60 days of the production

Amostra	Z-ave (d.nm)	PDI	ZP (mV)	Z-ave (d.nm)	PDI	ZP (mV)	Z-ave (d.nm)	PDI	ZP (mV)	Z-ave (d.nm)	PDI	ZP (mV)
HPH 3C	**24h**			**15 days**			**30 days**			**60 days**		
NLC 4	167.83±0.81^{hA}	0.158±0.013^{bcdeA}	-14.07±0.45^{abA}	164.00±1.73^{ghB}	0.154±0.006^{bcA}	-25.10±0.61^{gB}	168.10±0.60^{ghA}	0.154±0.021^{cdefA}	-33.77±0.67^{jD}	159.23±1.16^{hiC}	0.159±0.032^{bcA}	-27.30±0.79^{ghC}
NLC 5	18617±1.01^{cdA}	0.181±0.019^{abcA}	-21.00±0.78^{hA}	181.40±1.95^{dB}	0.147±0.023^{bcA}	-22.43±0.25^{fB}	186.37±1.65^{cdA}	0.207±0.023^{aA}	-25.13±0.75^{ghC}	181.83±1.29^{cdB}	0.165±0.032^{bcA}	-28.37±0.49^{hiD}
NLC 6	188.57±0.40^{cB}	0.162±0.012^{bcdeB}	-23.53±0.32^{iC}	184.40±1.21^{cdC}	0.161±0.018^{bB}	-22.47±0.29^{fB}	183.73±0.65^{deC}	0.179±0.015^{abcdB}	-22.37±0.40^{defB}	204.73±1.00^{aA}	0.223±0.027^{aA}	-16.23±0.55^{aA}
NLC 7	161.23±1.76^{iA}	0.133±0.012^{defgA}	-13.23±0.55^{aA}	155.07±0.90^{iB}	0.119±0.001^{bcA}	-14.90±0.40^{aB}	157.57±0.55^{iAB}	0.139±0.012^{defgA}	-24.30±0.56^{gC}	155.27±2.47^{iB}	0.120±0.005^{cdA}	-23.63±0.12^{eC}
NLC 8	180.07±1.18^{fB}	0.133±0.007^{defgAB}	-19.97±0.25^{ghA}	185.87±1.68^{cdA}	0.155±0.017^{bcA}	-21.40±0.66^{efB}	185.33±0.76^{cdA}	0.124±0.006^{fgB}	-27.33±0.12^{iC}	183.57±1.30^{cA}	0.139±0.004^{bcdAB}	-29.37±0.25^{iD}
NLC 9	170.67±1.19^{hA}	0.151±0.009^{cdeA}	-17.40±0.52^{deA}	169.27±1.29^{efA}	0.145±0.018^{bA}	-21.97±0.25^{efA}	170.80±0.95^{gA}	0.118±0.011^{fgA}	-23.60±0.78^{fgA}	170.23±2.29^{efA}	0.140±0.024^{bcdA}	-27.93±0.83^{hiC}
NLC 10	166.87±1.11^{hA}	0.132±0.011^{defgA}	-15.30±0.35^{bcA}	166.03±0.47^{fgAB}	0.110±0.017^{cA}	-18.70±0.40^{cdB}	164.70±0.95^{hiBC}	0.133±0.013^{efgA}	-20.70±0.62^{bcdC}	163.73±0.45^{ghC}	0.117±0.018^{cdA}	-26.07±0.15^{fgD}
NLC 11	156.33±1.23^{jB}	0.105±0.024^{efgA}	-19.13±0.78^{fgA}	159.73±1.89^{hiAB}	0.125±0.009^{bcA}	-20.87±0.35^{eB}	162.47±1.19^{iA}	0.102±0.010^{gA}	-26.20±0.72^{hiC}	159.90±2.00^{hiAB}	0.090±0.014^{dA}	-21.10±0.46^{dB}
NLC 12	171.10±1.10^{ghA}	0.118±0.009^{fgA}	-12.77±0.25^{aA}	172.42±1.68^{eA}	0.120±0.006^{bcA}	-18.90±0.61^{cdB}	174.63±0.64^{fA}	0.137±0.014^{defgA}	-19.47±0.23^{abB}	173.00±1.83^{eA}	0.144±0.025^{bcd}	-25.30±0.72^{fC}
HPH 5C	**24h**			**15 days**			**30 days**			**60 days**		
NLC 4	175.13±1.72^{gA}	0.175±0.010^{abcdA}	-16.73±0.15^{cdA}	169.97±1.96^{efB}	0.140±0.017^{bcB}	-19.43±0.55^{dB}	167.77±0.38^{ghBC}	0.135±0.007^{efgB}	-20.93±0.29^{bcdC}	165.10±1.13^{gC}	0.149±0.012^{bcAB}	-16.50±0.78^{aA}
NLC 5	200.33±1.86^{bA}	0.213±0.010^{aA}	-20.53±0.15^{gh}	194.57±1.00^{bB}	0.206±0.011^{aAB}	-21.60±0.30^{ef}	198.70±1.15^{bA}	0.186±0.009^{abcBC}	-21.83±0.67^{def}	190.13±1.12^{bC}	0.176±0.005^{b}	-20.07±0.25^{cdC}
NLC 6	208.10±1.25^{aA}	0.199±0.018^{abA}	-25.10±0.46^{jC}	206.93±2.4^{aA}	0.223±0.027^{aA}	-21.43±0.46^{efB}	206.93±1.19^{aA}	0.196±0.023^{abA}	-21.77±1.19^{cdeB}	181.33±1.72^{cdB}	0.179±0.002^{abA}	-17.47±0.31^{abA}
NLC 7	162.47±1.21^{iA}	0.149±0.010^{cdefA}	-15.63±0.70^{cA}	153.03±1.00^{iB}	0.147±0.012^{bcA}	-16.97±0.50^{bB}	157.90±0.30^{jB}	0.148±0.001^{cdefA}	-20.00±0.35^{abcC}	155.70±1.73^{iB}	0.141±0.006^{bcdA}	-22.87±0.29^{eD}
NLC 8	185.37±1.75^{cdeA}	0.160±0.012^{bcdeA}	-18.40±0.53^{efA}	186.93±1.63^{cA}	0.155±0.017^{bA}	-21.63±0.15^{efB}	188.20±1.39^{cA}	0.138±0.022^{defgA}	-24.97±0.12^{gh}	185.53±1.15^{bcA}	0.131±0.018^{bcdA}	-20.97±0.06^{dB}
NLC 9	181.60±2.82^{efA}	0.164±0.011^{bcdA}	-19.37±0.65^{fgA}	181.50±1.30^{dA}	0.156±0.080^{bcA}	-20.87±0.60^{eB}	180.53±0.85^{eA}	0.167±0.007^{abcdeA}	-21.93±0.12^{defB}	178.37±1.05^{dA}	0.163±0.011^{bcA}	-18.83±0.67^{bcA}
NLC 10	169.23±1.07^{hA}	0.131±0.031^{defgA}	-14.13±0.38^{abA}	167.40±0.85^{fgA}	0.144±0.017^{bcA}	-17.83±0.21^{bcB}	170.00±1.67^{gA}	0.123±0.001^{fgA}	-19.80±0.80^{abC}	167.27±2.15^{fgA}	0.136±0.006^{bcdA}	-28.43±0.12^{hiD}
NLC 11	161.90±0.44^{iB}	0.099±0.014^{gB}	-19.43±0.25^{fg}	165.57±2.37^{fgAB}	0.133±0.005^{bcA}	-22.57±0.31^{f}	167.97±2.18^{ghAB}	0.126±0.007^{efgAB}	-23.40±0.60^{efg}	165.27±2.02^{gAB}	0.111±0.016^{cdAB}	-23.17±0.78^{e}
NLC 12	183.13±1.12^{defA}	0.145±0.012^{cdefA}	-13.70±0.17^{aA}	183.20±0.53^{cdA}	0.151±0.015^{bcA}	-17.30±0.72^{bB}	186.03±1.85^{cdA}	0.157±0.010^{bcdefA}	-18.83±0.51^{aC}	183.17±1.72^{cdA}	0.133±0.019^{bcdA}	-20.30±0.26^{cdD}

Z-ave: hydrodynamic diameter; PDI: Polydispersity index; ZP: Zeta Potential; HP: High-Pressure Homogenization; 3C: three cycles of HPH; 5C: five cycles of cycles of HPH; Mean of three replicates ± Standard Deviation; Different upper-case letters on the same line indicate a significant difference related to the evaluation of each parameter (Z-ave, PDI and ZP) in 24h, 15, 30 and 60 days after prodution of each CLN evaluated at the probability level (p≤0.05) according to the Tukey Test; Lowercase letters in the same column indicate significant difference in probability (p≤0.05) according to the Tukey test related to the comparison between CLNs produced with 3 and 5 cycles of HPH for each parameter (Z-ave, PDI and ZP).

Along with Z-ave and PDI, another important parameter for the characterization of nanoparticles is the zeta potential. Although, the NLC developed in this study are based on natural fats and oils (neutral systems), the evaluation of ZP represents a valuable prerequisite, both in terms of characterization and in the evaluation of stability over the storage. ZP values above |30| mV characterize colloidal systems with good stability, considered to be close to |60| mV. The system is susceptible to destabilization and the occurrence of limited flocculation can be observed between 5 and 30mV; whereas for ZP values lower than 5mV, the system presents a great tendency for the coagulation of particles (Lacatusu, Mitrea, Badea, Stan, Oprea, & Meghea, 2013; Madureira, Campos, Gullon, Marques, Rodriguez-Alcala, Calhau, et al., 2016). The positive or negative charges of the values obtained for the ZP depending on the type of emulsifier applied. T80 is a non-ionic emulsifier, it is neutral, the sum of those charged in the molecule is close to zero. However, the negative charges observed in all ZP results (Table 1), are related to the type of emulsion obtained (oil-in-water). In the case of NLC, the nonpolar portion of the molecule, which is lipophilic, is positive and the polar portion, having a hydrophilic character, is negative. This negative portion is exposed on the surface of the particles, resulting in the negative ZP values to the systems. The results verified for the ZP varied between -13.23 to -23.53mV and -13.70 to -25.10mV, for the NLC obtained with 3 and 5 cycles of HPH, after processing, respectively (time of 24h, Table 1). These results indicated that NLC showed a possible susceptibility to destabilization soon after processing. But most of the systems proved to be stable over 60 days of evaluation, which will be further discussed. Based on this information, we found that NLC developed with 5 cycles of HPH presented the highest ranges of Z-ave and PDI values. It should be noted that there were few observed differences between 3 and 5 cycles. Thus, considering the application of this technology in industrial scale, we consider the use of 3 cycles of HPH the most appropriate in terms of economic viability. That is, the lower the number of homogenization cycles, the shorter the processing time and the equipment wear, thus increasing productivity and prolonging the equipment life. In this way, the discussion of the results in terms of LM composition and the other thermal and polymorphism evaluations were performed only for the systems developed with 3 cycles of HPH, since the use of 5 cycles was not considered feasible for industrial application.Evaluating the NLC developed with 3 cycles of HPH, it was observed that the NLCs

composed by CA had the lowest values of Z-ave (NLC 4: 167.83nm, NLC 7: 161.23nm and NLC 10: 166.87nm), while NLCs developed with CR presented higher values (NLC 6: 188.57nm, NLC 8: 170.67nm and NLC 12: 171.10nm) (Table 1). It was observed that the increase of HOSO (20, 40 and 60%) favored the reduction of the Z-ave composed by the mixture of CA and CR (NLC 5: 186.17nm, NLC 8: 180.07nm and NLC 11: 156.33nm), being statistically different at a 5% probability. It should be noted that NLC 11, which presented the lowest Z-ave among all the evaluated systems, presents in its composition the most heterogeneous mixture in relation to LM composition, being composed by the mixture of CA, CR and HOSO (20:20:60 m/m).

In relation to the stability of the systems evaluated with 3 cycles of HPH, it can be seen that NLC 6, composed of the lowest levels of unsaturated fatty acids, presented a ZP value closer to 30mV (-23.53mV), indicating that this nanoparticle system composed of 80% CR and 20% HOSO, has the best physical stability compared to other systems, even with the highest Z-ave (188.57nm) (Table 1). During the evaluation of the systems along the storage, looking at the intensity graphs shown in Figure 3, it is possible to verify that only NLC 4 and NLC 5 presented a second peak, referring to larger particles near 10.000nm for 30 and 60 days, respectively. However, the PDI did not show significant differences for both systems throughout the evaluation time (Table 1).

Significant reductions in the Z-ave of NLC 4, 5, 6 and 7 were observed after 15 days of processing, at NLC 10 after 30 days and at NLC 11 after 60 days. These reductions were not observed in NLC 8, 9 and 12. It should be noted that changes in the NLC 6 Z-ave continued to occur throughout storage, with a significant increase ($p < 0.05$) in Z-ave after 60 days, from 184.40nm (15 days) to 204.73nm (60 days). Associated with the Z-ave increase, occurs the increase of PDI (0.161 to 0.223) and ZP reduction from -23.53 to -16.23mV, showing the most unstable and susceptible to destabilization system. Furthermore, it was generally observed that the ZP values were closer to 30mV over the 60 days of storage. These values can indicate that the systems were organizing in the conditions of lower energy, that is, reaching the kinetic stability (Table 1).
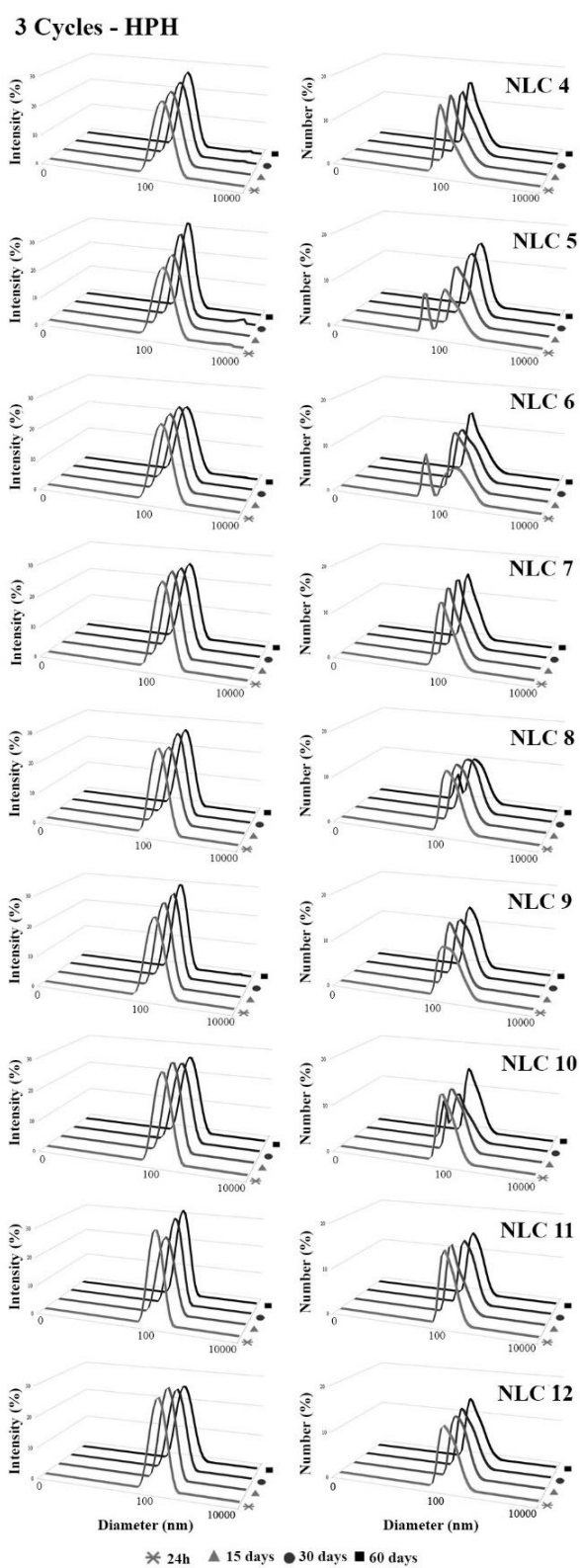
Fig. 3. Particle size distribution as a function of the intensity (A) and number (B) obtained from the dynamic light scattering (DLS) of the NLC obtained by 3 cycles of HPH after 24 hours (24 h), 15 days (15d), 30 days (30d) and 60 days (60d) of production.
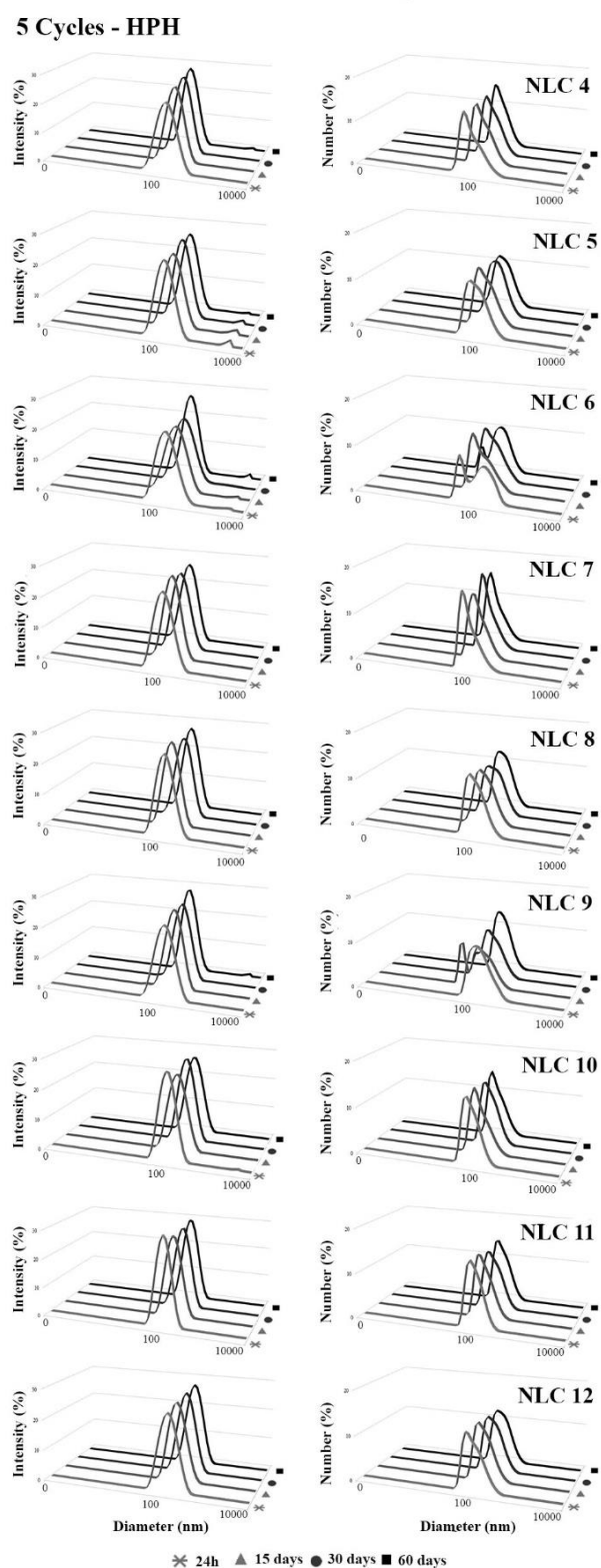
Fig. 4. Particle size distribution as a function of the intensity (A) and number (B) obtained from the dynamic light scattering (DLS) of the NLC obtained by 5 cycles of HPH after 24 hours (24 h), 15 days (15d), 30 days (30d) and 60 days (60d) of production.

Changes in Z-ave have been associated with changes in particle shape. Thus, the diffusion velocity of the particles is altered, and consequently changes the hydrodynamic values perceptible through the DLS technique (Tamjidi, Shahedi, Varshosaz, & Nasirpour, 2013). The change in the shape of lipid nanoparticles is directly related to the polymorphic transitions, to the more stable form ($\alpha \rightarrow \beta' \rightarrow \beta$), as discussed above. It should be pointed out that for some systems the Z-ave changes occurred with 15 days of storage and for others, it occurs only after 30 or 60 days. These changes are very dependent on the lipid composition and physical properties, as will be further discussed NLC.

3.3. Melting behavior

The most important aspects of the physical properties of oils and fats are related to phase changes, such as crystallization and melting. These thermal phenomena are generally verified by the monitoring of enthalpy and phase transition through DSC. A very sensitive and widely used technique for evaluating materials. In this study, we used the DSC to evaluate the melting behavior of lyophilized nanoparticles, obtained through 3 cycles of HPH. The obtained results are shown in Table 2. Additionally, in Figure 5, the thermograms are arranged, graphically representing the heat flow as a function of temperature. The parameters selected were: initial melt temperature (T_{im}), which refers to the beginning of the phase transition; maximum peak temperature of the melt (T_{max}), maximum thermal effect; final melting temperature (T_{off}) indicating the completion of the thermal effect; and the enthalpy of fusion (ΔH_m) or enthalpy of phase transition, measured by the area of the curve in relation to the baseline (Campos, 2005).

The results of the melting behavior of LM used in the development of nanoparticles were carried out by our research group in a previous study, under the same conditions of crystallization and stabilization used for the nanoparticles (V. S. Santos, Santana, Braz, Silva, Cardoso, & Ribeiro, 2018). Thus, for the comparison between macro and nanoscale fusion events, the LM results were recovered and included in Table 2 and Figure 5. Thus, the visualization of differences and similarities between both systems was facilitated.

Table 2. Melting behavior of solid lipid nanoparticles and nanostructured lipid carriers according to the parameters of initial melting temperature (T_{im}), maximum melting peak temperature (T_{max}), final melting temperature (T_{off}) and the melting enthalpy (ΔH_m)

LN		T_{im} (°C)	T_{max} (°C)	T_{off} (°C)	ΔH_m (J/g)	LM*	T_{im} (°C)	T_{max} (°C)	T_{off} (°C)	ΔH_m (J/g)
		SLNs lyophilized					**Lipid Matrices of SLNs**			
NLS 1	P_1	67.75±0.01	71.35±0.00	81.46±0.55	-128.70±0.17	LM 1	52.55±0.05	55.24±0.02	62.00±0.50	-88.96±1.62
	P_2	--	--	--	--		65.81±0.09	69.20±0.09	78.03±0.29	-30.82±1.45
NLS 2	P_1	62.74±0.01	65.76±0.00	75.47±0.43	-110.33±0.21	LM 2	53.41±0.02	58.46±0.23	73.79±1.73	-112.10±2.80
NLS 3	P_1	66.30±0.02	70.03±0.00	77.97±0.41	-115.10±0.36	LM 3	58.66±0.04	62.04±0.17	73.89±2.12	-113.20±1.10
		NLCs lyophilized					**Lipid Matrices of NLCs**			
NLC 4	P_1	70.01±0.00	71.18±0.00	81.23±0.85	-107.73±0.61	LM 4	62.16±0.00	70.22±0.13	82.27±0.36	-120.10±5.20
NLC 5	P_1	61.85±0.00	64.32±0.00	72.74±1.10	-107.87±0.93	LM 5	54.92±0.03	62.57±0.25	76.38±1.44	-113.00±1.40
NLC 6	P_1	65.68±0.01	70.17±0.00	80.53±1.27	-111.37±0.78	LM 6	56.20±0.05	65.38±0.02	81.62±0.29	-102.33±3.77
NLC 7	P_1	66.35±0.01	69.35±0.00	84.24±1.05	-68.34±0.54	LM 7	60.02±0.10	68.66±0.02	83.53±1.98	-88.63±0.91
NLC 8	P_1	59.76±0.02	64.10±0.00	83.07±2.45	-72.96±1.43	LM 8	54.18±0.04	61.70±0.23	78.46±1.36	-85.80±3.48
NLC 9	P_1	66.73±0.01	68.52±0.00	83.26±2.04	-68.66±1.48	LM 9	55.32±0.05	65.45±0.03	82.45±1.04	-83.15±1.67
NLC 10	P_1	70.01±0.00	71.18±0.00	81.23±0.85	-107.73±0.61	LM 10	57.62±0.07	66.27±0.10	81.01±0.32	-55.82±0.78
NLC 11	P_1	61.85±0.00	64.32±0.00	72.74±1.10	-107.87±0.93	LM 4	62.16±0.00	70.22±0.13	82.27±0.36	-120.10±5.20
NLC 12	P_1	65.68±0.01	70.17±0.00	80.53±1.27	-111.37±0.78	LM 5	54.92±0.03	62.57±0.25	76.38±1.44	-113.00±1.40

Mean of three replicates ± Standard Deviation. LN: Lipid nanoparticles; --: not detected; * Data of the lipid matrices (LM) used in these study to develop the solid lipid nanoparticles (SLN) and nanostructure lipid carriers (NLC), from an earlier study conducted by our research group (V. S. Santos, Santana, Braz, Silva, Cardoso, & Ribeiro, 2018).

In general, as can be seen in Figure 5, the thermal behavior of the nanoparticles was different from LM, mainly in terms of T_{max}. Indicating that nanoparticle lipid systems present higher thermal resistance than lipid systems in macroscale. Probably, because the TAG molecules were organized in a more compact crystalline structure. In other words, with very small dimensions the Van Der Waals interactions are more intense between the TAG molecules, unlike the macroscale, where TAGs have larger spaces to organize and form the less compacted crystalline structures. Furthermore, the higher thermal resistance may be related to the polymorphic form of the lipid fraction in the nanoparticles. Some authors reported that the polymorphic transition, to the most stable form, is accelerated in nanostructured systems (Mehnert & Mäder, 2012; Tamjidi, Shahedi, Varshosaz, & Nasirpour, 2013). It was also verified that the nanostructures composed of the mixtures of saturated and unsaturated fatty lipids (NLC) presented lower values of enthalpy (ΔH_m) than their respective LM. Possibly, the

change in physical state (solid to liquid) is facilitated due to the reduced size and consequent higher surface contact area of the nanoparticles compared to lipid systems crystallized macro scale.
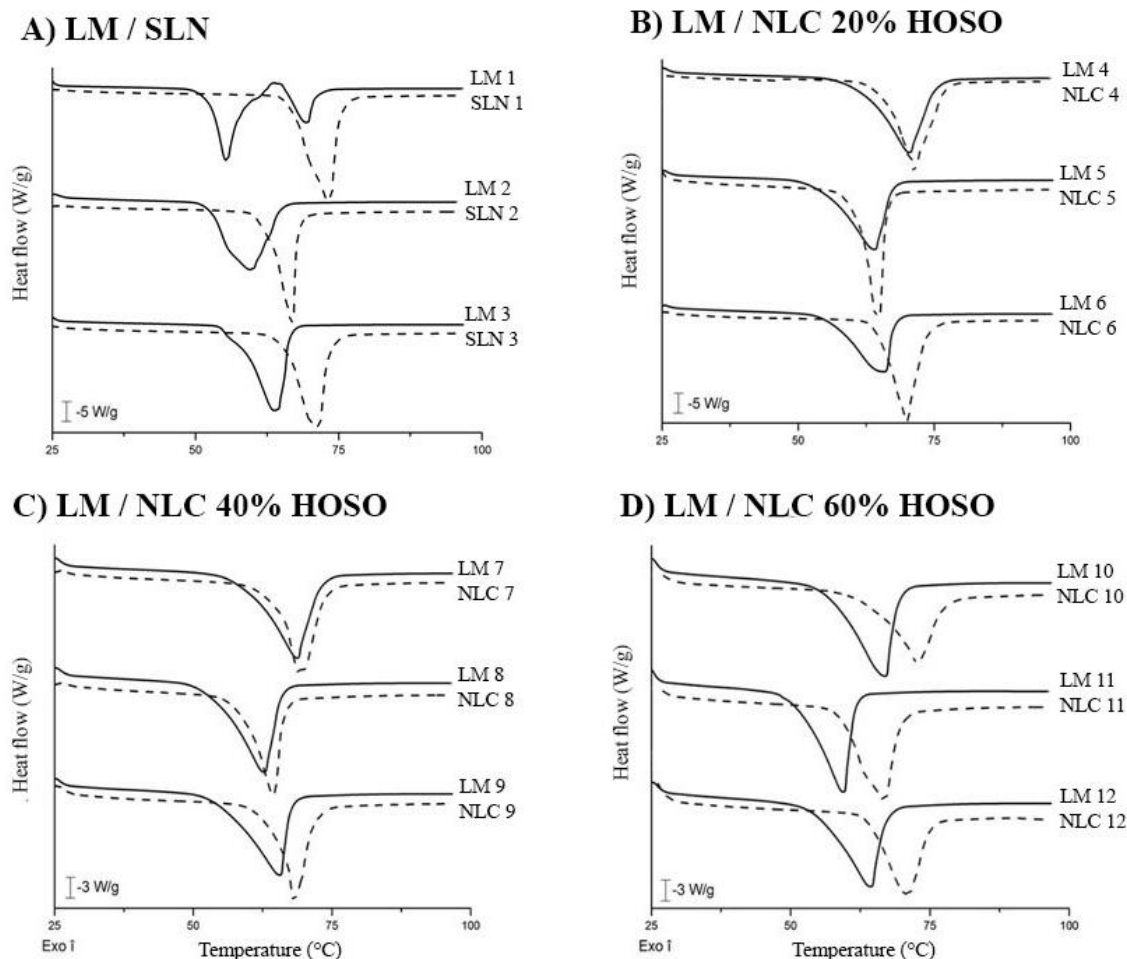
Figure 5. DSC melting curves of: A) Lipid matrices (LMs) composed by solid lipids (100% CA; mixture of CA and CR (50:50); 100% CR); B) LMs composed by mixtures of 80% of solid lipids (CA; mixture of CA and CR; CR) and 20% of the liquid lipid (HOSO); C) LM composed by mixtures of 60% of solid lipids (CA; mixture of CA and CR; CR) and 40% of the liquid lipid (HOSO); D) LMs composed of mixtures of 40% of solid lipids (CA; mixture of CA and CR; CR) and 60% of the liquid lipid (HOSO); E) NLSs developed with the LMs described in "A"; F) CLNs developed with LMs described in "B"; G) CLNs developed with the LMs described in "C"; and H) CLNs developed with the LMs described in "D". The data referring to MLs come from an earlier study conducted by our research group (V. S. Santos, Santana, Braz, Silva, Cardoso, & Ribeiro, 2018).

By evaluating the results obtained for the nanoparticles more critically and comparing them with the LM, it was observed that LM developed only with CA (LM 1) presented a wide melting range, starting at 52.55 °C and ending at 62.00 °C. In this range was possible to verify the presence of two melting peaks with T_{max} at 55.24 °C and 69.20 °C (Figure

5A). These two peaks may be related to the differentiated fusion of non-purified lipid materials of plant origin, since they present mixtures of different TAGs in their compositions (shown in the description of the materials used in this study). It is possible to relate the fatty acids chain size to the melting point, so the higher the number of carbons, the higher the melting point. According to Himawan, Starov, and Stapley (2006) this DSC behavior is generally observed for saturated monoacid TAGs, such as SSS, present in higher concentration in CA. The SLN 1 developed with LM 1 showed only a single melting peak (T_{max} of 71.35 °C), which may indicate that the fusion of the components at the nanoscale was uniform, or even that the TAGs after the nanostructure process were organized in the most stable polymorphic form. However, the DSC technique can only be used to infer about polymorphic transition and crystalline forms, the confirmation only happens through XRD, which will be further presented.

The SLN 3 composed of 100% CR showed a narrower melting peak than the SLN 1, indicating a more uniform melting of the TAGs in its formulation, presenting T max at 70,03 °C and lower energy to the phase transition (-115,10W/g) (Table 2). The SLN 2 composed of the mixture of CA and CR (50: 50m/m) presented an intermediate T_{max} value (65.76 °C) to the values found for SLN 1 and SLN 3. According to Himawan, Starov, and Stapley (2006) this effect tends to occur when the components of the systems differ in molecular volume, shape and/or polymorph, characterizing a eutectic behaviour, reducing the melting temperature when there is a mixture of CA and CR, compared to the use of the pure hardfats.

As can be seen in Figure 2, in all systems developed with the mixtures of CA and CR, for both the SLN and the NLC as for the correspondent LM, it is possible to verify the eutectic effect. In these systems, the eutectic effect is more related to the molecular volume of the constituents, since the AC presents 80% of SSS in its composition that has 54 carbons, whereas the CR presents a mixture of approximately 80% of TAG with carbonic chains ranging from 58 to 64 carbons (SBeBe, SSBe, SABe, and ABeBe). In addition, it should be noted that the eutectic effect increased with increasing HOSO in the systems (Figure 5B, C, and D), and was even more pronounced for NLC 11 and its LM 11 (Figure 5D). Therefore, it can be affirmed that the inclusion of HOSO increased the incompatibility between the components of the systems, a fact that can be explained by the HOSO composition, which presents approximately 66% of triolein (OOO), a triunsaturated TAG of 54 carbons. In this case, the eutectic effect is

more related to the structural form of the molecule, which has spatial organization different from the trisaturated TAGs, due to the presence of unsaturation.

It should be noted that the observed eutectic effect, related to the incompatibility between chain size of the saturated TAG molecules and accentuated by the presence of unsaturated molecules in the systems, contributed positively to the development of NLC reducing crystallinity and favouring the reduction of Z-ave of the particles. Confirmed by the results obtained in the previous topic regarding Z-ave and particle stability. The NLC 6, developed with 80% CR and 20% HOSO, showed the highest value of Z-ave (188.57nm) shortly after processing, and after 60 days of evaluation, it was the most unstable system, with a significant increase of Z-ave and PDI and undesirable ZP reduction after possible polymorphic transitions. While the NLC 11, which has the greatest heterogeneity in relation to the composition in TAG, composed by the mixture of 20% of CA, 20% and of 60% of HOSO, was the nanoparticle system that presented the lowest value of Z-ave (156.33nm) after processing, showing to be stable over 60 days of storage, even after possible polymorphic transition at 30 days storage.

Through these evaluations via DSC it was possible to observe that the LM composition used for the development of the nanoparticles had a direct influence on the thermal behavior of the nanostructures. Moreover, through the results obtained, it can be verified that the nanoparticles have different fusion behaviour of lipid systems in macroscale.

3.4. Polymorphic habit

X-ray diffraction is a consolidated technique for the crystalline characterization of continuous lipid systems as well as particulates (Bunjes & Unruh, 2007; Wu, Zhang, & Watanabe, 2011). Due to its different geometric configurations, the polymorphs diffract the x-rays at different angles. In this study the wide-angle X-ray scattering (WAXS) technique was used to provide information regarding the short spacings of the crystalline sub-cells in a way to obtains the polymorphic forms in the systems (Campos, 2005). In lipids, the most common polymorphs are in the α-form, which has a diffraction peak at 4.15Å, in the β 'form, characterized by two lines of diffraction at 3.8 and 4.2Å, and in the β form that is related to a line of higher intensity at 4.6 Å and peaks of lower intensities at 3.7 and 3.8Å (Rousseau & Marangoni, 2002).

The results concerning the crystalline forms of the nanoparticles developed in this work, after lyophilization process are shown in Table 3, where it is possible to verify also the shorts spacings presented for each sample. In addition, the results from the LM used in the development of nanoparticles, which were obtained in a previous study by our research group, are also described (V. S. Santos, Santana, Braz, Silva, Cardoso, & Ribeiro, 2018).

Table 3. Polymorphic forms, short spacings and peak intensities for solid lipid nanoparticles (SLN) and nanostructured lipid carriers (NLC) lyophilized.

Samples	Short spacings (Å)						Santos et al., 2018	
LN	4.6	4.1	4.2	3.8	3.7	Polymorphic Form	LM*	Polymorphic Form
SLNs lyophilized							LM of SLNs*	
SLN 1	4.60$_{VS}$	-	-	3.87$_M$	3.73$_M$	β	LM 1	α
SLN 2	4.61$_{VS}$	-	-	3.80$_M$	3.74$_M$	β	LM 2	α
SLN 3	-	-	4.23$_{VS}$	3.80$_M$	-	β'	LM 3	α
NLCs lyophilized							LM of NLCs*	
NLC 4	4.63$_M$	-	-	3.89$_M$	3.72$_M$	β	LM 4	$\beta'+\beta$
NLC 5	4.63$_{VS}$	-	-	3.82$_M$	3.76$_M$	β	LM 5	β
NLC 6	-	-	4.20$_{VS}$	3.81$_M$	-	β'	LM 6	β
NLC 7	4.60$_M$	-	-	3.88$_M$	3.71$_M$	β	LM 7	β
NLC 8	4.63$_M$	-	-	3.81$_M$	3.71$_M$	β	LM 8	$\beta'+\beta$
NLC 9	-	-	4.22$_{VS}$	3.80$_w$	-	β'	LM 9	$\beta'+\beta$
NLC 10	4.57$_{VW}$	-	-	3.86$_M$	3.69$_M$	β	LM 10	β
NLC 11	4.55$_{VW}$	-	-	3.88$_{VW}$	3.74$_{VW}$	β	LM 11	$\beta'+\beta$
NLC 12	-	-	4.23$_w$	3.79$_{VW}$	-	β'	LM 12	$\beta'+\beta$

Peak intensity: V - very, W - weak, M - medium, S - strong. *Data refering to lipid matrices (LM) came from an earlier study conducted by our research group (V. S. Santos, Santana, Braz, Silva, Cardoso, & Ribeiro, 2018).

As shown in Table 3, the LM used in the development of SLN, even after crystallization and crystalline stabilization, under the same conditions of processing of the nanoparticles showed diffraction peaks at 4.1Å, referring to crystals in the α-form (Figure 6A). According to the literature, the CA due to the high amount of SSS in its composition has the tendency to crystallize in β form, whereas the polymorphic habit of CR is the mixture of crystals in forms β 'and β. According to the authors, for the polymorphic transition to the more stable form, these systems required a specific temperature treatment or storage at 25 °C for 180 days (Oliveira, Stahl, Ribeiro, Grimaldi, Cardoso, & Kieckbusch, 2015; Ribeiro, Basso, & Kieckbusch, 2013). In the present study, it can be verified that the polymorphic transition was accelerated after the process of obtaining the nanoparticles developed with these LM (Figure

6A and 6E). The SLN 1 and SLN 2 showed diffraction peaks at 4.6 Å for crystallization in the most stable form β, and SLN 3 showed diffraction peaks at 4.2 and 3.8 Å for the intermediate polymorphic form β'. These results confirm that the SLN gelation process occurred due to the polymorphic transition of the lipid content ($\alpha \rightarrow \beta' \rightarrow \beta$) during the crystallization and stabilization steps performed shortly after the HPH production process, as previously described.

The NLC 6, NLC 9 and NLC 12 composed of CR with 20, 40 and 60% HOSO incorporation, respectively, presented diffraction peaks in 4.2 and 3.8Å, referring to the intermediate polymorphic form β', characteristic of the CR. It is noteworthy that in the results obtained for Z-ave of the nanoparticles referring to these systems, no changes in Z-ave were observed during the 60 days of evaluation. Indicating that there were no polymorphic transitions from the β' to β-form in the time and conditions studied. It is noteworthy that the x-ray diffraction was performed on the nanoparticles after the lyophilization process, which could have influenced the acceleration of the polymorphism of these nanoparticles. However, it does not occur for these systems, remaining in the intermediate β'-form , indicating that it really is the polymorphic habit of these systems. The other nanoparticles presented diffraction peaks at 4.6 Å for crystallization in the most stable β-form.

In addition, it was observed in the diffractograms shown in Figure 6 that the intensity of the peaks related to the crystalline forms was reduced with the increase of HOSO. It is an effect directly related to the reduction of the crystallinity of the systems by the incorporation of the unsaturated fraction.

In macroscale lipid systems, in terms of technological application, it is reported in the literature that crystals in the β'-form present intermediate stability, relatively small size and incorporate a large amount of liquid oil in the crystalline network, contributing to the formation of softer fats, with good aeration and creaminess properties. In contrast, crystals in the polymorphic form β are more stable and show dense packaging, which implies a higher consistency and melting point. In addition, they are initially small, but tend to grow into large, needle-shaped clusters, promoting in the mouth a sensation of undesirable sandiness (Sato, 2001; Timms, 1995).
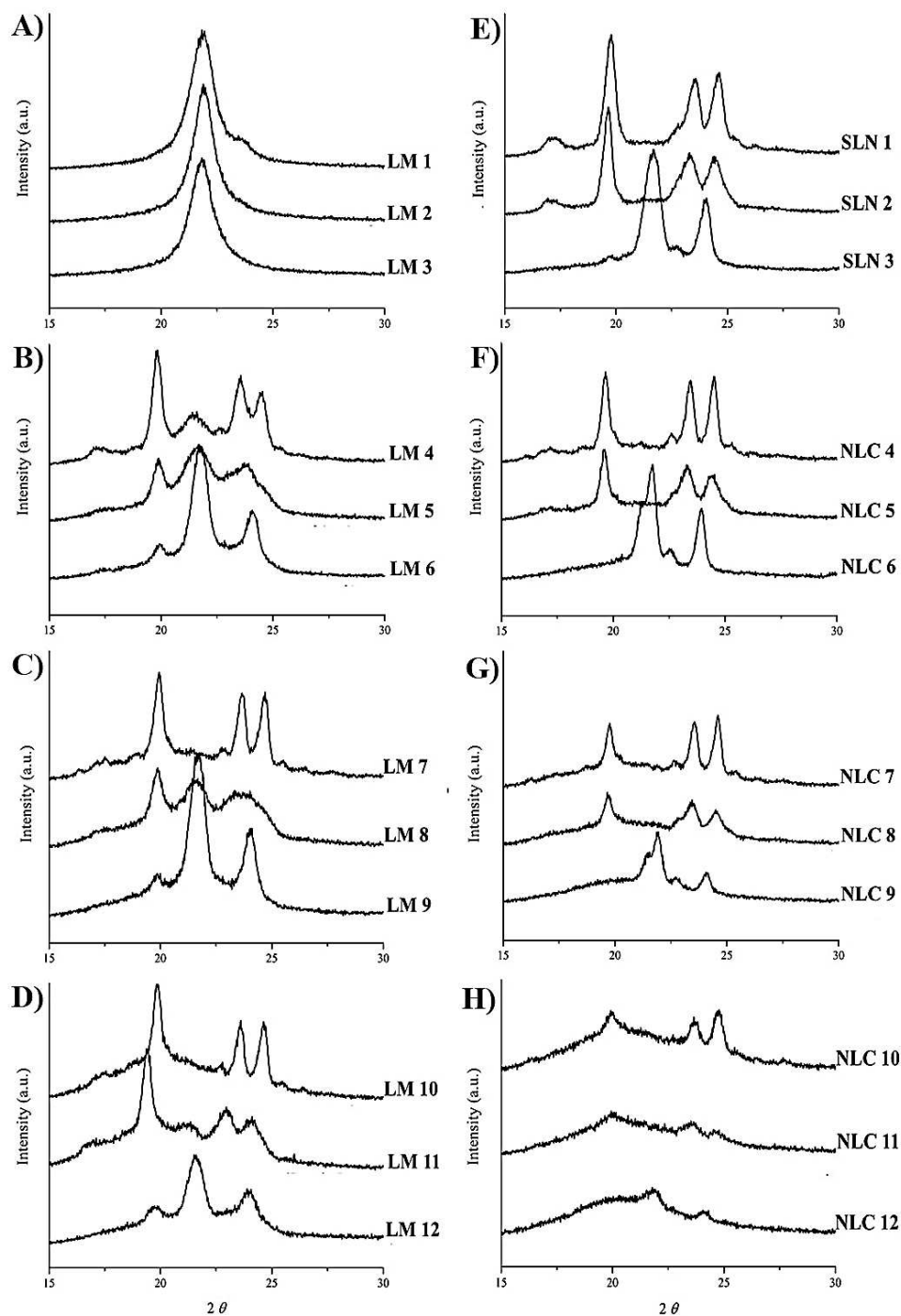
Fig. 6. Diffraction patterns of: A) Lipid matrices (LM) composed by solid lipids (100% CA; mixture of CA and CR (50:50); 100% CR); B) LM composed by mixtures of 80% of solid lipids (CA; mixture of CA and CR; CR) and 20% of liquid lipid (HOSO); C) LM composed by mixtures of 60% of solid lipids (CA; mixture of CA and CR; CR) and 40% of liquid lipid (HOSO); D) LM composed by mixtures of 40% solid lipids (CA; mixture of CA and CR; CR) and 60% of liquid lipid (HOSO); E) SLNs developed with the LMs described in "A"; F) NLCs developed with LMs described in "B"; G) NLCs developed with the LM described in "C"; and H) NLCs developed with the LM described in "D". The data referring to LMs come from an earlier study conducted by our research group (Santos, Santana, Braz, Silva, Cardoso, & Ribeiro, 2018).

Currently, there are no applications of lipid nanoparticles in foods reported in the literature, only indications about their efficiency in the transport of bioactive compounds, as well as medicines in the medical field, to facilitate absorption in the body. Thus, in this study, we can say that the developed NLC present potential application for the delivery of lipophilic bioactive compounds in foods, with consequent, delivery of these compounds in the body, mainly due to the high thermal resistance. In addition, the particles in the β'-form may have a higher incorporation capacity of bioactive compounds, due to the crystallinity characteristics related to less compact crystalline networks. Also, due to the reduced size, the nanoparticles can reduce the undesirable effects of technological application such as the sandiness characteristic of crystallized fats in the β-form, reported in the macroscale systems.

5. Conclusion

The use of other LM from plant origins, such as CA, CR, and HOSO, was positive for the production of lipid nanoparticles, with a clear viability of food application. The use of 3 cycles of PAH was sufficient to obtain systems with desirable characteristics. The NLC with mixed compositions of conventional oils and fats remained stable over 60 days, with few changes in Z-ave of the particles, PDI and ZP. The SLN composed only of the hardfats, presented gelation behavior very similar to the SLN developed with purified lipids, as reported in the literature. The thermal study allowed to identify differences between nanometric scale particles when compared to LM. The results show that the nanostructured lipid materials exhibit higher thermal resistance than the macroscale lipids. In addition, it was possible to detect an eutectic effect due to the heterogeneity of the constituent components of LM, which favoured the development of less crystalline nanoparticles in structural terms, with a consequent reduction in size and greater physical stability. Additionally, through the characterization of the polymorphic habit of the nanoparticles, it was verified that when in nanoscale polymorphic transitions are facilitated and the more stable form is reached more quickly. Therefore, the nanoparticles developed in this study have an economic and operational viability of food application. Mainly because they are composed of conventional fats and oils, in addition to the easy scaling of the production method to industrial scale. In terms of application, the developed systems presented a high potential for incorporation of bioactive compounds for application as delivery systems in food.

References

AOCS. (2009). *Official methods and recommended practices of the American Oil Chemists' Society*. Urbana (USA): AOCS Press.

Awad, T. S., Helgason, T., Weiss, J., Decker, E. A., & McClements, D. J. (2009). Effect of Omega-3 Fatty Acids on Crystallization, Polymorphic Transformation and Stability of Tripalmitin Solid Lipid Nanoparticle Suspensions. *Crystal Growth & Design, 9*(8), 3405–3411.

Basso, R. C., Ribeiro, A. P. B., Masuchi, M. H., Gioielli, L. A., Gonçalves, L. A. G., Santos, A. O. d., Cardoso, L. P., & Grimaldi, R. (2010). Tripalmitin and monoacylglycerols as modifiers in the crystallisation of palm oil. *Food Chemistry, 122*(4), 1185-1192.

Bunjes, H., Steiniger, F., & Richter, W. (2007). Visualizing the structure of triglyceride nanoparticles in different crystal modifications. *Langmuir, 23*(7), 4005-4011.

Bunjes, H., & Unruh, T. (2007). Characterization of lipid nanoparticles by differential scanning calorimetry, X-ray and neutron scattering. *Adv Drug Deliv Rev, 59*(6), 379-402.

Campos, R. (2005). Experimental methodology. In A. Marangoni (Ed.), *Fat Crystal Networks*, vol. 1 (pp. 267-349). New York: Marcel Dekker.

Cerqueira, M. A., Pinheiro, A. C., Silva, H. D., Ramos, P. E., Azevedo, M. A., Flores-López, M. L., Rivera, M. C., Bourbon, A. I., Ramos, Ó. L., & Vicente, A. A. (2014). Design of Bio-nanosystems for Oral Delivery of Functional Compounds. *Food Engineering Reviews, 6*(1-2), 1-19.

Himawan, C., Starov, V. M., & Stapley, A. G. (2006). Thermodynamic and kinetic aspects of fat crystallization. *Adv Colloid Interface Sci, 122*(1-3), 3-33.

Lacatusu, I., Mitrea, E., Badea, N., Stan, R., Oprea, O., & Meghea, A. (2013). Lipid nanoparticles based on omega-3 fatty acids as effective carriers for lutein delivery.

Preparation and in vitro characterization studies. *Journal of Functional Foods, 5*(3), 1260-1269.

Madureira, A. R., Campos, D., Gullon, B., Marques, C., Rodriguez-Alcala, L. M., Calhau, C., Alonso, J. L., Sarmento, B., Gomes, A. M., & Pintado, M. (2016). Fermentation of bioactive solid lipid nanoparticles by human gut microflora. *Food Funct, 7*(1), 516-529.

Marangoni, A. G., Acevedo, N., Maleky, F., Co, E., Peyronel, F., Mazzanti, G., Quinn, B., & Pink, D. (2012). Structure and functionality of edible fats. *Soft Matter, 8*(5), 1275-1300.

Martini, S., Awad, T., & Marangoni, A. G. (2006). Structure and Properties of Fat Crystals Networks. In F. Gunstone (Ed.), *Modifying Lipids for Use in Foods*, (pp. 142-169). NY: CRC Press.

Mehnert, W., & Mäder, K. (2012). Solid lipid nanoparticles. *Advanced Drug Delivery Reviews, 64*, 83-101.

Muller, R. H., Runge, S., Ravelli, V., Mehnert, W., Thunemann, A. F., & Souto, E. B. (2011). Oral bioavailability of cyclosporine: solid lipid nanoparticles (SLN) versus drug nanocrystals. *Int J Pharm, 317*(1), 82-89.

Oliveira, G. M. d., Stahl, M. A., Ribeiro, A. P. B., Grimaldi, R., Cardoso, L. P., & Kieckbusch, T. G. (2015). Development of zero trans/low sat fat systems structured with sorbitan monostearate and fully hydrogenated canola oil. *European Journal of Lipid Science and Technology, 117*(11), 1762-1771.

Qian, C., & McClements, D. J. (2011). Formation of nanoemulsions stabilized by model food-grade emulsifiers using high-pressure homogenization: Factors affecting particle size. *Food Hydrocolloids, 25*(5), 1000-1008.

Ribeiro, A. P. B., Basso, R. C., & Kieckbusch, T. G. (2013). Effect of the addition of hardfats on the physical properties of cocoa butter. *European Journal of Lipid Science and Technology, 115*, 301-312.

Rousseau, A. G., & Marangoni, A. (2002). *Food lipids: chemistry, nutrition, and biotechnology.* New York: CRC Press.

Salminen, H., Helgason, T., Kristinsson, B., Kristbergsson, K., & Weiss, J. (2013). Formation of solid shell nanoparticles with liquid omega-3 fatty acid core. *Food Chem, 141*(3), 2934-2943.

Santos, V. S., Ribeiro, A. P. B., Cardoso, L. P., & Santana, M. H. A. (2018). Crystallization, polymorphism and stability of nanostructured lipid carriers developed with soybean oil, fully hydrogenated soybean oil and free phytosterols for food application. *Food Chemistry, a ser submetido.*

Santos, V. S., Santana, M. H. A., Braz, B. B., Silva, A. Á., Cardoso, L. P., & Ribeiro, A. P. B. (2018). The thermal and crystalline behavior of lipid matrices with potential for application in lipid nanoparticles. *Química Nova, a ser submetido*.

Sato, K. (2001). *Crystallization behaviour of fats and lipids: a review* (Vol. 56). Oxford.

Scrimgeour, C. (2005). Chemistry of Fatty Acids: Part 1. Edible Oil & Fat Products: Chemistry, Properties, and Health Effects. In F. Shahidi (Ed.), *Bailey's Industrial Oil and Fat Products*, vol. 3 (pp. 629).

Severino, P., Andreani, T., Macedo, A. S., Fangueiro, J. F., Santana, M. H., Silva, A. M., & Souto, E. B. (2012). Current State-of-Art and New Trends on Lipid Nanoparticles (SLN and NLC) for Oral Drug Delivery. *J Drug Deliv, 2012*, 750891.

Severino, P., Santana, M. H., & Souto, E. B. (2012). Optimizing SLN and NLC by 2(2) full factorial design: effect of homogenization technique. *Mater Sci Eng C Mater Biol Appl, 32*(6), 1375-1379.

Tamjidi, F., Shahedi, M., Varshosaz, J., & Nasirpour, A. (2013). Nanostructured lipid carriers (NLC): A potential delivery system for bioactive food molecules. *Innovative Food Science & Emerging Technologies, 19*(Supplement C), 29-43.

Timms, R. E. (1995). *Crystallization of fats*. London: Blackie Academic.

Westesen, k., & Siekmann, b. (1997). Investigation of the gel formation of phospholipids stabilized solid lipid nanoparticles. . *Int J Pharm, 152*, 35-45.

Wu, L., Zhang, J., & Watanabe, W. (2011). Physical and chemical stability of drug nanoparticles. *Adv Drug Deliv Rev, 63*(6), 456-469.

Yang, Y., Corona, A., Schubert, B., Reeder, R., & Henson, M. A. (2014). The effect of oil type on the aggregation stability of nanostructured lipid carriers. *Journal of Colloid and Interface Science, 418*(Supplement C), 261-272.

Zimmermann, E., Müller, R. H., & Mäder, K. (2000). Influence of different parameters on reconstitution of lyophilized SLN. *International Journal of Pharmaceutics, 196*(2), 211-213.

ARTIGO 4

"Development of nanostructured lipid carriers loaded with free phytosterol for food applications" a ser submetido a *Food Structure.*

Development of nanostructured lipid carriers loaded with free phytosterol for food applications

V. S. Santos[1], A. P. B. Ribeiro[2], B. B. Braz[1], A. Á. Silva[2], L. P. Cardoso[3], M. H. A. Santana[1]

[1]*Department of Biotechnological Processes, School of Chemical Engineering, University of Campinas, 500 Albert Einstein Ave., Campinas, SP 13083-970, Brazil.*
[2] *Department of Food Technology, School of Food Engineering, University of Campinas, 80 Monteiro Lobato St., Campinas, SP 13083-970, Brazil.*
[3] *Department of Applied Physics, Institute of Physics Gleb Wataghin, University of Campinas, 777 Sérgio Buarque de Holanda St., 13083-859 Campinas, SP, Brazil.*

Abstract

The objective of this study was the development of nanostructured lipid carriers (NLC) with 30 and 50% of the free phytosterols (FP) using conventional fat and oils. Lipid matrices (LM) and NLC were produced with high oleic sunflower oil and fully hydrogenated canola (CA) and crambe (CR) oils by high-pressure homogenization (HPH) using Polyoxyethylene sorbitan monooleate as the emulsifier. The NLCs were evaluated for the physical stability during 60 days, by means of the verification of the hydrodynamic diameter (Z-ave), polydispersity index (PDI) and zeta potential (ZP). The LMs were characterized in terms of crystallinity and morphological characteristics. The melting behavior and polymorphic habit were investigated for both LM and NLC. The NLC presented particle sizes ranging from 148.23 to 342.10 nm, PDI from 0.275 to 0.481 and ZP between -22.27 and -29.70 mV. The best results were obtained for NLC with 30% of FP. The NLC presented higher thermal resistance than their LM, requiring more energy for the phase transition. The use of CA and CR separately in the NLC formulations favored the incorporation of FP. The FP showed a diffraction pattern with 14 peaks which has difficulted the triacylglycerols (TAG) peaks identification. Thus, possibly, both LM and NLC have presented crystals in β-form and also mixtures of β' and β forms, depending on CA and CR presence. When comparing to LM, the obtained NLC showed a different thermal and crystalline characteristics, whit high versatility for food applications. In this way, NLCs can be used for food enrichment, such as spreads, margarine, mayonnaise, beverages, among others.

Keywords

Nanotechnology; Lipids; Thermal properties; Crystallinity; Bioactive compounds; Functional Foods.

Abbreviations

CA   Fully hydrogenated canola oil
CR   Fully hydrogenated and crambe oil
DSC   Differential Scanning Calorimetry
FAC   Fatty acids composition

FP   Free Phytosterols
GRAS   Generally recognized as safe
GTI   Gastrointestinal tract
HLB   Hydrophilic-lipophilic balance
HOSO   High oleic sunflower oil
HPH   High-pressure homogenization
INPI   National Institute of Industrial Property
LM   Lipid matrix
LN   Lipid Nanoparticles
NLC   Nanostructured Lipid Carriers
PDI   Polydispersity index
T80   Polyoxyethylene sorbitan monooleate
TAG   Triacylglycerols
XRD   X-ray diffraction
Z-ave   Average diameter
ZP   Zeta Potential

1. Introduction

The benefits of nanotechnology have already been recognized by many industries and some products have already been manufactured and marketed. However, the study of nanotechnology in the food area very recent, considered non-existent in terms of industrial application, even recognizing the great potential of use. Up to date, the number of scientific studies focused on the development of nano-systems and its applications in food is still limited, but this number has been growing with a great potential for commercially viable applications in a close future (Beloqui, Solinis, Rodriguez-Gascon, Almeida, & Preat, 2016; Cerqueira, Pinheiro, Silva, Ramos, Azevedo, Flores-López, et al., 2014; I. Lacatusu, Badea, Stan, & Meghea, 2012; Rashidi & Khosravi-Darani, 2011).

Most of the developments in nanotechnology in the food area occurred after 2005, where researchers started reporting on several findings on nanoscale systems with potential for food application. The main highlighted topic in this field was the use of nanotechnology for the development of bioactive compound carriers for foods (Aditya, Aditya, Yang, Kim, Park, & Ko, 2015; Weiss, Takhistov, & McClements, 2006). These discoveries were initially encouraged by the use of carrier systems in pharmaceutical and cosmetic fields, where nanotechnology has been widely explored and applied for the delivery of many drugs and bioactive compounds. Even after the successful development of these nano-systems in the biomedical sectors, many challenges must be overcome for food uses such as the choice of raw

materials, since foods require compounds generally recognized as safe (GRAS) and/or under law limitations.

In this context, lipid nano-systems present a great potential for food applications, since a great variety of natural and modified fats and oils are already available for the food industry. In the scientific literature, it is possible to find a range of studies suggesting the development of solid lipid nanoparticles (SLN) and nanostructured lipid carriers (NLC) for the transport and protection of bioactive compounds for food applications (WEISS, TAKHISTOV, & McCLEMENTS, 2006; ADITYA & KO, 2015). The main interest in carrying bioactive compounds in food lies in the development of enriched or functional food products, in order to provide healthier food for consumers.

Bioactive compounds are commonly known for their functional properties related to disease prevention (McClements, Decker, & Weiss, 2007). However, many of these compounds are naturally present in foods, in very low amounts or with limited bioavailability. Currently, some of these compounds have been extracting from plant and animal sources to be directly incorporated in foods. However, this direct incorporation generally provides a low chemical stability and bioavailability which may reduce the functional effects of these compounds. In addition, bioactive compounds often have low solubility, which makes difficult their applications in foods (Hariklia Vaikousi, Athina Lazaridou, Costas G. Biliaderis, & Zawistowski, 2007).

Lipid nanoparticles are promising to deliver lipid-soluble bioactive compounds with low water solubility, such as carotenoids, tocopherols, omega-3, phytosterols, among others, widely used as ingredients in various food products. In addition, lipid nanoparticles can be used to protect these bioactive compounds from chemical degradation during food processing and storage. For instance, Awad (2008) evaluated the thermal and polymorphic behavior of NLS developed with tripalmitin loaded with ω-3. Ioana Lacatusu, Mitrea, Badea, Stan, Oprea, and Meghea (2013) studied NLC developed with fish oil, ω-3 rich, and tristearin for lutein carrying. Y. Liu and Wu (2010) developed NLC with tripalmitin and corn oil for the incorporation of lutein. I. Lacatusu, Badea, Stan, and Meghea (2012) developed NLC with grape seed and fish oils, and squalene to carry β-sitosterol. Additionally, authors report that due to the higher contact surface area of lipid nanoparticles, they may improve the bioavailability

and absorption of bioactive compounds during the gastrointestinal tract (Weiss, Decker, McClements, Kristbergsson, Helgason, & Awad, 2008).

As already cited, up to date the studies have been carried out using purified lipid as raw materials, such as isolated fatty acids and triacylglycerols (TAGs) as well as bioactive compounds of analytical grade. These compounds make it difficult, especially in terms of cost, the application of these systems in food products at industrial scale. For this reason, during the last 4 years, our research group has been working with the development of nanoscale systems based on the use of food grade vegetable fats and oils, widely used in the food industry. Thus, we have developed SLN with hardfats of canola and cambre oils, as well as NLC with high oleic sunflower oil and the hardfats of canola and cambre oils (V. S. Santos, Braz, Silva, Cardoso, A., & Ribeiro, 2018). In addition to these nanosystems, NLCs were also developed with soybean oils and soybean hardfat to carry food grade free phytosterols (FL) (V. S. Santos, Ribeiro, Cardoso, & Santana, 2018).

The hardfats are fully hydrogenated vegetable oils, with a melting point ranging from 40-72 ° C. They are obtained when all the double bonds of the fatty acids are saturated during the full catalytic hydrogenation of unsaturated oils. Hardfats are relative new industrial materials and affordable for use in food. They were initially developed as a raw material to interesterified low trans fats. Nowadays, besides the use as solid material for the development of NLS and NLC (V. S. Santos, Santana, Braz, Silva, Cardoso, & Ribeiro, 2018), hardfats have also been used as structuring agents of liquid oils (A. P. B. Ribeiro, Basso, & Kieckbusch, 2013; Tamjidi, Shahedi, Varshosaz, & Nasirpour, 2013).

It should be noted that our research group is a pioneer in the use of hardfats for the development of both NLS (alone) and NLC (combined to vegetable oils) for the transport of food grade lipophilic bioactive compounds, such as FL. The interest in carrying phytosterols into particles in foods is related, mainly to its health benefits.

Phytosterols, also known as plant sterols, are the main sterol fraction in plant extracts and vegetable oils. More than 10 types of phytosterols molecules can be naturally found, being β-sitosterol, Δ5-avenasterol, campesterol and stigmasterol the main species. The proportion of each sterol in the total content varies according to the plant source (Fernandes & Cabral, 2007; Goméz-Coca, Perez-Camino, & Moreda, 2015; Moreau, Whitaker, & Hicks, 2002).

Regarding the bioactivity and consumption of phytosterols by humans, many studies have been carried to demonstrate the good effects of phytosterols on the metabolism (Kritchevsky & Chen, 2005; Ostlund, 2002). The first reported effect was the prevention of coronary disease. Because of their similarity to cholesterol, phytosterols are known to compete with cholesterol for absorption, leading to lower blood cholesterol levels (Ling WH & PJ., 1995; Ntanios FY, MacDougall DE, & PJ., 1998). Studies indicate that the consumption of 2 g of phytosterols per day has a significant effect on the reduction of cholesterol levels and, consequently, the prevention of coronary heart disease (Moruisi, Oosthuizen, & Opperman, 2013; Wu, Fu, Yang, Zhang, & Han, 2009). In addition, the ingestion of phytosterols has been associated with cancer prevention. Recent studies indicate that the prevention of cancer by the consumption of phytosterols is related to the modulation of sterol biosynthesis, improvement of the immune response, and induction of tumor metastases (Shahzad, Khan, Md, Ali, Saluja, Sharma, et al., 2017).

From the technological point of view, our research group recently related that that food grade FL (composed of a mixture of phytosterols) have thermal and crystalline behavior very similar to isolated phytosterols such as β-sitosterol and stigmasterol (Gomes Silva et al., 2018). In addition, we have previously developed NLCs composed of soybean oil and fully hydrogenated soybean oil with the incorporation of 30% FP, being these systems promising for food application (V. S. Santos, Ribeiro, Cardoso, & Santana, 2018).

Thus, the central objective of this work was the development of NLC with other conventional raw materials, such as high oleic sunflower oil, and fully hydrogenated canola and crambe oils for food grade FL carriage. In addition, we aimed to extend the use of other vegetable oils and fats to obtain nanostructured systems with different crystalline characteristics and thermal stability for applications in different food products.

2. Materials & method

2.1. Materials

The solid lipid raw materials used for the development of lipid matrices (LM) and NlC were the fully hydrogenated canola (CA) and crambe (CR) oils provided by SGS Agricultura e Indústria Ltda©(Ponta Grossa - PR, Brazil). High oleic sunflower oil (HOSO), supplied by Cargill Agrícola S.A (Mairinque - SP, Brazil), was used as liquid lipid in the NLC

composition. The HOSO and both CA and CR were previous characterized according to the fatty acid (CAG) and triacylglycerols (TAG) compositions (V. S. Santos, Santana, Braz, Silva, Cardoso, & Ribeiro, 2018). HOSO presented 90.68% of unsaturated fatty acids, of which 78,60% was of oleic acid (O, C18:1) and 11,41% of linoleic acid (L, C18:2). The CA and CR presented 100% of saturated fatty acids. For the CA: 93.82% was of stearic acid (S, C18:0), 5.24% of palmitic acid (P, C16:0), and 0.94 % arachidonic acid (A, C20:0). For CR: 56.30% was of behenic acid (Be, C22:0), 31.70% of stearic acid (S, C18:0), 6.70 % of arachidonic acid (A, C20:0), 3.20% of palmitic acid (P, C16:0) and 2.10% of lignoceric acid (Lg, C24: 0). The TAGs present in the HOSO were: OOO representing approximately 65% of the total, followed by OLO (~ 15%), OOP (~ 10%) and OSL/PLO (~ 3%). CA presented 4 distinct TAGs, with the majority being SSS (~ 80%) and PSS (~ 13%) and in smaller proportions PPS (~ 4%) and SSA (~ 3%). In CR, 9 different TAGs were found, among which the predominant ones were SBeBe (~ 38%), SSBe (~ 17%), SABe (~ 17%) and in smaller proportions ABeBe (~6%), BeBeBe (~9%), BeBeLg (~8%), PSBe (~2%) and PSS (~ 0.5%). The ethoxylated sorbitan monooleate P1754 (Tween®80, T80), with a hydrophilic-lipophilic balance (HLB) of 14.0, was purchased from Sigma-Aldrich (St. Louis, Missouri, USA). The bioactive compounds were free phytosterols (FP), kindly provided by a national production initiative (still under development). FPs were 98% purity, composed of a mixture of sterols, being the main sterols β-sitosterol (~ 44%), stigmasterol (~ 27%) and campesterol (~ 23%).

2.2 Methods

2.2.1. Formulation of lipid matrix and lipid nanoparticles

The NLCs were developed with 10% (m/m) of total lipid phase and 90% (m/m) of the aqueous phase. The aqueous phase was composed of distilled water and 2% of the T80 as the emulsifier, as recommended by Aditya, Aditya, Yang, Kim, Park, and Ko (2015). For the composition of the lipid phase, 14 lipid matrices were formulated with liquid lipid (HOSO in proportions of 20, 40, 50 and 70%), solid lipids (30 and 50% of CA and CR and their mixtures) and the bioactive compound (30 and 50% FP), as shown in Figure 1. Each LM was used for the development of the NLC.
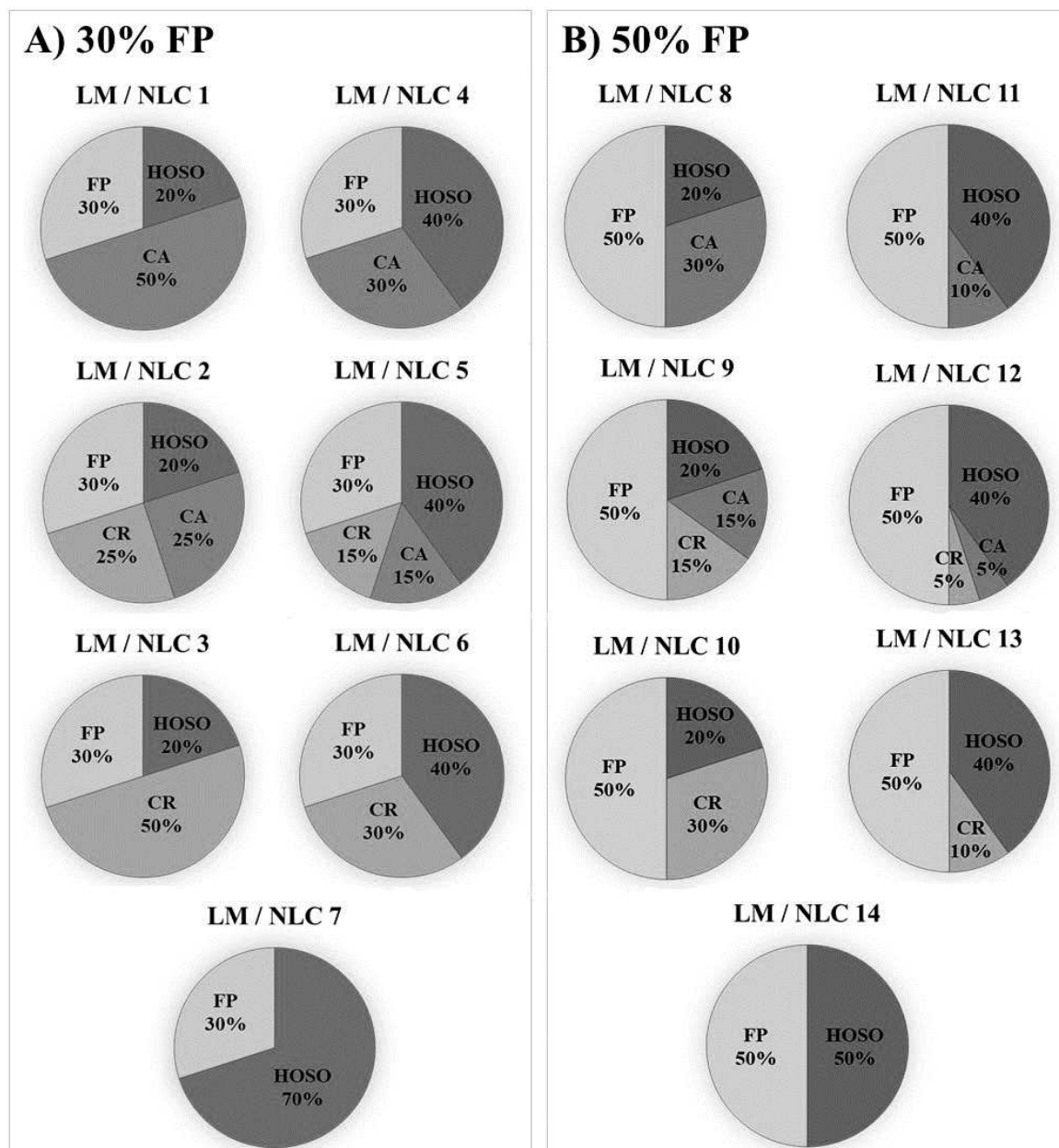
Fig. 1. Schematic representation of lipid matrices (LM) composition, used in the nanostructured lipid carriers (NLC) with free phytosterols (FP). A) LM and NLC, both developed with 30% FL, 20, 40 and 70% high oleic sunflower oil (HOSO), 15, 25, 30 and 50% of fully hydrogenated canola oil (CA) and crambe oil (CR); B) LM and NLC, both developed with 50% FL 20, 40 and 50% HOSO, 5, 10, 15 and 30% of CA and CR.

2.2.2. Production of lipid matrix and lipid nanoparticles

LMs were melted at 130 °C over magnetic stirring for 3 minutes, conditioned at 5°C for 24 h for lipid crystallization, followed by a further 24 h at 25 °C for crystalline stabilization and subsequent physical evaluations. The NLC preparation was performed

according to 4 steps: i) fusion of the lipid fraction; ii) formation of the emulsion; iii) nanoemulsification, and iiii) crystallization of the lipid phase. The lipid fraction (10%) was melted and homogenized on a magnetic stirrer at 300 rpm for 3 minutes. Subsequently, the aqueous phase (90%) was added at 90°C and the pre-emulsion was obtained in Ultra Turrax IKA T18 Basic (Germany) at 20,000rpm for 3 minutes. Then the pre-emulsion was subjected to 3 cycles of homogenization at 800 bar in a high pressure homogenizer (HPH, GEA Niro Soavi, model: NS 1001L PANDA 2K, Italy) as recommended by Zimmermann, Müller, and Mäder (2000), Bunjes, Steiniger, and Richter (2007) and Severino Patrícia Severino, Pinho, Souto, and Santana (2012). After the HPH process, the obtained nanoemulsions were stored at 5 °C/24 hours for lipid crystallization and obtaining the dispersions containing the NLC, which were subsequently stored at 25 °C/24h for crystalline stabilization (Qian & McClements, 2011; Yang, Corona, Schubert, Reeder, & Henson, 2014). A portion of the samples in aqueous suspension was maintained at 25°C for initial characterization and stability evaluation over 60 days storage and another part was dried by lyophilization, as described in the sequence.

2.2.3. Additional drying process of lipid nanoparticles

The NLCs in aqueous suspension, shortly after the crystallization and stabilization process described in the previous item, were frozen in ultra-freezer (-86 °C) for 2 hours and immediately afterward were subjected to lyophilization for 24h at -25 ° C under a vacuum of 0.370 mbar using lyophilizer (Liobras L101, Brazil). The NLCs were stored at 25 °C for further characterization.

2.2.4. Characterization of lipid matrix and lipid nanoparticles

2.2.4.1. Size, polydispersity index and zeta potential of lipid nanoparticles

The NLCs in aqueous dispersions were evaluated in triplicate for particle size by means of the hydrodynamic diameter (Z-ave) in nanometers (d.nm), polydispersity index (PDI) and zeta potential (ZP) after 24 hours, 15, 30 and 60 days of the production process by dynamic light scattering (DLS, Zetasizer Nano NS, Malvern, UK). The samples were diluted with distilled water to reduce the opalescence before the measurements. Data analysis was performed using the software included in the equipment system.

2.2.4.2.Thermal behavior in the melting of lipid matrix and lipid nanoparticles

The melting thermal behavior of the LM and the bioactive compound used to produce NLC, as well as lyophilized NLCs, were analyzed using the TA Instruments, model Q2000, attached to the RCS90 Refrigerated Cooling System (TA Instruments, Waters LLC, New Castle). Data were processed in the Universal V4.7A software (TA Instruments, Waters LLC, New Castle). LM used for the production of NLC were packed in aluminum hermetical capsules (~10mg) and melted at 150 °C to erase the crystalline history. Afterward, they were submitted to the same thermal treatment performed in the NLC after processing in HPH, referring to the crystallization and stabilization stages (5 °C/ 24h and 25 °C/24h), thus making it possible to compare the results during melting. The melting events were evaluated under isothermal condition at 25 °C for 10 minutes, followed by heating at 25°C to 10°C/min (Wang, Dong, Wei, Zhong, Liu, Yao, et al., 2014). To evaluate the NLC for the melting thermal behavior, the lyophilized samples (mass of ~10mg) were packed in hermetic aluminum capsules and submitted to the same DSC program, mentioned before. For all melting analysis were obtained the following parameters: initial melting temperature (T_{in}), peak melting temperature (T_{max}), final melting temperature (T_{off}) and melting enthalpy (ΔH_m).

2.2.4.3. The microstructure of lipid matrices

The determination of the microstructure (morphology and crystalline dimensions) of ML was performed by polarized light microscopy (PLM). The samples were previously melted at 150 °C in an oven and a droplet was placed on a glass sheet (also preheated at 150 °C), which was covered with a coverslip. The slides were then conditioned at 5 °C/24h followed by 24h at the analysis temperature (25 °C), according to the crystallization and stabilization treatment performed for LM and NLC. The morphology of the crystals was evaluated using the Microscope Microscope Olympus BX-51 (Olympus, Japan), with infinite correction optics UIS, coupled to the Evolt E-300 digital color video camera 5.0 Mpixel (Olympus, Japan). The images were captured using Image-Pro Plus software version 7.01 (Media Cybernetic, USA) under polarized light and magnification of 200 times. For each slide, three visual fields were analyzed, of which only one was chosen to represent the observed crystals. The evaluation parameters selected for the quantitative analysis of the images were the mean diameter of the crystals and the percentage of crystallized area (Campos, 2005).

2.2.4.4. X-ray diffraction analyses of lipid matrix and lipid nanoparticles

X-ray diffraction (XRD) analysis was performed on LMs used in nanoparticles production, lyophilized NLC and bioactive compound (FP) according to AOCS method Cj 2-95 (AOCS, 2009). FP and LM were subjected to a previous thermal treatment under the same conditions of the crystallization and stabilization of NLC, after the production process in HPH. Thus, the LM and the FP were melted at 150°C and conditioned at 5°C for 24 h, followed by a further 24 h at 25°C. The NLCs were subjected to XRD analysis after lyophilization. All XRD analyzes were performed on a Philips diffractometer (PW 1710) using Bragg-Brentano (θ:2θ) geometry with Cu-kα rad radiation (λ= 1.54056 Å, 40 KV voltage and 30 mA current). The measurements were obtained with steps of 0.02 ° in 2 ° and acquisition time of 2 seconds, with scans of 1.8 to 40° (2° scale) at 25 °C. The identification of the polymorphic forms of the LM and the lipid NLC were performed according to the typical short spacings of the lipid crystals (AOCS, 2009) and the diffraction peaks of the FP were enumerated and compared with results found in the literature.

2.2.5. Statistical analysis

Z-ave, PDI and ZP data were statistically analyzed by means of One-Way Analysis of Variance (ANOVA) with Statistica (V.12) Software (Statsoft Inc., Tulsa, UK). The Tukey test was applied to determine the significant differences between the means, at a probability level of 5% (p≤0.05).

3. Materials & method

3.1 Size, polydispersity index and zeta potential of lipid nanoparticles

The Z-ave, PDI and ZP are fundamental parameters for the characterization of nanostructured systems. These parameters can be used to verify the stability of the systems along of time. PDI values vary between 0 (monodisperse) and 1 (polydisperse) (T. S. Awad, Helgason, Weiss, Decker, & McClements, 2009). ZP over |30| mV characterizes colloidal systems with good stability, being |60| mV an optimum pint. The system is considered susceptible to destabilization and the occurrence of limited flocculation between 5 and 30mV (Madureira, Campos, Gullon, Marques, Rodriguez-Alcala, Calhau, et al., 2016). The results

obtained for Z-ave, PDI and ZP for the NLCs developed with 30 and 50% FP are described in Table 1 and plotted in Figure 2.

The NLCs with 30% of FP (Figure 2A) presented lower values of Z-ave in relation to NLC developed with 50% FP (Figure 2B), statistically different ($p \leq 0.05$). Z-ave values of particles obtained shortly after processing (24h), for NLCs with 30 and 50% FP, ranged from 148.23 to 250.00 nm and 205.97 to 342.10 nm, respectively. The values for PDI were also lower for NLCs with 30% FP, ranging from 0.275 to 0.410 and 0.343 to 0.481 for NLCs with 50% FP (Figures 2C and D). As for the ZP results, the values closer to 30mV were found for NLCs with 30% FP ranging from -24.40 to -29.70 mV, whereas for 50% FP incorporation these values were -22.27 at -26.47 mV. Similar values were found in NLC composed of solid lipids (palmitic and stearic fatty acids) and liquid lipids (squalene, grape seed oil, and fish oil) by I. Lacatusu, Badea, Stan, and Meghea (2012) with the incorporation of 1% β-sitosterol, using T80. These NLCs had Z-ave varying between 177 to 236 nm, PDI from 0.225 to 0.380 and ZP between -38 and -52 mV. It should be noted that the NLCs developed by these authors contained only 1% of β-sitosterol. In the present work, one of the challenges was the high incorporation of FP (30 and 50%) into the NLC, which may allow the development of enriched food products with functional properties.

In general, observing Figures 3A and 4A were the particle size distribution were expressed in terms of scattered light intensity, I distribution, the proportional diameter to the sixth power ($I \alpha d^6$). It is possible to verify that the NLCs with 30% of FP, had greater stability over time when compared to systems with 50% FP, even with a bimodal distribution. The differences between the two systems can be better understood by observing Figures 3B and 4B that showed the particle size distribution in terms of the number of particles, N distribution, proportional to the predominant diameter in the sample ($N \alpha d$).

Thus, it was possible to verify that the NLC with 30% of FP presented more homogeneous particle sizes, whereas, with 50% of FP, a greater polydispersity between the particles was noticed. In addition, it should be noted that the polydispersity of the particles with 50% FP increased over the time. It was observed that during the 60 days of evaluation the Z-ave of NLCs with 30% of FP remained very similar. In addition, it was found that the increase of HOSO in the NLC with 30% FP, favored the reduction of the particle size, being visible in Figure 2A. All NLCs developed with 40% HOSO showed Z-ave below 200 nm (NLC 4, 5 and

6). It should be noted that the NLC with the lowest values of particle size was NLC 7, composed only of liquid lipid and the bioactive compound (70% of HOSO and 30% of FP).

In a previous study, with NLC, soybean oil (20%) and fully hydrogenated soybean oil (50%) with 30% FP incorporation, Z-ave and PDI obtained were 164.97 nm and 0.235, respectively (V. S. Santos, Ribeiro, Cardoso, & Santana, 2018). The results obtained in the present work for NLC 1 with the same oil: fully hydrogenated oil ratio and bioactive compound (20% HOSO, 50% CA and 30% FP), but from different sources, Z-ave was 204.97 nm and PDI of 0.410. The differences between the values showed that the TAG composition of LM directly interferes in the characteristics of the NLC system. In this way, we can verify that it is very important to explore LMs composed of different vegetable fats and oils, to extend the range of raw materials compatible with the use in NLC and SLN, as well as to verify the best options for the incorporation of each bioactive compounds.

It was found that NLC 2 composed of the mixture of CA and CR (25:25m/m), 20% of HOSO and 30% of FP showed particles with 250 nm after 24h and this value was reduced to 219.23 nm after 15 days, and after 30 days of storage it was verified a reduction of to 212.77 nm, all changes with statistical differences at 5% probability level. Other reductions of Z-ave were detected in NLC with 30% of FP, but were not so intense as in NLC 2, and were not statistically different.

The NLCs with 50% FP showed many changes of Z-ave and PDI during 60 days of storage, and it was not possible to evaluate the influence of the increment of HOSO, as well as the chemical composition of the hardfats of the systems. It was observed that the incorporation of 50% FP influenced negatively the stability of the developed systems. With the exception of NLC 13 that presented size between 200 and 300 nm without many variations over the time. The ZP of this system increased from -26 to -31 mV approximately, indicating that this system presents greater stability in relation to the others, also developed with 50% FP. The behavior of this system can be observed in Figure 4B, in the results concerning the particle number distribution as a function of diameter (Nαd). It is possible to verify only one peak, indicating that the system is monodisperse, with less tendency to phenomena of destabilization.

The variations in the Z-ave of nanostructured particles, as seen for NLCs developed with 30% FP, have been related to TAG polymorphic changes during storage. In a previous study, founded that systems composed of more heterogeneous LMs, due to the TAG

composition, presented lower Z-ave and the reductions of the Z-ave were verified after 30 days of storage (V. S. Santos, Braz, Silva, Cardoso, A., & Ribeiro, 2018).

Table 1

Mean hydrodynamic diameter (Z-ave), polydispersity index (PDI) and zeta potential (ZP) of the nanostructured lipid carriers (NLC) with 30 and 50% of free phytosterols (FP) evaluated after 24 h, 15 days, 30 days and 60 days of production

NLC/ Time	Z-ave (d.nm)	PDI	ZP (mV)	NLC/ Time	z-ave (d.nm)	PDI	ZP (mV)
24 h		**30% FP**		**24 h**		**50% FP**	
NLC 1	204.97±3.45[cdefB]	0.410±0.026[abcA]	-28.30±0.95[hijklmB]	NLC 8	342.10±30.00[abdcA]	0.406±0.055[bA]	-23.57±0.72[bcdefA]
NLC 2	250.00±7.30[aA]	0.358±0.027[abA]	-24.40±0.56[cdeB]	NLC 9	217.10±10.70[hiB]	0.481±0.086[abA]	-22.27±0.92[abA]
NLC 3	214.40±6.91[bcdB]	0.310±0.062[ghijA]	-27.70±0.98[ghijklmB]	NLC 10	254.53±05.49[efghiA]	0.362±0.071[bA]	-23.07±0.93[abcdA]
NLC 4	179.77±3.74[jkB]	0.321±0.025[efghijA]	-29.17±0.21[jklmnB]	NLC 11	282.95±23.35[bcdefghiA]	0.378±0.052[bA]	-25.57±0.32[fghA]
NLC 5	184.70±3.01[fghiB]	0.315±0.031[fghijB]	-28.37±0.49[ijklmB]	NLC 12	265.55±18.15[defghiA]	0.384±0.006[bA]	-26.37±0.85[hijA]
NLC 6	177.33±4.29[kB]	0.275±0.028[ijB]	-29.70±1.35[lmnB]	NLC 13	205.97±03.79[iA]	0.392±0.028[bA]	-26.47±0.42[hijA]
NLC 7	148.23±0.55[mB]	0.276±0.025[ijA]	-26.13±0.46[efgB]	NLC 14	246.00±26.30[efghiA]	0.343±0.059[bA]	-24.73±0.55[cdefghA]
15 days				**15 days**			
NLC 1	202.27±4.42[defgB]	0.411±0.004[abA]	-27.83±0.15[ghijklmB]	NLC 8	482.75±18.88[aA]	0.478±0.055[abA]	-26.60±0.62[hijA]
NLC 2	219.23±2.46[bB]	0.384±0.031[abcdefgA]	-29.27±0.49[klmnA]	NLC 9	385.29±34.29[abcdA]	0.359±0.039[bA]	-29.60±0.57[klmA]
NLC 3	212.87±2.10[bcdeB]	0.399±0.011[abcdeA]	-27.27±0.71[ghijkA]	NLC 10	281.60±10.18[cdefghiA]	0.473±0.126[abA]	-28.00±0.36[ijkA]
NLC 4	184.77±2.65[ijkB]	0.348±0.200[abcdefghijB]	-28.00±0.44[ghijklmA]	NLC 11	382.50±18.95[bcdefA]	0.404±0.007[bA]	-31.55±0.92[nB]
NLC 5	190.10±3.90[hijB]	0.360±0.007[abcdefghA]	-27.10±0.75[ghijA]	NLC 12	368.20±00.99[bcdefA]	0.438±0.089[abA]	-29.37±0.95[klmB]
NLC 6	182.27±1.21[ijkB]	0.305±0.016[ghijB]	-26.17±0.47[efghA]	NLC 13	230.20±03.47[ghiA]	0.439±0.030[abA]	-28.97±0.49[klB]
NLC 7	152.77±2.66[lmB]	0.268±0.010[jB]	-30.60±0.35[noA]	NLC 14	308.13±42.93[bcdefghA]	0.397±0.075[bA]	-31.13±1.31[lmnA]
30 days				**30 days**			
NLC 1	201.83±1.86[efghB]	0.411±0.006[abA]	-24.53±0.49[defA]	NLC 8	366.50±25.70[abcA]	0.390±0.028[bA]	-23.83±0.59[bcdefgA]
NLC 2	208.03±3.40[cdeB]	0.347±0.029[abcdefghijA]	-22.37±0.71[abcA]	NLC 9	326.05±23.12[bcdefgA]	0.387±0.025[bA]	-24.80±0.57[cdefghB]
NLC 3	212.77±1.23[bcdeB]	0.390±0.010[abcdefB]	-21.50±0.20[abB]	NLC 10	328.87±02.75[bcdefgA]	0.444±0.005[abA]	-25.73±0.59[fghA]
NLC 4	191.40±8.39[ghijB]	0.301±0.032[hijB]	-29.90±1.35[mnB]	NLC 11	245.60±21.92[efghiA]	0.466±0.031[abA]	-22.65±0.35[abcA]
NLC 5	190.47±4.80[ghijB]	0.338±0.008[bcdefghijB]	-20.30±1.04[aA]	NLC 12	251.00±00.89[efghiA]	0.612±0.096[aA]	-24.47±0.74[cdefghB]
NLC 6	187.43±2.53[ijkB]	0.345±0.020[abcdefghijB]	-27.27±0.67[ghijkA]	NLC 13	236.57±02.80[ghiA]	0.448±0.300[abA]	-29.97±0.35[klmnB]
NLC 7	161.47±1.00[lB]	0.330±0.014[defghijA]	-35.60±0.10[pB]	NLC 14	286.67±27.45[bcdefghiA]	0.354±0.041[bA]	-28.33±0.46[jkA]
60 days				**60 days**			
NLC 1	208.93±4.23[bcdeB]	0.423±0.006[aA]	-21.87±0.35[abA]	NLC 8	337.75±05.35[bcdeA]	0.419±0.057[bA]	-24.70±0.70[cdefghB]
NLC 2	206.93±4.8[1cdeB]	0.375±0.048[abcdefghA]	-21.43±0.55[abA]	NLC 9	375.65±25.10[abA]	0.456±0.095[abA]	-25.27±0.29[efghB]
NLC 3	214.87±2.32[bcB]	0.408±0.016[abcdA]	-32.50±0.70[oB]	NLC 10	294.85±29.75[bcdefghiA]	0.460±0.052[abA]	-21.07±0.75[aA]
NLC 4	186.77±3.36[ijkB]	0.331±0.023[cdefghijB]	-26.67±0.40[fghiB]	NLC 11	273.27±32.00[cdefghiA]	0.429±0.055[abA]	-25.10±0.52[defghA]
NLC 5	193.17±3.61[fghiB]	0.345±0.032[abcdefghijA]	-24.93±0.40[defB]	NLC 12	258.67±20.90[efghiA]	0.382±0.045[bA]	-23.27±0.64[bcdeA]
NLC 6	188.03±1.14[ijkB]	0.368±0.005[abcdefghB]	-23.27±0.67[bcdA]	NLC 13	239.07±04.27[fghiA]	0.485±0.050[abA]	-31.37±0.71[mnB]
NLC 7	160.60±0.95[lB]	0.341±0.020[bcdefghijA]	-26.37±0.61[efghiA]	NLC 14	270.10±32.57[cdefghiA]	0.355±0.021[bA]	-25.83±1.10[ghiA]

*Average of three replicates ± Standard Deviation; Different lowercase letters in the same column indicate significant difference related to the evaluation of each parameter (Z-ave, PDI and ZP) in comparison to the time of production of NLC (24h, 15, 30 and 60 days after processing), at the probability level (p≤0.05) according to the Tukey Test; Capital letters on the same line indicate a significant difference in probability (p≤0.05) according to the Tukey Test related to the comparison between the NLC produced with different levels of incorporation of the bioactive compound (30 and 50% of FP) for each parameter (Z-ave, PDI and ZP).
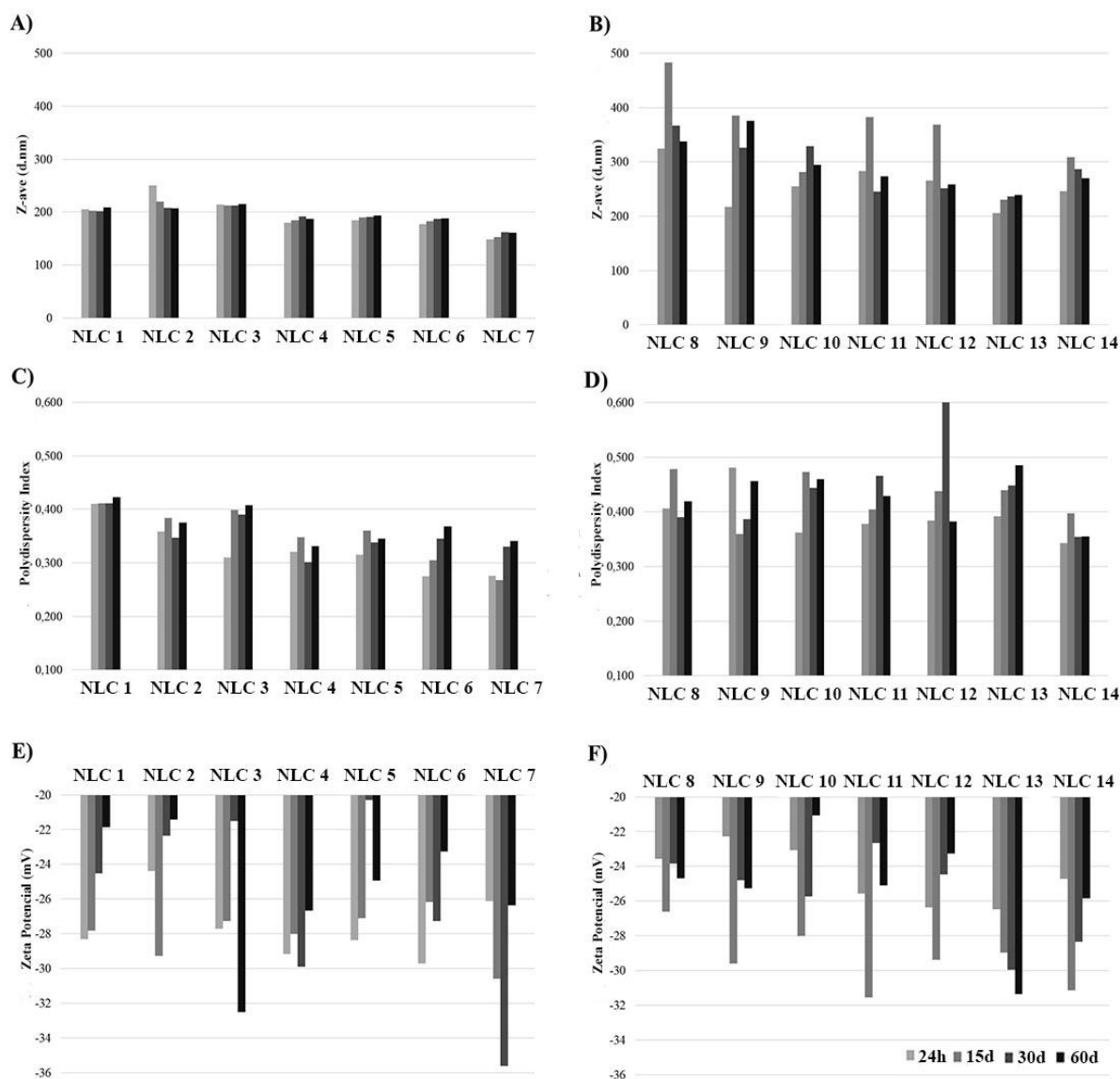
Fig. 2. Results represented graphically referring to the characterization of NLC obtained through DLS, evaluated after 24h, 15 days, 30 days and 60 days of processing, as: A) Mean hydrodynamic diameter, Z-ave (d.nm) of NLC with 30% of FP; B) Mean hydrodynamic diameter, Z-ave (d.nm) of NLC with 50% of FP; C) Polydispersity index of NLC with 30% of FP; D) Polydispersity index of NLC with 50% of FP; E) Zeta potential (mV) of NLC with 30% of FP; F) Zeta potential (mV) of NLC with 50% of FP.
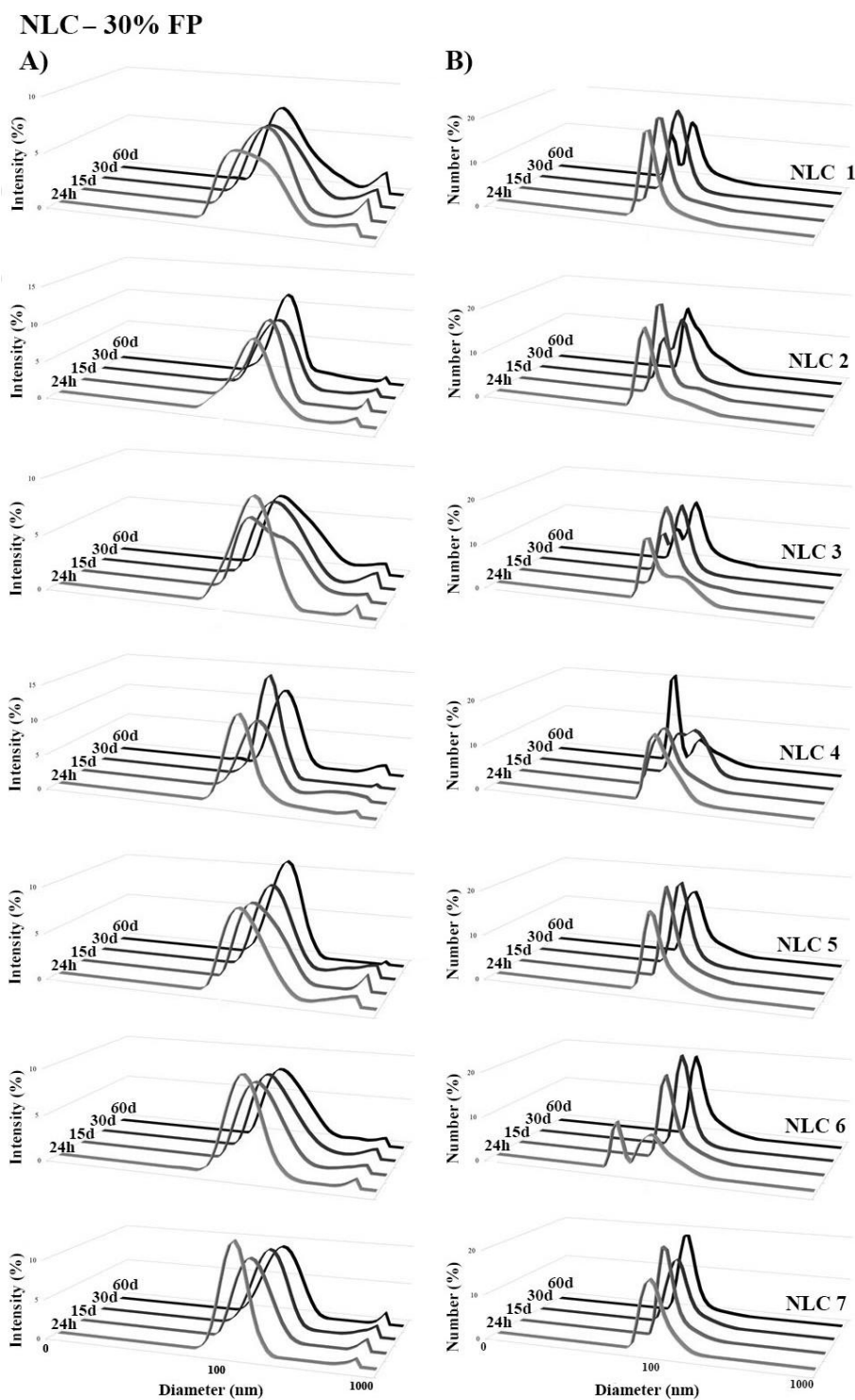
Fig. 3. Particle size distribution as a function of the intensity (A) and number (B) obtained from the dynamic light scattering (DLS) of the NLC with 30% of free phytosterols (FP) evaluated after 24 hours (24 h), 15 days (15d), 30 days (30d) and 60 days (60d) of production.

NLC - 50% FP
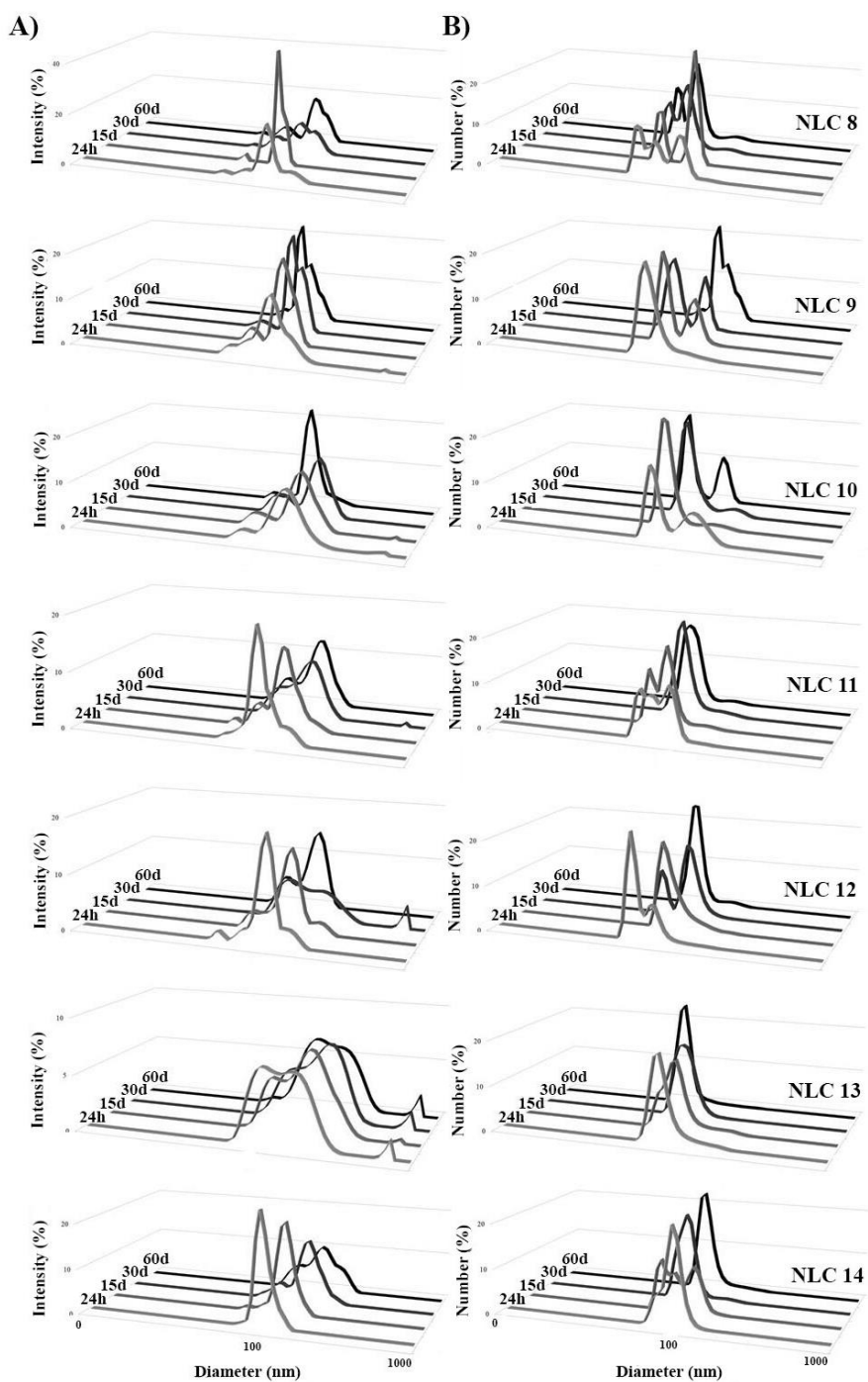
Fig. 4. Particle size distribution as a function of the intensity (A) and number (B) obtained from the dynamic light scattering (DLS) of the NLC with 50% of free phytosterols (FP) evaluated after 24 hours (24 h), 15 days (15d), 30 days (30d) and 60 days (60d) of production.

The authors reported that Z-ave reductions occur because of changes in the shape of lipid nanoparticles and correlated these reductions to polymorphic transitions of the lipid content to a more stable form ($\alpha \rightarrow \beta' \rightarrow \beta$). Thus, after the emulsification process, the lipids are dispersed in the water in droplets form surrounded by the emulsifier. After the crystallization of the lipid fraction, solid and spherical nanoparticles are obtained, nanostructured by TAGs in the most unstable polymorphic form (α-form). However, during storage, due to the polymorphic transitions of TAGs to the more stable form (β-form), the spherical nanoparticles become elongated, in platelets forms (Bunjes & Unruh, 2007; Salminen, Helgason, Kristinsson, Kristbergsson, & Weiss, 2013). The ability of the lipids to crystallize in different forms will be better elucidated in the topic related to XRD.

Additionally, according to Kuntsche, Horst, and Bunjes (2011), the NLC can present different forms, due to the polarity or differentiated solubility of the loaded compound. Nanoparticles of ubiquinone (vitamin Q10) consisting of tripalmitin presented a "spoon" format. This format was associated with the polymorphic transition of tripalmitin to the β-form, becoming elongated in the platelet form causing expulsion of vitamin Q10. However, vitamin Q10 was retained at one end of the structure, protected by the emulsifier layer, conferring this differentiated "spoon" shape to the nanosystems.

Thus, the large variations observed for NLC with 50% FP, may be related to the expulsion of the bioactive compound, with consequent contact of FP with the aqueous fraction. No detailed studies in the literature have been found elucidating the crystalline behavior of FP in nanostructured systems, being necessary the use of microscopic techniques to adequate elucidate this behavior. A recent study states that FPs dispersed in an aqueous phase in colloidal form can act as emulsion stabilizers through a mechanism known as Pickering, ie, FP crystals act on the coating of emulsified lipid droplets avoiding flocculation, through formation of fibrillary crystalline networks, providing gell-like properties to this systems (F. Liu & Tang, 2014).

3.2. Melting behavior of free phytosterols, lipid matrix, and Lipid nanoparticles

The evaluation of the melting thermal behavior was performed in the lyophilized NLC. For the FP and LM, the same thermal treatments of crystallization (5 °C/24h) and stabilization (25 °C/24h) of the NLC were carried out allowing the comparison between the systems in macro-scale and the nanostructured ones. The results obtained for the melting thermal behavior of FL, LM, and NLC are shown in Table 2 and the respective thermograms are shown in Figure 5. The parameters obtained were initial melting temperature (T_{im}), maximum peak temperature (T_{max}), final melting temperature (T_{off}), and the melting enthalpy (ΔH_m).

The FP showed only one melting peak at 130.29 °C T_{max} and melting range from 126.12 °C (T_{im}) to 136.14 °C (T_{off}), indicating that all FP components have similar melting properties (Figure 3C). As described in the materials topic, the FP used in this study are food grade and have a mixture of phytosterols in their composition. When comparing the thermal behavior of the FP mixture with the components in the purified form, we can verify that the melting point of the pure components is higher, being 141.60 °C for β-sitosterol (Villaseñor, Angelada, Canlas, & Echegoyen, 2002), 169.20°C for stigmasterol (Gomes Silva, Santos, Fernandes, Calligaris, Santana, Cardoso, et al., 2018) and 140.50 °C for campesterol (LI, HO, LI, TAO, & TAO, 2000).

Even though, the FP melting temperature is still high in relation to the melting properties of fats and oils, commonly used in food production, a characteristic that supports the great technological challenge of application of FP in food. In addition to this, FLs are lipophilic compounds with high water insolubility, which is another limiting factor in food use. As reported by Hariklia Vaikousi, Athina Lazaridou, Costas G. Biliaderis, and Zawistowski (2007) in their studies, the direct delivery of FP in food is considered a technological challenge, since the high crystallinity/insolubility can often become restrictive factors for the stability of several products. The great interest in using phytosterols in the free form is related to its higher nutritional functionality in reducing blood levels of cholesterol when compared to esterified ones (Hayes, Pronczuk, Wijendran, & Beer, 2002).

Table 2.

Melting behavior of the lipid matrices (LM) and NLC with 30 and 50% free phytosterols (FP), evaluated according to the parameters of initial melting temperature (T_{im}), maximum melting peak temperature (T_{max}), final melting temperature (T_{off}) and melting enthalpy (ΔH_m)

| Parameters	Peak	T_{im} (°C)	T_{max} (°C)	T_{off} (°C)	ΔH_m (J/g)		T_{On} (°C)	$T_{Máx}$ (°C)	T_{off} (°C)	ΔH_m (J/g)
FP	1	126.12±0.03	130.29±0.02	136.14±0.25	-16.61±0.32		-	-	-	-
			30% FP					**30% FP**		
LM 1	1	58.46±0.11	66.74±0.02	79.15±1.00	-70.03±3.18	NLC 1	65.13±0.03	70.08±0.00	89.73±0.43	-71.64±0.05
LM 2	1	50.97±0.04	59.57±0.00	75.72±0.94	-89.50±1.26	NLC 2	61.66±0.02	65.92±0.00	76.12±0.66	-40.11±0.13
	2	-	-	-	-		91.86±0.08	94.87±0.07	107.83±1.72	-4.24±0.49
LM 3	1	52.34±0.06	63.75±0.00	78.02±1.07	-79.78±0.52	NLC 3	64.89±0.03	68.68±0.00	80.68±1.12	-60.29±0.55
	2	-	-	-	-		88.56±0.01	93.55±0.00	117.93±1.36	-11.11±0.36
LM 4	1	55.59±0.02	64.19±0.00	76.59±0.24	-52.44±0.53	NLC 4	60.41±0.01	66.35±0.00	81.39±1.24	-37.34±0.37
	2	-	-	-	-		98.18±0.01	99.09±0.00	115.95±1.13	-5.67±0.45
LM 5	1	49.43±0.06	57.69±0.00	72.89±0.33	-43.87±0.82	NLC 5	55.91±0.06	60.71±0.00	88.56±0.63	-42.03±0.64
	2	-	-	-	-		127.33±0.01	127.73±0.00	143.59±0.56	-10.71±0.38
LM 6	1	52.85±0.06	62.23±0.00	77.41±0.53	-51.42±1.64	NLC 6	56.11±0.06	62.65±0.00	86.57±1.19	-15.47±0.51
LM 7	1	103.28±0.00	103.37±0.00	139.03±0.25	-16.67±0.57	NLC 7	44.73±0.56	50.06±0.64	59.51±0.31	-1.22±0.79
	2	-	-	-	-		66.43±0.06	77.10±0.02	95.48±0.56	-0.49±0.01
	3	-	-	-	-		106.54±0.04	126.87±0.04	144.75±0.25	-1.89±0.09
			50% FP					**50% FP**		
LM 8	1	57.39±0.06	65.37±0.00	81.76±0.56	-45.57±0.82	NLC 8	65.64±0.02	67.98±0.00	91.37±1.47	-44.9±1.19
		94.54±0.16	108.00±0.02	126.23±0.24	-5.27±0.46		-	-	-	-
LM 9	1	49.72±0.14	58.37±0.04	74.38±0.25	-50.17±0.16	NLC 9	56.84±0.02	62.31±0.00	79.06±0.64	-29.75±0.32
	2	91.23±0.62	108.15±0.02	126.31±1.56	-6.84±0.53		126.66±0.00	126.85±0.00	139.78±0.38	-11.77±0.17
LM 10	1	51.01±0.07	62.79±0.00	77.41±0.14	-48.30±0.78	NLC 10	60.63±0.10	65.23±0.00	91.91±1.59	-38.43±1.02
	2	93.97±0.20	109.03±0.04	127.43±3.1	-7.31±0.6		-	-	-	-
LM 11	1	51.01±0.09	59.99±0.00	73.30±0.32	-9.69±0.26	NLC 11	59.73±0.10	65.36±0.00	81.76±0.80	-35.66±0.77
	2	87.71±0.14	110.51±0.02	134.8±0.25	-14.06±0.35		102.01±0.01	102.44±0.00	116.90±0.75	-7.15±0.37
LM 12	1	47.05±0.09	53.76±0.02	68.21±0.07	-14.87±0.48	NLC 12	55.44±0.06	57.72±0.00	76.29±0.81	-8.79±0.28
	2	87.70±0.10	107.57±0.00	129.50±1.18	-8.29±0.09		104.39±0.00	105.34±0.00	126.80±0.85	-14.89±0.65
LM 13	1	51.80±0.03	58.40±0.00	71.69±0.26	-11.22±0.15	NLC 13	57.64±0.02	62.65±0.00	80.35±0.50	-10.72±0.16
	2	93.05±0.12	112.77±0.02	137.08±2.11	-13.13±0.5		-	-	-	-
LM 14	1	49.34±0.16	55.11±0.02	75.88±1.35	-7.22±0.57	NLC 14	48.05±0.06	55.20±0.00	71.03±0.63	-3.03±0.02
	2	89.81±0.04	108.36±0.02	129.46±0.49	-6.79±0.12		79.73±0.15	102.03±0.04	115.95±1.04	-4.07±0.29
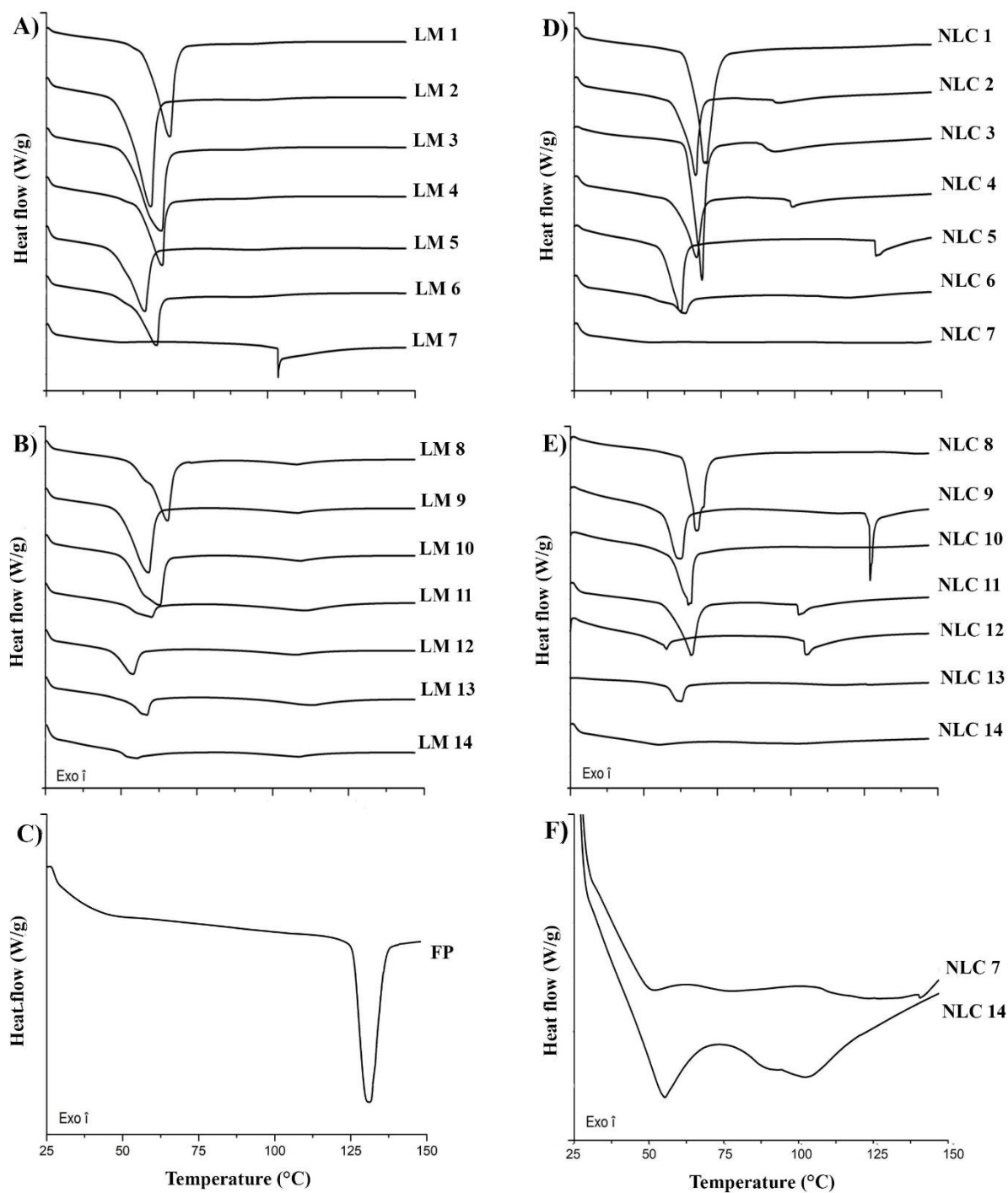
Fig. 5. Curves of the melting behavior of: A) Lipid matrices (LM) containing 30% of free phytosterols; B) Lipid matrices (LM) containing 50% of FP; C) Free Phytosterols (FP); D) NLC containing 30% of FP; E) NLC containing 50% of FP; F) Zoom of the melting curves of the NLC 7 and NLC 14.

The authors state that FPs compete directly with cholesterol in intestinal micelles, although the phytosterols esters are more dispersed in oils and fats and to be absorbed need to be first the hydrolyzed. Thus, aiming at the greater functionality of FP, the incorporation into NLC may be an alternative to allow the application of FP in food.

LMs developed with 30% FP presented only one melting peak, with T_{max}. ranging between ~57 and ~67 °C, as can be seen in Figure 5A. This behavior indicated the complete incorporation and solubilization of FP in these LM. Thus, it can be affirmed that the crystallinity of FP was reduced, being more pronounced in LM composed by the mixture of hardfats and HOSO. For the LM 7 formulated only with liquid lipid (70% HOSO) the T max was much higher than in the other LM (T max = 103.37 ° C) (Table 2).

Two melting peaks were observed for all LMs containing 50% FP, the first was found in the region of 47 to 82 °C, probably referring to the melting of the hardfat, HOSO and FL mixtures. While the second peak was found between 87 and 127 ° C, with a less intensity than the first, as can be observed in Figure 5. This second peak can be related to the melting of the fraction of FP that was not incorporated in LM, probably due to solubility (Figure 5B).

In addition, changes in peak intensities were observed with the increasing of HOSO from 20 to 40%, in both LM with 30 and with 50% FP incorporation. This effect can be observed through the ΔH_m of LM, systems containing 20% HOSO since they required higher energies for the phase transition. For LMs with 30 and 50% FP, were found values of approximately -70 to -89 J/g and -45 to -50 J/g for incorporation of 20% HOSO and -43 to -53 and -9 to -14 J/g to 40% HOSO, respectively. This effect was even higher for LM developed with 70% (LM 7) and 50% (LM 14) of HOSO with ΔH_m of -16.67 and -7.22 J/g, respectively. It was verified that the HOSO contributed to the reduction of the crystallinity of these LMs, developed with components of high melting points, like FP. Also, it should be noted that all the developed systems showed a melting temperature over to the body temperature, allowing the use of all LM for NLC application. This indication is based on their ability to maintain the structural integrity of the particles during the course of the gastrointestinal tract, according to recommendations found in the literature (P. Severino, Andreani, Macedo, Fangueiro, Santana, Silva, et al., 2012; Sharma, Diwan, Sardana, & Dhall, 2011; Tamjidi, Shahedi, Varshosaz, & Nasirpour, 2013). Additionally, as seen in the thermal behavior of LM 7 and 14, the lipophilic bioactive compound, such as FP, which have a high melting point, can also be used as solid

lipid to compose LM of NLC (Table 2). It presents differentiated properties of fusion, such as the high thermal resistance (above 100 °C), allowing the use of these LM for the development of NLC for application in food which will be thermally processed at high temperatures.

Comparing the melting behavior of the NLCs with those of the correspondent LMs, it was possible to verify that all the NLCs had higher T_{max} than the LMs. This behavior was also observed in our previous studies (V. S. Santos, Braz, Silva, Cardoso, A., & Ribeiro, 2018; V. S. Santos, Ribeiro, Cardoso, & Santana, 2018) and also by other authors (Tamjidi, Shahedi, Varshosaz, & Nasirpour, 2013). In this way, we can affirm that the developed NLC presented higher thermal resistance than their respective LM. In other words, the nanostructured systems required more energy to the phases transition (solid-liquid) than the lipid systems in macroscale. It is suggested that in NLC the TAGs constituents of the lipid fraction were organized in a more compact crystalline structure conferring greater thermal resistance to the nanoparticles. In contrast, in the macroscale, TAGs have larger spaces for their organization and formation of less compact crystalline networks.

In Figure 5D it is possible to visualize the melting thermal behavior of NLCs developed with 30% FP. It was noted that NLC 1 and NLC 6 showed only one melting peak (T max of 70.08 °C and 62.65 °C, respectively), indicating that all components of these nanoparticles exhibited similar melting behavior. However, in the other NLCs developed with 30% FP, a further melting peak was verified. It is suggested that in NLC 2, 3 and 4 the second peak is related to the melting of nanoparticles formed only by the FP covered by the emulsifier. Another suggestion related to the second peak would be the fusion of nanoparticles of smaller sizes present in the system, which require higher temperatures for the phase transition. However, in NLC5 it is suggested that undesired expulsion of the bioactive compound occurred, since the T max of this peak (127.73 °C) is very close to the FP T max (130.29 °C). In NL C7 developed only with FP and HOSO, 3 melting peaks with low ΔH_m values were verified, as can be seen in Figure 5F. These peaks indicate that formation of FP particles with different thermal melting behaviors occurred, which may be related to the Z-ave of the particles and not the expulsion of the FP, since neither a pronounced peak in the region of 130 °C was found.

In this way, it can confirm the possible formation of nanoparticles composed only by FP, suggested in the first hypothesis, or even the presence of FP in suspension, in the case of NLC 5. However, these behaviors did not compromise the physical stability of the systems

during 60 days of storage as previously discussed. It should be noted that the best Z-ave, PDI and ZP were obtained for NLC with 30% FP (Figure 2). Thus, NLCs developed with CA, CR and HOSO showed very promisingly for the delivery of 30% FP in food.

Another point to highlight in this study was the eutectic effect observed in LM and NLC developed with the mixture of CA and CR in both incorporation levels of 30% and 50% of FP. This behavior was also verified in our previous studies, where LM (V. S. Santos, Santana, Braz, Silva, Cardoso, & Ribeiro, 2018)and NLC (V. S. Santos, Braz, Silva, Cardoso, A., & Ribeiro, 2018) were developed with CA, CR, and HOSO, but without the incorporation of the bioactive compound. The eutectic effect was related to incompatibility between the chain sizes of the saturated TAG molecules, that was strengthened by the presence of unsaturated molecules in the systems. The results obtained in these studies showed that the eutectic effect has positively contributed to the development of NLC, reducing crystallinity and favoring the reduction of Z-ave (V. S. Santos, Braz, Silva, Cardoso, A., & Ribeiro, 2018).

In the present study, the eutectic effect observed for the solid lipids mixture in the formulations did not contribute to the incorporation of FP into the NLC. As can be observed in Figure 5E, NLC 9 with 50% FP, by the presence of two melting peaks, with the second peak being quite evident and related to the expulsion of the bioactive compound, with the T_{max} of 126.85 °C, very close to the value obtained for the T_{max} of the FP of 130.29 °C. In the NLCs developed with 50% FP with the isolated use of the CA or CR (NLC 8, NLC 10 and NLC 13) only one melting peak was verified. Proving that the use of these hardfats isolated is more effective for the development of NLC with 30 and 50 % FP. However, in general, NLCs developed with 50% FP presented many changes of Z-ave, PDI, and ZP, as previously seen in the results obtained through DLS. However, it is worth mentioning that the thermal behavior of the NLC 13, composed of 10% CR and 40% of HOSO, evidenced the best system to carry 50% FP even after 60 days of the physical stability evaluation.

3.3. Microstructure of lipid matrices

The evaluation of the microstructure of LM contributes to the understanding of the crystallinity of the systems since the images can show in detail the distribution of the crystals, including morphological and structural characteristics (Ana Paula B. Ribeiro, Grimaldi, Gioielli, & Gonçalves, 2009). In Table 3 are the mean diameter (D) of the crystals and

crystallized area of LM used in the development of NLC and in Figure 6 it is possible to visualize the images obtained through PLM. The D of the LM crystals developed with 30 and 50% FP varied between 1.29 and 2.45μm and 1.35 and 2.05μm, respectively. Larger crystals were observed in LM 7 developed only with FP and HOSO, where it is possible to verify the characteristic crystals of FP in the form of platelets and needles.

The percentage of crystallized LMs ranged from 2.42 to 15.47% for LMs developed with 30% FP and 2.08 to 14.04% for LMs composed of 50% FP (Table 3). As can be seen, the presence of the FP collaborated to increase the crystallinity of the LMs and the difference between the crystallinity of the LMs with 30 and 50% of FP is higher than 10%, being visually perceptible that the formation of the crystals is different in these LMs. The LM with the highest amount of HOSO (70%), as said before, presented more spaces between the FP, being possible to observe crystals in the form of platelets and needles, whereas with the reduction of HOSO in LM to 50%, the crystalline network formed is totally different, and it is possible to verify the formation of a continuous crystalline network with smaller and more uniform crystals. It was observed that the crystalline networks formed in LM 1, 2 and 3 developed with 20% of HOSO, were homogeneous and dense. It was observed that the increase of HOSO (40%) reduced the crystallized area and it was possible to verify the presence of needle-shaped crystals characteristic of FP in LM 4, developed with CA only. In addition, it was possible to verify that the increment of CR increased the crystallized area in both systems (Figure 6).

Table 3
Mean diameter and the crystallized area of the lipid matrices (LM) developed with free phytosterols (FP), composed by fully hydrogenated canola (CA) and/or crambe (CR) oils, and/or high oleic sunflower oil (HOSO)

LM	Diameter of crystals (μm)	Crystallized Area (%)	LM	Diameter of crystals (μm)	Crystallized Area (%)
30% FP			50% FP		
LM 1	1.63±1.26	10.54±0.50	LM 8	1.37±1.13	7.76±1.11
LM 2	1.97±1.53	13.49±1.61	LM 9	1.90±1.59	12.13±1.40
LM 3	1.93±1.50	15.47±0.90	LM 10	1.35±1.05	9.06±0.34
LM 4	1.29±1.29	6.34±2.04	LM 11	1.59±1.67	2.08±0.60
LM 5	1.38±1.02	9.50±1.08	LM 12	1.96±1.69	13.88±0.60
LM 6	1.86±1.56	11.10±0.13	LM 13	2.05±2.15	12.98±0.88
LM 7	2.45±2.60	2.42±0.45	LM 14	1.86±1.85	14.04±3.46

A) 30% FP
B) 50% FP

LM 1   **LM 4**   **LM 8**   **LM 11**

LM 2   **LM 5**   **LM 9**   **LM 12**

LM 3   **LM 6**   **LM 10**   **LM 13**

LM 7   **LM 14**
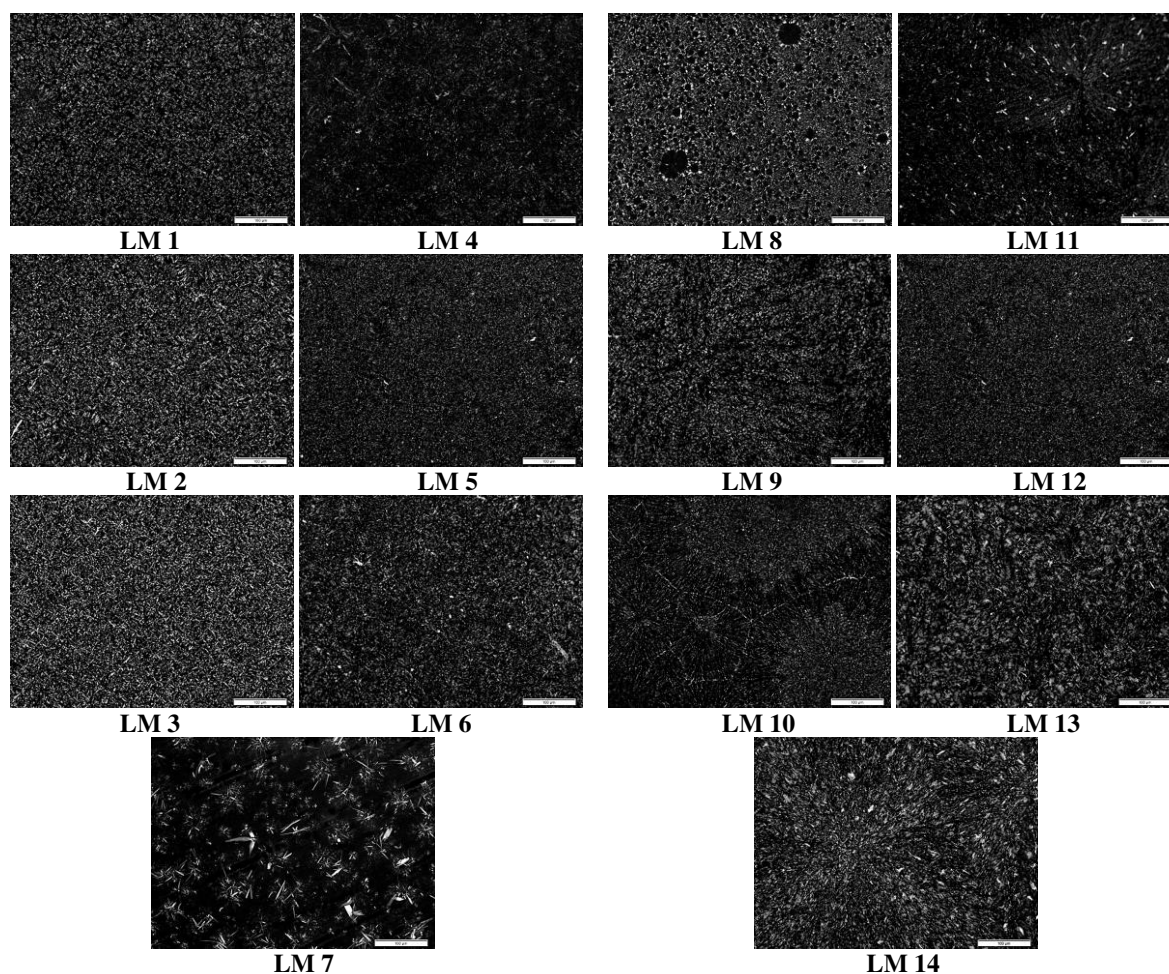
Fig. 6. Polarized light microscopy images of lipid matrices (LM) composed of high oleic sunflower oil (HOSO) and fully hydrogenated canola (CA) and/or crambe (CR) oils, with incorporation of: A) 30% of free phytosterols (FP) and B) 50% of free phytosterols (FP), obtained after thermal treatment (crystallization at 5 °C/24 h followed by crystalline stabilization at 25 °C/24 h) with increase of 200X.

In LMs formulated with 50% FP, the images revealed well differentiated crystalline formations in all systems. It was not possible to establish a relationship between the components and the crystalline forms observed. It only can be said that in the presence of 50% FP the use of the mixture of CA and CR favored the development of more crystalline LM than when used separately. More homogeneous Z-ave and crystalline networks were obtained in the presence of 20 and 40% HOSO, of 1.90 and 1.96 μm, respectively. This strong crystalline behavior of the LM developed with the hardfat mixture, is directly related to the expulsion of the FP, as verified in the thermal behavior melting curves discussed in the previous topic. It can be stated

that the use of CA and CR separately in NLC formulations for incorporation of 30 and 50% FP favored the incorporation of the bioactive compounds.

3.4. X-Rays Diffraction

Lipids have the ability to crystallize in different crystalline structures, resulting in different molecular packagings. According to the current polymorphic nomenclature for TAGs, there are three specific types of sub-cells referring to polymorphs α, β' and β, denominated according to the classification of Brava Networks as hexagonal, perpendicular orthorhombic, and triclinic crystals, respectively. In addition, lipids exhibit monotropic polymorphic transitions, which is a process of irreversible transition from less stable polymorphic form to the more stable ($\alpha \rightarrow \beta' \rightarrow \beta$) (Martini, Awad, & Marangoni, 2006; Sato, 2001). These forms exhibit characteristic diffraction peaks, with the α-form having a single diffraction peak at 4.15Å, the β'-form is characterized by two diffraction lines at 3.8 and 4.2Å, and the β-form is related with a higher intensity line at 4.6Å, and lower intensity peaks at 3.7 and 3.8Å (Rousseau & Marangoni, 2002).

In this study, in order to verify the crystalline behavior of LM, NLC and the incorporated bioactive compound (FP), the XRD analysis was applied to obtain the diffraction patterns of each sample. For the FP, a series of peaks was identified, with theta-2theta ($\theta:2\theta$) of: 5.20, 12.18, 12.80, 15.08, 15.80, 16.92, 17.86, 18.64, 19.70, 20.88, 21.82, 22.96, 24.06 and 25.28. In addition, in a recent study conducted by our research group, it was found that FP had a very similar diffraction pattern to the pure sterols (Gomes Silva, et al., 2018). In this way, it was verified that β-sitosterol, the main sterol of the FP mixture, crystallizes in the simple orthorhombic form, according to the crystallographic information verified through the Structural Database-CSD, with registration in CCDC 933712.
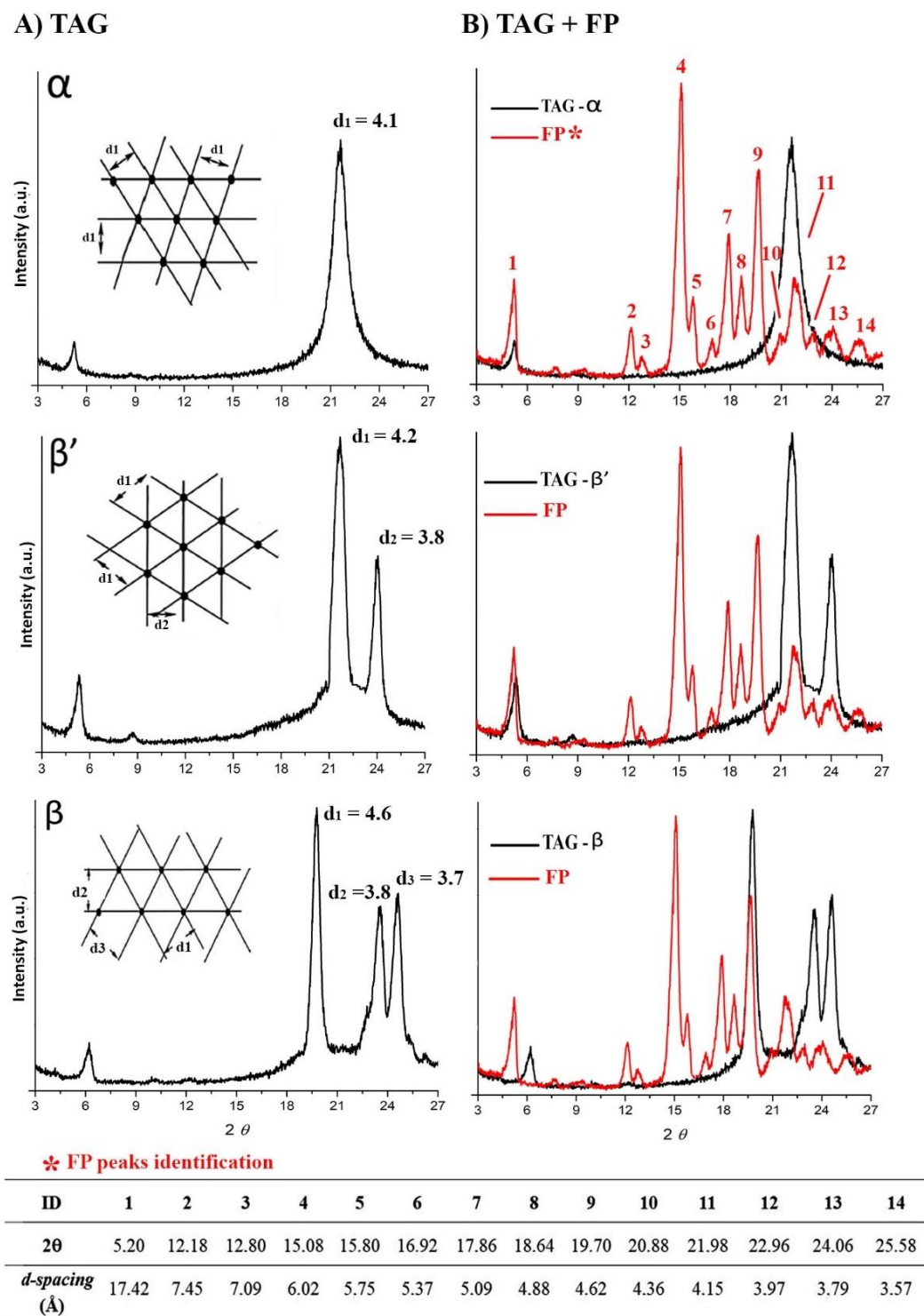
**Fig. 7.** Schematic representation of: (a) X-ray diffraction patterns (XRD) for triacylglycerols (TAG) in the most commonly polymorphic forms α, β' and β; B) Experimental XRD patterns and peak identification of the free phytosterols (FP) with the peaks overlaping each TAG polymorphic form.

The crystalline structure of FP is very similar to the β'-form of TAG, which is classified as perpendicular orthorhombic, differing only in the angles of crystallization and in the deformations of the unit cell, where the simple orthorhombic form is deformed on one side of the square and the orthorhombic perpendicularly shows deformation along the diagonal of the base square. For this reason, some FP peaks showed a very similar diffraction pattern to those used for the identification of the polymorphs in the TAG. It is possible to observe in Figure 7 a schematic representation of the 3 most common polymorphs of the TAG (Figure 7A) and the peaks of XRD of the FP with the identification of each peak and their respective values of 2θ and d-spacing (Figure 7B). Thus, it was possible to visualize the overlapping of the FP diffractograms with each of the α, β' and β forms characteristic of the TAGs. The diffraction peaks of FP that showed overlap with the TAG peaks were peaks 9, 11, 12 and 13 with d-spacing of 4.62, 4.15, 3.97 and 3.79Å, respectively (Figure 7).

In this way, the possible identifications of the crystalline forms of the TAGs with the respective overlapping peaks of the FP were performed, as described in Table 4.

It was observed that in the diffraction patterns of LM and NLC the peaks related to FP had lower intensities, as shown in Figure 8. It is suggested that the intensity of the FP diffraction peaks was reduced by the incorporation, solubilization and co-crystallization effects of the FP with the lipid materials. Moreover, no diffraction lines were observed at 4.15Å, referring to the α form of the TAG and the FP peak 11.

The results showed that both LM and NLC presented possible crystalline forms of intermediate crystallization form (β'), in the most stable form (β) and the mixture of β' and β forms, as can be seen in Table 4. Furthermore, LM developed only with HOSO and 30 and 50% FP, with LM 7 and LM 14, respectively, presented similar diffraction patterns. It was observed that, when compared to the respective NLC, it is possible to observe a greater distance from the baseline, which may indicate a lower crystallinity when nanostructured (Figure 8).

Table 4
Short spacings and peak intensities of the diffractograms obtained for lipid matrices (LM) and nanostructured lipid carriers (NLC), developed with free phytosterols (FP), and polymorphic forms related to the TAG crystalline behavior

Samples	Short spacings (Å)				Polymorphic form of
	4.6	4.2	3.8	3.7	TAG
Lipid matrix - 30% FP					
LM 1	4.60(TAG*)/4.62(FP**)	-	3.89(TAG)/3.97(FP)	3.73(TAG)/3.79(FP)	β
LM 2	4.63(TAG)/4.62(FP)	4.22(TAG)	3.81(TAG)/3.97(FP)	3.73(TAG)/3.79(FP)	β'+β
LM 3	4.68(TAG)/4.62(FP)	4.21(TAG)	3.81(TAG)/3.97(FP)	-	β'+β
LM 4	4.60(TAG)/4.62(FP)	-	3.86(TAG)/3.97(FP)	3.71(TAG)/3.79(FP)	β
LM 5	4.61(TAG)/4.62(FP)	4.20(TAG)	3.89(TAG)/3.97(FP)	3.70(TAG)/3.79(FP)	β'+β
LM 6	4.64(TAG)/4.62(FP)	4.20(TAG)	3.80(TAG)/3.97(FP)	-	β'+β
LM 7***	-	-	-	-	-
Lipid matrix - 50% FP					
LM 8	4.61(TAG)/4.62(FP)	-	3.87(TAG)/3.97(FP)	3.73(TAG)/3.79(FP)	β
LM 9	4.66(TAG)/4.62(FP)	4.20(TAG)	3.84(TAG)/3.97(FP)	-	β'+β
LM 10	4.66(TAG)/4.62(FP)	4.20(TAG)	3.81(TAG)/3.97(FP)	-	β'+β
LM 11	4.61(TAG)/4.62(FP)	-	3.88(TAG)/3.97(FP)	3.71(TAG)/3.79(FP)	β
LM 12	4.60(TAG)/4.62(FP)	-	3.87(TAG)/3.97(FP)	3.70(TAG)/3.79(FP)	β
LM 13	4.65(TAG)/4.62(FP)	4.20(TAG)	3.80(TAG)/3.97(FP)	-	β'+β
LM 14***	-	-	-	-	-
Lyophilized nanostructured lipid carriers - 30% FP					
NLC 1	4.63(TAG)/4.62(FP)	-	3.89(TAG)/3.97(FP)	3.73(TAG)/3.79(FP)	β
NLC 2	4.64(TAG)/4.62(FP)	-	3.89(TAG)/3.97(FP)	3.73(TAG)/3.79(FP)	β
NLC 3	-	4.21(TAG)	3.80(TAG)/3.97(FP)	-	β'
NLC 4	4.64(TAG)/4.62(FP)	-	3.88(TAG)/3.97(FP)	3.74(TAG)/3.79(FP)	β
NLC 5	4.63(TAG)/4.62(FP)	-	3.86(TAG)/3.97(FP)	3.72(TAG)/3.79(FP)	β
NLC 6	-	4.20(TAG)	3.80(TAG)/3.97(FP)	-	β'
NLC 7***	-	-	-	-	-
Lyophilized nanostructured lipid carriers - 50% FP					
NLC 8	4.66(TAG)/4.62(FP)	-	3.89(TAG)/3.97(FP)	3.73(TAG)/3.79(FP)	β
NLC 9	4.62(TAG)/4.62(FP)	-	3.88(TAG)/3.97(FP)	3.72(TAG)/3.79(FP)	β
NLC 10	4.66(TAG)/4.62(FP)	4.20(TAG)	3.81(TAG)/3.97(FP)	-	β'+β
NLC 11	4.62(TAG)/4.62(FP)	-	3.88(TAG)/3.97(FP)	3.72(TAG)/3.79(FP)	β
NLC 12	4.66(TAG)/4.62(FP)	4.20(TAG)	3.81(TAG)/3.97(FP)	-	β'+β
NLC 13	4.66(TAG)/4.62(FP)	4.20(TAG)	3.81(TAG)/3.97(FP)	-	β'+β
NLC 14***	-	-	-	-	-

*Short spacings characteristic of the triacylglycerols; **Short spacings characteristic of the free phytosterols; ***Sample does without solid lipids, with only HOSO and FP.
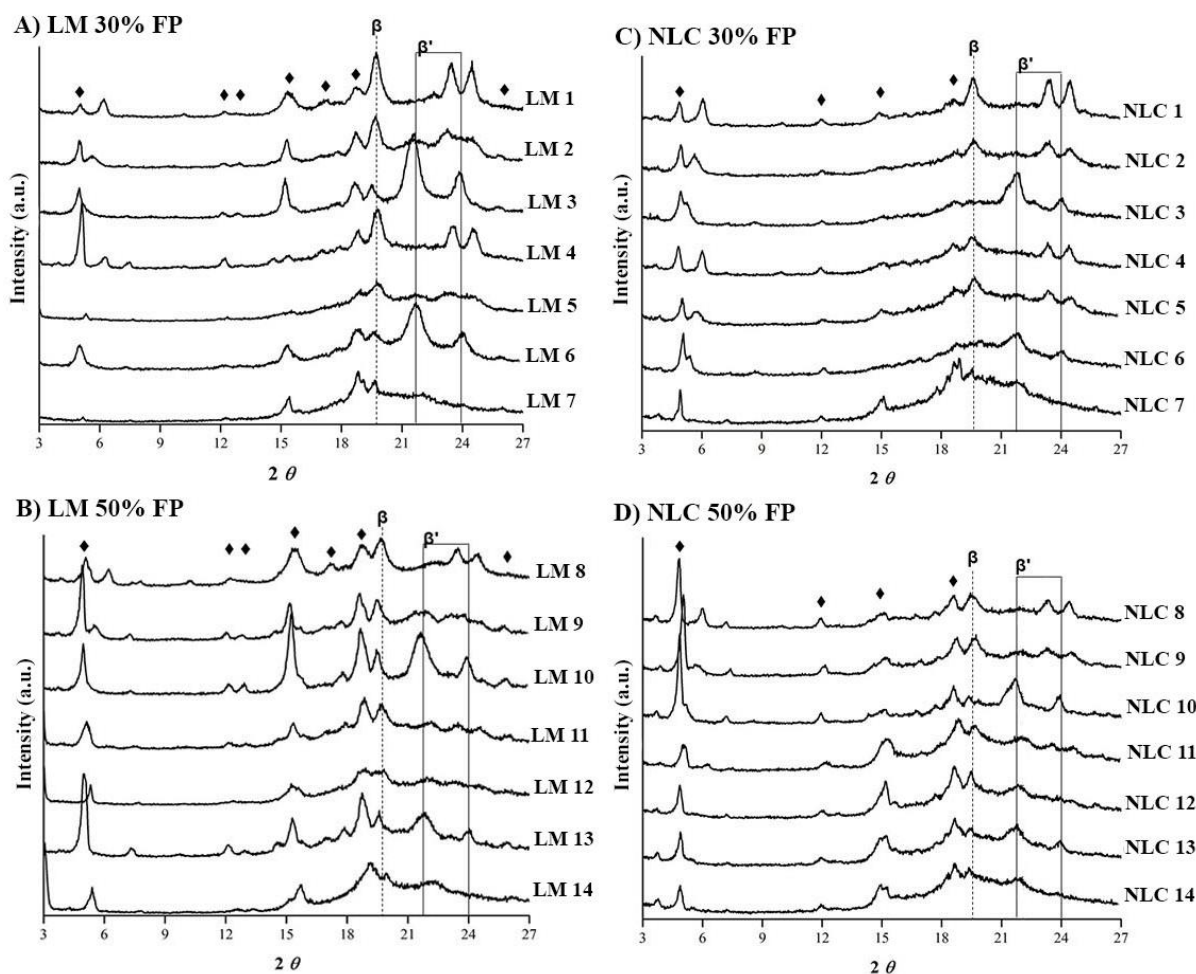
Fig. 8. X-ray diffraction patterns from: A) Lipid matrices (LM) developed with the fully hydrogenated canola (CA) and/or crambe (CR) oils, and/or high oleic sunflower oil (HOSO) containing 30% of free phytosterols (FP); B) LM developed with CA and/or CR, and/or HOSO containing 50% of FP; C) Nanostructured lipid carriers (NLC) with 30% of FP; D) NLC with 50% of FP.

LMs with the incorporation of FP in the proportions of 30 and 50% were found to have the same crystalline forms. Differing only LM 5 and LM 12, composed of the mixture of CA and CR, where the presence of 50% FP favored the polymorphic transition from $\beta' + \beta$ to β (Table 4). Comparing the NLCs with 30% FP with the respective LM, varying only in the composition of the solid lipids, it was observed that in the NLC 1 and NLC 4 compounds only by CA the β-form was maintained in NLC 3 and NLC 6 composed only with CR the polymorphic transitions were delayed from $\beta' + \beta$ to β'. In the NLC 2 and NLC 5 composed by the mixture of CA and CR, the polymorphic transition was accelerated to β. According to Oliveira et al. (2015) the polymorphic habit of CA is the β form and according to A. P. B.

Ribeiro, Basso, and Kieckbusch (2013) the polymorphic habit of CR is the mixture of crystals in forms β' and β. Thus, it can be affirmed that these results, even with the interference of the FP peaks, have agreed with the crystallization behavior of the lipid raw materials used in the formulation of LM and NLC. It should be noted that NLC 3 and NLC 6 will probably undergo polymorphic transition, presenting the mixture of $\beta' + \beta$ forms, according to the polymorphic habit of CR.

Similar results regarding the composition of the hardfat were found for NLC containing 50% FP, NLC 10, NLC 12 and NLC 13, composed of CR, CA + CR and CR presented a mixture of crystals in the $\beta' + \beta$ forms, whereas the NLC 8, NLC 9 and NLC 11 composed of CA, CA + CR and CA showed crystals in the most stable β-form. The use of CR enabled the development of NLC with the β-form and the mixture of polymorphic forms β' and β, a feature not found in our previous studies with soy-based raw materials. In this way, it can extend the applications in foods, as for example in margarines or spreads, where the form β' is desirable. According to Sato (2001), the crystals in the form β' contribute to the formation of softer fats, with good aeration and properties of creaminess.

4. Conclusion

The LMs developed with the CA and CR and with HOSO presented promising for the development of NLC for the incorporation of bioactive compounds. For the development of NLC with FP, the LM composed by CA and CR separately in the formulations showed adequate thermal behavior, where it was possible to verify the complete incorporation of FP. The incorporation of FP promoted the increase of the thermal resistance of LM, increasing also the crystallinity of the developed systems. In addition, the proportions of 30 and 50% of FP promoted the formation of different crystalline networks, with crystals in needle and platelet forms, with crystals characteristic of FP in LM with greater increase of HOSO. Its important to emphasize that in this study the incorporation of high levels of PF in the lipid nanoparticles was effective. NLCs developed with 30% FP incorporation presented the best results regarding Z-ave, PDI and ZP when compared to NLC with 50% FP during 60 days of evaluation. It should be noted that the NLC developed in this study presented very different thermal and crystalline behavior than the systems developed in our previous study with soybean based raw materials. Thus, it was found that the use of natural raw materials, such as vegetable oils and fats, confer

different characteristics depending on the vegetable source. Note the NLC obtained with the polymorphic β'-form, for applications in food products, where the characteristics of soft and creamy are desirable.

References

Aditya, N. P., Aditya, S., Yang, H., Kim, H. W., Park, S. O., & Ko, S. (2015). Co-delivery of hydrophobic curcumin and hydrophilic catechin by a water-in-oil-in-water double emulsion. Food Chem, 173, 7-13.

AOCS. (2009). Official methods and recommended practices of the American Oil Chemists' Society. Urbana (USA): AOCS Press.

Awad, T. S., Helgason, T., Weiss, J., Decker, E. A., & McClements, D. J. (2009). Effect of Omega-3 Fatty Acids on Crystallization, Polymorphic Transformation and Stability of Tripalmitin Solid Lipid Nanoparticle Suspensions. Crystal Growth & Design, 9(8), 3405–3411.

Beloqui, A., Solinis, M. A., Rodriguez-Gascon, A., Almeida, A. J., & Preat, V. (2016). Nanostructured lipid carriers: Promising drug delivery systems for future clinics. Nanomedicine, 12(1), 143-161.

Bunjes, H., Steiniger, F., & Richter, W. (2007). Visualizing the structure of triglyceride nanoparticles in different crystal modifications. Langmuir, 23(7), 4005-4011.

Bunjes, H., & Unruh, T. (2007). Characterization of lipid nanoparticles by differential scanning calorimetry, X-ray and neutron scattering. Adv Drug Deliv Rev, 59(6), 379-402.

Campos, R. (2005). Experimental methodology. In A. Marangoni (Ed.), Fat Crystal Networks, vol. 1 (pp. 267-349). New York: Marcel Dekker.

Cerqueira, M. A., Pinheiro, A. C., Silva, H. D., Ramos, P. E., Azevedo, M. A., Flores-López, M. L., Rivera, M. C., Bourbon, A. I., Ramos, Ó. L., & Vicente, A. A. (2014). Design of

Bio-nanosystems for Oral Delivery of Functional Compounds. Food Engineering Reviews, 6(1-2), 1-19.

Fernandes, P., & Cabral, J. M. S. (2007). Phytosterols: Applications and recovery methods. Bioresource Technology, 98, 2335-2350.

Gomes Silva, M., Santos, V. S., Fernandes, G. D., Calligaris, G., Santana, M. H. A., Cardoso, L. P., & Ribeiro, A. P. B. (2018). Phytosterols and phytosterol-oil blends under the perspective of thermal behaviour and phase transitions. Food Research International, Submeted.

Goméz-Coca, R. B., Perez-Camino, M. C., & Moreda, W. (2015). Analysis of Neutral Lipids: Unsaponifiable Matter. In L. Nollet & F. Toldrá (Eds.), Handbook of Food Analysis, vol. third). Boca Raton, Florida, USA: CRCPress.

Hariklia Vaikousi, Athina Lazaridou, Costas G. Biliaderis, & Zawistowski, J. (2007). Phase Transitions, Solubility, and Crystallization Kinetics of Phytosterols and Phytosterol-Oil Blends. J. Agric. Food Chem., 55, 1790−1798.

Hayes, K. C., Pronczuk, A., Wijendran, V., & Beer, M. (2002). Free Phytosterols Effectively Reduce Plasma and Liver Cholesterol in Gerbils Fed Cholesterol. The Journal of Nutrition, 132(7), 1983-1988.

Kritchevsky, D., & Chen, S. C. (2005). Phytosterols—health benefits and potential concerns: a review. Nutrition Research, 25(5), 413-428.

Kuntsche, J., Horst, J. C., & Bunjes, H. (2011). Cryogenic transmission electron microscopy (cryo-TEM) for studying the morphology of colloidal drug delivery systems. Int J Pharm, 417(1-2), 120-137.

Lacatusu, I., Badea, N., Stan, R., & Meghea, A. (2012). Novel bio-active lipid nanocarriers for the stabilization and sustained release of sitosterol. Nanotechnology, 23(45), 455702.

Lacatusu, I., Mitrea, E., Badea, N., Stan, R., Oprea, O., & Meghea, A. (2013). Lipid nanoparticles based on omega-3 fatty acids as effective carriers for lutein delivery. Preparation and in vitro characterization studies. Journal of Functional Foods, 5(3), 1260-1269.

LI, J., HO, C. T., LI, H., TAO, H., & TAO, L. (2000). Separation of sterols and triterpene alcohols from unsaponifiable fractions of three plant seed oils. Journal of Food Lipids, 7(1), 11-20.

Ling WH, & PJ., J. (1995). Dietary phytosterols: a review of metabolism, benefits and side effects. Life Scienci, 57 (3), 195-206.

Liu, F., & Tang, C.-H. (2014). Phytosterol Colloidal Particles as Pickering Stabilizers for Emulsions. Journal of Agricultural and Food Chemistry, 62(22), 5133-5141.

Liu, Y., & Wu, F. (2010). Global burden of aflatoxin-induced hepatocellular carcinoma: a risk assessment. Environ Health Perspect, 118(6), 818-824.

Madureira, A. R., Campos, D., Gullon, B., Marques, C., Rodriguez-Alcala, L. M., Calhau, C., Alonso, J. L., Sarmento, B., Gomes, A. M., & Pintado, M. (2016). Fermentation of bioactive solid lipid nanoparticles by human gut microflora. Food Funct, 7(1), 516-529.

Martini, S., Awad, T., & Marangoni, A. G. (2006). Structure and Properties of Fat Crystals Networks. In F. Gunstone (Ed.), Modifying Lipids for Use in Foods, (pp. 142-169). NY: CRC Press.

McClements, D. J., Decker, E. A., & Weiss, J. (2007). Emulsion-based delivery systems for lipophilic bioactive components. J Food Sci, 72(8), R109-124.

Moreau, R. A., Whitaker, B. D., & Hicks, K. B. (2002). Phytosterols, phytostanols, and their conjugates in foods: structural diversity, quantitative analysis, and health-promoting uses. Progress in lipid research, 41, 457–500.

Moruisi, K. G., Oosthuizen, W., & Opperman, A. M. (2013). Phytosterols/Stanols Lower Cholesterol Concentrations in Familial Hypercholesterolemic Subjects: A Systematic Review with Meta-Analysis. Journal of the American College of Nutrition, 25(1), 41-48.

Ntanios FY, MacDougall DE, & PJ., J. (1998). Gender effects of tall oil versus soybean phytosterols as cholesterol-lowering agents in hamsters. Can J Physiol Pharmacol., 76.(7-8), 780-787.

Ostlund, R. E., Jr. (2002). Phytosterols in human nutrition. Annu Rev Nutr, 22, 533-549.

Qian, C., & McClements, D. J. (2011). Formation of nanoemulsions stabilized by model food-grade emulsifiers using high-pressure homogenization: Factors affecting particle size. Food Hydrocolloids, 25(5), 1000-1008.

Rashidi, L., & Khosravi-Darani, K. (2011). The Applications of Nanotechnology in Food Industry. Critical Reviews in Food Science and Nutrition, 51, 723-730.

Ribeiro, A. P. B., Basso, R. C., & Kieckbusch, T. G. (2013). Effect of the addition of hardfats on the physical properties of cocoa butter. European Journal of Lipid Science and Technology, 115, 301-312.

Ribeiro, A. P. B., Grimaldi, R., Gioielli, L. A., & Gonçalves, L. A. G. (2009). Zero trans fats from soybean oil and fully hydrogenated soybean oil: Physico-chemical properties and food applications. Food Research International, 42(3), 401-410.

Rousseau, A. G., & Marangoni, A. (2002). Food lipids: chemistry, nutrition, and biotechnology. New York: CRC Press.

Salminen, H., Helgason, T., Kristinsson, B., Kristbergsson, K., & Weiss, J. (2013). Formation of solid shell nanoparticles with liquid omega-3 fatty acid core. Food Chem, 141(3), 2934-2943.

Santos, V. S., Braz, B. B., Silva, A. Á., Cardoso, L. P., A., S. M. H., & Ribeiro, A. P. B. (2018). Thermal and crystalline properties of lipid nanoparticles developed with conventional vegetable fats and oils for food applications. Food Chemistry, to be submitted.

Santos, V. S., Ribeiro, A. P. B., Cardoso, L. P., & Santana, M. H. A. (2018). Crystallization, polymorphism and stability of nanostructured lipid carriers developed with soybean oil, fully hydrogenated soybean oil and free phytosterols for food application. Food Chemistry, a ser submetido.

Santos, V. S., Santana, M. H. A., Braz, B. B., Silva, A. Á., Cardoso, L. P., & Ribeiro, A. P. B. (2018). The thermal and crystalline behavior of lipid matrices with potential for application in lipid nanoparticles. Química Nova, a ser submetido.

Sato, K. (2001). Crystallization behaviour of fats and lipids: a review (Vol. 56). Oxford.

Severino, P., Andreani, T., Macedo, A. S., Fangueiro, J. F., Santana, M. H., Silva, A. M., & Souto, E. B. (2012). Current State-of-Art and New Trends on Lipid Nanoparticles (SLN and NLC) for Oral Drug Delivery. J Drug Deliv, 2012, 750891.

Severino, P., Pinho, S. C., Souto, E. B., & Santana, M. H. A. (2012). Crystallinity of Dynasan®114 and Dynasan®118 matrices for the production of stable Miglyol®-loaded nanoparticles. Journal of Thermal Analysis and Calorimetry, 108(1), 101-108.

Shahzad, N., Khan, W., Md, S., Ali, A., Saluja, S. S., Sharma, S., Al-Allaf, F. A., Abduljaleel, Z., Ibrahim, I. A. A., Abdel-Wahab, A. F., Afify, M. A., & Al-Ghamdi, S. S. (2017).

Phytosterols as a natural anticancer agent: Current status and future perspective. Biomed Pharmacother, 88, 786-794.

Sharma, V. K., Diwan, A., Sardana, S., & Dhall, V. (2011). Solid lipid nanoparticles system: an overview. International Journal of Research in Pharmaceutical Sciences, 2(3), 450-461.

Tamjidi, F., Shahedi, M., Varshosaz, J., & Nasirpour, A. (2013). Nanostructured lipid carriers (NLC): A potential delivery system for bioactive food molecules. Innovative Food Science & Emerging Technologies, 19(Supplement C), 29-43.

Villaseñor, I. M., Angelada, J., Canlas, A. P., & Echegoyen, D. (2002). Bioactivity studies on β-sitosterol and its glucoside. Phytotherapy Research, 16(5), 417-421.

Wang, J. L., Dong, X. Y., Wei, F., Zhong, J., Liu, B., Yao, M. H., Yang, M., Zheng, C., Quek, S. Y., & Chen, H. (2014). Preparation and characterization of novel lipid carriers containing microalgae oil for food applications. J Food Sci, 79(2), E169-177.

Weiss, J., Decker, E. A., McClements, D. J., Kristbergsson, K., Helgason, T., & Awad, T. (2008). Solid Lipid Nanoparticles as Delivery Systems for Bioactive Food Components. Food Biophysics, 3(2), 146-154.

Weiss, J., Takhistov, P., & McClements, D. J. (2006). Functional Materials in Food Nanotechnology. Journal of Food Science, 71(9), R107-R116.

Wu, T., Fu, J., Yang, Y., Zhang, L., & Han, J. (2009). The effects of phytosterols/stanols on blood lipid profiles: a systematic review with meta-analysis. Asia Pac J Clin Nutr, 18(2), 179-186.

Yang, Y., Corona, A., Schubert, B., Reeder, R., & Henson, M. A. (2014). The effect of oil type on the aggregation stability of nanostructured lipid carriers. Journal of Colloid and Interface Science, 418(Supplement C), 261-272.

Zimmermann, E., Müller, R. H., & Mäder, K. (2000). Influence of different parameters on reconstitution of lyophilized SLN. International Journal of Pharmaceutics, 196(2), 211-213.

PATENTE

"*Nanopartículas Lipídicas Sólidas (NLS) e Carreadores Lipídicos Nanoestruturados (CLN) para aplicação em alimentos, processo para obtenção de NLS e CLN e uso das NLS e dos CLN*" no âmbito de Privilégio de Invenção - INPI BR 10 2017 006471 9.

Título: NANOPARTÍCULAS LIPIDICAS SÓLIDAS (NLS) E CARREADORES LIPÍDICOS NANOESTRUTURADOS (CLN) PARA APLICAÇÃO EM ALIMENTOS, PROCESSO PARA OBTENÇÃO DE NLS E CLN E USO DAS NLS E DOS CLN

Autores:

VALERIA DA SILVA SANTOS

ANA PAULA BADAN RIBEIRO

MARIA HELENA ANDRADE SANTANA

Unidade: FEQ

Data de Protocolo: 29.03.17

Número do Processo: BR 10 2017 006471 9

Natureza do Pedido: Privilégio de Invenção - PI

Resumo

A presente invenção refere-se à nanopartículas lipídicas sólidas (NLS) e carreadores lipídicos nanoestruturados (CLN) obtidos a partir de óleos e gorduras comestíveis e compostos bioativos, tais como fitoesteróis, para aplicação em alimentos. Ainda, os óleos e gorduras comestíveis consistem em óleos de soja, girassol, linhaça, girassol alto oléico, canola, algodão, palma, milho, gergelim, coco e os azeites de oliva, abacate e dendê, *hardfat*s dos óleos de soja, algodão, palma, palmiste, canola e crambe, e suas misturas. Adicionalmente, a invenção refere-se ao processo de obtenção de NLS e CLN utilizando homogeneização a alta pressão a quente (HAP); e seu uso em alimentos, produtos de grau alimentício, fármacos e cosméticos, principalmente, para melhorar as propriedades estruturais, reduzir o teor de ácidos graxos saturados, e enriquecer produtos ou alimentos com compostos bioativos como carreador dos mesmos.

DISCUSSÃO GERAL

DISCUSSÃO GERAL

No cenário atual, a nanotecnologia ainda se encontra em fase exploratória na área de alimentos e inexistente em termos de aplicações em indústrias e produtos alimentícios. O estímulo para a utilização desta tecnologia na área de alimentos se deu pelo conhecimento das propriedades diferenciadas de partículas lipídicas em escala nanométrica muito utilizadas na área médica, farmacêutica e de cosméticos. Sendo que, as propriedades mais interessantes destes materiais são a proteção, o carreamento e liberação de compostos ativos, em medicamentos e cosméticos. Deste modo, foi possível visualizar o potencial destes sistemas nanométricos para aplicação em alimentos. Porém, nos deparamos com o elevado custo das matérias-primas, uma vez que, até o presente momento se utilizam apenas materiais purificados, como por exemplo, triestearina, trioleína, ácido graxo esteárico, ácido graxo oleico, entre outros, sendo, portanto, um impasse para a viabilização desta tecnologia para aplicação em escala industrial alimentícia.

Assim, o grande desafio deste estudo residiu na utilização de matérias-primas comumente empregadas na indústria alimentícia para a produção de nano partículas lipídicas. Estes materiais já estão presentes nas formulações alimentícias em geral, sem restrições de uso quanto aos aspectos regulatórios das legislações em alimentos. Foram utilizados neste estudo *hardfats* dos óleos de soja, canola e crambe e os óleos de soja e girassol alto oleico. Estas matérias-primas são óleos e gorduras vegetais que apresentam misturas de TAGs em suas composições, diferente das matérias-primas purificadas, utilizadas em fármacos e cosméticos. Deste modo, pela elevada complexidade química e fisica dos lipídios e falta de conhecimento do comportamento destes materiais em escala nanométrica, foram realizados diferentes estudos de comportamente. Buscou-se, principalmente, elucidar o comportamento térmico e cristalino de nanopartículas lipídicas com ML compostas por diferentes *hardfats* e óleos. Além disso, considerando a possibilidade de carreamento de compostos biotivos em NLS e CLN, foram incorporados FL nas ML das nanopartículas. Os FL, foram escolhidos como compostos de inclusão nestes sistemas pelos efeitos benéficos a saúde, como a redução comprovada dos níveis de colesterol no sangue. Além disso, por questões tecnológicas de aplicação, uma vez que, estes compostos bioativos lipofílicos são pouco explorados na área alimentícia, principalmente por questões de elevada hidrofobicidade e cristalinidade, o que dificulta a incorporação em produtos alimentícios, pois ocasionam problemas de estabilidade física. Sendo as NLS e CLN

desenvolvidas ao longo deste trabalho uma opção de veiculação de fitoesteróis livres para enriquecimento nutricional e funcional de alimentos.

Os FL utilizados como compostos bioativos nas nanoparticulas foram caracterizados química e fisicamente, apresentando em sua composição uma mistura de esteróis, com predominância do β-sitosterol (~44%), estigmasterol (~27%) e campesterol (~23%). Cabe destacar que, mesmo sendo uma mistura de esteróis, apresentaram comportamento térmico homogêneo, com elevadas temperaturas de cristalização (126,37°C) e fusão (137,94°C), mas isto não impediu a incorporação de FL nas ML e CLN, como será discutido na sequência.

No inicio do estudo, foram desenvolvidos CLN compostos por óleo de soja e *hardfat* do óleo de soja com e sem a inclusão de 30% de FL. Foram avaliados três diferentes emulsificantes (monooleato de sorbitano - S60, BLH = 4,7, lecitina de soja - LS, BHL = 7,0 e monoestearato de sorbitano etoxilado - T80, BHL = 15,0). Foram empregados dois métodos de produção das nanopartículaculas: i) Homogeneização a alta pressão (HAP), com avaliação de 3 e 5 ciclos de homogeneização a 800 bar e ii) Ultrasson (US), com ponta de titânio 13 mm, potência de 60W e exposição as ondas de ultrassom por 5 e 10 minutos. Os resultados de Z-ave de partículas não foram promissores para os CLN com FL desenvolvidos com US, apresentando valores de aproximadamente 700 nm, assim como para os resultados de PDI, que ficaram próximos de 0,7 indicando distribuição de tamanho de partículas muito amplo, caracterizando baixa estabilidade física. Deste modo, apenas a HAP foi utilizada para dar sequência nos estudos e os resultados obtidos foram descritos no "**Artigo 1**".

Verificou-se que a HAP se mostrou muito eficaz no desenvolvimento de CLN, principalmente nos CLN desenvolvidos com FL. Pois, a elevada temperatura durante o processamento de HAP evitou a recristalização dos FL, favorecendo a obtenção de sistemas estáveis e com reduzidos tamanhos de partículas. O número de ciclos utilizados na HAP, de maneira geral, não interferiu no Z-ave e PDI das nanopartículas, mas colaborou para a redução do PDI dos CLN desenvolvidos com os FL. Contudo, estes resultados não são apenas dependentes do número de ciclos e pressão utilizados, sendo extremamente importante considerar o efeito do sistema emulsificante empregado, para garantir a manutenção e estabilidade após a cristalização da fração lipídica. Assim, com este estudo, também foi possível acompanhar a eficiência dos diferentes emulsificantes em conjunto com as condições de

processamento, como pressão e número de ciclos da HAP. De maneira geral, os melhores resultados obtidos para os CLN compostos de óleo de soja e *hardfats* de óleo de soja com e sem a incorporação de FL, em relação a Z-ave de partículas e PDI foram através do emprego do emulsificante T80, sendo de aproximadamente 167 e 164 nm (3 ciclos de HAP) e 161 e 164 nm (5 ciclos de HAP) com PDI variando entre 0,1 e 0,3. Por questões de problemas no equipamento utilizado para fazer a medida de PZ, estas medidas não foram realizadas nas nanopartículas obtidas neste estudo.

Foi possível verificar que a incorporação do composto bioativo nas ML modificou as suas propriedades térmicas e cristalinas, devido a elavada cristalinidade dos FL. Além disso, verificou-se que as nanopartículas apresentaram comportamento térmico diferenciado das ML. Este fato possibilita afirmar que os lipídios quando estão nanoestruturados em forma de partículas, necessitam de maiores energias para que ocorra a transição de fase. Todos os CLN compostos por óleo de soja e *hardfat* do óleo de soja apresentaram partículas com hábito polimórfico em *β*, enquanto que nas ML correspondentes foram predominantes a mistura das formas polimórficas *β'+β*. O que indicou que as transições polimórficas são aceleradas em materiais nanoestruturados.

Afim de verificar o comportamento de ML e nanopartículas desenvolvidas com outros óleos e *hardfats*, podendo ampliar a gama de aplicações de NLS e CLN, o restante do estudo foi realizado com óleo de girassol alto oleico e com os *hardfats* dos óleos de canola e crambe. Varios fatores foram considerados para a utilização destas outras fontes vegetais, como: i) características físico-químicas diferenciadas, como por exemplo, maior estabilidade química do óleo de girassol alto oleico em relação ao óleo de soja; ii) tamanho da cadeia carbônica dos ácidos graxos majoritários dos *hardfats*, para verificar a influência na cristalinidade dos sistemas; iii) efeito nutricional no organismo dos ácidos graxos, como citado na "**Introdução Geral**".

No "**Artigo 2**", foi realizado um estudo detalhado das propriedades térmicas e cristalinas das matérias-primas e misturas desenvolvidas com o óleo de girassol alto oleico e os *hardfats* do óleo de canola e crambe. Neste caso, o principal objetivo foi caracterizar o comportamento de cada componente e suas misturas para aplicação como ML de sistemas nanoestruturados. Com os resultados obtidos verificou-se que as ML desenvolvidas com estas matérias-primas apresentaram comportamento térmico e cristalino diferenciado de compostos

purificados. Além disso, foi observado um efeito eutético nas ML desenvolvidas com misturas destas materias-primas. Este eveito provavelmente está relacionado à grande diferença entre os tamanhos das cadeias carbônicas dos ácidos graxos esteárico e behênico, predominantes nos *hardfats* de canola e crambe, respectivamente, e também à presença de insaturações provenientes das moléculas dos ácidos graxos oleico predominantes no OGAO. Contudo, este comportamento foi considerado benéfico para a produção de NLS e CLN, podendo colaborar na redução da cristalidade dos sistemas, favorecendo a incorporação de compostos bioativos.

No "**Artigo 3**", algumas destas hipóteses foram confirmadas com o desenvolvimento de NLS e CLN através da aplicação das ML descritas no Artigo 2. A utilização do *hardfat* do óleo de crambe nas ML aumentou a resistência térmica dos sistemas, em comparação as nanopartículas desenvolvidas apenas com o *hardfat* do óleo de canola. Portanto, o tamanho da cadeia carbônica, no caso do crambe, composta por 22 carbonos, realmente interferiu nas características físicas das ML e dos CLN. Além disso, o efeito eutetico verificado no Artigo 2 para as ML se repetiu nas nanopartículas, e favoreceu o desenvolvimento de nanopartículas menos cristalinas em termos estruturais, com consequente redução do tamanho das partículas e maior estabilidade física, durante 60 dias de avaliação. Em termos de processamento, verificou-se que o emprego de 3 ciclos de HAP foi suficiente para se obter sistemas com características desejáveis, assim como foi verificado para os CLN desenvolvidos com óleo de soja e hardfat do óleo de soja no Artigo 1.

Cabe destacar, no Artigo 3 o comportamento diferenciado das NLS compostas apenas pelos *hardfats* de canola e crambe, separados e em mistura (50:50m/m). Estas NLS gelificaram durante o processo de cristalização e estabilização cristalina, etapas realizadas logo após o processamento em HAP, permanecendo sólidas durante todo o período de avaliação (60 dias). Este comportamento é muito relatado na literatura para NLS desenvolvidas com matérias-primas purificadas. No entanto, este comportamento foi verificado apenas para as NLS, não sendo observados para os demais sistemas obtidos. Os CLN obtidos com os *hardfats* de canola e crambe e com OGAO apresentaram Z-ave de partículas variando entre 156 a 189 nm (3 ciclos de HAP) e 162 a 208 nm (5 ciclos de HAP), com PDI variando entre 0,1 e 0,2. Adicionalmente, foi verificado o PZ destes sistemas e os valores encontrados variaram entre -13 a -24 mV e -13 a -25 mV, para os CLN obtidos com 3 e 5 ciclos de HAP, respectivamente. Os CLN desenvolvidos com os *hardfats* de canola e crambe e com o OGAO, apresentaram maior

resistência térmica do que suas ML avaliadas em macroescala no Artigo 2. Fato que também foi verificado no Artigo 1, reforçando ainda mais que materiais lipídicos nanoestruturados necessitam de maiores energias para que ocorra transição de fase. Comportamento muito favorável para aplicação de CLN em alimentos processados termicamente, podendo-se manter a integridade estrutural das nanopartículas. As NLS e CLN obtidas neste estudo apresentaram-se na forma *β'* ou *β*, diferentemente das nanopartículas compostas pelo óleo de soja e *hardfat* do óleo de soja obtidas no Artigo 1, que apenas foram encontradas nanopartículas na forma mais estável (forma *β*). Estes resultados confirmaram também que as transições polimórficas são aceleradas em sistemas lipídicos em escala nanométrica, mas que estas transições são dependentes do hábito polimórfico das materias-primas utilizadas para a composição das ML. Assim, foi possível afirmar que foram obtidas nanopartículas com propriedades térmicas e cristalinas diferentes das obtidas no Artigo 1, principalmente pela composição química diferenciada das matérias-primas utilizadas.

No **Artigo 4**, foram desenvolvidas ML e CLN compostos por OGAO e os *hardfats* dos óleos de canola e crambe, com a incorporação de 30 e 50% de FL. O maior desafio neste estudo foi a incorporação de grandes quantidades de FL nas ML e nos CLN. Pois, nos trabalhos relatados na literatura, geralmente os autores trabalham com contrações muito baixas de compostos bioativos, em torno de 1%. Como visto no Artigo 1, foram obtidos resultados promissores para a incorporação de 30% de FL nos CLN a base de óleo de soja e *hardfat* do óleo de soja. Neste artigo 4, com outras matérias-primas, os resultados obtidos para os CLN com incorporação de 30 e 50% de FL foram de partículas com tamanho variando entre, 148 a 250 nm e 206 a 342 nm aproximadamente; PDI de 0,2 a 0,4 e de 0,3 a 0,4; com PZ entre -24 a -30 mV e -22 a -27 mV, respectivamente. De maneira geral, os CLN desenvolvidos com 30% de FL mantiveram-se mais estáveis do que os CLN com 50% de FL durante 60 dias de avaliação. De qualquer maneira, pode-se afirmar que foi possível desenvolver CLN com altos teores de FL, fato inédito para o desenvolvimento de NL.

O efeito eutético também foi observado nas ML e CLN desenvolvidos com FL. Vale ressaltar que nos artigos anteriores este efeito se mostrou efetivo na redução da cristalinidade dos sistemas desenvolvidos, com consequente redução do tamanho das partículas. No entanto, na presença dos FL este efeito de incompatibilidade proveniente das diferenças de tamanho dos ácidos graxos não foi positivo, e pode estar relacionado a expulsão dos compostos

bioativos das nanoparticulas. Sendo os melhores resultados obtidos para os CLN desenvolvidos com os *hardfats* em separado nas formulações.

Assim como no Artigo 1, no Artigo 4 nos deparamos com a dificuldade de identificação do hábito polimórfico das ML e CLN desenvolvidos com FL, devido a alguns picos de difração dos FL serem muito próximos aos picos que caracterizam as formas polimórficas de TAG. Deste modo, não foi possivel afirmar a forma cristalina destes sistemas, e sim supor quais são as possíveis formas. Além disso, nestes sistemas desenvolvidos com FL verificou-se que as ML apresentaram cristais na forma mais estável (forma β), comportamento diferente das ML desenvolvidas no Artigo 1, que se encontravam na forma inicial (forma α) ou misturas da forma intermediaria com a mais estavel (formas $\beta' + \beta$). Portanto, inferiu-se que os FL promoveram a estabilização das ML e CLN desenvolvidos com OGAO e os *hardfats* dos óleos de canola e crambe, no hábito preferencial, não sendo notado efeitos de aceleração de transição polimórfica, causado pela nanoestruturação.

De maneira geral, as nanopartículas obtidas neste estudo apresentaram diâmetro médio de partículas e PDI muito semelhantes, confirmando a efetividade do sistema emulsficante e do método de produção. Deste modo, foi possível considerar a HAP muito promissora para o desenvolvimento de NLS e CLN. Além disso, outros fatores tornam essa técnica muito vantajosa para aplicação a nível industrial. Sendo, a HAP um processo muito rápido, podendo-se obter as nanopartículas em poucos minutos e com quantidades reduzidas de emulsificantes. Outro ponto a ressaltar é a versatilidade do uso de temperaturas, podendo ser utilizadas altas temperaturas para facilitar a solubilização dos compostos bioativos com elevado ponto de fusão, como os fitoesteróis livres, ou temperaturas intermediárias à brandas se for de interesse incorpor comportos bioativos termolábeis. Destaca-se que a transposição de escala do processo é facilitada pela disponibilidade comercial da HAP, usado na principal etapa do processo, e além disso é uma tecnologia que não utiliza solventes orgânicos no processo, sendo considerado um fator muito importante para as indutrias, por questões ambientais.

Além disso, com a compilação de todos os resultados obtidos neste estudo, foi possivel verificar os benéficos da utilização de sistemas nanoestruturados desenvolvidos com lipídios, como as NLS e os CLN, para aplicação em alimentos. Destaca-se a questão estrutural sólida das nanopartículas, que foram desenvolvidas com materiais lipidícos de alta resistência térmica e também com óleos liquidos, em proporções que mantiveram estes sistemas com ponto

de fusão acima da temperatura corporea. Deste modo, garantindo a integridade fisica destas nanopartículas durante todo o processo digestório, para a entrega dos compostos bioativos de interesse até o momento de absorção dos lipídios no trato gastrointestinal. Além disso, parte das nanoparticulas desenvolvidas apresentaram ponto de fusão mais elevado, em torno de 60 a 70°C, possibilitando a inclusão direta destas partículas em alguns alimentos processados termicamente, sem a necessidade de alteração do processo de obtenção.

Do ponto de vista de utilização de óleos e gorduras vegetais disponíveis no cenário industrial alimentício, as materias-primas propostas neste estudo podem possibilitar a utilização destes nanosistemas e suas propriedades diferenciadas em alimentos, principalmente, através da redução de custos desta tencnologia, pela utilização de matérias-primas comuns e não purificadas. Deste modo, para fins de comparação de custos foi realizado um levantamento de preços dos materiais purificados mais relatados na literatura científica, tanto para emprego em nanopartículas para aplicação em fármacos e cosméticos quanto para aplicação em alimentos, comparando-os com as matérias-primas utilizadas neste estudo. Verificou-se que a triestearina e o ácido graxo esteárico, ambos purificados de grau técnico, com 95% de pureza, utilizados como material sólido nas nanopartículas lipidícas apresentaram valores de R$ 1.596,00/Kg e 169,00/Kg, respectivamente. Os contituintes lipídicos líquidos purificados, trioleato de glicerila com 65% de pureza e o ácido graxo oleico de grau técnico com 90% de pureza, os valores encontrados foram de R$ 934,00/L e R$ 273,00/L, respectivamente. Enquanto que, para os *hardfats* utilizados neste estudo como material sólido das nanopartículas, os valores variam entre R$ 3 a 5,00/Kg, dependente da fonte de óleo, e os óleos de soja e girassol alto oléico, utilizados como material liquido das nanopartículas, os valores encontrados foram de R$ 3,00 e 10,00/L, respectivamente. Portanto, o uso de materiais lipídicos puros para o desenvolvimento de nanopartículas lipídicas é economicamente inviável na área de alimentos, devido aos volumes de produção e escalabilidade característicos da indústria de alimentos. Deste modo, os *hardfats* e óleos vegetais foram considerados matérias-primas de baixo custo, quanto comparado com os materiais que vêm sendo utilizados para o desenvolvimento de nanopartículas lipidícas, e de alto potencial para o uso como lipídios saturados e insaturados na produção de NLS e CLN. Além disso, os lipídios são considerados sistemas promissores para carreamento de compostos bioativos lipofílicos, pois possuem polaridade semelhante o que facilita a sua solubilização. Adicionalmente, o carreamento e proteção de compostos bioativos

em NLS e CLN podem ser uma alternativa viável para resolver alguns problemas de enriquecimento nutricional em alguns produtos. Contudo, estes sistemas possuem grande potencial de aplicação em diferentes produtos, podem ser empregados tanto em alimentos de base lipídica quanto aquosa. Como sugestões de aplicação, seria interessante utilizar as nanoparticulas para veicular FL em alimentos de base aquosa, onde a dispersão dos FL geralmente é dificultada pelo alto ponto de fusão e solubilidade limitada. Além disso, pode-se sugerir o emprego das nanoparticulas secas em estufa ou liofilizados, como sementes de cristalização em alimentos de base lipídica, para a indução das formas polimórficas β' e β. Por outro lado, estes sistemas podem também serem expandidos para outros setores industriais, principalmente visando redução de custos, como nas áreas farmacêuticas e de cosmético para carreamento de compostos bioativos e fármacos. Porém, ressalta-se que ainda não existe legislação para regulamentação de sistemas nanoestrutrados, apenas um incentivo internacional para inclusão no rótulo que o produto foi obtido utilizando-se nanotecnologia.

CONCLUSÕES GERAIS

CONCLUSÕES GERAIS

Foi possível desenvolver diferentes nanopartículas lipídicas, utilizando matérias-primas lipídicas comumente utilizadas na indústria de alimentos para a incorporação de altos teoreos de fitoesteróis livres (30 e 50%), com potencial para de incorporação de outros compostos bioativos lipofílicos.

As diferentes fontes lipídicas vegetaisutilizadas neste estudo conferiram características diferenciadas aos sistemas nanoestruturados, principalmente em termos de propriedades térmicas e cristalinas.

Dentre os emulsificantes utilizados, o emuslficiante monooleato de sorbinata etoxilado, mostrou-se o mais promissor, favorecendo a obtenção de nanopartítculas com menores diâmetros médios e com tamanhos de partículas mais homogêneos, em relação aos demais emulsficantes utilizados.

A homogeneização a alta pressão foi muito efeitiva para a obtenção de NLS e CLN com 3 ciclos de homogeneização a 800bar, mostrando grande potencial de escalonamento para produção em escala indústrial.

Através do estudo térmico foi possivel identificar diferenças entre partículas em escala nanométrica quando comparadas as ML, comprovando que os materiais lipídicos nanoestruturados apresentam maior resistência térmica do que em macroescala.

A partir da caracterização do hábito polimórfico das nanopartículas, verificou-se que nos lipídios nanoestruturados, de maneira geral, as transições polimórficas são facilitadas e a forma mais estável é atingida mais rapidamente.

As nanopartículas desenvolvidas neste estudo têm viabilidade econômica e operacional para aplicação em alimentos em escala industrial.

Os sistemas desenvolvidos neste estudo são de caracter inovador, em termos de composições das matrizes lipídicas e apresentam alto potencial para a aplicação em alimentos, com possibilidade de utilização em fármacos e cosméticos.

SUGESTÕES PARA TRABALHOS FUTUROS

SUGESTÕES PARA TRABALHOS FUTUROS

- Utilização de outros emulsificantes para o desenvolvimento destes sistemas, principalmente, os emulsificantes naturais;

- Explorar outros tipos de lecitinas, com diferentes BHL e composições químicas;

- Verificar a eficiencia da utilização de co-emulsificantes, na estabilização dos sistemas desenvolvidos neste estudo;

- Desenvolver nanopartículas lipídicas com outros óleos e gorduras vegetais, para ampliar a gama de aplicações;

- Utilizar outros compostos bioativos nestas matrizes lipídicas e caracterizar os sistemas em macro e nanoescala;

- Desenvolver nanopartículas com hábito polimórfico em α, para verificar a estabilidade física quanto a expulsão do composto bioativo;

- Aplicar estes nanosistemas em alimentos e verificar as suas estabilidades;

- Desenvolver produtos com nanopartículas lipídicas e validar as propriedades diferenciadas promovidas pela inclusão destes nanosistemas;

- Avaliar estes sistemas *in* vitro e *in* vivo, para verificar a absorção das nanopartículas e dos compostos bioativos carreados.

REFERÊNCIAS

REFERENCIAS GERAIS

ABUASAL, B. S. et al. Enhancement of intestinal permeability utilizing solid lipid nanoparticles increases γ-tocotrienol oral bioavailability. **Lipids**, *47*(5): 461–469, 2012.

ADITYA, N. P. et al. Co-delivery of hydrophobic curcumin and hydrophilic catechin by a water-in-oil-in-water double emulsion. **Food Chemistry**, v. 173, p. 7-13, 2015.

ADITYA, N. P. et al. Curcumin and genistein coloaded nanostructured lipid carriers: in vitro digestion and antiprostate cancer activity. **Journal of Agricultural and Food Chemistry**, 61:1878−1883, 2013.

ADITYA, N. P., KO. S. Solid lipid nanoparticles (SLNs): delivery vehicles for food bioactives. **RSC Advances***, 5*:30902–30911, 2015.

ALBERIO, C. et al. A new sunflower high oleic mutation confers stable oil grain fatty acid composition across environments. **European Journal of Agronomy,** v. 73, p. 25-33, 2016.

ALEX, A. M. R. et al. Lopinavir loaded solid lipid nanoparticles (SLN) for intestinal lymphatic targeting. **European Journal of Pharmaceutical Sciences**, 42:11–18, 2011.

AMANI, A. et al. Factors affecting the stability of nanoemulsions - Use of artificial neural networks. **Pharmaceutical Research**, 27(1):37–45, 2010.

ANTONIOSI, F. N. R., MENDES, O. L., LANÇAS, F. M. Computer prediction of triacylglycerol composition of vegetable oils by HRGC. **Chromatographia,** v. 40, n. 9, p. 557-562, 1995.

AOCS. **Official methods and recommended practices of the American Oil Chemists' Society**. Urbana (USA): AOCS Press, 2009.

ASUMADU-MENSAH, A., SMITH, K. W., RIBEIRO, H. S. Solid lipid dispersions: potential delivery system for functional ingredients in foods. **Journal of Food Science**, v.78, p.1000–1008, 2013.

ATTAMA, A. A., MULLER-GOYMANN, C. C. Effect of beeswax modification on the lipid matrix and solid lipid nanoparticle crystallinity. **Colloids and Surfaces A: Physicochemical and Engineering Aspects**, v.315, p.189–195, 2008.

AWAD, A. B., CHINNAM, M., FINK, C. S., BRADFORD, P. G. D-Sitosterol activates Fas signaling in human breast cancer cells. **Phytomedicine,** v.14, n.11, p.747–754, 2007.

AWAD, T. S. et al. Effect of Omega-3 Fatty Acids on Crystallization, Polymorphic Transformation and Stability of Tripalmitin Solid Lipid Nanoparticle Suspensions. Crystal Growth & Design, v. 9, n. 8, p. 3405–3411, 2009.

AWAD, T. S. et al. Applications of ultrasound in analysis, processing and quality control of food: A review. **Food Research International**, v.48, p.410–427, 2012.

AWAD, T. S., HELGASON, T., KRISTBERGSSON, K., DECKER, E. A., WEISS, J., McCLEMENTS, D. J. Effect of cooling and heating rates on polymorphic transformations and gelation of tripalmitin solid lipid nanoparticle (SLN) suspensions. **Food Biophysics**, v.3, p.155–162, 2008.

AWAD, T. S., HELGASON, T., WEISS, J., DECKER, E. A., MCcLEMENTS, D. J. Effect of omega-3 fatty acids on crystallization, polymorphic transformation and stability of tripalmitin solid lipid nanoparticle suspensions. **Crystal Growth & Design**, v.9, p.3405–3411, 2009.

BADEA, G. et al. Use of various vegetable oils in designing photoprotective nanostructured formulations for UV protection and antioxidant activity. **Industrial Crops and Products**, v.67, p.18–24, 2015.

BASTIDA-RODRÍGUEZ, J. The food additive polyglycerol polyricinoleate (E-476): structure, applications, and production methods. **International Scholarly Research Notices, Chemical Engineering**, v.2013, p.1-21, 2013.

BELOQUI, A. et al. Nanostructured lipid carriers: Promising drug delivery systems for future clinics. Nanomedicine, v. 12, n. 1, p. 143-61, 2016.

BELOQUI, A. et al. Nanostructured lipid carriers: Promising drug delivery systems for future clinics. **Nanomedicine: Nanotechnology, Biology, and Medicine**, v.12, p.143–161, 2016.

BERTON-CARABIN, C. C., COUPLAND, J. N., ELIAS, R. J. Effect of the lipophilicity of model ingredients on their location and reactivity in emulsions and solid lipid nanoparticles. **Colloids and Surfaces A: Physicochemical and Engineering Aspects**, v,431, p.9-17, 2013.

BLASCO, C., PICÓ, Y. Determining nanomaterials in food. **Trends in Analytical Chemistry**, v.30, n.1, p.84-99, 2011.

BOUCHEMAL, K. et al. Nano-emulsion formulation using spontaneous emulsification: Solvent, oil and surfactant optimisation. **International Journal of Pharmaceutics**, v.280, p.241–25, 2004.

BUCHGRABER, M., ULBERTH, F., EMONS, H., ANKLAN, E. Triacylglycerol profiling by using chromatographic techniques. **European Journal of Lipid Science and Technology,** v.106, n.9, p.581-651, 2004.

BUNJES, H. Characterization of Solid Lipid Nano and Microparticles. In.: C. Nastruzzi (Ed.), **Lipospheres in Drug Targets and Delivery: Approaches, Methods, and Applications.** (pp. 43-70). Boca Raton: CRC Press LLC, 2005.

BUNJES, H., SIEKMANN, B. Manufacture, Characterization, and Applications of Solid Lipid Nanoparticles as Drug Delivery Systems. In.: S. Benita Ed., **Microencapsulation - Methods and Industrial Applications.** (pp. 213-268), London CRC Press: Taylor & Francis Group, 2006.

BUNJES, H., STEINIGER, F., RICHTER, W. Visualizing the structure of triglyceride nanoparticles in different crystal modifications. **Langmuir**, v. 23, n. 7, p. 4005-11, 2007.

BUNJES, H., UNRUH, T. Characterization of lipid nanoparticles by differential scanning calorimetry, X-ray and neutron scattering. **Advanced Drug Delivery Reviews**, v. 59, n. 6, p.379-402, 2007.

CAMPOS, R. Experimental methodology. In: MARANGONI, A. (Ed.). **Fat Crystal Networks**. (p.267-349). New York: Marcel Dekker, v.1, 2005.

CARVALHO, S. M. et al. Optimization of α-tocopherol loaded solid lipid nanoparticles by central composite design. **Industrial Crops and Products**, *49*:278–285, 2013.

CERQUEIRA, M. A. et al. Design of Bio-nanosystems for Oral Delivery of Functional Compounds. **Food Engineering Reviews**, v. 6, n. 1-2, p. 1-19, 2014. ces/ucm257698.htm> Acessed: 2017, April 23.

CHAKRABORTY, S. et al. Utilization of adsorption technique in the development of oral delivery system of lipid-based nanoparticles. **Colloids and Surfaces B: Biointerfaces**, v.81, n.2, p.563–569, 2010.

CHAUDHRY, Q., CASTLE, L. Food applications of nanotechnologies: An overview of opportunities and challenges for developing countries. **Trends in Food Science & Technology, v.**22, p.595–603, 2011.

CHEONG, J. N., TAN, C. P. Palm-based functional lipid nanodispersions: preparation, characterization and stability evaluation. **European Journal of Lipid Science and Technology**, v.112, p.557–564, 2010.

CHO, Y. H., SHIM, H. K., PARK, J. Encapsulation of fish oil by an enzymatic gelation process using TGase cross-linked protein. **Journal of Food Science**, v.68, p.2717–2723, 2003.

CHOI, K., ADITYA, N. P., KO, S. Effect of aqueous pH and electrolyte concentration on structure, stability and flow behavior of non-ionic surfactant based solid lipid nanoparticles. **Food Chemistry**, v.147, p.239–244, 2014.

CONTO, L. C., GROSSO, C. R. F., GONÇALVES, L. A. G. Chemometric as applied to the production of OMEGA-3 microcapsules by complex coacervation with soy protein isolate and gum Arabic. **LWT- Food Science and Technology**, *53*:218–224, 2013.

COSTALES, R., FERNANDEZ, A. Hidrogenación e interesterificación. In.: BLOCK, J. M. B.-A., D. (Ed.). **Temas Selectos en Aceites y Grasas - Volumen 1/ Procesamiento.** (v.1, p.1-29). São Paulo: Blucher, 2009.

CURI, R. et al. **ENTENDENDO A GORDURA: OS ÁCIDOS GRAXOS**. 1. Brasil: Editora Manole LTDA, 2002.

CUSHENA, M. et al. Nanotechnologies in the food industry e Recent developments, risks and regulation. **Trends in Food Science & Technology**, v.24, p.30-46, 2012.

DE MORAIS, J. et al. Physicochemical characterization of canola oil/water nano-emulsions obtained by determination of required HLB number and emulsion phase inversion methods. **Journal of Dispersion Science and Technology**, v.27, n.1, p.109–115, 2006.

DION, M. A. M. L. et al. Review of Analytical Methods for the Identification and Characterization of Nano Delivery Systems in Food. **Journal of Agricultural and Food Chemistry**, v.56, n.18, p.8231–8247, 2008.

DOKTOROVOVÁ, S. et al. Formulating fluticasone propionate in novel PEG-containing nanostructured lipid carriers (PEG-NLC). **Colloids and Surfaces B: Biointerfaces**, v.75, n.2, p.538-542, 2010.

DOMINGO, C., SAURINA, J. Review An overview of the analytical characterization of nanostructured drug delivery systems: Towards green and sustainable pharmaceuticals: A review. **Analytica Chemical Acta**, v.744, p.8–22, 2012.

DOMINGUES, M. A. F. et al. Sucrose behenate as a crystallization enhancer for soft fats. **Food Chemistry,** v.192, p.72–978, 2016.

DORA, C. L. et al. Physicochemical and morphological characterizations of glyceryl tristearate/castor oil nanocarriers prepared by the solvent diffusion method. **Journal of the Brazilian Chemical Society**, v.23, p.1972-1981, 2012.

DURÁN, N., MARCATO, P. D. Nanobiotechnology perspectives. Role of nanotechnology in the food industry: A review. **International Journal of Food Science and Technology**, v.48, p.1127–1134, 2013.

ELTAYEB, M. et al. Preparation of solid lipid nanoparticles containing active compound by electrohydrodynamic spraying. **Food Research International**, v.53, p.88–95, 2013.

ENGELT, R., SCHUBERT, H. Formulation of phytosterols in emulsions for increased dose response in functional foods. **Innovative Food Science and Emerging Technologies**, v.6, p.233– 237, 2005.

FERNANDES, P., CABRAL, J. M. S. Phytosterols: Applications and recovery methods. **Bioresource Technology**, v.98, p.2335-2350, 2007.

Food and Drug Administration - FDA Contains Nonbinding Recommendations: Assessing the Effects of Significant Manufacturing Process Changes, Including Emerging Technologies, on the Safety and Regulatory Status of Food Ingredients and Food Contact Substances, Including Food Ingredients that are Color Additives, 2014. Available from: <http://www.fda.gov/RegulatoryInformation/Guidan

GARNETT, M. C., KALLINTERI, P. Nanomedicines and nanotoxicology: some physiological principles. **Occupational medicine**, v.56, n.5, p.307–311, 2006.

GARZÓN, M. L. S. et al. Efecto de los componentes de la formulación em las propriedades de las nanopartículas sólidas. **Revista Mexicana de Ciências Farmacéuticas**, v.40, n.2, p.26-40, 2009.

GARZÓN, M. L. S., et al. Preparación de nanopartículas sólidas lipídicas (SLN), y de Acarreadores lipídicos nanoestructurados (NLC). **Revista Mexicana de Ciencias Farmacéuticas**, v.39, n.4, p.50-66, 2008.

GASCO, M. R. G. Lipid nanoparticles: perspectives and challenges. **Advanced Drug Delivery Reviews**, v.59, p.377–378, 2007.

GHOSH, V. et al. Cinnamon oil nanoemulsion formulation by untrasonic emulsficantion: investigation of its bactericidal activity. **Journal of Nanoscience and Nanotechnology**, v.13, n.1, p.114-122, 2013.

GOMES SILVA, M. et al. Phytosterols and phytosterol-oil blends under the perspective of thermal behaviour and phase transitions. **Food Research International**, v. Submeted., 2018.

GÓMEZ-COCA, R. B., PÉREZ-CAMINO, M. C., MOREDA, W. Analysis of Neutral Lipids: Unsaponifiable. In.: **Handbook of Food Analysis**, 3rd ed., NOLLET, L., TOLDRÁ F. Eds., CRC Press: Boca Raton, (pp.459-491), 2015.

GUEDES, A. M. M. et al. Physicochemical Properties of Interesterified Blends of Fully Hydrogenated Crambe abyssinica Oil and Soybean Oil. **Journal of the American Oil Chemists' Society,** v.91, n.1, p.111-123, 2014.

GUNSTONE, F. D. Vegetable Oils. In: SHAHIDI, F. (Ed.). **Bailey's Industrial Oil and Fat Products. Edible Oil and Fat Products: Chemistry, Chemical properties, and health effects**. New Jersey: Hoboken, John Wiley & Sons, v.2, 2005.

HAN. F. et al. Effect of surfactants on the formation and characterization of a new type of colloidal drug delivery system: nanostructured lipid carriers. **Colloids and Surfaces A: Physicochemical and Engineering Aspects**, v.315, p.210–216, 2008.

HARTMAN, L., LAGO, R. Rapid preparation of fatty acid methyl esters from lipids. **Laboratory Practice,** v.22, p.475–476, 1973.

HASKELL, R. J. Physical Characterization of Nanoparticles. In.: GUPTA, R. B., KOMPELLA, U. B. Eds., **Nanoparticle Technology for Drug Delivery,** (pp. 103-138) Boca Raton: CRC Press, 2006.

HAYES, K. C. et al. Free Phytosterols Effectively Reduce Plasma and Liver Cholesterol in Gerbils Fed Cholesterol. **The Journal of Nutrition**, v.132, n.7, p.1983-1988, 2002.

HEJRI, A. et al. Optimisation of the formulation of β-carotene loaded nanostructured lipid carriers prepared by solvent diffusion method. **Food Chemistry**, v.141, p.117–123, 2013.

HELGASON, T. et al. Impact of surfactant properties on oxidative stability of β-carotene encapsulated within solid lipid nanoparticles. **Journal of Agricultural and Food Chemistry**, v.57, p.8033–8040, 2009.

HENTSCHEL, A. et al. β-Carotene-loaded nanostructured lipid carriers. **Journal of Food Science**, v.73, n.2, p.1-6, 2008.

HIMAVAN, C., STAROV, V. M., STAPLEY, A. G. F. Thermodynamic and kinetic aspects of fat crystallization. **Advances in Colloid and Interface Science**, v.122, p.3-33, 2006.

HOET, P. H. M., BRÜSKE-HOHLFELD, I., SALATA, O. V. Nanoparticles - known and unknown health risks. **Journal of Nanobiotechnology**, v.2, n.12, p.1-15, 2004.

HOLSER, R. Encapsulation of polyunsaturated fatty acid esters with solid lipid articles. **Lipid Insights**, v.5, p.1-5, 2012.

HOU, D. Z. et al. The production and characteristics of solid lipid nanoparticles (SLNs). **Biomaterials**, 24:1781-1785, 2003.

HUANG, Q., YU, H., RU, Q. Bioavailability and delivery of nutraceuticals using nanotechnology. **Journal of Food Science**, v.75, p.50-57, 2010.

HUMPHREY, K. L., NARINE, S. S., A comparison of lipid shortening functionality as a function of molecular ensemble and shear: microstructure, polymorphism, solid fat content and texture. **Food Research International**, v.37, n.1, p.28-38, 2004.

IZADI, Z., NASIRPOUR, A., GAROUSI, G. Optimization of Phytosterols Dispersion in an Oil/Water Emulsion Using Mixture Design Approach. **Journal of Dispersion Science and Technology**, v.33, n.12, p.1715-1722, 2012.

JAFARI, S. Nanoencapsulation of Food Bioactive Ingredients. Principles and Applications. Seid Jafari Ed. p.500, 2017.

JANNIN, V., MUSAKHANIAN, J., MARCHAUD, D. Approaches for the development of solid and semi-solid lipid-based formulations. **Advanced Drug Delivery Reviews**, v.60, p.734-746, 2008.

JORES, K. et al. Investigations on the structure of solid lipid nanoparticles (SLN) and oil-loaded solid lipid nanoparticles by photon correlation spectroscopy, field-flow fractionation and transmission electron microscopy. **Journal of Controlled Release**, v.95, p.217– 227, 2004.

JORES, K. et al. Solid Lipid Nanoparticles (SLN) and Oil-Loaded SLN Studied by Spectrofluorometric and Raman Spectroscopy. **Pharmaceutical Research**, v.22, n.11, p.1887-1897, 2005.

JORES, K., MEHNERT, W., MÄDER, K. Physicochemical Investigations on Solid Lipid Nanoparticles and on Oil-Loaded Solid Lipid Nanoparticles: A Nuclear Magnetic Resonance and Electron Spin Resonance Study. **Pharmaceutical Research**, v.20, n.8, p.1274-1283, 2003.

JOSEPH, S. et al. Stability of the Metastable α-Polymorph in Solid Triglyceride Drug-Carrier Nanoparticles. **Langmuir**, v.31, p.6663−6674, 2015.

JOSEPH, S., BUNJES, H. Preparation of nanoemulsions and solid lipid nanoparticles by premix membrane emulsification. **Journal of Pharmaceutical Sciences**, v.101, p.2479-2489, 2012.

KAMAL-ELDIN, A. Minor Components of Fats and Oils. In.: F. Shahidi (Ed.), **Bailey's Industrial Oil and Fat Products. Edible Oil and Fat Products: Chemistry, Chemical properties, and health effects** (pp. 319−359). Hoboken, New Jersey: John Wiley & Sons, 2005.

KAMBOJ, S., BALA, S., NAIR, A. B. Solid lipid nanoparticles: an effective lipid bases technology for poorly water-soluble drugs. **International Journal of Pharmaceutical Sciences Review and Research**, v.5, p.78-90, 2010.

KENTISH, S. et al. The use of ultrasonics for nanoemulsion preparation. **Innovative Food Science and Emerging Technologies**, v.9, p.170–175, 2008.

KLANG, V. et al. Electron microscopy of nanoemulsions: An essential tool for characterization and stability assessment. **Micron,** v.43, n.2–3, p.85–103, 2012.

KOJIMA, M. et al. Structured triacylglycerol containing behenic and oleic acids suppresses triacylglycerol absorption and prevents obesity in rats. **Lipids Health Disease Journal,** v.9, p.77, 2010.

KRITCHEVSKY, D., CHEN, S. C. Phytosterols—health benefits and potential concerns: a review. Nutrition Research, v.25, n.5, p.413-428, 2005.

KUMBHAR, D. D., POKHARKAR, V. B. Engineering of a nanostructured lipid carrier for the poorly water-soluble drug, bicalutamide: Physicochemical investigations. **Colloids and Surfaces A: Physicochemical and Engineering Aspects**, v. 416, p.32– 42, 2013.

KUNTSCHE, J., HORST, J. C., BUNJES, H. Cryogenic transmission electron microscopy (cryo-TEM) for studying the morphology of colloidal drug delivery systems. **International Journal of Pharmaceutics**, v. 417, n.1-2, p.120-37, 2011.

LACATUSU, I. et al. Novel bio-active lipid nanocarriers for the stabilization and sustained release of sitosterol. **Nanotechnology**, v.23, n. 45, p. 455702, 2012.

LACATUSU, I. et al. Lipid nanoparticles based on omega-3 fatty acids as effective carriers for lutein delivery. Preparation and in vitro characterization studies. **Journal of Functional Foods**, v.5, n.3, p.1260-1269, 2013.

LASON, E., OGONOWSKI, J. Solid lipid nanoparticles – Characteristics, application and obtaining. **Chemik**, v.65, n.10, p.964-967, 2011.

LAWLER, P. J., DIMICK, P. S. Crystallization and polymorphism of fats. In.: C. C. Akoh (Ed.), **Food Lipids: Chemistry, Nutrition, and Biotechnology** (pp. 275-300). Boca Raton: CRC Press, 2002.

LEONG, W. F. et al. Optimization of Processing Parameters for the Preparation of Phytosterol Microemulsions by the Solvent Displacement Method. **Journal of Agricultural and Food Chemistry**, v.57, p.8426–8433, 2009.

LEONG, W. F. et al. Preparation and characterization of water-soluble phytosterol nanodispersions. **Food Chemistry**, v.129, p.77–83, 2011a.

LEONG. W. F. et al. Effect of sucrose fatty acid esters on the particle characteristics and flow properties of phytosterol nanodispersions. **Journal of Food Engineering,** v.104, p.63–69, 2011.

LI, J. et al. Separation of sterols and triterpene alcohols from unsaponifiable fractions of three plant seed oils. **Journal of Food Lipids**, v.7, n.1, p.11-20, 2000.

LING, W. H., JONES, P. J. Dietary phytosterols: a review of metabolism, benefits and side effects. **Life Scienci**, v. 57 n. 3, p. 195-206, 1995.

LIU, C. H., WU, C. T. Optimization of nanostructured lipid carriers for lutein delivery. **Colloids and Surfaces A: Physicochemical and Engineering Aspects**, v.353, n.2-3, p.149–156, 2010.

LIU, F., TANG, C. Phytosterol Colloidal Particles as Pickering Stabilizers for Emulsions. **Journal of Agricultural and Food Chemistry**, v.62, n.22, p.5133−5141, 2014.

LIU, G. Y., WANG, J. M., XIA, Q. Application of nanostructured lipid carrier in food for the improved bioavailability. **European Food Research and Technology**, v.234, p.391–398, 2012.

LIU, Y., WU, F. Global burden of aflatoxin-induced hepatocellular carcinoma: a risk assessment. **Environ Health Perspect**, v.118, n.6, p.818-24, 2010.

LOBATO, K. B. S. et al. Characterization and stability evaluation of bixin nanocapsules. **Food Chemistry**, v.141, p.3906–3912, 2013.

LOVEJOY, J. C. et al. Effects of Diets Enriched in Saturated (Palmitic), Monounsaturated (Oleic), or trans (Elaidic) Fatty Acids on Insulin Sensitivity and Substrate Oxidation in Healthy Adults. **Diabetes Care,** v.25, n.8, p.1283-1288, 2002.

LUYKX, D. M. A. M. et al. A Review of Analytical Methods for the Identification and Characterization of Nano Delivery Systems in Food. **Journal of Agricultural and Food Chemistry**, v.56, p.8231–8247, 2008.

MADUREIRA, A. R. et al. Fermentation of bioactive solid lipid nanoparticles by human gut microflora. **Food Functional**, v.7, n.1, p.516-29, 2016.

MADUREIRA, A. R. et al. Characterization of solid lipid nanoparticles produced with carnauba wax for rosmarinic acid oral delivery. **RSC Advances**, v.5, p.22665-22673, 2015.

MANDAWGADE, S. D., PATRAVALE, V. B. Development of SLNs from natural lipids: application to topical delivery of tretinoin. **International Journal of Pharmaceutics**, v.363, p.132–138, 2008.

MAO, L. K. et al. Effects of small and large molecule emulsifiers on the characteristics of beta-carotene nanoemulsions prepared by high pressure homogenization. **Food Technology and Biotechnology**, v.47, p.336–342, 2009.

MARANGONI, A. G., ACEVEDO, N., MAKELY, F., CO, E. Structure and functionality of edible fats. **Soft Matter,** v.8, p.1275-1300, 2012.

MARANGONI, A. G., ROUSSEAU, D. Engineering triacylglicerols: the role of interesterification. **Trends in Food Science and Technology,** v.6, p.329-336, 1995.

MARTINI, S., AWAD, T., MARANGONI, A. G. Structure and Properties of Fat Crystals Networks. In.: GUNSTONE, F. (Ed.). **Modifying Lipids for Use in Foods**. (pp.142-169). NY: CRC Press, 2006.

MASUCHI, M. H., GRIMALDI, R., KIECKBUSCH, T. G . Effects of Sorbitan Monostearate and Monooleate on the Crystallization and Consistency Behaviors of Cocoa Butter**. Journal of the American Oil Chemists' Society**, v.91, p.1111-1120, 2014.

McCLEMENTS D. J. Edible lipid nanoparticles: Digestion, absorption, and potential toxicity. **Progress in Lipid Research**, v.52, p.409–423, 2013.

McCLEMENTS, D. J. et al. Structural design principles for delivery of bioactive components in nutraceuticals and functional foods. **Critical Reviews in Food Science and Nutrition**, v.49, p.577–606, 2009.

McCLEMENTS, D. J. Nanoscale Nutrient Delivery Systems for Food Applications: Improving Bioactive Dispersibility, Stability, and Bioavailability. **Journal of Food Science,** v.80, n.7, p. N1602-11, 2015.

McCLEMENTS, D. J., DECKER, E. A., WEISS, J. Emulsion-based delivery systems for lipophilic bioactive components. **Journal of Food Science**, v.72, p.109-124, 2007.

McCLEMENTS, D. J., RAO, J. Food-grade nanoemulsions: formulation, fabrication, properties, performance, biological fate, and potential toxicity. **Critical Reviews in Food Science and Nutrition**, v.51, n.4, p.285-330, 2011.

McKEON, T. A. Transgenic Oils. In.: SHAHIDI, F. (Ed.). **Bailey's Industrial Oil and Fat Products. Edible Oil and Fat Products: Chemistry, Chemical properties, and health effects**. Hoboken, New Jersey: John Wiley & Sons, v.2, 2005.

MEHNERT. W., MÄDER, K. Solid lipid nanoparticles: production, characterization and applications. **Advanced Drug Delivery Reviews**, v.64, p.83-101, 2012.

MENSINK, R. P. Effects of stearic acid on plasma lipid and lipoproteins in humans. **Lipids,** v.40, n.12, p.1201-1205, 2005.

MITRI, K. et al. Lipid nanocarriers for dermal delivery of lutein: preparation, characterization, stability and performance. **International Journal of Pharmaceutics**, v.414, p.267– 275, 2011.

MOJAHEDIAN, M. M. et al. A novel method to produce solid lipid nanoparticles using n-butanol as an additional co-surfactant according to the o/w microemulsion quenching technique. **Chemistry and Physics of Lipids**, v.174, p.32– 38, 2013.

MOREAU, R. A., WHITAKER, B. D., HICKS, K. B. Phytosterols, phytostanols, and their conjugates in foods: structural diversity, quantitative analysis, and health-promoting uses. **Progress in Lipid Research**, v.41, p. 457–500, 2002.

MOREIRA, D. K. T. et al. Production and characterization of structured lipids with antiobesity potential and as a source of essential fatty acids. **Food Research International,** v.99, p.713-719, 2017.

MORUISI, K. G., OOSTHUIZEN, W., OPPERMAN, A. M. Phytosterols/Stanols Lower Cholesterol Concentrations in Familial Hypercholesterolemic Subjects: A Systematic Review with Meta-Analysis. **Journal of the American College of Nutrition**, v.25, n.1, p 41-48, 2013.

MOZAFARI, M. R. et al. Recent trends in the lipid-based nanoencapsulation of antioxidants and their role in foods. **Journal of the Science of Food and Agriculture**, v.86, p.2038-2045, 2006.

MÜHLEN, A. Z., SCHWARZ, C., MEHNERT, W. Solid lipid nanoparticles (SLN) for controlled drug delivery – Drug release and release mechanism. **European Journal of Pharmaceutics and Biopharmaceutics**, v.45, n.2, p.149–155, 1998.

MÜLLER, R. H. et al. Oral bioavailability of cyclosporine: solid lipid nanoparticles (SLN) versus drug nanocrystals. **International Journal of Pharmaceutics**, v.317, n.1, p.82-9, 2006.

MÜLLER, R. H. et al. Oral bioavailability of cyclosporine: Solid lipid nanoparticles (SLN®) versus drug nanocrystals. **International Journal of Pharmaceutics,** v.317, p.82–89, 2006.

MÜLLER, R. H., RADTKE, M., WISSING, S. A. Nanostructured lipid matrices for improved microencapsulation of drugs. **International Journal of Pharmaceutics,** v.242, n.1-2, p.121-128, 2002.

NAKAJIMA, M. et al. Nano-Science-Engineering-Technology Applications to Food and Nutrition. **Journal of Nutritional Science and Vitaminology**, v.61, p. S180-2, 2015.

NGUYEN, H. M. et al. Enhanced payload and photo-protection for pesticides using nanostructured lipid carriers with corn oil as liquid lipid. **Journal of Microencapsulation**, v.29, n.6, p.596-604, 2012.

NICHOLS, D. S, SANDERSON, K. The nomenclature, structure and properties of food lipids. In.: Sikorski, Z. E, Kolakowska, A., editors. **Chemical and Functional Properties of Food Lipids.** (pp.29–60). Boca Raton: CRC Press., 2003.

NIK, A. M., LANGMAID, S., WRIGHT, A. J. Nonionic surfactant and interfacial structure impact crystallinity and stability of β-carotene loaded lipid nanodispersions. **Journal of Agricultural and Food Chemistry**, v.60, p.4126−4135, 2012.

NTANIOS, F. Y., MAcDOUGALL, D. E., JONES, P. J. Gender effects of tall oil versus soybean phytosterols as cholesterol-lowering agents in hamsters. **Canadian Journal of Physiology and Pharmacology**, v.76., n.7-8, p.780-787, 1998.

O'BRIEN, R. D. **Fats and Oils: Formulating and Processing for Applications**, CRC Press, New York (USA), 2009.

OLIVEIRA, A. C. et al. Fontes Vegetais Naturais de Antioxidantes. **Química Nova**, v.32, n.3, p.689-702, 2009.

OLIVEIRA, G. M. D. et al. Development of zero trans/low sat fat systems structured with sorbitan monostearate and fully hydrogenated canola oil. **European Journal of Lipid Science and Technology,** v.117, n.11, p.1762-1771, 2015.

OSTLUND, R. E. Phytosterols in human nutrition. **Annual Review of Nutrition,** v. 22, p. 533-49, 2002.

PARDEIKE, J., HOMMOSS, A., MÜLLER, R. Lipid nanoparticles (SLN, NLC) in cosmetic and pharmaceutical dermal products. **International Journal of Pharmaceutics**, v.366, p.170-184, 2009.

PATEL, M. R., MARTIN-GONZALEZ, F. S. Characterization of ergocalciferol loaded solid lipid nanoparticles. **Journal of Food Science**, v.71, p.8-13, 2012.

PEY, C. M., MAESTRO, A., SOLE, I., GONZALEZ, C., SOLANS, C., & GUTIERREZ, J. M. Optimization of nano-emulsions prepared by low-energy emulsification

methods at constant temperature using a factorial design study. **Colloids and Surfaces a-Physicochemical and Engineering Aspects**, v.288, n.1–3, p.144–150, 2006.

PORTER, C. J. H., WILLIANS, H. D., TREVASKIS, N. Recent advances in lipid-based formulation technology. **Pharmaceutical Research**, v.30, p.2971–2975, 2013.

QIAN, C., DECKER, E. A., XIAO, H., McCLEMENTS, D. J. Impact of lipid nanoparticle physical state on particle aggregation and β-carotene degradation: potential limitations of solid lipid nanoparticles. **Food Research International**, v.52, p.342–349, 2013.

QIAN, C., DECKER, E. A., XIAO, H., McCLEMENTS, D. J. Inhibition of β-carotene degradation in oil-in-water nanoemulsions: Influence of oil-soluble and water-soluble antioxidants. **Food Chemistry**, v.135, n.3, p.1036-1043, 2012.

QIAN, C., McCLEMENTS, D. Formation of nanoemulsions stabilized by model food-grade emulsifiers using high pressure homogenization: Factors affecting particle size. **Food Hydrocolloids**, v.25, n.5, p.1000-1008, 2011.

QIAN, C., McCLEMENTS, D. J. Formation of nanoemulsions stabilized by model food-grade emulsifiers using high-pressure homogenization: Factors affecting particle size. **Food Hydrocolloids**, v.25, n.5, p. 1000-1008, 2011.

RAMEL, P. R. et al. Structure and functionality of nanostructured triacylglycerol crystal networks. **Progress in lipid research,** v.64, p.231-242, 2016.

RAMISETTY, K. A., PANDIT, A. B., GOGATE, P. R. Ultrasound assisted preparation of emulsion of coconut oil in water: Understanding the effect of operating parameters and comparison of reactor designs. **Chemical Engineering and Processing: Process Intensification**, v.88, p.70–77, 2015.

RASHIDI, L., KHOSRAVI-DARANI, K. The Applications of Nanotechnology in Food Industry. **Critical Reviews in Food Science and Nutrition,** v.51, p.723-730, 2011.

REDDY, R. N., SHARIFF, A. Solid lipid nanoparticles: an advanced drug delivery system. **International Journal of Pharmaceutical Sciences and Research**, v.4, n.1, p.161-171, 2013.

REGITANO-D'ARCE, M. A. B., VIEIRA, T. M. F. S. **Fuentes de Aceites y Grasas**. In.: BLOCK, J. M., BARRERA-ARELLANO, D. (Org.). Temas Selectos en Aceites y Grasas - Volumen 1/Procesamiento. 1 ed. (pp.1-29). São Paulo: Blucher, 2009.

RELKIN, P., YUNG, J. M., KALNIN, D., OLLIVON, M. Structural behaviour of lipid droplets in protein-stabilized nano-emulsions and stability of α-tocopherol. **Food Biophysics**, v.3, p.163–168, 2008.

RIBEIRO, A. P. B. et al. Physico-chemical properties of Brazilian cocoa butter and industrial blends. Part II - Microstructure, polymorphic behavior and crystallization characteristics. **Grasas y Aceites,** v.63, n.1, p. 89-99, 2012.

RIBEIRO, A. P. B. et al. Zero trans fats from soybean oil and fully hydrogenated soybean oil: Physico-chemical properties and food applications. **Food Research International,** v.42, n.3, p.401-410, 2009b.

RIBEIRO, A. P. B. et al. Instrumental methods for the evaluation of interesterified fats. **Food Analytical Methods,** v.2, p.282-302, 2009c.

RIBEIRO, A. P. B. et al. Interesterificação química de óleo de soja e óleo de soja totalmente hidrogenado: influência do tempo de reação. **Química Nova**, v.32, n.4, p.939-945, 2009a.

RIBEIRO, A. P. B. et al. Thermal Behavior, Microstructure, Polymorphism, and Crystallization Properties of Zero Trans Fats from Soybean Oil and Fully Hydrogenated Soybean Oil. **Food Biophysics**, v.4, p.106–118, 2009d.

RIBEIRO, A. P. B., BASSO, R. C., KIECKBUSCH, T. G. Effect of the addition of hardfats on the physical properties of cocoa butter. **European Journal of Lipid Science and Technology,** v.115, p.301-312, 2013.

RIBEIRO, H. S., SCHUBERT, H. Stability of lycopene emulsions in food systems. **Journal of Food Science**, v.68, p.2730-2734, 2003.

RIBEIRO, M. D. M. M. et al. Synthesis of structured lipids containing behenic acid from fully hydrogenated Crambe abyssinica oil by enzymatic interesterification. **Journal of Food Science and Technology,** v.54, n.5, p.1146–1157, 2017.

ROBLES, L. V. et al. Nanopartículas lipídicas sólidas. **Revista Mexicana de Ciências Farmacêuticas**, v.39, n.1, p.38-52, 2008.

ROUSSEAU, A. G., MARANGONI, A. **Food lipids: chemistry, nutrition, and biotechnology.** New York: CRC Press, 2002.

RUBIO-RODRÍGUEZ, S. B. N. et al. Production of omega-3 polyunsaturated fatty acid concentrates: A review. **Innovative Food Science and Emerging Technologies**, v.11, p.1-12, 2010.

SALMINEN, H. et al. Formation of solid shell nanoparticles with liquid omega-3 fatty acid core. **Food Chemistry**, v.141, n.3, p.2934-43, 2013.

SANTOS, G. S. et al. Desenvolvimento e caracterização de nanopartículas lipídicas destinadas à aplicação tópica de dapsona. **Química Nova**, v.35, n.7, p.1388-1394, 2012.

SANTOS, V. S. et al. Crystallization, polymorphism and stability of nanostructured lipid carriers developed with soybean oil, fully hydrogenated soybean oil and free phytosterols for food applications. **Food Chemistry,** 2018 *(a ser submetido).*

SANTOS, V. S. et al. Thermal and crystalline properties of lipid nanoparticles produced with conventional vegetable fats and oils for food applications. **Food Chemistry**, 2018 *(a ser submetido).*

SANTOS, V. S. et al. Comportamento térmico e cristalino de matrizes lipídicas com potencial de aplicação em nanopartículas lipídicas. **Química Nova**, 2018. *(a ser submetido).*

SATO, K. Crystallization behaviour of fats and lipids: a review. **Chemical Engineering Science**, v.56, n.7, p.2255-2265, 2001.

SCRIMGEOUR, C. Chemistry of Fatty Acids. In.: F. Shahidi (Ed.) **Bailey's Industrial Oil and Fat Products. Edible Oil and Fat Products: Chemistry, Chemical properties, and health effects.** (pp. 1-43). New Jersey: John Wiley & Sons, 2005.

SEVERINO, P. et al. Crystallinity of Dynasan® 114 and Dynasan® 118 matrices for the production of stable Miglyol®-loaded nanoparticles. **Journal of Thermal Analysis and Calorimetry,** v.108, n.1p.101-108, 2011.

SEVERINO, P. et al. Current State-of-Art and New Trends on Lipid Nanoparticles (SLN and NLC) for Oral Drug Delivery**. Journal of Drug Delivery**, v. 2012, p. 750-891, 2012.

SEVERINO, P. et al. Review Article: Current State-of-Art and New Trends on Lipid Nanoparticles (SLN and NLC) for Oral Drug Delivery. **Journal of Drug Delivery**, p. 750-891, 2012.

SEVERINO, P., SANTANA, M. H. A., SOUTO, E. B. Optimizing SLN and NLC by 2^2 full factorial design: effect of homogenization technique. **Materials Science and Engineering**, v.2, n.6, p.1375-1379, 2012.

SHAH, R. et al. **Lipid Nanoparticles: Production, Characterization and Stability.** Springer. (2015). ISBN: 978-3-319-10711-0

SHAHZAD, N. et al. Phytosterols as a natural anticancer agent: Current status and future perspective. **Biomedicine & Pharmacotherapy**, v.88, p.786-794, 2017.

SHANGGUAN, M. et al. Binary lipids-based nanostructured lipid carriers for improved oral bioavailability of silymarin. **Journal of Biomaterials Applications**, v.28, p.887–896, 2014.

SHARMA, P. et al. Formulation and pharmacokinetics of lipid nanoparticles of a chemically sensitive nitrogen mustard derivative: Chlorambucil. **International Journal of Pharmaceutics**, v.9, n.367, p.187–194, 2009.

SHARMA, V. K. et al. Solid lipid nanoparticles system: an overview. **International Journal of Research in Pharmaceutical Sciences**, v.2, n.3, p.450-461, 2011.

SHILEI, N. et al. Quercetin loaded Nanostructured Lipid Carrier for food fortification: Preparation, Characterization and in vitro study. **Journal of Food Process Engineering**, v.38, p.93-106, 2014.

SIMOVIC, S. et al. Assembling nanoparticle coatings to improve the drug delivery performance of lipid based colloids. **Nanoscale**, v.4, p.1220–1230, 2012.

SOUTO, E. B. et al. Nanopartículas de lipídios sólidos: métodos clássicos de produção laboratorial. **Química Nova**, v. 34, p.1762-1769, 2011.

SOZER, N., KOKINI, J. L. Nanotechnology and its applications in the food sector. **Trends in Biotechnology**, v.27, n.2, p.82-89, 2009.

TAKEUCHI, M., UENO, S., SATO, K. Synchrotron Radiation SAXS/WAXS Study of Polymorph-Dependent Phase Behavior of Binary Mixtures of Saturated Monoacid Triacylglycerols. **Crystal growth & design**, v.3, n.3, p.369-374, 2003.

TAMJIDI, F. et al. Nanostructured lipid carriers (NLC): A potential delivery system for bioactive food molecules. **Innovative Food Science & Emerging Technologies,** v.19, n. Supplement C, p.29-43, 2013.

TAN, C. P., CHE MAN, Y. B. Differential scanning calorimetric analysis of palm, palm oil based products and coconut oil: effects of scanning rate variation. **Food Chemistry**, v.76, p.9-102, 2002.

TAN, C. P., NAKAJIMA, M. β-Carotene nanodispersions: preparation, characterization and stability evaluation. **Food Chemistry**, v.92, p.661–671, 2005.

TANG, D., MARANGONI, A. **Quantitative study on the microstructure of interface techniques**. Boca Raton: CRC Press, 2006.

TEO, B. S. X. A potential tocopherol acetate loaded palm oil esters-in-water nanoemulsions for nanocosmeceuticals. **Journal of Nanobiotechnology**, v.8, n.4, p.1–12, 2010.

Timms, R. E. Crystallization of fats, in Developments in Oils and Fats, Hamilton, R.J., Ed., Blackie Academic, London, 1995, p.204.

TRUJILLO, C. C., WRIGHT, A. J. Properties and stability of solid lipid particle dispersions based on canola stearin and poloxamer 188. **Journal of American Oil Chemists' Society**, v.87, p.715–730, 2010.

VAIKOUSI, H. et al. Phase Transitions, Solubility, and Crystallization Kinetics of Phytosterols and Phytosterol-Oil Blends. **Journal of Agricultural and Food Chemistry**, v.55, p.1790−1798, 2007.

VILLASEÑOR, I. M. et al. Bioactivity studies on β-sitosterol and its glucoside. **Phytotherapy Research**, v.16, n.5, p.417-421, 2002.

WALSTRA, P. **Physical Chemistry of Foods**, Marcel Decker, New York, NY., 2003.

WANASUNDARA, P. K. J. P. D., SHAHIDI, F. Antioxidants: Science, Technology, and Applications. In.: F. Shahidi (Ed.), **Bailey's Industrial Oil and Fat Products. Edible Oil and Fat Products: Chemistry, Chemical properties, and health effects** (pp. 431-489). New Jersey: John Wiley & Sons, 2005.

WANG, J. L. et al. Preparation and characterization of novel lipid carriers containing microalgae oil for food applications. **Journal of Food Science**, v.79, p.169-177, 2014.

WANG, T. Soybean oil. In.: GUNSTONE, F. D. **Vegetable Oils in Food Technology Composition, Properties and Uses.** Boca Raton, Florida, U.S.A: CRC Press LLC, (pp. 18-52), 2002.

WANG, X. Y. Enhancing anti-inflammation activity of curcumin through O/W nanoemulsions. **Food Chemistry**, v.108, n.2, 419–424, 2008.

WEISS, J. et al. Solid lipid nanoparticles as delivery systems for bioactive food components. **Food Biophysics**, v.3, p.146-154, 2008.

WEISS, J., TAKHISTOV, P., MCCLEMENTS, D. J. Functional Materials in Food Nanotechnology. **Journal of Food Science**, v.71, n.9, p. R107-R116, 2006.

WISSING, S. A., KAYSER, O., MÜLLER, R. H. Solid lipid nanoparticles for parenteral drug delivery. **Advanced Drug Delivery Reviews**, v.56, n.9, 1257–1272, 2004.

WOOSTER, T., GOLDING, M., SANGUANSRI, P. Impact of oil type on nanoemulsion formation and Ostwald ripening stability. **Langmuir**, v.24, n.22, p.12758–12765, 2008.

WU, L., ZHANG, J., WATANABE, W. Physical and chemical stability of drug nanoparticles. **Advanced Drug Delivery Reviews**, v.63, p.456-469, 2011.

WU, T. et al. The effects of phytosterols/stanols on blood lipid profiles: a systematic review with meta-analysis. **Asia Pacific Journal of Clinical Nutrition**, v.18, n.2, p.179-86, 2009.

WULFF-PEREZ, M. et al. Delaying lipid digestion through steric surfactant Pluronic F68: A novel in vitro approach. **Food Research International**, v.43, n.6, p.1629–1633, 2010.

YANG, Y. et al. The effect of oil type on the aggregation stability of nanostructured lipid carriers. **Journal of Colloid and Interface Science**, v. 418, n. Supplement C, p.261-272, 2014.

YIN, L. et al. Performance of selected emulsifiers and their combinations in the preparation of [beta]-carotene nanodispersions. **Food Hydrocolloids**, v.23, n.6, p.1617–1622, 2009.

YOON, G., PARK, J.W., YONN, I. Solid lipid nanoparticles (SLNs) and nanostructured lipid carriers (NLCs): recent advances in drug delivery. **Journal of Pharmaceutical Investigation**, v.43, p.353–362, 2013.

YUAN, H. et al. Studies on oral absorption of stearic acid SLN by a novel fluorometric method. **Colloids and Surfaces B-Biointerfaces**, v.58, n.2, p.157–164, 2007.

YUCEL, U., ELIAS, R. J., COUPLAND, J. N. Localization and reactivity of a hydrophobic solute in lecithin and caseinate stabilized solid lipid nanoparticles and nanoemulsions. **Journal of Colloid and Interface Science**, v.394, p.20-25, 2013.

ZEITOUN, M. A. M., NEFF, W. E. MOUNTS, T. L. Physical properties of interesterified fat blends. **Journal of the American Oil Chemists' Society**, v.70, n.5, p.467-471, 1993.

ZHANG, L. et al. Transparent dispersions of milk-fat-based nanostructured lipid carriers for delivery of β-carotene. **Journal of Agricultural and Food Chemistry**, v.61, p.9435−9443, 2013.

ZHENG, K. et al. The effect of polymer surfactant emulsifying agent on the formation and stability of α-lipoic acid loaded nanostructured lipid carriers (NLC). **Food Hydrocolloids**, v.32, p.72-78, 2013.

ZHU, J. et al. Preparation and characterization of novel nanocarriers containing krill oil for food application. **Journal of Functional Foods**, v.19, p.902– 912, 2015.

ZIANI, K., FANG, Y., McCLEMENTS, D. J. Encapsulation of functional lipophilic components in surfactant-based colloidal delivery systems: vitamin E, vitamin D, and lemon oil. **Food Chemistry**, v.134, p.1106–1112, 2012.

ZIMMERMANN, E., MÜLLER, R.H, MÄDER, K. Influence of different parameters on reconstitution of lyophilized SLN. **International Journal of Pharmaceutics**, v.196, p. 211–213, 2000.

ANEXOS

ANEXO 1

Comprovante de submissão do Artigo de Revisão

Submission Confirmation

Food Research International <eesserver@eesmail.elsevier.com>

seg 18/09/2017 23:10

Para:santosilvaleria@hotmail.com <santosilvaleria@hotmail.com>; santosilvaleria@gmail.com <santosilvaleria@gmail.com>;

Dear Valeria,

Your submission entitled "Solid lipid nanoparticles as carries for lipophilic compounds for applications in foods" of Review Article has been received by Food Research International

You may check on the progress of your paper by logging on to the Elsevier Editorial System as an author. The URL is https://eeslive.elsevier.com/foodres/.

Your username is: santosilvaleria@hotmail.com
If you need to retrieve password details, please go to: http://ees.elsevier.com/foodres/automail_query.asp

Your manuscript will be given a reference number once an Editor has been assigned.

Thank you for submitting your work to this journal.

Kind regards,

Elsevier Editorial System
Food Research International

Important information to authors concerning the manuscript processing at Food Research International and correspondence with the Editorial Office

All papers submitted to FRI undergo a process of pre-review evaluation which will determine whether they are sent for external review (see Guide for Authors).

FRI submissions have increased by over 40% over the past three years, and while editors try to process them rapidly as possible, the pre-review evaluation of many papers cannot be completed in a short time. When a paper is marked "With Editor" in EES, the pre-evaluation review is being completed.

Papers that are accepted for external review are sent to peer reviewers. Finding reviewers who are both specialized in the same field as the manuscript topic and who are available to review can be a long and time-consuming process. Papers marked "Under Review" have not been forgotten, but frequently it takes multiple attempts to find two peer reviewers who will actually review the submission.

Authors should only send correspondence to the journal about technical issues - e.g. password difficulties, missing data, adding another author, or some other item that was forgotten or overlooked when the paper was uploaded into EES. Enquiries concerning the status of papers, given the very small staff at the FRI Editorial Office, and its part-time operation, will delay the processing of manuscripts; there is no guarantee that such enquiries will be answered.

For further assistance, please visit our customer support site at http://help.elsevier.com/app/answers/list/p/7923. Here you can search for solutions on a range of topics, find answers to frequently asked questions and learn more about EES via interactive tutorials. You will also find our 24/7 support contact details should you need any further assistance from one of our customer support representatives.

ANEXO 2

Deposito de Pedido de Patente

INSTITUTO NACIONAL DA PROPRIEDADE INDUSTRIAL
Sistema de Gestão da Qualidade
Diretoria de Patentes

DIRPA	Tipo de Documento:	DIRPA	Página:
	Formulário		2/3
Título do Documento:		Código: FQ001	Versão: 01
Depósito de Pedido de Patente		Procedimento: DIRPA-PQ006	

6. **Inventor (72):**

☐ Assinale aqui se o(s) mesmo(s) requer(em) a não divulgação de seus nome(s), neste caso não preencher os campos abaixo.

6.1 Nome: VALERIA DA SILVA SANTOS

6.2 Qualificação: BRAS,UN.EST, QUÍM

6.3 CPF: 011.732.180-09

6.4 Endereço Completo: RUA GILBERTO PATTARO, 150, BAIRRO ALTO, EM CAMPINAS - SP

6.5 CEP: 13084-586

6.6 Telefone: (19)984072784   6.7 FAX:

6.8 E-mail: santosilvaleria@hotmail.com

☒ continua em folha anexa

7. **Declaração de divulgação anterior não prejudicial.** ☐
Artigo 12 da LPI – período de graça.
Informe no item 11.13 os documentos anexados, se houver.

8. **Declaração na forma do item 3.2 da Instrução Normativa nº 17/2013:**

☐ Declaro que os dados fornecidos no presente formulário são idênticos ao da certidão de depósito ou documento equivalente do pedido cuja prioridade está sendo reivindicada.

9. **Procurador (74):**

9.1 Nome: FERNANDA LAVRAS COSTALLAT SILVADO

9.2 CNPJ/CPF: 295.166.068-57   9.3 API/OAB: 210.899

9.4 Endereço Completo: PROCURADORIA GERAL DA UNICAMP, EM CAMPINAS - SP

9.5 CEP: 13083-970

9.6 Telefone: 19 3521-4771   9.7 FAX: 19 3521-4944

9.8 E-mail: proc-geral@pg.unicamp.br

☐ continua em folha anexa

10. **Listagem de sequências biológicas.**
Informe nos itens 11.9 ao 11.12 os documentos anexados, se houver. ☐

< Uso exclusivo do INPI >

INPI INSTITUTO NACIONAL DA PROPRIEDADE INDUSTRIAL
PROTOCOLO GERAL

mariarosa
29/03/2017   018170000778
15:13   DESP

BR 10 2017 006471 9

Espaço reservado para o protocolo   Espaço reservado para a etiqueta   Espaço reservado para o código QR

INSTITUTO NACIONAL DA PROPRIEDADE INDUSTRIAL
Sistema de Gestão da Qualidade
Diretoria de Patentes

DIRPA	Tipo de Documento: Formulário	DIRPA	Página: 1/3
Título do Documento: **Depósito de Pedido de Patente**		Código: FQ001	Versão: 01
		Procedimento: DIRPA-PQ006	

Ao Instituto Nacional da Propriedade Industrial:
O requerente solicita a concessão de um privilégio na natureza e nas condições abaixo indicadas:

1. Depositante (71):

1.1 Nome: UNIVERSIDADE ESTADUAL DE CAMPINAS - UNICAMP

1.2 Qualificação: PESSOA JURÍDICA DE DIREITO PÚBLICO, AUTARQUIA ESTADUAL

1.3 CNPJ/CPF: 46.068.425/0001-33

1.4 Endereço Completo: CIDADE UNIVERSITÁRIA "ZEFERINO VAZ"

1.5 CEP: 13083-970

1.6 Telefone: 19 3521-5015   1.7 Fax: 19 3521-5210

1.8 E-mail: patentes@inova.unicamp.br

☒ continua em folha anexa

2. Natureza: ☒ Invenção   ☐ Modelo de Utilidade   ☐ Certificado de Adição

3. Título da Invenção ou Modelo de Utilidade (54):

"NANOPARTICULAS LIPIDICAS SÓLIDAS (NLS) E CARREADORES LIPÍDICOS NANOESTRUTURADOS (CLN) PARA APLICAÇÃO EM ALIMENTOS, PROCESSO PARA OBTENÇÃO DE NLS E CLN E USO DAS NLS E DOS CLN"

☐ continua em folha anexa

4. Pedido de Divisão: do pedido Nº   **Data de Depósito:**

5. Prioridade: ☐ Interna (66)   ☐ Unionista (30)

O depositante reivindica a(s) seguinte(s):

País ou Organização do depósito	Número do depósito (se disponível)	Data de depósito

☐ continua em folha anexa

INSTITUTO NACIONAL DA PROPRIEDADE INDUSTRIAL
Sistema de Gestão da Qualidade
Diretoria de Patentes

DIRPA	Tipo de Documento: Formulário		DIRPA	Página: 3/3
Título do Documento: Depósito de Pedido de Patente			Código: FQ001	Versão: 01
			Procedimento: DIRPA-PQ006	

11.   Documentos Anexados:

(Assinale e indique também o número de folhas):
(Deverá ser indicado o número total de somente uma das vias de cada documento).

		Documentos Anexados	folhas
☒	11.1	Guia de Recolhimento da União (GRU).	1
☒	11.2	Procuração.	1
☐	11.3	Documentos de Prioridade.	
☐	11.4	Documento de contrato de trabalho.	
☒	11.5	Relatório descritivo.	27
☒	11.6	Reivindicações.	6
☒	11.7	Desenho(s) (se houver). Sugestão de figura a ser publicada com o resumo: nº, ___1___ por melhor representar a invenção (sujeito à avaliação do INPI).	4
☒	11.8	Resumo.	1
☐	11.9	Listagem de sequências em arquivo eletrônico: _____nº de CDs ou DVDs (original e cópia).	
☐	11.10	Código de controle alfanumérico no formato de código de barras referente às listagem de sequências.	
☐	11.11	Listagem de sequências em formato impresso.	
☐	11.12	Listagem de sequências - Declaração de acordo com a Resolução INPI nº 70/2013.	
☐	11.13	Outros (especificar)	

12.   Total de folhas anexadas: 40   fls.

13.   Declaro, sob as penas da Lei que todas as informações acima prestadas são completas e verdadeiras.

CAMPINAS, SP, EM 09.03.2017

_____
Local e Data

_____
Assinatura e Carimbo

FERNANDA LAVRAS COSTALLAT SILVADO
Procuradora de Universidade Subchefe
Matrícula nº 309279
OAB/SP nº 210.899

ANEXO 3

Parecer do orientador no exterior.

EPSRC Centre for Doctoral Training in Complex Particulate Products and Processes
(CDT CP3)

School of Chemical and Process Engineering
University of Leeds, Leeds LS2 9JT

T +44 (0) 113 343 0499
E cp3-cdt@leeds.ac.uk
W www.engineering.leeds.ac.uk/particulates

UNIVERSITY OF LEEDS

14 November 2017

To whom it may concern

Valeria da Silva Santos, PhD student in the Department of Materials and Bioprocess Engineering, Faculty of Chemical Engineering at the State University of Campinas, Brazil.

This is to confirm that Valeria da Silva Santos recently completed a research visit to the University of Leeds to develop part of her doctoral thesis studies.

Her research in 'Development of lipid nanoparticle carriers of phytosterols for application in margarine' was carried out in the EPSRC Centre for Doctoral Training in Complex Particulate Products and Processes, based in the School of Chemical and Process Engineering at the University of Leeds.

Valeria's visit took place from 1 July 2017 to 31 October 2017. During that time, Valeria was supported with the entire necessary scientific infrastructure and the advice of my research group. Valeria and I met regularly to discuss the progress of her research project and to ensure that she successfully completed the activities outlined in her application for funding.

Please do not hesitate to contact me should you require further information.

Yours faithfully

Kevin J Roberts

Brotherton Professor of Chemical Engineering

Director, EPSRC Centre for Doctoral Training in Complex Particulate Products and Processes